Integrated Scale Down Of The Primary Downstream Purification Process And Assessment Of Alternative Process Options For The Production Of An Ovine Polyclonal Antibody Based Anti-Venom

A thesis submitted to the University of London

for the degree of Doctor of Engineering

By

Gregory Edward Neal

DEPARTMENT OF BIOCHEMICAL ENGINEERING
UNIVERSITY COLLEGE LONDON
TORRINGTON PLACE
LONDON
WC1E 7JE

~~2004~~
2005

ProQuest LLC
789 East Eisenhower Parkway
P.O. Box 1346
Ann Arbor, MI 48106-1346

Abstract

This thesis describes the development of a linked 1000^{th} scale mimic of four distinct unit operations, including precipitation and centrifugation. These operations are utilised during the production of an anti-snake venom Fab fragment. A new approach has been used to define the important engineering parameters that impacted on the recovery process; the effect of these was verified by experimental work. The mimic requires only millilitre quantities of material to predict changes in the physical and biological properties of key components, such as particle size and antibody activity. The potential impact of several process changes on the characteristics of the feed stream and on purification steps further downstream has been assessed, which is not possible without a linked system.

Microfiltration has been examined as a possible alternative to the current centrifugal method of recovering the antibody particles. A small-scale stirred cell device was used to carry out a number of operations in a single piece of equipment; these included separation, concentration and buffer exchange. An overall increase in the yield of 10% was observed. This was attributed to the ability of microfiltration to reduce material losses by integrating a number of operations.

A preliminary investigation has been conducted into the possibility of utilising Protein G affinity chromatography in place of the current four-step precipitation and centrifugation recovery operation. A mathematical model capable of predicting the size and shape of the breakthrough curves has been developed; the predicted curves were tested by comparison with breakthrough curves produced under different experimental conditions. The initial results demonstrated the feasibility of utilising affinity chromatography as a one step recovery process. However the predicted breakthrough curves varied from the experimental curves suggesting that the mathematical model requires refinement.

Acknowledgements

Over the past four years numerous people have contributed both emotionally and intellectually to the development of this thesis. I would especially like to thank the following people. In no particular order: Protherics PLC for making this project possible especially; Keiran O'Donovan, Tony Newcombe, Aline Denton, Garnet Lewis and Richard Francis for always answering my questions, supplying me with material and making me feel welcome when I visited.

I would also like to thank Eli Keshavarz-Moore and Parviz Shamlou for their guidance, help and unswerving belief in my capabilities when my own belief failed.

Finally but by no means last special thanks go to Victoria Smalley for always supporting me and putting up with my despondent phases when I thought I would never finish and my Mum and Dad who provided a haven down in Somerset for when the big smoke got too much.

"As an adolescent I aspired to lasting fame, I craved factual certainty, and I thirsted for a meaningful vision of human life - so I became a scientist. This is like becoming an archbishop so you can meet girls".

M. Cartmill

Contents

List of Figures

List of Tables

Nomenclature

ω = angular velocity = $2\pi n$ (rps)

θ = half disc angle (rad)

Σ = Sigma (m^2)

μ = viscosity (mPa.s)

υ = volume of matrix (cm^3)

ξ = Power input per unit volume of suspension (WKg^{-1})

ΔP = pressure (bar)

ΔP_{TM} or TMP = transmembrane pressure (bar)

ϕ_v = volume fraction of particles = $\pi d^3 N_0 / 6$ (-)

Δp = density difference between the particle and the suspending fluid (gcm^{-3})

A = filter area (m^2)

b = channel height (m)

B = Solubility constant (-)

C = particle concentration ($Kg.m^{-3}$)

C_0 = initial protein concentration (mg/ml)

Ca = Camp number (-)

C_b = bulk concentration of cells in the feed stream ($Kg.m^{-3}$)

C_M = concentration of solute in the mobile phase (mg/ml)

C_S = concentration of adsorbed solute at equilibrium (mg/ml)

C_w = wall concentration of cells ($Kg.m^{-3}$)

D = diffusion coefficient (cm^2s^{-1})

D = impeller diameter (m)

d = particle diameter (m)

d_s = particle diameter (m)

$E_f = \varepsilon_v t$ = time integrated shear stress (Nm^{-2})

F_0 = initial flux ($L.m^{-2}.hr^{-1}$)

F_1 = correction factor applied to account for the presence of the spacer chalks (-)

g = gravitational acceleration ($m.s^{-2}$)

G = mean velocity gradient (-)

I = ionic strength of solution (mols)

J = flux ($L.m^{-2}.hr^{-1}$)

K = mass transfer coefficient ($Kg.m^{-2}.s^{-1}$)

K_1 = forward rate constant ($m^3/Kg/hr$)

K_{-1} = reverse reaction rate constant ($m^3/Kg/hr$)

K_2 = backward rate constant ($m^3/Kg/hr^{1}$)

K_A = association constant (Kg/m^3)

K_b = Boltzman constant ($J.K^{-1}$)

K_D = disassociation constant (Kg/m^3)

k_p = proportionality constant (-)

L = channel length (m)

n = impeller speed (rps)

N_0 = particle number concentration (-)

N_{crit} = rotational speed (rps)

N_{rd} = rotational speed of laboratory rotating disc device (rps)

p = density of the bulk suspension (Kgm^{-3})

P = power input (W)

P_0 = power number (-)

P_1 = feed inlet pressure (bar)

P_2 = retentate outlet pressure (bar)

P_3 = permeate outlet pressure (bar)

P_l = liquid density (gcm^{-3})

P_p = particle density (gcm^{-3})

Q = volumetric flowrate (m^3s^{-1})

q_m = maximum monolayer capacity of the matrix (mg/ml)

r = distance from the axis of rotation (m)

R_0 = outer disc radius (m)

R_1 = inner disc radius (m)

R_c = cake resistance ($m.Kg^{-1}$)

r_{crit} = critical radius of the structure (m)

r_e = equivalent min and max radius (m)

R_{max} =maximum radius (m)

R_{min} = minimum radius (m)

r_p = radius of the diffusing particle (m)

R_t = sum of the membrane resistance ($m.Kg^{-1}$)

R_t = total hydrodynamic resistance defined for a given membrane and a pure solvent (water) ($m.Kg^{-1}$)

S = solubility (-)

s_e = equivalent settling distance (m)

T = absolute temperature (K)

t = time (s)

T = torque (Nm)

V = volume (m^3)

V_{crit} = tip-velocity ($m.s^{-1}$)

V_f = volume of filtrate required to double the resistance to flow compared to the filter alone (L)

V_g = Stokes settling velocity ($m.s^{-1}$)

V_{max} = maximum volume filtered (L/m^2)

V_t = volume filtered (L)

w = channel width (m)

z = number of discs in the stack (-)

α = effectiveness factor of collisions in forming aggregates (-)

Abbreviations

d_{10} / d0.1 = particle size of 10% and less of the total volume of particles

d_{50} / d0.5 = particle size of 50% and less of the total volume of particles

d_{90} / d0.9 = particle size of 90% and less of the total volume of particles

1 Introduction

1.1 Background Of Protherics

The estimated annual number of world-wide deaths from snakebites are around 100,000 (Smith, 2001). In the USA alone roughly 8000 people are bitten each year. The incidence of snakebites is rising as more and more people come into contact with snakes, hence there is an increasing need for an effective anti-venom (Chippaux, 1998).

Snake venom is composed of a complex mixture of proteins; these are injected into a victim when bitten. The venom's poisonous action depends on its exact composition:

- Some destroy red blood cells and prevent clotting
- Some effect the nervous system and interfere with movement
- Others are destructive to the tissue around the bite

DNA immunisation targeting specific venom toxin molecules has the potential to treat large groups of the population in the affected areas of the world. However, the technique is in its infancy (Harrison, 2000) and it will be many years before a product becomes available on the market. As such, a snakebite victim is currently treated through the use of antibodies developed against the venom, extracted from animal serum and purified for human use. Traditionally anti-venom has been produced by immunising animals, such as horses with a cocktail of venoms from across the board. Serum would be harvested from the animal and injected into the patient. Due to the "foreign" nature of the anti-venom antibodies produced in this fashion allergic reactions by the patients are commonplace and could be fatal.

Protherics PLC (Wales, UK) has developed a new rattlesnake venom specific Fab fragment that is approved by the US Food and Drug Administration. It is expected

to open up a market worth an estimated $35 million a year. Since the action of the anti-venom is determined entirely by the Fab region, the Fc region of the antibody is removed during the purification process. This results in a significant reduction in allergic responses due to the Fc fragment being highly glycoslylated. Without the Fc region the patient's immune system cannot readily identify the Fab fragment as being "foreign" in nature. Further reductions in the allergic reaction are due to the highly purified nature of the anti-venom. In addition a Fab fragment, when compared to a whole antibody, can more quickly leave the blood stream; has faster diffusion rates into the affected tissues and the small Fab-venom complex can be more rapidly cleared from the body. This results in an anti-venom, that is more effective.

There are thirty-two species of rattlesnake and sixty five to seventy subspecies. In order for the anti-venom to be effective one single treatment for all types of rattlesnake is required. Investigation into the different rattlesnake venoms identified similarities in their composition. Four species of snake were identified the venom from which when used to develop antibodies that are blended together, would give protection against all species. These were:

- *Agkistrodon piscvorous* (Western cottonmouth)
- *Crotalus atrox* (Western diamondback)
- *Crotalus adamanteus* (Eastern diamondback)
- *Crotalus scutulatus* (Mojave rattlesnake)

The antibody fragments, administered via intravenous injection, work by binding to and thereby neutralising the venom toxins; facilitating their redistribution away from the target tissues and their elimination from the body.

The very first stage in the production of the anti-venom requires separate groups of sheep to be immunised with each different type of venom. The polyclonal antibody Fab fragments against each type of venom are then isolated from the serum. The four products are then blended in equal quantities to produce one anti-venom effective against all North American rattlesnake venoms.

The sheep (kept in Australia) are immunised on a monthly schedule using venom collected in Arizona USA, which has been processed into sheep dose vials then freeze-dried in Wales, UK. The venom is mixed with Freunds adjuvant (a solution of oils which increases the immune response) and injected into the sheep. Each sheep is bled once a month with each bleed producing 750-800mls of blood. The blood is clotted and centrifuged which leaves roughly 400mls of serum. This process takes twenty minutes after which the serum is pooled, dead end filtered, frozen and sent to Wales (UK) for purification.

1.2 Industrial Scale Purification Of Fab Fragments From Ovine Serum

The entire industrial scale downstream purification process is shown in figure 1.1.

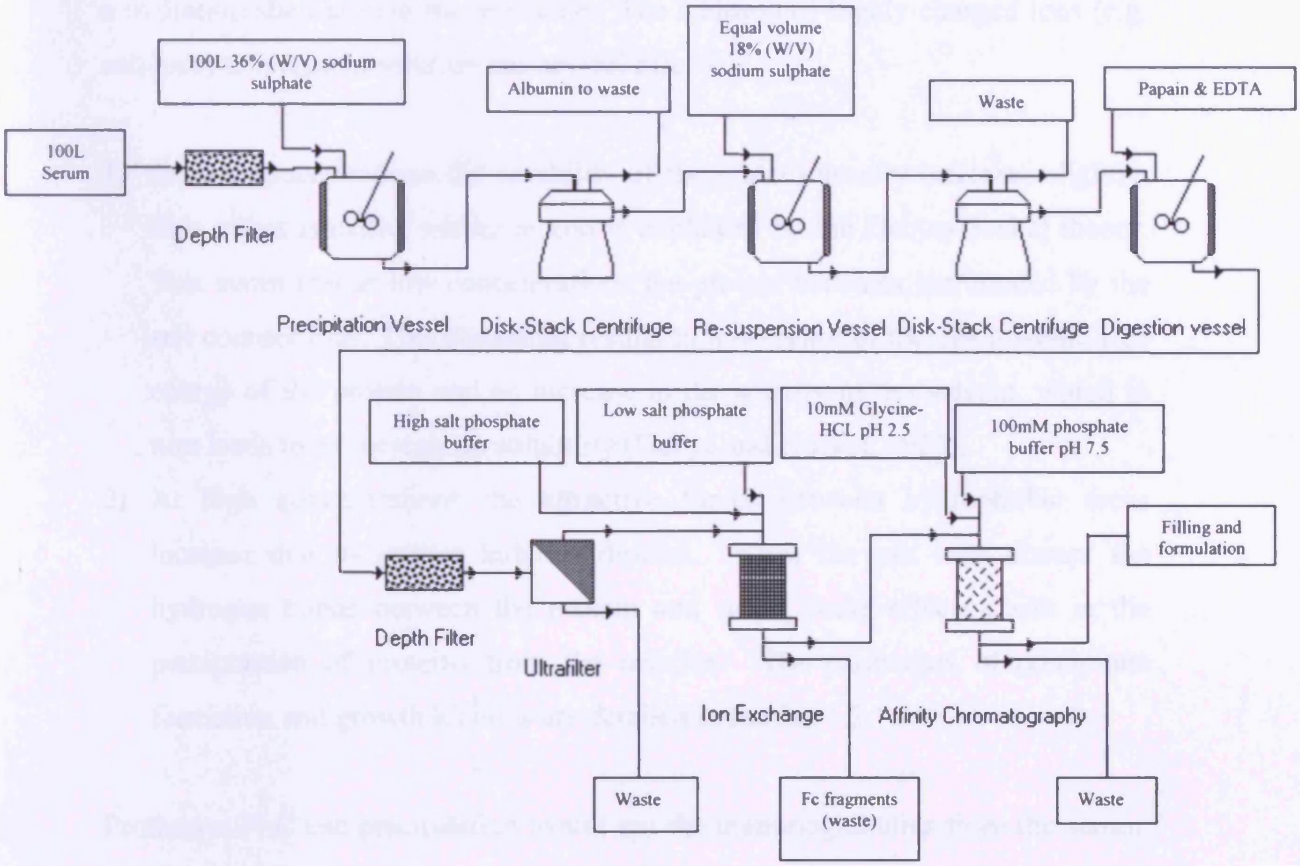

Figure 1.1 Process flow sheet for the purification of polyclonal Fab fragments from ovine serum

The following section describes the purpose of the purification steps; the initial step, which is not described in detail, is the 0.2μm depth filtration of the thawed serum which removes cyro-precipitates.

1.2.1 Precipitation

Precipitation is a fast way of concentrating proteins from solution. Under normal conditions proteins are associated with various levels of bound water. These form a hydration shell around the molecule. The addition of highly charged ions (e.g. sulphate) to a protein solution has several effects:

1. At low concentrations the solubility of the protein usually increases slightly. This effect is called salting in and is explained by the Debye-Huckel theory. This states that at low concentrations the protein becomes surrounded by the salt counter ions. This screening results in a decrease in the electrostatic free energy of the protein and an increase in the activity of the solvent, which in turn leads to an increase in solubility (Debye and Huckel, 1923).
2. At high concentrations the attractive forces between hydrophobic areas increase due to greater induced dipoles. Also, the salt ions disrupt the hydrogen bonds between the protein and water, these effects result in the precipitation of proteins from the solution. The particulars of precipitate formation and growth kinetics are detailed in section 1.3.1.

Protherics PLC use precipitation to salt out the immunoglobulins from the serum. Precipitation is a good first step choice because it reduces the volume of feed material and provides an acceptable level of initial purification. An equal volume of 36%(w/v) liquid sodium sulphate solution is added to the serum, resulting in a final concentration of 18%(w/v) sodium sulphate. This solution is left stirring overnight. Sodium sulphate is used in preference of ammonium sulphate because ammonium sulphate is corrosive and toxic. The immunoglobulins are precipitated out as a white paste whilst the majority of the albumin, the main contaminant at this stage, remains in solution.

Post precipitation disc stack centrifugation is used to separate the two phases. The serum/sodium sulphate solution is pumped into the centrifuge which is spinning at 7500rpm at a flow rate of 120 to 130L/hr. The supernatant flows out via the waste pipe (albumin fraction). The precipitate is desludged at regular intervals along with a hood flush of 18% (w/v) sodium sulphate. Following the completion of the

batch, the precipitated IgG is resuspended in 18% (w/v) sodium sulphate and centrifuged again in order to further reduce the levels of albumin contamination.

1.2.2 Centrifugation

Centrifugal separation is a sedimentation operation accelerated by centrifugal force. As such, a prerequisite for separation is a density difference between phases. This technique can be used to separate two liquid phases or a solid/liquid mixture. Protherics PLC utilise a continuous flow disc stack centrifuge (Westfalia separator serial number SAM R3036, type SA14, bowl volume 6.9L with a max speed of 7500rpm, 6288g) to separate the precipitated antibodies from the proteins remaining in solution.

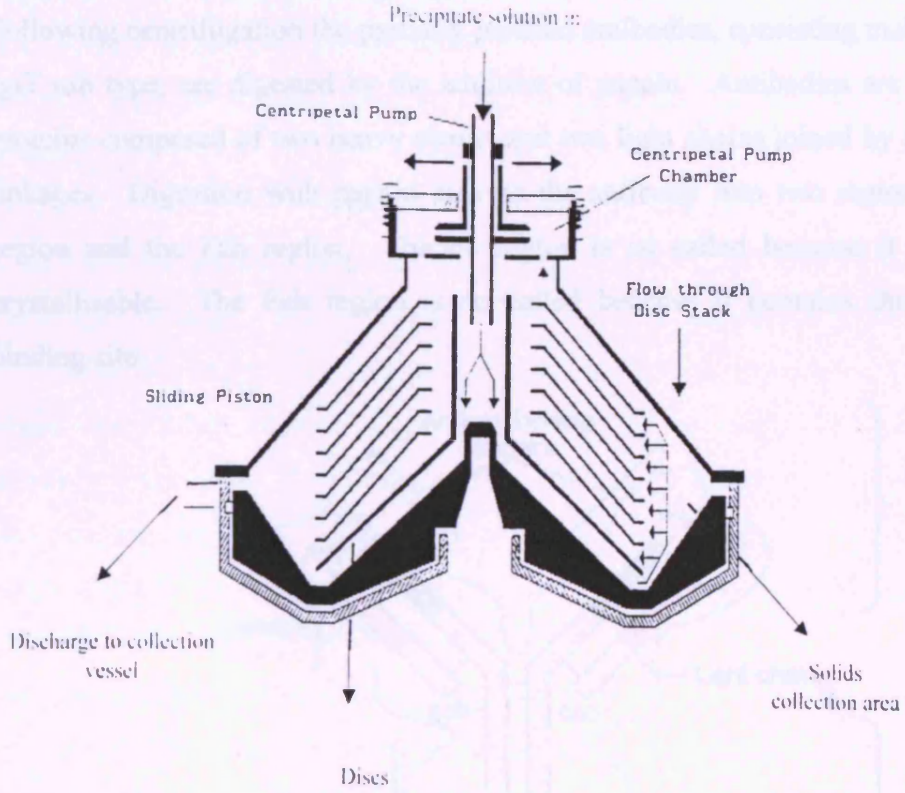

Figure 1.2 A disc stack centrifuge

The precipitate solution is pumped into the centrifuge (feed flow rate is between 120-130L/hour) where it collects in the feed chamber at the bottom of the stack. During normal operation the stack is spinning at 7500rpm this causes the solid precipitate to be thrown outwards and collect on the underside of the discs. It then slides down into the collection chamber, which is located by the discharge ports. The liquid part containing the unwanted proteins flows out the top of the machine to waste. At a time interval, set by the percentage solids content of the feed stream, pressurised water is used to open the sliding bowl resulting in the collected solid being ejected into a clean vessel. If the interval is too long a situation called breakthrough arises whereby the solid collection area becomes full and the solids begin to go out via waste.

1.2.3 Digestion

Following centrifugation the partially purified antibodies, consisting mainly of the IgG sub type, are digested by the addition of papain. Antibodies are Y shaped proteins composed of two heavy chains and two light chains joined by disulphide linkages. Digestion with papain cleaves the antibody into two regions: the Fc region and the Fab region. The Fc region is so called because it is readily crystallisable. The Fab region is so called because it contains the antibody binding site.

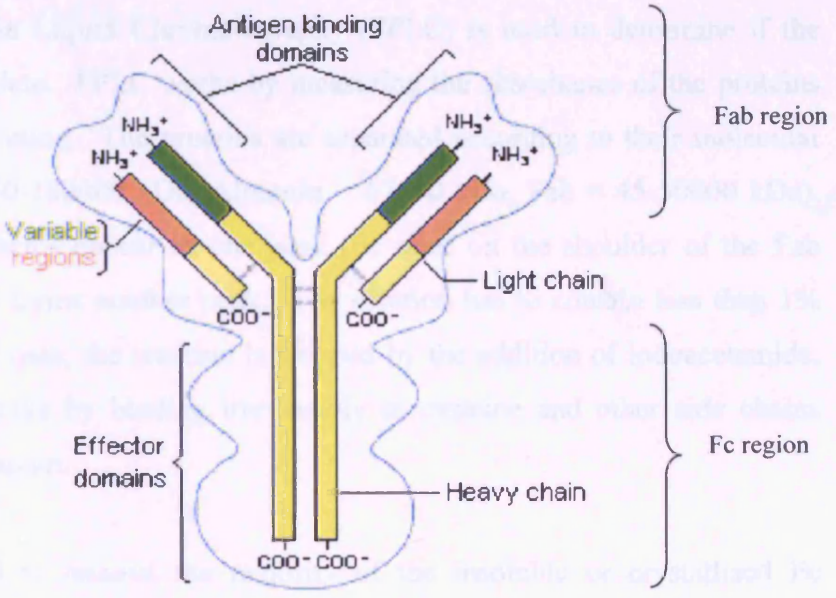

Figure 1.3 Stylised representation of the sub-unit structure of an IgG antibody

The Fc region mediates some aspects of the immune response, but differences in the glycosylation pattern between species mean that foreign antibodies are easily recognised by a patient's immune system as being foreign in origin. For this reason when antibodies from one species are injected into another an allergic reaction is often observed. This is caused by the patient's immune system attacking the antibodies. The functions of the Fc region are not, however, required by the anti venom. The binding of the Fab fragment to the venom is enough to neutralise it.

Protherics PLC utilise the unique action of the enzyme papain to cleave the heavy chain on the $COOH^-$ terminal side of the disulphide bond that links the heavy and light chains. This results in the formation of two Fab fragments and one Fc fragment. The Fc fragment can then be purified out further downstream resulting in a product which has been modified sufficiently to reduce recognition by the patient's immune system. This dramatically reduces the risk of harmful side effects.

A solution of papain, cysteine and EDTA is added to the product of the centrifugation stage. This solution is then left in a stirring vessel overnight at 37°C. The following morning a sample is taken to the quality control laboratories where Fast Protein Liquid Chromatography (FPLC) is used to determine if the digestion is complete. FPLC works by measuring the absorbance of the proteins contained in a solution. The proteins are separated according to their molecular weight (IgG = 150-180000 kDa, Albumin = 67000 kDa, Fab = 45-50000 kDa). Fab and Fc fragments appear as one peak (Fc rides on the shoulder of the Fab peak), whilst IgG forms another peak. The solution has to contain less than 1% IgG. If this is the case, the reaction is stopped by the addition of iodoacetamide. Iodoacetamide works by binding irreversibly to cysteine and other side chains neutralising the papain.

Filtration is used to remove the majority of the insoluble or crystallised Fc fragments. However the product solution now also contains a large concentration of other chemicals such as EDTA and soluble Fc fragments. Ultrafiltration is

used to remove these chemicals, concentrate the product and change the buffer to one compatible with the next purification stages. This is achieved by passing the solution across a filter with pores that are small enough to block the passage of Fab fragments but large enough to allow other contaminants to pass to waste. At this stage the product is known as total Fab and is eighty percent pure. It can be stored for up to eight weeks before final processing.

1.2.4 Ion Exchange

Ion exchange chromatography is used to separate the Fc fragments and other blood proteins from the Fab fragments. Separation on an ion exchange column depends upon the reversible binding of charged molecules to immobilised ion exchange groups of an opposite charge. There are two types of ion exchange column: cationic exchangers and anionic exchangers. Cationic exchangers bind molecules with a net positive charge, whilst anionic exchangers bind molecules with a net negative charge.

The pH/ionic strength of the solution a protein is dissolved in effects its binding affinity. By altering the pH or ionic strength of the solution, proteins can be given either a net positive or a net negative charge. Different proteins have different charges at different pH/ionic strength. This phenomenon can be used to separate one protein from a solution containing many.

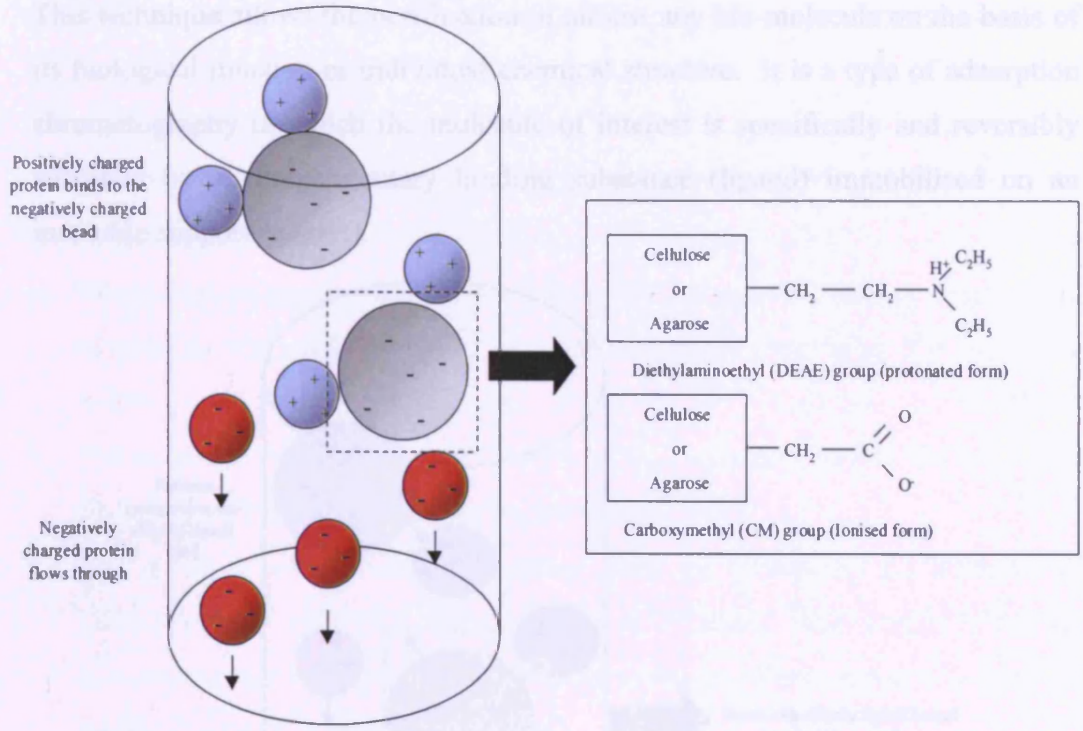

Figure 1.4 Schematic representation of Ion Exchange chromatography (adapted from the Ion Exchange chromatography handbook, Pharmacia)

As the column has a finite capacity (column dimension 30cm diameter, 19-20cm bed height), the total Fab produced to date must be divided up and loaded batch wise. As the solution is passed over the matrix the unwanted proteins, such as the Fc fragments and albumin, bind reversibly whilst the Fab fragments go straight through and are collected. The portion which remains bound to the column is then removed by washing with 10mM phosphate, 1M NaCl. The column is then cleaned and sanitised by application of 1M sodium hydroxide. Before the next batch can be processed the column must be re-equilibrated by the addition of 10mM phosphate buffer. This ensures that the matrix and the solution the Fab is contained in are compatible.

1.2.5 Affinity Chromatography

The final purification step is the separation of the component specific antibodies from the other unspecific antibodies. Protherics PLC utilise affinity chromatography to achieve this.

This technique allows the purification of almost any bio-molecule on the basis of its biological function or individual chemical structure. It is a type of adsorption chromatography in which the molecule of interest is specifically and reversibly adsorbed by a complementary binding substance (ligand) immobilised on an insoluble support (matrix).

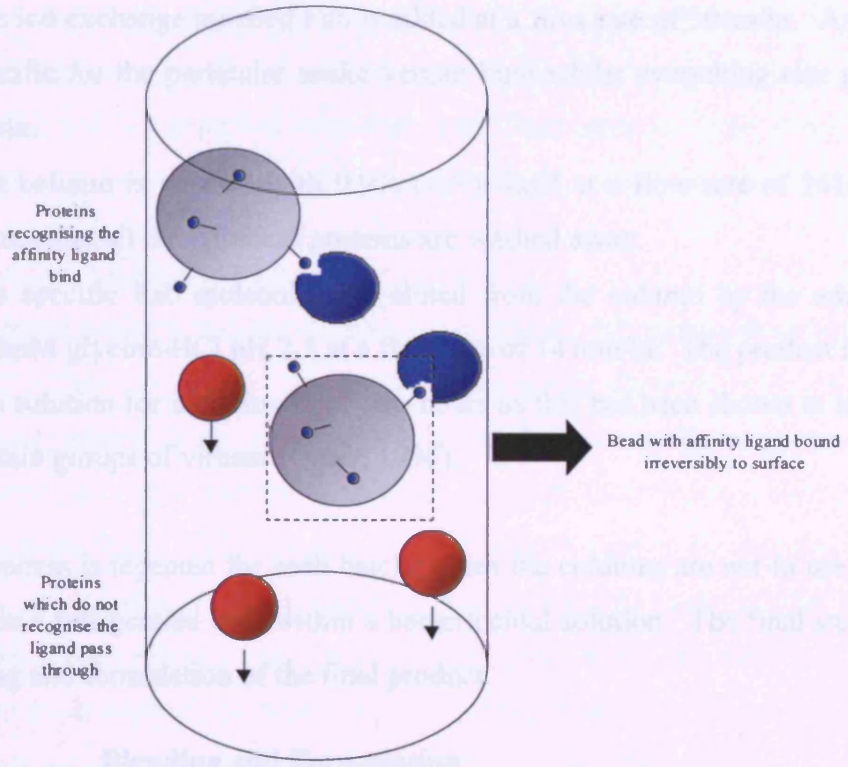

Figure 1.5 Schematic representation of affinity chromatography

Successful separation requires a bio-specific ligand that can be covalently attached to a chromatographic bed material, the matrix.

Protherics PLC utilise the snake venom specific for the anti-venom as the ligand. This is bound irreversibly to the matrix (Controlled pore glass, Millipore, Watford UK). Thus, as each component recognises a different type of venom, each component of the anti-venom requires its own column (Column dimensions 30cm diameter, 28.5 to 32cm bed height). This means that there are four columns in total. Once again the column has a finite capacity so the product is split into equal

volumes and each is loaded separately batch wise. Separation proceeds as follows:

- The column is equilibrated with 100mM Phosphate buffer pH 7.5 at a flow rate of 141cm/hr.
- The ion exchange purified Fab is added at a flow rate of 30cm/hr. Antibodies specific for the particular snake venom bind whilst everything else passes to waste.
- The column is washed with 0.9% (w/v) NaCl at a flow rate of 141cm/hr to ensure that all the unbound proteins are washed away.
- The specific Fab molecules are eluted from the column by the addition of 100mM glycine-HCl pH 2.5 at a flow rate of 141cm/hr. The product is held in this solution for a minimum of two hours as this has been shown to inactivate certain groups of viruses (Omar, 1996).

This process is repeated for each batch. When the columns are not in use they are stored in a refrigerated area within a bacteriocidal solution. The final stage is the blending and formulation of the final product.

1.2.6 Blending and Formulation

With the downstream processing complete, the final step is the blending and formulation of the individual components into a solution suitable for freeze-drying. This solution is then concentrated so that each vial contains a consistent potency of product.

- The four anti-venom components are equally blended together forming a pure product, which contains between 1g/L to 3g/L.
- Ultrafiltration concentrates the product to 12g/L and exchanges the buffer to sodium acetate, which is compatible with the next stage.
- The product is passed through a 15nm viral filter. This has been shown to be an effective viral removal step (O'Grady, 1996). This gives Protherics PLC two validated steps for virus removal.

- Ultrafiltration exchanges the buffer for low salt phosphate, which is suitable for freeze-drying. This causes some of the Fab to precipitate out these are removed by depth filtration.
- Final ultrafiltration concentrates the product to 70g/L.
- Contractors are used to freeze dry the product and place it in to vials. One vial holds a maximum of 14mls. The bulk formulated solution is tested by external contractor for its potency to neutralise the venoms activity. The vial fill volume is calculated such that vials from batch to batch always contain sufficient neutralising potency to meet the final product specification.

1.2.7 Conclusion

Anti-venom prepared by this method is not cheap; full treatment normally costs $10000. From a process engineering perspective, there is now very intense pressure on companies to establish techniques that can rapidly assess new process options to produce a potential new drug candidate in sufficient quantities for its perceived demand. This pressure is compounded further by the fact that such process information is needed often early in the life cycle of the new drug candidate. Unfortunately this is when pilot plant trials are either not feasible, because the company has no access to suitable facilities, or not practical because only very small quantities of relevant materials are available for tests.

This thesis describes an engineering approach to the development and verification of small scale devices/processes that mimic industrial scale operations. This allows key unit operations and options to be investigated early on in the product development life cycle, providing the process engineer with invaluable information. It also seeks to investigate alternative process options for the production of the anti-venom.

1.3 Background Theory and Practice of Downstream Unit Operations

This section details the research already conducted on the techniques of interest and the impact on this study. It endeavours to cover the work related to and the concepts important to the running and mimicking of each purification process utilised. It also aims to provide an overview of the methods available for protein purification, which are applicable to the purification of antibodies from ovine serum.

1.3.1 Precipitation

Precipitation has been used as a method to separate proteins for 130 years. It is well established in the separation of proteins from blood plasma, microbial extracts and plant extracts (Foster, 1994). Precipitation exploits the differences in protein solubility in order to achieve separation. The proteins are precipitated as a non-crystalline solid.

Precipitation is often used near the start of a purification process for a variety of reasons. These include:

- Precipitation methods can inexpensively process a large volume of crude material, resulting in a reduction of the volume of material. Although the purification factors of 3-10 that are typically achieved are low compared to say chromatographic methods (Bell, et al. 1983; Chisti and Moo-young, 1991). The ability to process large volumes of crude material mean this method is a good first choice purification step.
- The process is easily scale-able allowing processing options to be easily studied before the license is agreed.
- Protein precipitates are compact and stable, thereby allowing the purification process to be held at an intermediate stage.
- Precipitation places the protein into an environment depleted of proteolytic enzymes and other biologically active substances.

Since part of this thesis describes the mimicking of the precipitation stage it is important to understand the factors controlling the formation and growth of

precipitate particles. Knowledge of these parameters will allow an accurate mimic of the process to be designed and operated.

Particle formation usually consists of two phases; an induction phase involving the formation of the nuclei, followed by a growth phase during which other solute molecules attach to the nuclei. The precipitate particles continue to grow until equilibrium is reached. In order for particle formation to occur the soluble solute concentration must be greater than the normal equilibrium value. As nucleation and growth are energy consuming processes, there is a need for the solution to attain a certain level of supersaturation. It is the excess solute concentration relative to the equilibrium solubility value that contributes the necessary energy.

The formation and growth of precipitate particles follows a set series of well defined stages.

Stage 1. Addition of the precipitant, achievement of supersaturation and nuclei formation. Nucleation times can range from a few seconds to several minutes depending on the type of precipitant and the specific protein. Parker and Dalgleish (1977) used light scattering and turbidity measurements in order to study the kinetics of this process.

Stage 2. Perikinetic growth of nuclei to form primary precipitate particles. The rate of growth of these particles will be determined by the collision frequency. Particles up to the size of 1μm are not affected by mixing conditions, so collisions will be determined by diffusion, this is shown in equation 1.3.

$$\left[\frac{-dN_0}{dt}\right] = K_a N_0^{\,2}$$

(equation 1.1)

$$K_a = 8\pi Dd$$

(equation 1.2)

Where N_0 is the particle number concentration, d is the particle diameter and D is the diffusion coefficient.

$$D = \frac{K_b T}{3\pi\mu d}$$

(equation 1.3)

Where K_b is the Boltzman constant, T is the absolute temperature and μ is the viscosity of the solution.

The above equations imply that there will be a greater rate of collisions and hence a greater growth rate at higher temperatures. They also imply a linear rate of increase of particle volume, mass or molecular weight with time.

Stage 3. Orthokinetic growth occurs once the particles have reached a size of 1 μm. Fluid motion then causes the particles to collide and form macroscopic precipitate particles.

$$\frac{-dN_0}{dt} = \frac{2}{3}\alpha G d^3 N_0^2$$

(equation 1.4)

$$= \frac{4}{\pi}\alpha\phi_v G N_0$$

(equation 1.5)

Where ϕ_v is the volume fraction of particles which equals $\pi\ d^3\ N_0 / 6$, α is the effectiveness factor of collisions in forming aggregates and G is the mean velocity gradient.

These equations imply that the growth rate of the particles should increase with a larger mean velocity gradient and greater particle concentration. They also imply that the size of particles should increase exponentially with time.

Stage 4. Batch aging and conditioning. Centrifugation is often used in order to separate the precipitate particles from solution. For efficient separation the best particles are large, dense and strong. Batch aging can produce particles with these attributes. This is where the precipitate is stirred in the tank for a given period of time. The average size of the final precipitate will be a result of the balance between orthokinetic growth and hydrodynamic shear induced break up of particles. Increasing the intensity of mixing will result in smaller particles. Larger sized particles will be obtained at lower shear rates, however these particles are unlikely to be very strong and so more likely to break up when subjected to the high shear field found in equipment such as centrifuges.

Shear conditions within a reactor can be defined by the Camp number Gt, where G is the average shear rate, or mean velocity gradient and t is the time of exposure to the shear. Bell and Dunnill (1982a) found that the aggregate strength was dependent on the extent and duration of agitation. They determined an optimum value of the aging parameter Gt of 10^5 (see figure 1.6).

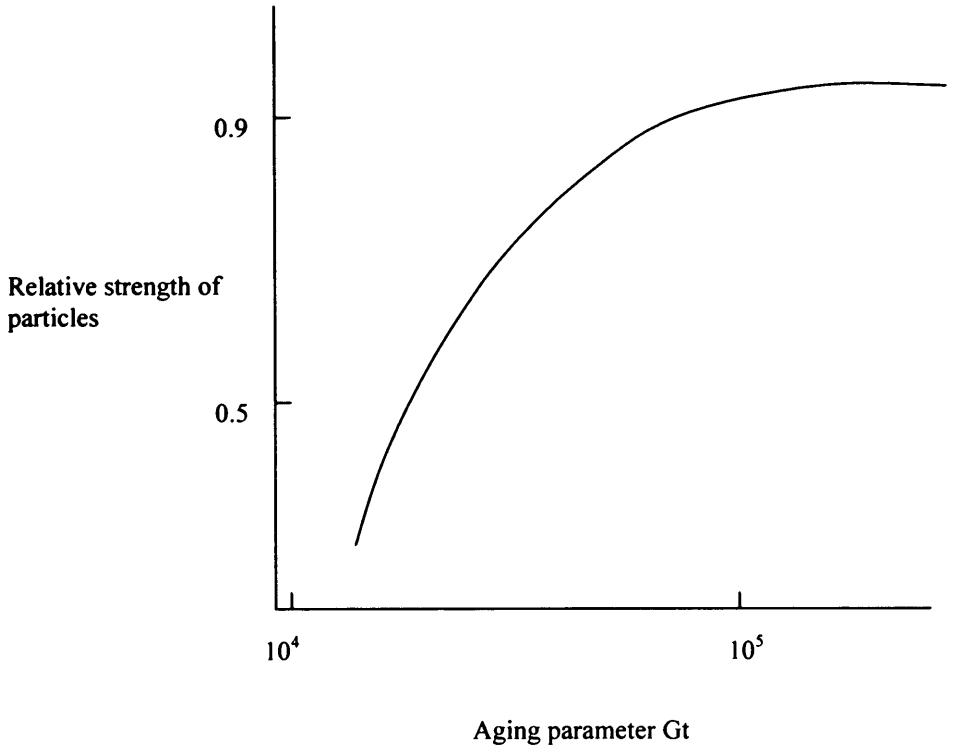

Figure 1.6 Effect of aging on the strength of particles (Bell and Dunnill 1982)

Particles produced by this aging parameter were found to be the most resistant to shear break-up. This suggested that precipitates produced under low conditions of shear should be aged for longer in order to strengthen them. The improved strength at Gt values of 10^5 were thought to be due to rearrangement and infilling with smaller particles giving a closer, denser and more stable particle. Other studies by Hoare (1982) and Clarkson, et al. (1996a) confirmed this finding. Hoare (1982) examined the batch aging of ammonium sulphate precipitated casein and found that the maximum stable precipitate size was achieved at a Gt value of 10^5. While Clarkson, et al. (1996a) showed that bakers yeast protein precipitated with ammonium sulphate had a reduction in fine aggregates of approximately 1.5μm and an increase in the proportion of larger aggregates of 2 to 4μm at a Gt value of 10^5.

There are several methods of altering protein solubility, bringing about protein precipitation:

- Coagulation by heat may be used to precipitate out unwanted heat labile proteins from a solution of more stable ones. When a protein reaches a certain critical temperature it denatures allowing hydrophobic residues buried within its structure to interact with each other bringing the protein out of solution.
- Isoelectric precipitation may be used to separate pH stable proteins. This method is based on the fact that at their isoelectric point proteins have no net charge. This results in a reduction in the repulsive forces between protein molecules allowing them to contact each other forming an agglomeration.
- Metal ions such as zinc or calcium can be used to precipitate proteins. These work by binding to the surface of the protein molecules again reducing the repulsion between the molecules.
- High concentrations of non-ionic polymers (~20%w/v) such as polyethylene glycol tend to induce precipitation by removal of water from the protein environment.

- Ionic polyelectrolytes induce precipitation, probably by a mixture of methods including charge patch neutralization and polymer bridging. Very low concentrations are required and the addition of excess quantities leads to re-solubilisation of the protein. Reagents used include polyethyleneimine, although that particular reagent is difficult to remove further downstream.

The most widely used method of protein precipitation is the addition of high concentrations of neutral salts. This process is known as "salting-out". At low salt concentrations proteins are very soluble as a result of polar interactions with the aqueous solvent, ionic interactions with the salt present and to some extent repulsive electrostatic forces between like charged molecules or aggregates (Scopes, 1988). This effect is often called "salting in". At higher salt concentrations solubility depends more on the hydrophobicity of the protein. The most hydrophobic and hence the least hydrated protein tend to be the first to come out of solution (Zhang, et al. 1995). Each protein has a distribution of hydrophilic and hydrophobic residues on its surface; these will determine its solubility behavior. When hydrophobic residues are forced into contact with an aqueous environment, water molecules become bound in place around these residues. When large amounts of salt are added, the salt molecules become solvated and, as water molecules become scarce, pull away the bound molecules from the hydrophobic residues. The exposed residues can then interact to form a protein aggregate. Once these reach a size no longer favorable to the soluble phase, precipitation of the solid phase occurs (Foster, 1994).

Precipitation reactions generally follow the Cohn equation (Chisti and Moo-young, 1991).

$$\ln S = B - K_s I$$

(equation 1.6)

Where S is the solubility and I is the ionic strength of solution. The constants K and B represent the slope of the linear portion of the salting-out curve and the y

intercept respectively. B is a function of both pH and temperature and is at a minimum at the proteins iso-electric point. K is a function of the type of salt used and the individual protein. The constants B and K have also been found to vary according to the mode and rate of addition of the precipitant (Foster, et al. 1976). This implies that although the precipitate may be in a stable form this does not represent a true equilibrium state.

The differing reagents discussed above have different precipitation kinetics. These are discussed in a paper by Chan, et al. (1986).

The relative effectiveness of neutral salts in salting out, in particular the anions, is given by the lyotrophic or Hofmeister series (Hofmeister, 1888; Cacace, et al. 1997):

Citrate > phosphate > sulphate > acetate ~ chloride > nitrate > thiocynate

The series is in order of decreasing effectiveness of anion to cause salting out and increasing likelihood of destabilising the protein.

One of the most commonly utilised salts is ammonium sulphate due to its high solubility, cheapness and stabilising effect on some enzymes. However ammonium sulphate is corrosive and evolves ammonia at high pH. This makes it difficult to process at a large scale (Richardson, 1987).

The main factors, which determine protein solubility and therefore the extent of precipitation are listed in table 1.1. The effects on the resulting particles of altering some of them are discussed afterwards.

Protein Characteristics	Solution properties
Size of molecule	Solvent availability e.g. Water
Amino acid composition	pH
Amino acid sequence	Ionic strength
Number of ionisable residues	Dielectric constant
Ratio of polar/non-polar residues	Temperature
Distribution of polar/non-polar residues	Specific ion effects
Dissociation constants	
Protein conformation	
Protein charge	
Ion binding properties	
Chemical nature of amino acids	

Table 1.1 Factors determining the solubility of proteins from Foster (1994)

The effects of altering the pH on the solubility of the protein and the resulting particle size of the precipitate are shown below.

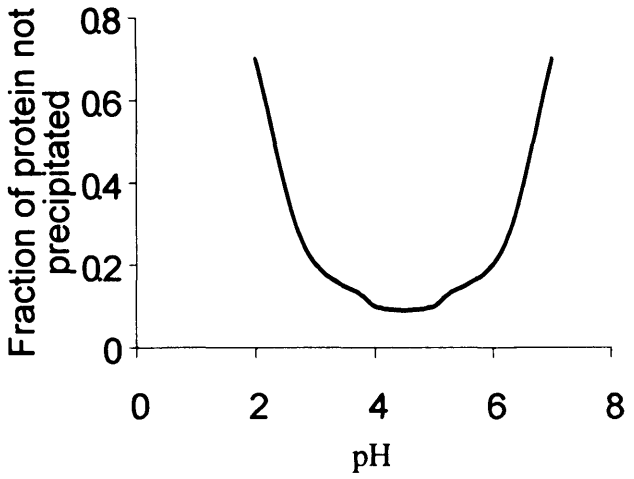

Figure 1.7 The effect of pH on soya protein solubility (Virkar, et al. 1982)

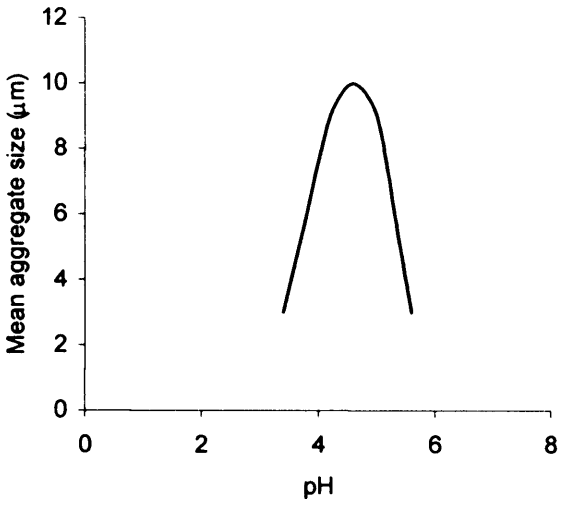

Figure 1.8 Effect of pH on precipitate particle size (Chan, et al. 1986)

As can be seen the least solubility and highest particle size occur at roughly the same point.

The effect of ionic strength on protein solubility:

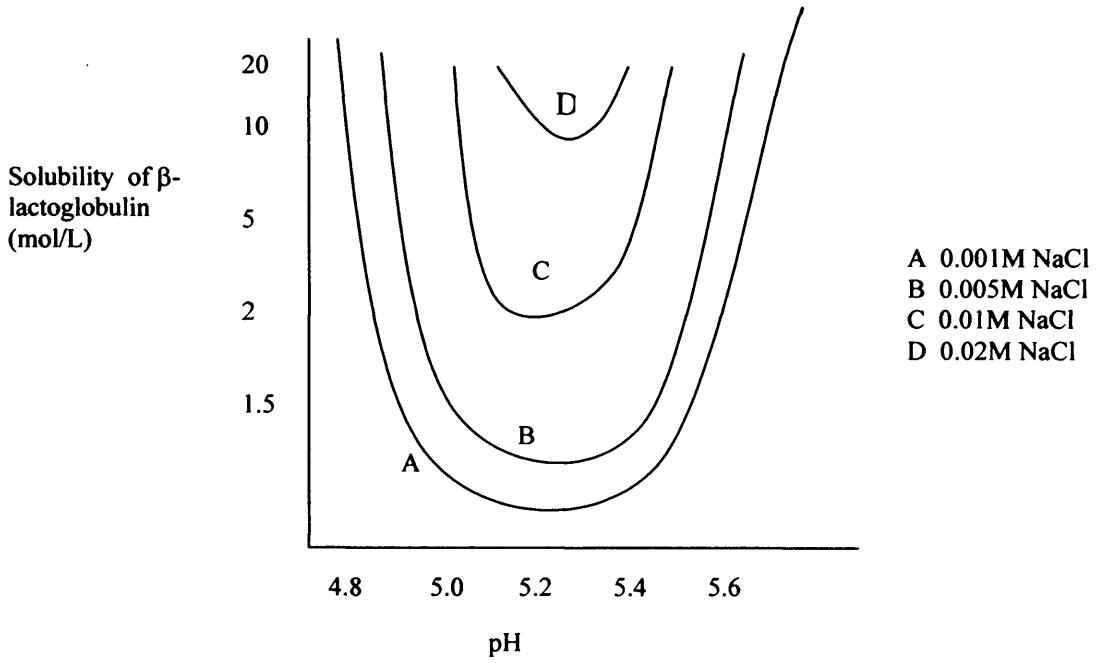

Figure 1.9 The effect of ionic strength on protein solubility (Gronwall 1942)
As can be seen there is a salting in effect at lower concentrations.

It can be concluded from previous research that the pH, temperature, ionic strength, the rate and mode of addition of the precipitant, the type of salt and the mixing conditions will all need to be kept similar between the scales of operation in order to achieve an accurate mimic.

1.3.2 Centrifugation

Centrifugal separation is a mechanical method of separating the components of a mixture of liquids or of liquid and solid particles. Centrifugation takes advantage of the density differences between the liquid phases or solid and liquid phases. The material is accelerated in a centrifugal field, which acts in the same manner as a gravitational field. The centrifugal field can however be varied by adjusting the rotational speed and equipment dimensions. Commercial centrifugal equipment can reach an acceleration of 20000 times gravity (20000 g), where as laboratory equipment can reach up to 360000 g.

1.3.2.1 Types of centrifuge

The application and design of centrifugal separators has been reviewed by Axelsson (1985) and Brunner, et al. (1988). There are five main types of centrifuge, which are required in order to deal with the variety of process materials produced. The choice of separator depends on the characteristics of the process stream, including the particle size, the difference in density between the solid and liquid phases, the solids content and the tendency for the process stream to form emulsions. Centrifuges are mainly used for cell harvest and washing after fermentation and for recovery of solid particles following extraction, crystallisation or precipitation.

Tubular bowl

The simplistic design of the tubular bowl accounts for its ease of operation. Fluid enters at the bottom and the solids sediment against the wall as the fluid flows up and out via an inner ring dam or centripetal pump. The centrifuge is capable of operating at high rotational speeds. This leads to good clarification and good dewatering. There is however no automated solids discharge; solids have to be

removed manually at the end of the run. Therefore, it is best used with process streams that have a low solids content and small batch volume.

Decanter/Scroll

This centrifuge design was derived from the tubular bowl. The main difference is that solids discharge is achieved via a conveyer screw which rotates at a different speed to the bowl. This has the effect of concentrating solids in streams with high solids content. It is best suited to process streams, which contain large dense particles due to the low centrifugal forces achievable because of the imbalance inherent to the design. This machine is attractive because it is capable of handling a high solids content and obtaining good dewatering. It is mainly used for sludge dewatering in wastewater treatment.

Multichamber bowl

This centrifuge contains up to five concentric chambers. These have the effect of increasing the axial flow path and increasing the area available for sedimentation. Large particles sediment out in the inner chamber, whilst smaller particles sediment out in the outer chambers where there is a higher centrifugal force. The effect of shear in the feed zone is decreased since it is flooded. Therefore material which enters the feed zone is accelerated slowly. This increases the performance of the centrifuge since less fine particles are produced. Discharge of collected solids is manual but the increased size means that it can handle process streams with a higher solids content than a tubular bowl.

Carr Powerfuge

The Carr powerfuge is a tubular bowl centrifuge with an automated solids discharge mechanism. The bowl is constructed of titanium, which can tolerate higher g forces. As a result, the machine can operate at higher rotational speeds. Solids discharge is achieved by means of a scraper that moves into position near the bowl wall. Collected material is then removed from the walls and drops into a collection vessel whilst the centrifuge is spinning slowly. The powerfuge can be both cleaned in place and steamed in place minimising process stream contamination.

Disc Stack

The disc stack centrifuge is one of the most commonly employed machines for the separation of biological materials in the biotechnology industry. Applications include the separation of cells from fermentation broth (Higgins, et al. 1978; Datar and Rosen, 1987), the removal of cell debris after cell disruption (Mosqueira, et al. 1981; Clarkson, et al. 1993a), the recovery of inclusion bodies (Jin, et al. 1994) and the recovery of precipitates (Bell, et al. 1983; Clarkson, et al. 1996b).

The disc stack centrifuge consists of a bowl containing a series of conical discs stacked one on top of the other. The discs are separated by spacer bars roughly 1mm in height. During normal operation the process material splits into thin layers and flows between the discs. Settling solids are thrown outwards and collect on the underside of the discs and the bowl wall (figure 1.10).

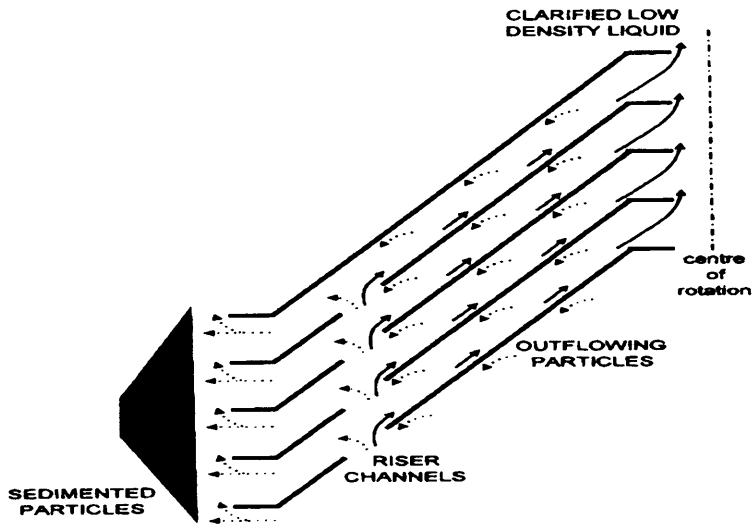

Figure 1.10 Disc stack centrifugation

This configuration provides a large settling area and constant flow path, which unlike tubular bowl centrifuges, is not reduced by the previously separated solids (Atkinson, et al. 1987). The flow between the discs is usually laminar, which makes particle settling easier and reduces the settling distance (Axelsson, 1985). Solids discharge is achieved using a hydraulic bowl opening mechanism.

Important factors which affect the performance of the centrifuge are:

- The properties of the material being separated
- The centrifuge design and operating conditions

1.3.3 Recovery of biological solids

Centrifuges encounter some problems during the recovery of biological solids. These are mainly caused by small particle size, a low density difference between phases and shear or denaturation at air liquid interfaces.

Separating cells

A low density difference and high viscosity lead to separation difficulties. These are amplified by the small size of some cells. Bacteria range between 1μm and 3μm, yeast range between 4μm and 8μm and fungi are bigger still, although fungi are easily sheared and so recovery is not necessarily easier.

Cell debris

Cells are mainly disrupted by either homogenisation or by a bead mill in order to release intracellular proteins. Removal of the debris produced by these operations is difficult due to, for example, the presence of DNA or the small size of the debris (Bonnerjea, 1988) but it is very important. For example, affinity chromatography is a high resolution operation but the column is easily fouled, so cell debris is usually removed before this step. Homogenisation of cells also results in debris with a broad size distribution; some particles may be less than 0.2μm. This can cause problems.

Precipitates

As discussed in section 1.3.1 the density and size of precipitate particles depend on the protein, the precipitant and the system (Bell and Dunnill, 1982a & b). Typically precipitate particles range in size from 5μm to 25μm, although some can be as small as 1μm (Clarkson, et al. 1993a). The density difference between phases is usually in the order of $10kgm^{-3}$ to $150kgm^{-3}$ therefore a low flow rate may be required. This will result in an increase in the temperature of the feed stream unless the centrifuge has bowl cooling. Other problems are due to the

nature of proteins, which cause foaming and air entrapment. This causes low settling velocities and denaturation. High shear stresses in the feed zone also cause precipitates to break-up (Boychyn, et al. 2001; Neal, et al. 2003).

Once separated, solid material must be discharged from the bowl. The disc stack, scroll and Carr powerfuge are the only models with automated discharge. In the other models the collected solids have to be removed manually. Maybury (1999) states that feed rates calculated theoretically are higher than in practice, due to hindered settling which occurs in process streams with a high percentage of solids. For process streams containing 0-2 percent of solids (v/v) two thirds the predicted flow should be used and for 5 percent solids half the predicted flow rate should be used (Clarkson, et al. 1993b). The percentage solids content is very important when choosing which centrifuge to utilise, since only certain centrifuges can handle certain solids load. Figure 1.11 (Brunner and Hemfort, 1988) illustrates which centrifuges can handle what solids concentration.

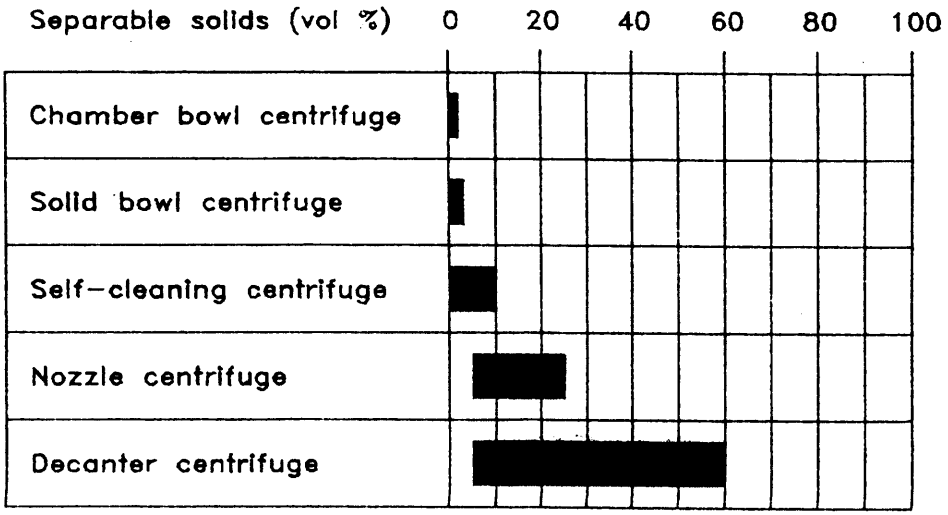

Figure 1.11 Guide to suitable centrifuge design with respect to feed solids concentration (Brumner and Hemfort, 1988)

1.3.4 Sigma theory

The Σ concept is the most commonly used quantity to characterise centrifuges, it was presented by Ambler (1952 and 1959). In his derivation he considered particles with a critical diameter that were separated to 50 percent. Today however the most commonly used definition of the critical diameter (d_c) is a particle that is separated to 100 percent. This does not influence the formulas for the sigma value but the value for the feed flow rate (Q) will be halved. Σ is defined as:

$$Q_{theor} = V_g . \Sigma$$

(equation 1.7)

Where, V_g is stokes settling velocity

Σ has the general expression:

$$\Sigma = \frac{V\omega^2 r_e}{g s_e}$$

(equation 1.8)

The equation for critical diameter becomes

$$d_c = \left(\frac{18\mu Q_{theor}}{(P_p - P_l)} \cdot \frac{s_e}{V\omega^2 r_e} \right)^{1/2}$$

$$= \left(\frac{18\mu Q_{theor}}{\Sigma (P_p - P_l) g} \right)^{1/2}$$

(equation 1.9)

Where, μ is the dynamic viscosity of fluid, P_p is the particle density, P_l is the liquid density, s_e is the equivalent settling distance, g is gravity V is volume, ω is angular velocity and r_e is the equivalent min and max radius.

The derivation in equation 1.9 assumes the following:

- Viscous drag is determining particle movement
- The flow in disc bowls between the discs is laminar and symmetrical
- The liquid rotates at the same speed as the bowl
- There is no hindered settling
- The particle always moves at its final settling velocity

Sigma theory allows a centrifuge to be described in terms of a separation area and is independent of process parameters. The sigma value indicates the required area of a gravity settling tank, with the same clarifying capacity as the centrifuge, under the same conditions. Sigma is used as an index to compare the performance of a centrifuge during scale up and between centrifuges of different types. Protherics PLC disc stack centrifuge has a sigma value of $8400m^2$.

The information detailed within this section indicates that in order to mimic a centrifuge the settling conditions need to be maintained and the shear conditions recreated.

1.3.5 Filtration

Filtration is a vacuum or pressure driven process that separates the components of a feed stream. Separation is based on size differences rather than density differences, through the use of a selectively permeable membrane. This is of particular importance in certain situations where centrifugation is not applicable i.e. where there is only a small density difference between components. Cheryan, et al. (1988) contains an excellent review on the reasons for choosing filtration. Over the past two decades there have been significant advances in membrane technology, such as increased control of pore size distribution, driven by the need for increasingly pure pharmaceutical products. Separation technology has reached the stage now where it is no-longer limited to the separation of solutes differing in size by about ten fold (Van Reis, et al. 1997). As such, filtration is increasingly

becoming an attractive process option for applications which would have traditionally utilised centrifugation.

Membrane filtration has several applications within the bioprocess industry. These include:

- Cell harvesting/recycling
- Cell removal
- Debris removal
- Product sterilisation

During filtration the feed stream is either pumped perpendicular to the membrane or parallel to it. Figure 1.12 depicts the two differing modes of operation. If the feed is pumped perpendicular to the membrane, then the operation is termed normal flow filtration (NFF) or dead end filtration. During this type of operation a layer of particles builds up on the surface of the membrane. This is termed the cake. This cake blocks the membrane pores and forms a barrier to filtration, in effect fouling the membrane. This results in a decrease in the observed flux rate through the membrane as the operation progresses. If the flux rate is to be maintained, then the pressure will have to be altered to compensate for the fouling caused by the cake.

If the feed stream is pumped parallel to the surface of the membrane then the operation is termed tangential flow filtration (TFF). TFF utilises high flow rates to generate shear forces at the membrane surface. These act to "sweep" the surface of the membrane clear of particles, thereby helping to reduce cake formation and prolong higher flux rates.

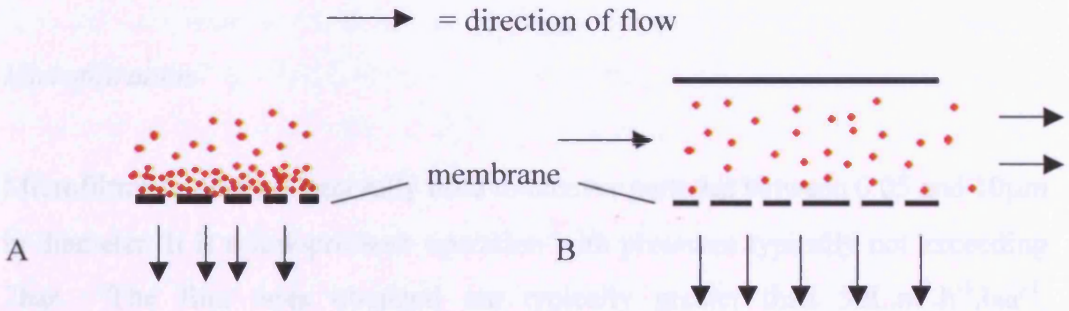

Figure 1.12 Diagrammatic representation of Dead end filtration (A) and Tangential flow filtration (B)

The stirred cell depicted in figure 1.13 is a dead end filtration process that utilises a stirrer bar placed close to the surface of the membrane. When spinning, the stirrer bar will generate a shear field, without having to utilise a high flow rate. These devices have been successfully used to increase the flux rate for a given filtration system, but have not found widespread use in industry due to problems during scale up. Lee, et al. (1995) utilised a stirred cell for the concentration of recombinant yeast cells. The results showed that flux increased with disc rotation speed. The author attributed this to the fact that at higher speeds the observed cake build up was minimal and hence membrane fouling was reduced. Vogel and Kroner (1999) also utilised a stirred cell to develop a novel technique for the separation of animal cells.

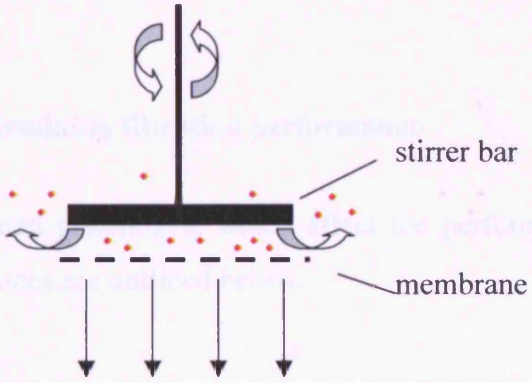

Figure 1.13 Diagrammatic representation of the stirred cell filtration device

Filtration processes are normally classified according to the dimensions of the membrane pores and the size of the material to be separated.

Microfiltration

Microfiltration (MF) is generally used to recover particles between 0.05 and 10μm in diameter. It is a low-pressure operation with pressures typically not exceeding 2bar. The flux rates obtained are typically greater than $50L.m^2.h^{-1}.bar^{-1}$. Examples of material removed by MF processes include bacteria, moulds and yeast (Winston Ho and Sirkar, 1992). Microfiltration operations can be run in several ways. Which one is chosen depends upon the nature of the feed stream. They include, batch, fed-batch, feed and bleed, continuous and diafiltration.

Ultrafiltration

Ultrafiltration (UF) relies on the same principles as microfiltration, but is generally used during the recovery of particles and polymeric solutes between 10 and 150kDa. It is high pressure operation and may be run utilising pressures as high as 5bar. The flux rates obtained are typically between 10 and $50L.m^2.h^{-1}.bar^{-1}$. One of the most common uses for UF is during diafiltration, when one buffer liquid is replaced by another. The membrane retains the protein of interest, whilst the old buffer flows to waste new buffer is added to system gradually replacing the old. UF is also used to concentrate solutions by decreasing the volume of a process solution (Winston Ho and Sirkar, 1992).

1.3.5.1 Factors determining filtration performance

There are several feed related parameters, which affect the performance of the filtration process; the main ones are outlined below.

Buffer composition

The pH and ionic strength of the buffering solution can greatly influence the performance of the filtration process. By altering a proteins surface charge, the solubility of the protein may be affected. At its iso-electric point a protein will have no net charge. As a result, the degree of adsorption of the protein into the surface of the membrane will be increased (Bowen and Gan, 1991; Hanemaaijer, et al. 1989). It has also been observed that a maximum transmission is achieved at the protein's iso-electric point, with a second maximum between the protein and the membrane's iso-electric point (Burns and Zydney, 1999).

Particle properties

The shape and compressibility of feed stream components will influence the filtration. The compressibility of a particle will affect the nature of the cake layer formed and impact on performance. The shape of the particle will determine the void volume within the bed, which again influences the flux rate. Of particular importance is the size difference between solutes; this will determine the degree of separation achievable.

Viscosity

The viscosity of the feed stream determines its resistance to flow; an increase in viscosity results in lower flow rates and higher pressures to obtain an equivalent flux rate.

Temperature

The temperature of the solution can affect the flux in two ways (Kroner, et al. 1984). Increasing the temperature can lead to protein aggregation and hence an increase in fouling with concurrent decrease in flux. Increasing the temperature will also decrease the viscosity. This will result in an increase in flux if all other parameters remain unchanged (Kroner, et al. 1984; Lojkine, et al. 1992).

1.3.5.2 System related factors

Operating mode

The actual physical membrane is rarely the true filtering medium. In reality the true filtering medium is the initial thin layer of precipitate that forms on the surface of the membrane at the start of the operation. A consequence of this is that this initial layer is of prime importance in ensuring a satisfactory filtration operation.

If full pressure is applied at the start of the process, as is the case with constant pressure filtration where the flux is allowed to decline over time, then the first layer of particles will be compacted into a tight mass that largely blocks the pores of the filter. This may result in a low flux rate for the rest of the filtration. If the initial pressure is low, as in constant flux filtration, the initial precipitate layer will be open resulting in increased flux rates during the filtration. During constant flux filtration, the pressure is gradually increased in order to maintain the flux rate throughout the process. A draw back of this is that the maximum pressure is applied only at the end of the process so the whole cycle is run at less than maximum capacity. Studies by Field et al, (1995) and Howell (1995), have suggested that operating in constant flux mode will result in higher flux rates and hence a better performing separation operation.

The advantages and disadvantages of the two types of operation depend to a large degree on the nature of the feed. If the particles are compressible then increasing the pressure may not necessarily result in an increase in the flux rate. With a compressible cake, as the pressure is increased so the resistance of the cake increases. Eventually the increase in the resistance of the cake to flow becomes more than the increase in the flow rate caused by the increase in pressure. At this point further increases in pressure will have no effect and may even result in a decrease in flux.

Process configuration

The membrane separation may be run in a number of different modes. The most common configurations are diafiltration, batch concentration and feed and bleed (Winston Ho and Sirkar, 1992). Each configuration has its own advantages and disadvantages. Which one is used depends on the feed stream and process requirements.

During diafiltration, buffer is added to the retentate tank as the process continues in order to replace any permeate that has been removed. Diafiltration helps to overcome the low fluxes associated with high concentrations or to achieve greater removal of permeable species.

Batch concentration requires the minimum membrane area and is the most flexible. However, tank volume requirements may be high, the equipment may have a large footprint and the residence time can be excessive. As the permeate is removed the concentration of retained species increases. This is particularly useful when dealing with large process volumes, as the volume of feed can be reduced.

During a feed and bleed process the permeate is removed as is a small portion of the retentate. The remaining retentate is passed on to a fresh filter for further concentration; this helps to maintain a high crossflow velocity and reduce membrane fouling.

1.3.5.3 Transmembrane pressure

Increasing the pressure on the upstream side of the membrane, with reference to the downstream side, results in process fluid being forced through the membrane. The difference in pressure between the two sides of the membrane is known as transmembrane pressure (TMP) and for TFF is defined as:

$$TMP = \frac{P_1 + P_2}{2} - P_3$$

(equation 1.10)

Where P_1 is the feed inlet pressure, P_2 is the retentate outlet pressure and P_3 is the permeate outlet pressure.

During the filtration process any material retained by the membrane may be deposited on the surface. This phenomenon is called concentration polarisation. At the same time that material is deposited it is also removed by back transport mechanisms (proposed mechanisms include Brownian motion, inertial lift and shear enhanced diffusion). As TMP is increased the rate of solute convection towards the membrane will increase. Eventually this rate will exceed the rate of back transport. At this point the flux rate will be unchanged by further increases in the TMP; the membrane is said to be concentration polarised. Porter (1972) first noticed this phenomenon during UF it has also been observed during MF (Brown and Kavanagh, 1987; Shimizu, et al. 1994).

Operating at an initial higher TMP may give a higher initial flux rate but it may lead to lower flux and transmission performance as polarisation and other fouling effects will be increased (Lee, et al. 1995; Haarstrick, et al. 1991; Field, et al. 1995). If a lower TMP is used initially it is often possible to operate the process for longer periods of time without a significant decline in the flux rate. The TMP can then be gradually increased to maintain the flux as fouling occurs (Maiorella, et al. 1991; Van Reis, et al. 1991).

1.3.5.4 Crossflow velocity

The pumping of the feed stream parallel to the surface of the membrane generates shear stress that acts to sweep the membrane, minimising the build up of any fouling layer. Increasing the crossflow velocity will increase the rate of back transport, increasing the flux rate achievable for a given TMP. This removal of

the fouling layer by crossflow has been demonstrated by a number of researchers (Culkin, 1998; Mikulasek, 1994). Crossflow velocity cannot however be increased indefinitely in order to increase the flux rate. For one, the crossflow velocity has no impact on the degree of internal fouling, which occurs within the structure of the membrane and determines transmission. Also higher flow velocities require bigger pumps and higher energy consumptions, which impacts on the economics of the process.

1.3.5.5 Fouling

The term fouling is used to describe any phenomenon that is detrimental to a membranes performance. Fouling can take several different forms, the simplest of which is pore plugging.

Figure 1.14 Representation of pore plugging

This results when a particle is sufficiently small to enter a pore but does not pass through it (Hermia, 1982).

Pore narrowing or constriction is caused by the adsorption of proteins to the membrane.

Figure 1.15 Representation of pore narrowing or constriction

The pores become smaller and it may result in the smallest pores becoming blocked. Each particle that is retained within the pore will reduce the pore volume.

The equation below is used to describe systems where pore plugging is the main method of fouling.

$$\frac{t}{V} = K_2\left(\frac{t}{2}\right) + \frac{1}{F_o}$$

(equation 1.11)

Where F_0 is the initial flux rate, K_2 is an empirical constant obtained from experimental data, t is time and V is the volume filtered. If pore plugging is the main mode of fouling then a plot of t/V versus t should produce a straight line where the gradient is $K_2/2$ and the intercept is $1/F_0$ (Jornitz and Metzler, 1988).

Gel or cake layer formation results in a decrease in flux due to irreversible accumulation of particles at the membranes surface. The thickness of the layer increases as the volume of filtered fluid increases.

Figure 1.16 Representation of gel or cake layer formation

Assuming that the cake is incompressible and that the pressure is constant the filtration should follow the equation outlined below (Jornitz and Meltzer, 1988).

$$\frac{t}{V} = K_1\left(\frac{V}{2}\right) + \frac{1}{F_o}$$

(equation 1.12)

Where t is time, V is the volume filtered and K_1 is another empirical constant obtained from experimental data.

If surface retention is the primary method of fouling, then a plot of t/V versus V should result in a straight line where the gradient is K_1 and the intercept is V. This model is not ideal for biological solutions because often the solids are compressible.

The hydrophobicity/hydrophilicity of the particle or membrane are key characteristics in determining these interactions. The type of membrane will also affect the type of fouling. Marshall, et al. (1993) concluded that proteins reduce the performance of UF membranes by surface deposition in the form of a gel layer but during MF the main mechanism of fouling was found to be pore plugging. It has also been suggested that the mechanism of fouling is influenced by the concentration of the feed stream. Pore plugging is the main factor at dilute concentrations but surface deposition dominates at high concentrations.

Manufacturers of membranes have developed a wide range of products with different properties in order to combat fouling. There are also several commercial systems available which use mechanical methods to decrease fouling. JP. Postlethwaite (2004) contains a good review of these systems (Postlewaite, et al. 2004).

1.3.5.6 Models of flux prediction

Concentration polarisation model

Porter (1972) proposed that the permeate flux can be predicted from the following model.

$$J = K\left(\ln\frac{C_w}{C_b}\right)$$

(equation 1.13)

Where J is the flux, K is the mass transfer coefficient, C_w is the wall concentration of protein, C_b is the bulk concentration of protein in the feed stream.

This model was developed based on the assumption that a boundary layer or gel layer of high concentration solutes builds up on the membrane surface and that this layer forms the limiting resistance to flow. From this, it is possible to calculate the transport rate of water through the membrane on the basis of the mass transfer of membrane retained solutes from the surface back into the bulk stream. Porter (1972) assumes that the layer has a fixed concentration (C_g) but is free to vary in terms of thickness and porosity.

The mass transfer coefficient (K) can be calculated using the heat transfer correlation described by Dittus and Boelter (1930).

$$K = k_p\left(\frac{Q}{bwL}\right)^{0.5}\frac{D^{0.66}}{V^{0.17}}$$

(equation 1.14)

Where k_p is the proportionality constant, Q is the volumetric flowrate, D is the diffusion coefficient, b is the channel height, w is the channel width, L is the channel length and V is the kinematic viscosity of the broth.

The diffusion coefficient is described by the Stokes-Einstein relationship for diffusity.

$$D = \frac{K_b T}{6\pi\mu r_p}$$

(equation 1.15)

Where K_b is the boltzman constant, T is the temperature, μ is the viscosity and r_p is the radius of the diffusing particle.

Assuming that the proteins at the membrane surface resemble a layer of closely packed spheres having 65-75% solids by volume, the experimental values to calculate k_p can be used to predict the steady state permeate flux.

This theory has been utilised by many researchers (Wakeman and Williams, 2002; Mignard and Glass, 2001) whilst attempting to predict membrane flux and fouling.

Membrane fouling model

This theory assumes that the molecules from the feed stream plug the membrane pores. The resulting hydrodynamic resistance can be used to predict flux based on the following equation.

$$J = \frac{\Delta P_{TM}}{\mu R_t}$$

(equation 1.16)

Where R_t is the total hydrodynamic resistance defined for a given membrane and a pure solvent (water).

According to Davies, et al. (2000) R_t can be defined as the sum of the membrane resistance (R_m) the cake resistance (R_c) and the resistance due to pore blockage (R_b). Davies, et al. (2000) goes on to state that membrane resistance can be measured using pure water flux data.

If using pure water as the feed, the flux equation can be rewritten:

$$J = \frac{\Delta P_{TM}}{\mu R_m}$$

(equation 1.17)

The resistance of the membrane can then be calculated from a plot of flux against ΔP_{TM} with the gradient equalling $1/R_m\mu$.

1.3.6 Chromatography

Separation by chromatographic means generally exploits a facet of the protein of interests unique physio-chemical properties. These properties include: size (size exclusion/gel filtration), charge (ion exchange), hydrophobicity (hydrophobic interaction) and bio-specific interactions (affinity). Ion exchange is used in 75% of purification processes (Bonnerjea, et al. 1986). This wide spread use was attributed to the ease of scale up, the wide availability of cost efficient, robust matrixes and the acceptance of the technique by regulatory bodies. Affinity chromatography was found to be used in 60% of processes and gel filtration in 50% of processes. Chromatographic systems can achieve an excellent level of purification in a small number of steps. They are also apt for dealing with large volumes of material containing only small concentrations of the target protein. The different types of ligand are described in the following sections.

1.3.6.1 Ion Exchange Chromatography

Ion exchange chromatography has found wide spread use for the purification of proteins, both in the lab and in the production plant. In 1956 it became the first type of interaction to be successfully employed for the separation of charged macromolecules onto oppositely charged moieties (Peterson and Sobers, 1956). This technique has also been employed for the purification and separation of proteins, nucleic acids, polypeptides, polynucleotides and other charged molecules (Bonnerjea, et al. 1986).

Separation during ion exchange chromatography is dependent on the reversible binding of charged solute molecules to an immobilised matrix consisting of oppositely charged groups. There are two types of exchanger: anion exchangers are positively charged and bind negatively charged molecules and cation exchangers that are negatively charged and bind positively charged molecules.

Separation is achieved by giving either the target protein or the main contaminants an opposite charge to the matrix. The protein(s) of interest will then be retained by the solid support whilst all other proteins flow out. This selective charge is obtained by looking at a proteins iso-electric point. Above its iso-electric point the protein will have a net negative charge, below it the protein will have a net positive charge. Once the protein of interest is bound to the matrix unbound proteins are washed away by applying the starting buffer. Elution is achieved by changing either the pH or the ionic strength. The protein of interest will elute from the matrix and can be collected.

There has been extensive research into ion-exchange chromatography including the development of new media, modelling of column dynamics/retention characteristics, process characteristics and process scale up (Lin, et al. 1987; Regnier, 1984; Scopes, 1981; Velayudban and Horvath, 1988; Wankat, 1986; Yamamoto, et al. 1983). The major disadvantage of ion-exchange chromatography is that it is not as specific as affinity chromatography as more than one species of protein may bind to the matrix at the same time.

1.3.6.2 Affinity Chromatography

Affinity chromatography is considered to be the most specific separation technology currently available. It exploits the unique binding characteristics inherent to a ligand-biomacromolecule interaction. Since the technology relies on biological recognition rather than physio-cheimcal interactions affinity chromatography preserves the biological activity of the target protein.

Affinity chromatography is a type of adsorption chromatography in which the molecule to be purified is specifically and most importantly reversibly adsorbed by a complementary binding substance immobilised on an insoluble support, the matrix.

The technique was first utilised in 1910 to selectively adsorb Amylase onto insoluble starch. However the complex organic chemistry required to produce the matrix prevented widespread use of the technique. In 1967 Axen, Porath and Ernback (Axon, et al. 1967) reported that molecules containing primary amino groups could be coupled to polysaccharide matrices activated by cyanogen bromide. This method is still commonly used today to couple ligands to the matrix. Its development opened the way for the widespread use of affinity chromatography.

Advances in technology have resulted in the development of new media, with increased stability in high or low pH and increased binding capacity which lowers the cost. Verdoliva, et al. (2002) reports the development of an all D synthetic peptide with higher binding capacities than protein A or G and very high stability in terms of ligand leakage and stability. Gulich, et al. (2002) reports the development of a genetically engineered version of protein G which has increased alkaline stability. Therefore columns utilising this ligand can be cleaned with sodium hydroxide, which standard protein G columns cannot be.

Process scale affinity chromatography

Process scale matrices need to fulfil certain criteria (Cabrera and Wilchek, 1988; Janson and Kristiansen, 1990). The perfect resin would be:

Inert, non-biodegradable, chemically and physically resistant, easily derivatized, easily packed and macroporous. However by their very nature, most protein affinity columns are biodegradable, chemically and physically unstable and deform at high flow rates.

The three most important characteristics are high adsorption capacity, high mass transfer coefficient and high liquid flow rate through the bed (Katoh, 1987). From a commercial point of view cost, reuse or ligand leakage and the purity of the eluted product are also equally important.

The optimisation and scale up of chromatographic processes

In order to successfully scale up an affinity chromatographic separation a thorough understanding of the fundamental processes involved in the separation mechanism are required. Liapis, 1989; Chase, 1988 and McCormick, 1988 contain reviews of scale up methodology. The authors also address the predictions, implications and limitations of the affinity chromatography models.

Column and matrix based parameters to consider are: the length and diameter of the column, the particle size and pore size of the affinity support. Small-scale studies should be carried out utilising a matrix that is suitable for large-scale separations. Physical properties that should be considered are: the sample volume, flow rates, temperature and pH (Liapis, 1989). Since each separation is unique each process must be individually optimised. However several groups are developing algorithms to predict the optimum flow rates, gradients, buffer compositions and temperatures (Janson and Hedman, 1987).

Affinity ligands

Any component that may be coupled to a base matrix can be used as a ligand for purifying its respective binding substance i.e.

Enzyme: Substrate
Antibody: Antigen
Hormone: Receptor

This list contains only three possible ligands. Narayanan (1994) contains a good review of the available ligands and matrices. Protein G is of specific interest in the context of this thesis (as opposed to protein A) because of its affinity for ovine antibodies. It is therefore applicable to the purification of the anti-venom antibodies contained with the ovine serum.

Protein G

Protein G (Akerstrom, et al. 1985; Frank, 1997; McCormick, 1988; Akerstrom and Bjorck, 1986) is a bacterial surface protein found in group G *streptococcal* strains (Forsgen and Sjoquist, 1966; Reis, et al. 1984). It recognises and binds to the Fc part of a wide variety of IgG antibodies:

IgG type	Binding Strength	IgG type	Binding Strength
Human IgG1	++	Rat IgG2c	++
Human IgG2	++	Rabbit IgG	++
Human IgG3	++	Bovine IgG1	++
Human IgG4	++	Bovine IgG2	++
Mouse IgG1	+	Sheep IgG1	++
Mouse IgG2a	++	Sheep IgG2	++
Mouse IgG2b	++	Goat IgG1	++
Mouse IgG3	++	Goat IgG2	++
Rat IgG1	+	Horse IgG(ab)	++
Rat IgG2a	++	Horse IgG(c)	++
Rat IgG2b	+	Horse IgG(T)	(+)

Table 1.2 Summary of different antibody subtype binding patterns to protein G (adapted from Bjorrck and Kronvall, 1984)

Protein G will bind most strongly to the majority of different immunoglobulin types, at or near neutral pH, but readily dissociates from these solutes when placed in a buffer with a lower pH. The native protein contains an albumin binding region. This is genetically deleted in modern versions of protein G used for binding immunoglobulins in order to minimise non-specific binding.

1.3.6.3 Gel filtration

Gel filtration has occupied a key position in laboratory scale purification for more than 30 years (Porath and Flodin, 1959; Janson, 1987). Separation of molecules during gel filtration is based on molecular size and shape. The solution containing molecules of differing sizes is fed down a column containing a hydrophilic cross-linked gel with pores of finite size. By varying the degree of cross-linking within the gel, different pore sizes can be produced resulting in media that covers the whole range of molecular sizes.

Molecules which are larger than the pore size of the gel will be excluded from the matrix and are therefore eluted first from the column. Smaller molecules will enter the pores within the gel to various extents. This retards their progress through the column and they will elute according to their molecular size (largest first).

Gel filtration is not suitable for recovery of target proteins present in only relatively small concentrations since load volumes should not exceed 10% of the column volume. It is also not suitable for large-scale recovery due to the large volumes of gel required for large process volumes. As a result gel filtration is often employed towards the end of a process as a polishing step and within the biopharmaceutical industry to remove aggregates.

1.3.6.4 Hydrophobic Interaction Chromatography

The basis of hydrophobic interaction chromatography (HIC) is an entropy driven attraction between non-polar groups in an aqueous environment; the specifics are summarised in (Eriksson, 1998). It has been described as "The unusually strong attraction between non-polar molecules and surfaces in water" (Israelachvili, 1985). Chromatographic separation of proteins by HIC were first reported separately by two groups in 1972 (Er-El, et al. 1972; Yon, 1972).

The separation is normally run at high salt concentrations. Hydrophobic pockets on the surface of proteins adsorb onto the support. The protein is eluted by lowering the salt concentration. Proteins with high surface hydrophobicity will elute first (Hammond and Scawen, 1989). Typically HIC is classified as a mild separation technique, as proteins can be eluted from the support in their native state. However, it has not found wide spread use in industry due to the fact that "classical commercial hydrophobic adsorbents are inadequate due to their high hydrophobicity" (Oscarsson et al 1995). As a result proteins readily bind to the support but they are difficult to elute in their native state because the binding is too strong. However, it has been successfully employed during the purification of periplasmic human interferon α2c expressed in E.coli (Voss, et al. 1994) and human growth hormone (Wu, et al. 1990; Pavlu & Gellerfors, 1993).

1.3.6.5 Adsorption Models

The simplest model used to describe the adsorption process that occurs during chromatography assumes that the solute (S) confined within the aqueous phase (aq) is adsorbed by the ligand (L) of a solid chromatography matrix. The equation shown below describes this adsorption process:

$$S(aq) + L(s) \underset{k_2}{\overset{k_1}{\rightleftharpoons}} S - L(s)$$

(equation 1.18)

The rate at which the solute will be adsorbed by the ligand is governed by an association constant K_A, ($K_A = K_1/K_2$) where $K_1$is the forward rate constant and K_2 is the backward rate constant. The disassociation constant $K_D = 1/K_A$.

K_A can be calculated from the equation detailed below:

$$C_S = \frac{C_M q_m}{C_M + K_D} = \frac{C_M q_m K_A}{C_M K_A + 1}$$

(equation 1.19)

Where C_S is the concentration of adsorbed solute at equilibrium, C_M is the concentration of solute in the mobile phase and q_m is the maximum monolayer capacity of the matrix.

Isotherms

Rearranging equation 1.19 forms equation 1.20 shown below:

$$K_A = \frac{[S-L^*]}{[S^*][L^*]} = \frac{C_S}{C_M(q_m - C_S)}$$

(equation 1.20)

It can be concluded from this equation that the concentration of adsorbed solute is asymptotically approaching the maximum capacity of the matrix. This will be reached at lower mobile phase concentrations for solutes that have a higher association constant. It can therefore be concluded that buffering conditions which increase the association constant will lead to more of the solute that binds to the matrix being bound, resulting in a more efficient separation process. The graph resulting from a plot of the concentration of bound solute (C_S) against the concentration of solute in the mobile phase (C_M) is called the adsorption isotherm.

The relationship shown in figure 1.17 is called Langmuir isotherm (Langmuir, 1918).

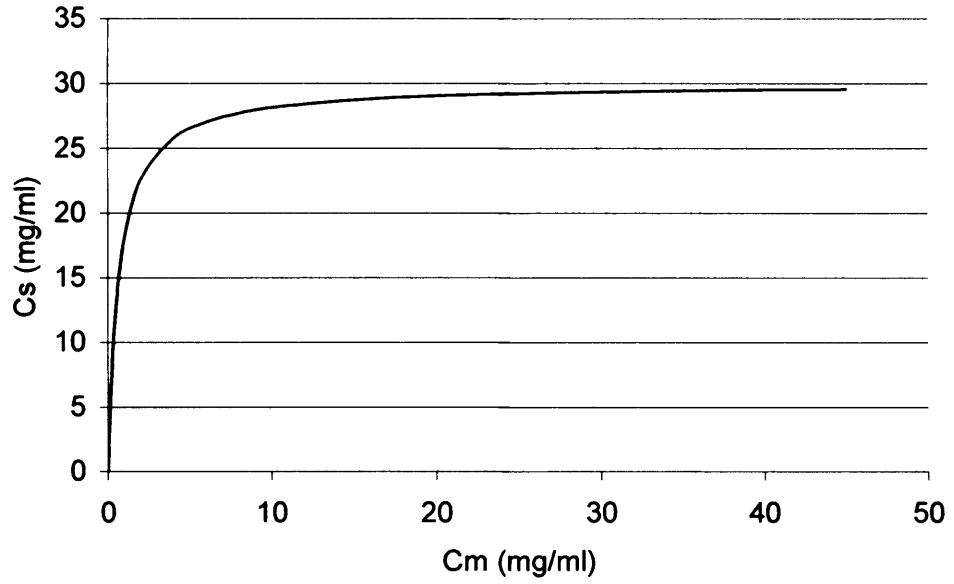

Figure 1.17 Hypothetical Langmuirian adsorption isotherm

The Langmuir model was originally developed to portray the chemisorption on a set of distinct localised adsorption sites. As a result it is only valid for monolayer adsorption of a single solute species in a one to one binding relationship, which is not affected by the presence of other solutes. Generally adsorption of proteins onto ion-exchangers or affinity media is of a form similar to the favourable model described by Langmuir (Horstmann and Chase, 1989; Skidmore and Chase, 1988). Langmuir isotherms have been successfully employed on several occasions (Weaver and Carta, 1996; Chase, 1984; Skidmore, et al. 1990; Yoshida, et al. 1993; Mao, et al. 1995). Deviations from the model can be explained by contaminating proteins competing for binding sites or proteins binding to the matrix by other means. These deviations are discussed by (Gill, et al. 1994).

A multi-component mixture may be described by the multi-component Langmuir isotherm.

$$C_{S,i} = \frac{C_{M,i} K_{A,i} q_{m,i}}{1 + \sum C_{M,J} K_{A,J}}$$

(equation 1.21)

Several other isotherms have been developed to account for different conditions. For instance, the Freundlich isotherm (Freundlich, 1907) describes adsorption to a heterogeneous surface. The flow rate through a column and its impact on residence time will also affect the isotherm. A good review discussing the various merits of the different isotherms can be found in Bellot and Condoret (1993).

1.4 Scale Down Of Industrial Bio-Separation Techniques

Early bioprocess development is often hampered by the availability of material for experiments investigating different downstream processing options. The production of laboratory scale devices that accurately mimic industrial scale purification processes allows options to be considered with out the use of large amounts of valuable material. It also provides a powerful tool for minimising bioprocess development times.

Successful scale down requires a detailed understanding of the mechanisms involved in order to identify the key parameters influencing a system. Once identified, these parameters can be mimicked on a small scale thereby ensuring an accurate model.

1.4.1 Current approach to the scale down of precipitation

As described in section 1.3.1 the physical properties of a protein precipitate are affected by several factors. Each of these have to be maintained or taken into account in order to obtain a final product with similar characteristics to that produced on an industrial scale.

Mechanical parameters, which have to be kept constant between the scale down mimic and the industrial scale operation, include:

- Tank geometry (the height to diameter ratio)
- Impeller type
- Diameter of the impeller relative to that of the tank
- Placement of the impeller
- Baffle geometry (if any)

However, even if all of the above factors are kept constant fluid flow patterns will still alter between the small and industrial scale devices, which could result in differences between the final material.

Process parameters that need to be maintained include:

- Temperature of operation
- pH
- Ionic strength
- Type of salt
- Mean velocity gradient, aging parameter (Camp number) and residence time

The mean velocity gradient is a measurement of the power dissipated (P) per unit volume (Smoluchowski, 1917).

$$\overline{G} = \left(\frac{P}{V\mu}\right)^{\frac{1}{2}}$$

(equation 1.22)

Where μ equals dynamic viscosity, V is the volume and P is the power input.

The power input, P, is calculated by:

$$P = P_0 p N^3 D^5$$

(equation 1.23)

Where P_0 is the power number, p is the density of the bulk suspension, N the impeller speed and D is the impeller diameter (Rushton, et al. 1950).

The controlling parameter of a precipitation operation is the Camp number; this is a measurement of the amount of energy inputted into a system over time and is defined by the equation below.

$$Ca = Gt$$

(equation 1.24)

Where G is the mean velocity gradient and t is time.

By maintaining the Camp number between scales of operation it is possible to mimic a precipitation operation. This has been successfully achieved for protein precipitant formation (Boychyn, et al. 2000; Maybury, 1999; Neal, et al. 2003).

1.4.2 Scale down of centrifugation

The scale down of centrifugation has been achieved through two different methods (Mannweiler and Hoare, 1992; Boychyn, et al. 2000). The first involves the insertion of blank discs into a disc stack centrifuge in order to reduce the feed flow requirement. The second involves the utilisation of an in house shearing device. Each method will be discussed separately.

1.4.2.1 Scaling down by reducing the number of active discs

The smallest disc stack centrifuge is a pilot scale model that operates with a bowl capacity of 0.69 litres. This means that in order to run the centrifuge more than 10 litres of feed material are required. During the early stages of process development the amount of material available for study is small. By scaling down

the amounts required for centrifugation studies the purification process can be more extensively studied and alterations made without the need for large amounts of valuable material.

Work by Mannweiler and Hoare (1992), Rumpus (1997) and Maybury (1999) concentrated on scaling down a disc stack centrifuge by reducing the number of active discs. Maybury, et al. (1998) achieved a 76% scale down of the settling area in conjunction with a 70% reduction in bowl volume whilst still maintaining a separation performance that matched that of the full-scale machine. The reduction in feed requirements was achieved by blanking off the stack; this was done by utilising stainless steel inserts specially made by Westfalia separators. These inserts reduced the number of active discs, therefore reducing the separation area, bowl volume and solids holding capacity. There are two different types of insert. The top inserts reduce the bowl volume and solids holding space, whilst a bottom insert reduces the bowl volume and lifts the stack off the bottom of the centrifuge.

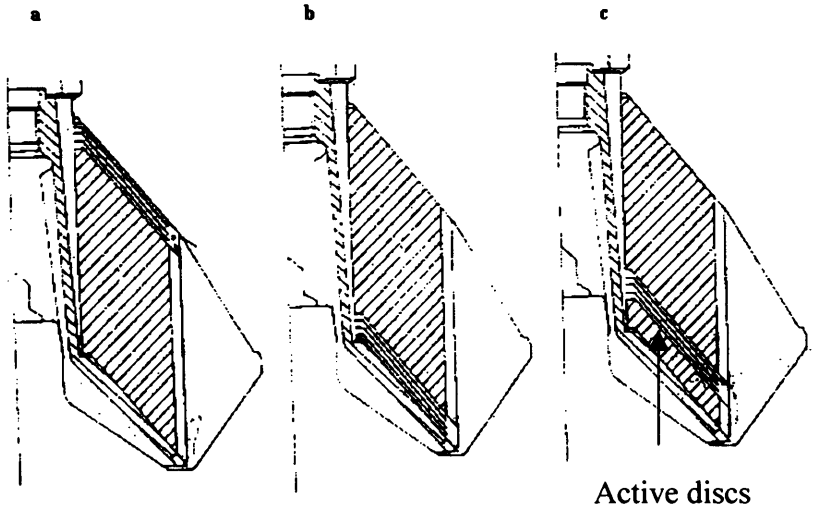

Figure 1.18 Diagrammatic representation of a disc stack centrifuge showing different regions blanked out. a) Top position b) Bottom position c) On top of insert equivalent to 7 discs (Maybury, et al. 1998)

Work by Maybury, et al. (1998) highlighted the importance of the positioning of the active discs within the stack. If the active discs are positioned at the bottom, the recovery performance was found to be inferior to the full-scale machine. This was attributed to turbulence associated with the region of the centrifuge where the feed stream enters the settling region resulting in re-entrapment of sedimented solids. Positioning of the active discs at the top of the stack was found to give a superior performance; this was attributed to solid particles settling out as the feed stream passed through the solids holding space before reaching the active discs. When the discs were positioned a small distance from the bottom above the turbulent region, the recovery performance was found to be similar to the full-scale machine.

Scaling down by this method changes the bowl geometry, since the bowl height is reduced whilst the diameter remains the same. Although this change may be expected to alter the recovery performance, Maybury, et al. (1998) concluded that it does not. This method has advantages in the fact that the bowl speed and diameter remain unchanged and hence dewatering of collected solid should remain the same. However this method still requires several litres of material. A more useful mimic would require only millilitres of material per run.

1.4.2.2 Scaling down using the shearing device

There are several methods for comparing the performance of centrifuges. One popular method is the Sigma or settling area based on Stokes law which describes the sedimentation of a particle in a centrifugal field (Ambler 1959). In theory, by maintaining the same flow rate (Q) to settling area (Σ) the end product should have the same clarification for all centrifuges. However correction factors must be introduced to account for non-ideal flow conditions.

Mannweiler, et al. (1989) demonstrated that the entrance zone of a centrifuge is the area where the highest flow stresses prevail. Therefore when a shear sensitive material enters the feed zone of a centrifuge, breakage of the particles occurs. This increases the proportion of fines resulting in a reduction in the clarification of the material. Within a laboratory scale batch centrifuge, this break up of process

material does not occur since the process material is still relative to the wall of the tube. This means that the laboratory centrifuge will achieve a higher degree of clarification than an industrial device, even if the flow rate to settling area is maintained between different centrifuges.

The rotating disc device works on the principle that by mimicking the feed zone of an industrial centrifuge, the sample can be sheared thus producing the same fine particles and decrease in particle size distribution as found at an industrial scale. Once sheared samples are centrifuged whilst maintaining the same relative settling area between industrial and laboratory scale centrifuge, as a result the same degree of clarification should then be observed.

The rotating disc device consists of a Perspex chamber of diameter 40mm. The rotating elements are fabricated from smooth aluminium alloy coated with a thin layer of PTFE mounted on a stainless steal shaft. The Perspex chamber is constructed of four interchangeable sections that can be arranged to give different heights from 10mm to 40mm. The shaft of the rotating elements is extended through a top cover via a relatively airtight PTFE bearing and connected to a high speed DC motor. The motor is powered by a set of trickle batteries which via a transformer, are capable of delivering a series of fixed voltages between 2 and 12 volts, thus providing six fixed speeds of rotation. The whole assembly is mounted on a heavy metal base to stop vibration whilst it is being operated. A full description can be found elsewhere (Levy, et al. 1998).

The first step in designing a device that could mimic the shear fields within the feed zone of an industrial scale centrifuge was to accurately map the complex flow fields found within an industrial scale centrifuge. Boychyn, et al. (2001) used computational fluid dynamics (CFD) coupled with a modern computer to solve the necessary equations. Therefore they provided a method where-by the complex flow field in an industrial centrifuge could be quantified. Once quantified the CFD analysis can be used to predict the speed of disc rotation that would be required to mimic the feed zone. When used in combination with a laboratory scale centrifuge, accurate predictions of the behaviour of an industrial

device can be made. This method has been validated by correlation to boundary layer theory (Schlichting, 1979, Boychyn, et al. 2001). It is however laborious and time consuming.

A less laborious method is based on maintaining a constant tip velocity between the rotating disc device and the critical structure in the feed zone of the centrifuge. The critical structure is identified as the area where initial contact and acceleration of the process stream occurs. In a disc stack machine the lock nut represents the initial point of contact for the feed suspension. Once the structure has been identified the critical radius must be selected. For the lock nut this is the radius at its top. The tip velocity can be converted into a maximum power dissipation as discussed below and this can be used to predict the performance.

The flow over a disc of radius R, rotating at an angular velocity ω, has been theoretically described by Schlichting (1979) and verified by CFD analysis (Levy, et al. 1999). The maximum power dissipation is given by:

$$\varepsilon = \frac{P}{pV} = \frac{\omega T}{pV}$$

(equation 1.25)

Where P is the power dissipation, p is the density of the bulk fluid, V is the volume of the boundary layer, ω is the angular velocity and T is the torque.

The magnitude of forces occurring in the feed zone of a continuous centrifuge may be estimated by determining the tip-velocity (V_{crit}) of the critical structure:

$$V_{crit} = r_{crit}\omega_{crit} = 2\pi N_{crit} r_{crit}$$

(equation 1.26)

Where r_{crit} is the critical radius of the structure and N_{crit} is the rotational speed. The critical velocity is then maintained in the laboratory rotating disc device, its rotational speed is determined by:

$$N_{rd} = \frac{r_{crit} N_{crit}}{r_{rd}}$$

(equation 1.27)

From this an associated maximum energy dissipation rate can be calculated.

Thus the rotating disc device can be used to mimic the feed zone of an industrial centrifuge and a batch laboratory scale centrifuge can be used to mimic the settling conditions. This provides an effective method of scaling down centrifugation so that process options can be studied using only millilitres of material.

1.5 Aims

Downstream purification process development and optimisation currently requires large quantities of material and time, commodities that are in short supply during the initial stages of drug development. Research into methods of accurately scaling down purification operations has been on going for a number of years.

The aims of this project are to develop novel or utilise current scale down methodologies in order to mimic the primary industrial scale purification stages used during the production of polyclonal Fab fragments. These mimics are to be tested by comparison to the feed stream produced at an industrial scale and used to study the effects of changes to the purification process. Alternative purification options for the removal of the precipitated antibodies such as the use of microfiltration will be investigated. Chromatographic methods for purification of the antibodies directly from the serum, without the need for precipitation or centrifugation will also be investigated. These investigations may lead to improvements in the yield or in the ease of operation of the process.

2 Materials And Methods

2.1 Introduction

Unless otherwise stated all chemicals and materials were obtained from Sigma, Poole UK. This chapter details the methods, analytical techniques and experiments that were conducted during the preparation of this thesis.

All assay variances quoted within the results sections of this thesis (standard deviations and standard errors) were calculated from the actual results.

Section 2.2 describes the design of the scale down mimics, section 2.3 describes the analytical techniques and section 2.4 describes the running of the scale down mimics and other small-scale experiments.

2.2 Application Of Existing Scale Down Theory

2.2.1 Scaled down precipitation

The application of the theories and experimental conclusions outlined in section 1.4.1 allows a large-scale precipitation reaction to be mimicked and accurately reproduced at a laboratory scale.

The first step in any scale down work is to investigate the equipment and the process used at the large scale.

2.2.1.1 Industrial scale vessel parameters and operating conditions

Table 2.1 shown below details the dimensions of the precipitation vessel used during the industrial scale precipitation operation.

Vessel height	0.6m
Vessel diameter	0.686m
Volume of liquid	200L
Construction material	Stainless steel
Impeller type	3-bladed marine propeller
Impeller diameter	0.175m
Impeller placement	Bottom corner
Height of impeller	0.20m

Table 2.1 Dimensions of the industrial scale precipitation vessel

The precipitation reaction is operated under the conditions outlined in table 2.2

Speed of impeller rotation during addition phase	125rpm
Speed of impeller rotation during conditioning phase	500rpm
Conditioning time	15 hours
Rate of addition of precipitant	4L/minute

Table 2.2 Operating parameters for the industrial scale precipitation reaction

2.2.1.2 1000 fold scale down mimic

In order to produce an accurate scale down mimic the vessel geometry and power input into the precipitation system needs to be maintained between scales.

Scale down of precipitation vessel

By maintaining vessel geometry between scales a 1000 fold scale down version of the industrial scale vessel described in the previous section was produced. It has the following dimensions, shown in table 2.3.

Vessel height	0.06m
Vessel diameter	0.0686m
Volume of liquid	0.2L
Construction material	Perspex
Impeller type	3 bladed marine propeller
Impeller diameter	0.02m
Impeller placement	Bottom middle
Height of impeller	0.02m

Table 2.3 Dimensions of the 1000 fold scaled down precipitation vessel

As can be seen there are some differences between this vessel and the industrial one, such as the material of construction. The industrial scale vessel also has a curved bottom where as the scale down vessel has a flat bottom. The main difference is in the placement of the impeller: in the scale down version the impeller is in the middle. These differences will affect the flow conditions within the reactor. However the controlling factor, which is the power input into the system, remains unchanged, which should result in an accurate mimic.

Scale down of operating conditions

In order to recreate the mixing conditions experienced by the precipitate particles during the precipitation process, the total power input into the system needs to be calculated. This is expressed as the Camp number. The first step is to calculate the power inputted into the industrial scale system. Solving equation 1.23 (shown below for reference) using the parameters from tables 2.1, 2.2 and the density experiments (described later), allows the power input into the precipitation system during the conditioning phase to be calculated.

$$P = P_0 p N^3 D^5$$

(equation 2.1)

If P_0 = 0.8 (standard power number for a three bladed marine impeller from Rushton, et al. 1950), p = 130Kgm^{-3} N = 8.3rps and D = 0.175m the resulting power input equals 9.7W.

Using equation 1.22 (shown below for reference), the power input calculated above, the volume shown in table 2.1 and the value for the viscosity deduced from experiments described later, the mean velocity gradient for the precipitation reaction can be calculated.

$$\overline{G} = \left(\frac{P}{V\mu}\right)^{\frac{1}{2}}$$

(equation 2.2)

If P = 9.7W, V = 0.2m^3 and μ = 0.0024Pa.s then the mean velocity gradient is 142.

From this the Camp number can be calculated where:

$$Ca = Gt$$

(equation 2.3)

The conditioning time is 15 hours, therefore the Camp number is 7668000s^{-1}.

The mean velocity gradient can be mimicked at the laboratory scale by calculating the power input required to achieve the level found at the industrial scale and then calculating the impeller speed required to give that power input.

Rearranging equation 2.2 to make the power input the subject gives

$$P = G^2V\mu$$

(equation 2.4)

Solving this equation where G = 142 (calculated above), V = 0.0002m^3 (from table 2.3) and μ = 0.0024Pa.s gives a power input of 0.0097W. The recalculated

power input is then inserted into equation 2.1 which has been rearranged to make the impeller speed the subject.

$$N^3 = \frac{P}{P_0 p d_i^5}$$

(equation 2.5)

Solving this equation where P = 0.0097W, P_0 = 0.8, p= 130Kgm^{-3} and d_i = 0.02m (from table 2.3) yields an impeller speed of 1840 rpm to be used during the conditioning phase. This speed needs to be divided by 3.33 to give the impeller speed used during the addition phase of the precipitation reaction.

Table 2.4 (shown below) summarises the operating conditions of the scaled down precipitation reaction that should mimic the industrial scale operation.

Speed of rotation during addition phase	555rpm
Speed of rotation during conditioning phase	1840rpm
Conditioning time	15 hours
Rate of addition of precipitant	4ml/minute

Table 2.4 Operating parameters of the scaled down precipitation reaction

2.2.2 Mimicking centrifugation

It was decided to use the method described in section 1.4.2.2 to scale down the centrifugation stage; since this offered the possibility of producing a mimic that would require only millilitres of material. The disc stack centrifuge mimicked has the following dimensions and operating conditions:

Number of discs	95
Outer disc radius	0.1m
Inner disc radius	0.045m
Half disc angle	55^0
Diameter of lock nut	0.08m
Rotational speed	125rps
Feed flow rate	120L/hr
Sigma Value	$8400m^2$
Correction factor	0.25

Table 2.5 Dimensions and operating conditions of the industrial scale disc stack centrifuge

Calculating the tip velocity of the critical structure and then mimicking this with the in house shear device, mimicked the shear conditions in the centrifuge. Equation 1.27 (shown below) was solved in order to determine the speed that the in house shear device would be run at, in order to mimic the industrial centrifuge.

$$N_{rd} = \frac{r_{crit} N_{crit}}{r_{rd}}$$

(equation 2.6)

Where N_{crit} = 125rps and r_{crit} = 0.04m and r_{rd} = 0.015m a rotational speed within the shear device of 20000rpm should recreate the shear conditions found within the industrial scale machine.

Once sheared the settling conditions were modelled by maintaining the same Q/Σ between scales. The sigma value for the industrial disc stack centrifuge can be calculated from the equation below (Axelsson, 1985):

$$\Sigma = \frac{2}{3g} \pi z \omega^2 \cot\theta (R_0^{\ 3} - R_1^{\ 3}) F_1$$

(equation 2.7)

Where z is the number of discs in the stack, $\omega = 2\pi n$ (n is the rotational speed), θ is the half disc angle, R_0 is the outer disc radius, R_1 is the inner disc radius and F_1 is the correction factor applied to account for the presence of the spacer chalks. Solving this equation using the parameters in table 1.6 gives a sigma value of $8400m^2$.

The sigma value of the Beckman J2.M1 lab centrifuge fitted with a swing out bucket rotor (JA 13.1) with the following dimensions and operated under the following conditions can be calculated by utilising equation 2.8.

Maximum radius	0.14m
Minimum radius	0.041m
Volume	$3x10^{-5}m^3$
Rotational speed	100rps
Sigma	$2.76m^2$

Table 2.6 Dimensions and operating parameters of the in-house shear device and lab centrifuge

$$\Sigma_{lab} = \frac{V\omega^2}{g \ln\left(\frac{2R_{max}}{R_{max} + R_{min}}\right)}$$

(equation 2.8)

Where R_{max} is the maximum radius, R_{min} is the minimum radius. Altering the volume of material to be separated and the length of centrifugation can account for the difference between the Sigma values. The flow rate to Sigma ratio (Q/Σ) can be maintained by utilising the following equation:

$$\frac{Q_{ind}}{\Sigma_{ind} F_1} = \frac{V_{lab}}{\Sigma_{lab} F_1 t}$$

(equation 2.9)

Rearranging equation 2.9 in order to make time the subject gives the following equation:

$$t = \frac{V_{lab}}{\Sigma_{lab} F_1 \left(\frac{Q_{ind}}{\Sigma_{ind} F_1} \right)}$$

(equation 2.10)

Where Q_{ind} is the volumetric flow rate at the industrial scale and F_1 is the correction factor applied to account for irregularities in the flow. Solving this equation shows that the lab scale centrifuge should be run at 6000rpm, with 25ml of sample for 9.6minutes in order to recreate the settling conditions. The methodology based on these calculations can be found in section 2.4.2.

2.2.3 Conclusion

This section describes how the operating conditions detailed in section 2.4 were determined. Operating the scale down mimics under these conditions should accurately mimic the industrial scale operations.

2.3 Analytical Techniques

2.3.1 Biological assays

2.3.1.1 Total protein

Total protein concentration was determined by the method of coomassie (Pierce, Rockford, USA). The method is a modification of the work of Bradford (1976). The binding of protein to the reagent suppresses protonation and results in a colour change from brown to blue. Samples to be assayed were diluted to within

the working range of the reagent (200-1000μg/ml of protein), using phosphate buffered saline. This also ensured that the levels of possible interfering buffers, such sodium sulphate, were below the level where they could interfere with the assay. 50μl of sample were mixed with 950μl of commassie reagent in a cuvette. The change in absorbance at 595nm was measured using a spectrophotometer (Kontron instruments model 922) after 10 minutes. Comparison of the reading with a standard curve produced, using bovine serum albumin or ovine IgG depending on the nature of the sample being tested, enabled the protein concentration to be determined. Each sample was measured in triplicate to give a mean value.

2.3.1.2 ELISA (Enzyme Linked Immuno Sorbant Assay)

The percentage of active anti-snake venom antibodies was determined using enzyme-linked immuno sorbant assay, which allows the identification and quantification of an antigen from within a mixed solution. The assay was carried out according to the following protocol. A series of wells were coated with 100μl each of snake venom (Protherics, Wales, UK) diluted (1:2000) with PBS pH 7.4 and incubated for two hours at room temperature. Each well was washed three times with a PBS/Tween 20 buffer, pH 7.4 and blocked by the addition of 100μl of 1% skimmed milk diluted in PBS, pH 7.4. After 30 minutes the wells were then washed three times with the PBS/Tween 20 buffer. Serial dilutions, using PBS, pH 7.4, of each sample were prepared in the range of 1:2000 to 1:320000 for samples where the levels of antibody present were expected to be low e.g. the supernatant and 1:40000 to 1:1280000 for sample where the levels of antibody were expected to be high e.g. ovine serum and precipitated solids. 100μl of each sample was pipetted in duplicate into the coated wells and incubated at room temperature for 2hr. The wells were washed three times with PBS/Tween 20 buffer, pH 7.4. 100μl of anti sheep alkaline phosphatase diluted 1:5000 with PBS/Tween 20, pH 7.4 were added to each well. The wells were incubated at room temperature for 1hr, after which they were washed again with PBS/Tween 20, pH 7.4. Finally, 100μl of alkaline phosphate yellow substrate was added to each well. When the yellow colour developed, after approximately 30 minutes,

the reaction was stopped by the addition of 25µl of 3M sodium hydroxide. The absorbance of the contents of each well was measured at 405nm by using a plate reader (Dynatech MR7000, Guernsey, Channel islands).

The total concentration of ovine IgG was also measured using an ELISA assay. A series of wells were coated with 100µl of ovine IgG diluted using PBS, pH 7.4 to concentrations between 1000ng/ml and 25ng/ml in order to produce a standard curve. Each sample to be assayed was serially diluted using PBS, pH 7.4 to within the working range of the assay and then 100ul were added to each well. The plates were incubated for either two hours at room temperature or over night at 4^0C. Each well was washed three times with a PBS/Tween 20 buffer, pH 7.4 and blocked by the addition of 100µl of 1% skimmed milk diluted in PBS, pH 7.4. After 30 minutes the wells were then washed three times with the PBS/Tween 20 buffer. 100µl of anti-ovine IgG diluted 1:2000 with PBS/Tween 20, pH 7.4 was added to each well and allowed to incubate for 1hr. The wells were washed three times with PBS/Tween 20 buffer, pH 7.4. 100µl of anti sheep alkaline phosphatase conjugate diluted 1:5000 with PBS/Tween 20, pH 7.4 were added to each well. The wells were incubated at room temperature for 1hr, after which they were washed again with PBS/Tween 20, pH 7.4. Finally, 100µl of alkaline phosphate yellow substrate solution was added to each well. When the yellow colour developed, after approximately 30 minutes, the reaction was stopped by the addition of 25µl of 3M sodium hydroxide. The absorbance of the contents of each well was measured at 405nm by using a plate reader (Dynatech MR7000, Guernsey, Channel islands).

2.3.1.3 Albumin concentration

The concentration of the contaminating albumin in each sample was determined by using albumin reagent, bromocresol green BCG. Albumin binds to BCG to produce a blue/green colour with an absorbance maximum at 628nm (Corcoran, 1977). 50µl of each sample was mixed with 1ml of BCG in a cuvette. After 5 minutes the colour change was measured using a spectrophotometer (Kontron

instruments model 922). The concentration of albumin was determined by comparing the result with the standard curve produced using bovine serum albumin. Each sample was measured in triplicate in order to obtain a mean value.

2.3.2 Physical properties

2.3.2.1 Solid/Aqueous fraction determination

The percentage solid content of each sample was determined by pipetting 1ml of precipitated material into an eppendorf and spinning it at 13000 rpm for 10 minutes. The volume of the sample occupied by solid material could then be measured by comparison to a graduated eppendorf. The percentage of solid was then calculated by dividing by the total volume. Each sample was analysed in triplicate in order to calculate the mean value.

2.3.2.2 Liquid density

The density of the suspending solution containing the antibodies of interest was measured using a specific gravity bottle. 70ml of sample was spun at 12100g using a Beckman J2 M1 centrifuge with a JA 20 rotor for 30 minutes in order to remove all solid material. 10ml of the supernatant was decanted into a specific gravity bottle and weighed. This was repeated three times in order to obtain an average reading.

2.3.2.3 Precipitate density

The density of the antibody solid fraction was determined by measuring the gravity settling velocity i.e. the time taken for the precipitate particles to settle out. Then using Stokes law of free settling and assuming laminar flow the density of the particles could be calculated, given that both the viscosity and the density of the liquid through which the particles were settling had been determined. This was considered reasonable considering the relatively small size of the particles.

2.3.2.4 Viscosity

Sample viscosity was determined using the Contraves Rheomat 115 rheometer (Contraves AG, Zurich, Switzerland). The Rheomat 115 is a rotational

viscometer; its coaxial measuring systems operate according to the Searle principle. A coaxial cylinder arrangement, which rotates in the substance to be measured was used to measure the viscosity of the sample at 15 different shear rates. The shearing speed prevailing in the sample is a function of the cylinders rotational speed and the shear stress is a function of the braking torque. The samples viscosity, or its flow behaviour respectively can be deduced from these values.

20ml of sample at a temperature of 20 to 25^{0}C were used for each run and each was repeated in triplicate in order to determine a mean value.

2.3.3 Gel Electrophoresis

2.3.3.1 Reducing SDS-Page gel electrophoresis

The proteins contained within each sample were separated and visualised according to size under denaturing conditions by using SDS polyacrylamide gel electrophoresis (SDS-PAGE). A 12% resolving, 4% stacking gel was prepared using the method of Laemmli (1970). The separated protein bands were visualised by staining with Coomassie brilliant blue R250 protein dye for 30 to 60 minutes. Once stained, the gels were destained by shaking in 45% (v/v) methanol, 10% (v/v) acetic acid in deionised water.

Each sample was diluted to 1mg/ml. They were then diluted 1 in 2 with sample buffer containing 10% (v/v) glycerol, 20% (v/v) of 10% (w/v) SDS, 12.5% (v/v) 0.5 M Tris-HCl pH 6.8, 5% (v/v) β-mercaptoethanol, 5% (v/v) of 0.5% bromophenol blue and 47.5% (v/v) deionised water to give a final concentration of 0.5mg/ml. Each sample was boiled for one minute to ensure that the proteins were fully denatured. 15μl of each sample were loaded into each well. The gel was run at 80V for 30 minutes and then at 150V until the tracking dye reached the bottom.

2.3.3.2 Non-reducing SDS page gel electrophoresis

The proteins within certain samples were separated under non-denaturing condition. Each sample was diluted to 5mg/ml and then diluted 1:8 in native sample buffer (Invitrogen Ltd, Paisley, UK) to give a final concentration of 0.6mg/ml. Each sample was then placed in boiling water for 1 minute. 15ul of sample were loaded into a pre-cast 4-20% Tris-Glycine gel (Invitrogen Ltd, Paisley, UK). The gels were run at 150 volts for roughly 1.5 hours or until the tracking dye reached the bottom. The proteins were visualised by staining with Coomassie Brilliant blue R250 (Biorad, Hertfordshire, UK) for 30 to 60 minutes. Destaining was achieved by shaking in 45% (v/v) methanol, 10% (v/v) acetic acid in deionised water.

2.3.4 Particle size analysis

2.3.4.1 Laser particle sizing

Particle size analysis was carried out using the Malvern Mastersizer 2000 laser sizer (Malvern, Worcestershire, UK). Laser diffraction, more accurately called Forward Light Scattering measures particles in the range of 0.1 to 2000 microns. The instrument consists of three major parts; a schematic is shown in figure 2.1.

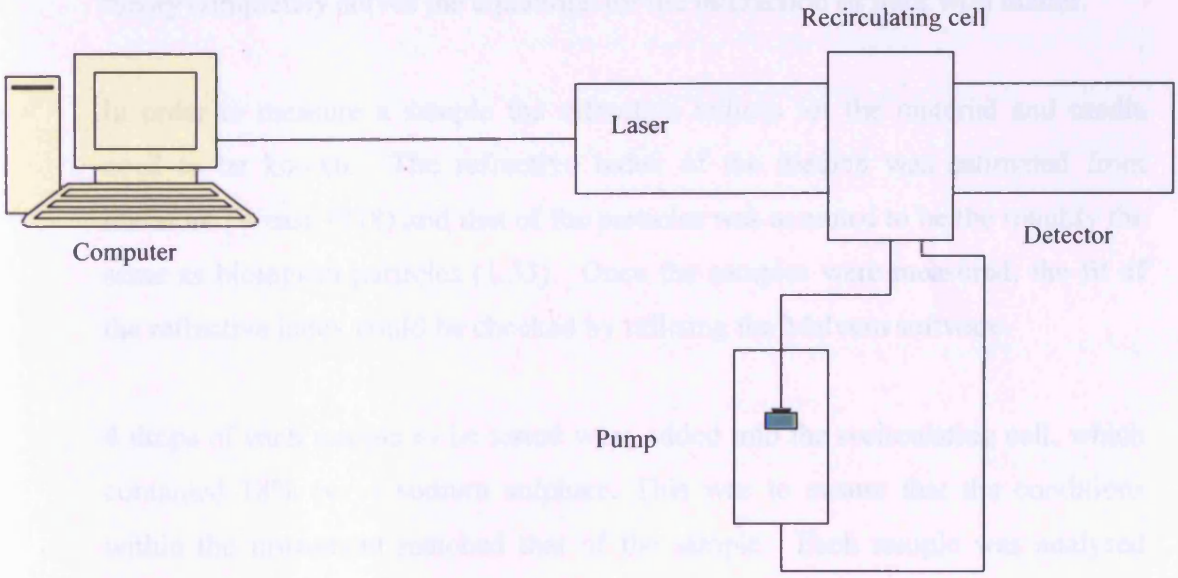

Figure 2.1 Schematic of the Malvern Mastersizer 2000

- The laser, which acts as a source of coherent intense light of a fixed wavelength. The lower the wavelength of the light the more stable the system is and the better the signal to noise ratio becomes. The standard He-Ne gas lasers operate at a wavelength of 0.633μm. It is expected however that the smaller laser diodes, with wavelengths as low as 600nm, will begin to replace the bulkier gas lasers once they become more reliable.
- A detector: this consists of a slice of photosensitive silicon with a number of discrete detectors. It has been shown that the optimum number of detectors is between 16 and 32. Increasing the number of detectors does not necessarily result in an increase in the resolution.
- A means of passing the sample through the laser beam. Aerosols can be sprayed directly through the beam. Dry powders can be measured by being blown through the beam and collected by a vacuum cleaner to prevent dust being released to the environment. Particles in suspension can be measured by recirculating the sample in front of the laser beam.

The Malvern Mastersizer uses the Mie theory to "assume" the volume of the particle and then convert this into the diameter of an equivalent sphere. This theory completely solves the equations for the interaction of light with matter.

In order to measure a sample the refractive indices for the material and media need to be known. The refractive index of the median was estimated from literature (Weast 1978) and that of the particles was assumed to be the roughly the same as biological particles (1.33). Once the samples were measured, the fit of the refractive index could be checked by utilising the Malvern software.

4 drops of each sample to be tested were added into the recirculating cell, which contained 18% (w/v) sodium sulphate. This was to ensure that the conditions within the instrument matched that of the sample. Each sample was analysed three times in order to obtain a mean value.

2.4 Ultra Scale Down Techniques

2.4.1 Ultra scale down precipitation

The precipitation reaction is the first stage in Protherics PLC purification process; by mimicking this stage it becomes possible to predict the effect changes will have on the large-scale operation and also study the existing process. The operating parameters and vessel dimensions were determined in section 2.2

100ml of serum (Protherics, Llandusul, U.K.) were thawed overnight. The serum was then filtered through a 0.2μm filter (Millipore, Watford UK) in order to remove any cryoprecipitates. The amount of filtrate was measured and this was then poured into the scaled down reaction vessel. The vessel was placed into a water bath set to 30°C and the serum allowed to equilibrate with the water temperature. Once the temperature of the serum had reached 30°C, an equal amount of 36% (w/v) sodium sulphate (Protherics, Llandusul, U.K.) temperature 30°C was added at a rate of 4ml/minute by using a Watson Marlow pump model 101U/R (Watson Marlow, Falmouth, U.K.). Whilst adding the precipitate the impeller was set to 555rpm (as determined in section 2.2.1.2). The speed was controlled by using a variable speed stirrer (Eurostar Digital, IKA, Lobotechnik). Once all the sodium sulphate had been added (approximately 30 minutes), the impeller was turned up to 1840rpm and the water bath was switched off. After 15 hours, the final solution was characterised according to the methods detailed in section 2.3.

2.4.2 Ultra scale down centrifugation

Following precipitation at an industrial scale the solid fraction is removed by disc stack centrifugation. This operation was mimicked through the use of the in house shear device and a standard swing out bucket lab centrifuge. The operating conditions were determined in section 2.2.2.

30ml of the precipitated antibody solution, prepared as per the method detailed in section 2.4.1, was sheared in the in-house shear device at 20000rpm for 1minute.

Once sheared the solid was then spun down in a Beckman JA20 with a swing out bucket rotor for 9.6minutes at 6000rpm. The solids fraction was then re-suspended in 18% (w/v) sodium sulphate. Once re-suspended this solution was then sheared again at 20000rpm for 1 minute before being spun down under the same conditions as before (at this point samples were taken for particle size analysis). Finally, the resulting solids fraction was re-suspended in PBS pH 7.4.

2.4.3 Scaled down filtration

Previously, precipitated immunoglobulins were recovered from the liquor containing contaminating proteins by disc stack centrifugation. This process is time consuming and requires very strict monitoring for validation purposes. A small-scale stirred cell filtration device (Millipore, Watford, UK) has been used to study the effects of replacing the centrifuge with a filter. The precipitated antibody feed used in these experiments was produced as per the method in section 2.4.1.

2.4.4 Stirred cell methodology

The stirred cell device was operated in two different modes: batch and continuous. It has a diameter of 0.063m with a total volume of 200ml and was modified for use as a small-scale microfiltration device. A 3μm (pore size) cellulose acetate membrane 90mm in diameter (Millipore, Watford, UK) was cut to the correct diameter, as 3μm pore size membranes were not available in the correct diameter. These were then placed at the bottom of the cell. The cell was equipped with a single paddle impeller (width = 4.3mm, height = 8.4mm, length = 49.6mm) positioned centrally in the cell in close proximity to the surface of the filter membrane. The shaft was driven from the top by a variable speed motor having a maximum speed of 242rpm. The rotational speed of the shaft was measured using a digital tachometer. The cell was hermetically sealed, once the lid was screwed in place, and was supplied with an air inlet and pressure control system allowing precise setting of the air pressure above the solution in the cell during operation.

During continuous (diafiltration) operation the working liquid volume in the cell was maintained at a constant level by continuously feeding a wash/diafiltrate buffer (18% Na_2SO_4 w/v) to the vessel at a rate equal to the permeate rate.

2.4.4.1 Batch filtration

Standard batch filtration tests were carried out as follows: 75ml of suspension containing the precipitated antibody was placed in the stirred cell. The rotational speed of the paddle was set at a pre-determined value and an air pressure applied. The permeate was collected (sample 2a, Figure 5.1b) until the permeate flow stopped and a filter cake formed on the membrane. In the second part of the test, the cake was washed, as described next. The operation was stopped, 150ml of 18% sodium sulphate (w/v) was added to the vessel and the paddle speed was set to the same speed as before. The mixture was stirred for ten minutes to break and resuspend the cake of precipitated antibody. The air pressure was re-applied and the filtrate was collected and measured every minute until the permeate flow stopped.

2.4.4.2 Continuous filtration

In diafiltration mode, 75ml of precipitated antibody was placed in the cell. The speed of the paddle was set at the pre-determined value and air pressure applied. A buffer solution of 18% sodium sulphate (w/v) was drawn in at the same rate that the permeate was collected, thus maintaining a constant level of liquid in the vessel. The flow of buffer was stopped after 150ml of buffer solution had been added and the operation switched to cake-filtration mode until the permeate flow stopped and a filter cake of the antibody precipitate formed. The 225ml of permeate was collected in three separate 75ml fractions for analysis.

The final step for both modes of operation consisted of adding 75ml of warm (37°C) phosphate buffered saline (PBS) pH 7.4 to the solid cake in the cell. The antibody rich filter cake was allowed to dissolve over approximately ten minutes. The air pressure was applied as before and the antibody rich permeate collected for analysis.

2.4.4.3 Loading and wash volume determination

75ml and 100ml respectively of precipitated serum were placed into the stirred cell. The rotational speed was set to 121rpm and an air pressure of 1bar applied. The permeate was collected until the permeate flow stopped. The layer of

precipitated antibodies, which had formed on the surface of the membrane, was then washed as described below. The operation was stopped and an equal volume in the first set of experiments and twice the initial load volume in the second set of experiments of 18% sodium sulphate (w/v) was added to the vessel. The paddle speed was set to the same speed as before and the mixture was stirred for ten minutes to break and re-suspend the cake of precipitated antibody. The air pressure was re-applied and the filtrate was collected.

2.5 Chromatography

Precipitation followed by centrifugation is an unwieldy and time consuming method of achieving the initial separation. Affinity chromatography utilising the unique properties of protein G (as detailed in section 1.3.6.2) offers a simple one step procedure for isolating and concentrating the ovine immunoglobulins from all the other contaminating proteins.

A preliminary investigation into the feasibility of this process option has been carried out. Computer modelling has been utilised to predict breakthrough curves of column separations based on equilibrium data obtained at the laboratory scale.

2.5.1 24 hour equilibrium

Equilibrium binding experiments were used to determine experimental values of the amount of IgG bound to the matrix and the amount remaining soluble in solutions of different concentrations after 24 hours. This data can then be fitted to model isotherm equations such as the Langmuir curve.

100µl of Protein G sepharose 4 fast flow matrix (Amersham Biosciences, Buckinghamshire, UK) equilibrated in 0.2M sodium phosphate buffer pH 7.4 (binding buffer) was pipetted into a series of eppendorfs. Samples of purified ovine IgG (prepared according to section 2.5.3) and Albumin were prepared at concentrations of 40, 35, 30, 25, 20, 15, 10, 8, 6, 4, 2, 1, and 0.5mg/ml by dilution with binding buffer. The protein solutions remained clear and there was no visible precipitation.

100µl of each sample was pippeted into a separate eppendorf. The tubes were closed and placed on an end over end stirrer. After 24 hours, the eppendorfs were spun in a microfuge (Biofuge 13, Heraeus sepatech, Germany) at 13000rpm for two minutes in order to pack the matrix to the bottom of the tube. (Measuring the concentration of a control sample that had been left at room temperature for 24 hours checked the stability of the protein. This showed that no degradation of the protein was occurring). 80µl of the mobile phase was then removed and analysed by Bradford assay for total protein content and ELISA for total IgG content as per sections 2.3.1.1 and 2.3.1.2. Each run was repeated three times in order to determine a mean value.

2.5.2 Dynamic equilibrium determination

2ml of protein G sepharose 4 fast flow matrix (Amersham Biosciences, Buckinghamshire, UK), equilibrated by washing in 10ml of 0.2M sodium phosphate buffer pH 7.4, was pippetted into a stirred cell (Millipore, Watford UK) (model 8010). The mixer was turned on at a slow speed in order to ensure good mixing. 2ml of each sample (IgG 30mg/ml and Albumin 30mg/ml) was then added to the stirred cell. 30ul samples were removed at 15, 30, 45, 60, 90, 120, 300, 600, 900, 1200, 1500 and 1800 seconds. Any matrix contained with the sample was immediately removed by centrifugation through a centrifugal filter fitted with a 1µm pore diameter filter (Millipore, Watford UK). This ensured that no further adsorption of protein to the matrix would occur. The collected samples were assayed for total protein content and total IgG content as per sections 2.3.1.1 and 2.3.1.2.

2.5.3 Purification of ovine IgG by adsorption to Protein G

A 2.5cm high by 0.7cm diameter protein G column (Amersham Biosciences, Buckinghamshire, UK) was used to purify the ovine IgG from the serum, forming a source of pure IgG for further experiments. 1ml of 0.2µm depth filtered serum was mixed with 1ml of binding buffer, in order to ensure buffering conditions suitable for the binding of IgG to protein G. This was loaded onto the column at a

flow rate of 157cm/hr. Any unbound proteins were then washed away by the addition of 6 column volumes (CVs) of binding buffer. The bound IgG was then eluted by the addition of 8 CVs of 0.1M glycine-HCl buffer pH 2.7. Samples were collected in one millilitre fractions and the elutant samples were immediately quenched to pH 7.0 by the addition of 46µl of 1.0M Tris-HCL pH 9.0 buffer. This ensured that the acid labile immunoglobulins were not denatured by the harsh elution conditions. Following elution, the column was immediately re-equilibrated with 8 CVs of binding buffer. After every five runs, the column was cleaned by running a solution of 0.1% Triton 100 detergent through the column for one minute (as recommended by the manufacturer). This should remove any proteins or lipids that remained bound to the column.

The eluted fractions were pooled, concentrated and a buffer exchange affected. This was achieved by centrifugal filtration through a 100KDa membrane (Millipore, Watford, UK) until a final concentration of IgG in excess of 40mg/ml (determined by measurement of the absorbance at 280nm) was reached. This product could then be diluted as necessary (6 runs were generally required to produce 3ml of final product). The flow through, wash and elution fractions were assayed for total protein content and the proteins contained in the samples were visualised by non denaturing SDS page as per section 2.3.1.1 and 2.3.3.2.

2.5.4 Breakthrough curves

Purified and concentrated IgG was produced as per the method in section 2.5.3. This was diluted with binding buffer to 30mg/ml and 15mg/ml as determined by absorbance at 280nm. Columns with the dimensions and bed heights shown below in table 2.7 were poured:

Bed Height (cm)	Bed Diameter (cm)	Column Volume (ml)
2.5	0.7	0.96
5	1	3.95
10	1	7.9
15	0.8	7.5

Table 2.7 Chromatography bed dimensions for breakthrough curve experiments

The purified IgG was then pumped onto the column at the flow rates and concentrations shown below in table 2.8. A range of flow rates, feed concentrations and bed heights were chosen in order to generate differing breakthrough curves and test the ability of the mathematical model to accurately predict the shape of the breakthrough curves.

Bed Height (cm)	Feed Concentration (mg/ml)	Flow rate (cm/h)
2.5	30	157
2.5	30	316
2.5	15	157
2.5	15	316
5	30	76
5	15	76
10	30	76
10	30	38
15	30	120
15	30	60

Table 2.8 Feed concentrations and flow rates used during the breakthrough curve experiments

Each column was run until the absorbance reading of the effluent levelled out and was within 0.1AU of the feedstock.

3 An Ultra Scale Down Approach For The Predication Of Full Scale Recovery Of Ovine Polyclonal Immunoglobulins Used In The Manufacture Of Snake Venom Specific Fab Fragment

3.1 Introduction

The results presented in this chapter have been published (Neal, et al. 2003). This chapter describes a new approach that allows the prediction of the performance of a large-scale integrated process for the primary recovery of a therapeutic antibody from an analysis of the individual unit operations and their interactions in an ultra scale-down mimic of the process. The recovery process consisted of four distinct unit operations (figure 3.1a). Using the new approach the important engineering parameters in each operation that impacted the overall recovery process were defined and in each case its effect was verified by a combination of modelling and experimentation.

Immunoglobulins were precipitated from large volumes of dilute blood plasma and the precipitate particles were recovered by centrifugal separation from the liquor containing contaminating proteins including albumin. The fluid mechanical forces acting on the particles and the time of exposure to these forces were used to define a time-integrated fluid stress. This was used as a scaling factor to predict the properties of the precipitate particles at large scale. In the case of centrifugation, the performance of a full-scale disc stack centrifuge was predicted. This was achieved from a CFD analysis of the flow field in the centrifuge coupled with experimental data obtained from the precipitated immunoglobulin particles using the scale down precipitation tank, a rotating shear device, and a standard swing-out rotor centrifuge operating under defined conditions. In this way, the performance of the individual unit operations, and their linkage, was successfully analysed from a combination of modelling and experiments. These experiments required only millilitre quantities of the process material. The overall performance of the large-scale process was predicted by tracking the changes in physical and

biological properties of the key components in the system including the size distribution of the antibody particles and antibody activity through the individual unit operations in the ultra scale-down process flowsheet.

This chapter is concerned with the initial downstream recovery of ovine polyclonal immunoglobulins as part of a process for the preparation of monovalent Fab fragments developed as an antidote to rattlesnake bites. The preparation of the anti-venom is detailed in chapter 1.

From a process engineering perspective, there is now very intense pressure on companies to establish techniques that can rapidly assess new process options to produce a potential new drug candidate in sufficient quantities for its perceived demand. This pressure is compounded further by the fact that such process information is needed often early in the life cycle of the new drug candidate when pilot plant trials are either not feasible, because the company has no access to suitable facilities, or not practical because only very small quantities of relevant materials are available for tests. Recently an engineering approach that allowed key process information to be generated from small mimics of large industrial unit operations was developed. This provided experimental evidence that demonstrated the applicability of the technique in two separate operations, one involving the recovery of a protein precipitate using a multichamber centrifuge (Boychyn, et al. 2001) and the other the recovery of a monoclonal antibody fragment in solution from fermentation broth using a filtering centrifuge (Boulding, et al. 2002). This chapter provides experimental evidence to demonstrate the capacity of the approach to link two neighbouring operations of precipitation and centrifugation used in sequence in the primary recovery of the immunoglobulins.

3.2 Methodology

All experiments were carried out with the same stock of anti-venom serum supplied by, Protherics PLC (Llandusul, Wales, UK).

Figure 3.1a shows the sequence of operations in the large-scale process flowsheet for the primary recovery of the immunoglobulins. The process starts with a precipitation step during which the immunoglobulins, primarily IgG, are precipitated from the serum solution by the addition of an equal volume of 36% (w/v) solution of sodium sulphate (final concentration 18% w/v). This is followed by a solid-liquid separation step in a disc stack centrifuge to remove the precipitated antibodies from the liquor containing the contaminating proteins including albumin. The solid fraction containing the immunoglobulins are then resuspended in a fresh solution of 18% (w/v) sodium sulphate and centrifuged again to remove the residual contaminating proteins.

In the large-scale process, the precipitation step was carried out in a 0.68m diameter cylindrical stainless steel, dished-bottom tank having a height of 0.6m. The liquid height in the vessel was maintained at 0.5m giving a working volume of 200L. The vessel was equipped with a 3-bladed stainless steel marine propeller, positioned off-centre in the tank. The impeller shaft entered the vessel through the side-bottom of the tank, 1/5 of the liquid height from the base of the vessel, at an angle of approximately 45°. The impeller was driven by an electric motor with the speed of agitation set at 150rpm. Agitation was maintained at this speed for 30 min to complete the precipitation process, following which the impeller speed was increased to 500rpm and maintained at this speed for 15hr to condition (age) the precipitate. The whole operation (precipitation and aging) was carried out at 30°C. The precipitated antibody was separated from the liquor containing the other biomolecules by using a continuous flow disc stack centrifuge (Model SAMR 3036, Westfalia, UK) with a bowl volume of 6.9L operating at a speed of 7500rpm and a flow rate of 120Lhr^{-1}. The solids were collected intermittently, pooled and resuspended in an equal volume of 18% (w/v) sodium sulphate in a tank with identical configuration to the precipitating vessel and operating under the same speed. The resuspended antibody particle was then centrifuged under operating conditions similar to those used in the first centrifuge. The solids from the second centrifuge were pooled and resuspended in phosphate buffered saline (PBS) solution before being transferred to the fractionation vessel for treatment with papain.

Figure 3.1b shows the ultra scale-down flowsheet used to mimic the operations in the full-scale process (Figure 3.1a). The precipitation tank was scaled-down by factor of 1000, based on the working volume of the liquid. The main dimensions of the scale-down precipitation vessel were as follows: tank diameter = 0.068m; tank height = 0.06m; liquid height = 0.05m; and impeller diameter = 0.02m. There were major geometrical differences between the full-scale precipitation tank and its mimic. For example, in the scale-down configuration, both the vessel and the three bladed marine propeller were constructed from plastic, the vessel had a flat bottom and the impeller was positioned in the centre of the tank and driven via a shaft from the top of the vessel by a small electric motor with a variable speed control. The impeller was placed approximately 1/3 of the vessel diameter from the base of the vessel and the ratio of impeller to tank diameter was different to that used in the full-scale unit.

3.2.1 Computational Fluid Dynamics simulation

The velocity profile and the associated local energy dissipation rates in the entrance region of the disc stack centrifuge were simulated using a commercially available package (CFX 4.1, AEA Technology, Oxfordshire, UK). A finite volume code was used to solve the integrated form of the governing flow equation (Versteeg and Malalasekera, 1955). The flow of the fluid in the entrance is highly turbulent, and the high Reynolds number form of the k-ε turbulence model (RNG k-ε turbulence model) was built into the CFX-4.1 code and used for calculation purposes. Previously described experimental results validate simulations made by CFX (Soon et al, 2001). This package is now used routinely to assess the flow in complex process geometry (Boychyn, et al. 2001; Boulding, et al. 2002).

For the purpose of flow analysis, the two-liquid phase mixture was treated as a continuum having the physical properties of the continuous aqueous phase. This is a reasonable assumption given the relatively low solid concentration in the feed (12% v/v). The antibody suspension flows into the empty space of the entrance chamber, and in its normal mode of operation the flow is considered as a two-phase, gas-liquid system with the liquid expanding through the air space of the

chamber. The homogeneous two-phase flow model was used to describe the gas-liquid interaction. It was assumed that the solution fields for each phase were identical except for the volume fractions, which were found by solving separate continuity equations for each phase. This approximation was considered to be reasonable because the majority of the volume fractions are close to zero or unity, with the exception of those at the interface. The two-phase fluid flow was assumed to be transient, weakly compressible for the gas phase and Newtonian, non-isothermal and homogeneous with constant density and viscosity (incompressible) for the liquid phase. Gravity effects were assumed to be negligible and were not included in the calculations.

Because of the symmetry of flow the simulations were carried out only for a quarter of the centrifuge volume. In terms of CFD analysis of flow in the centrifuge, an important consideration is the treatment of boundary conditions at moving surfaces. The simulation programme used in the present study is a cell centred code in which the variables are calculated and stored at a node in the centre of the cell. Therefore, unlike other codes that have active vertices on the wall, for example a finite element code, CFX4 does not require the specification of turbulence values on the wall.

The entrance region of the centrifuge forming the computational domain was "body fitted" for grid generation and the governing equation solved using a personal computer (Hewlett Packard, Vectra, Pentium II 400 MHz). Grid independent solutions were obtained by using a mesh design consisting of 90,000 grids. The grids were refined to allow the details of flow to be examined in regions where rapid changes in flow occurred.

3.2.2 Analytical techniques

Biological assays

The activity of antibodies, the total protein concentration and the concentration of albumin within the samples were determined as per the methods in section 2.2.1.

The proteins contained within each sample were separated according to size under denaturing conditions by sodium dodecyl sulphate polyacrylamide gel electrophoresis (SDS-PAGE). The methodology is described in section 2.2.3

Physical properties

To assess the physical state of the precipitated antibody particles, particle size measurements were performed on samples removed from the full-scale process as well as the scale-down mimic. The sampling locations are shown in Figures 3.1a and 3.1b. Particle size measurements were obtained as per section 2.2.4.

Density measurement of the liquid and solid fractions, viscosity measurements and percent solids content were determined as per the methods in section 2.2.2.

3.3 Results

Figures 3.1a and 3.1b are process flow sheets detailing the initial purification steps used during the production of rattlesnake anti-venom. Figure 3.1a shows the industrial scale process which consists of precipitation, centrifugation, re-suspension and a second centrifugation step. Figure 3.1b shows the scaled down mimic process which consists of precipitation, shearing, centrifugation, re-suspension, a second shearing step and a second centrifugation.

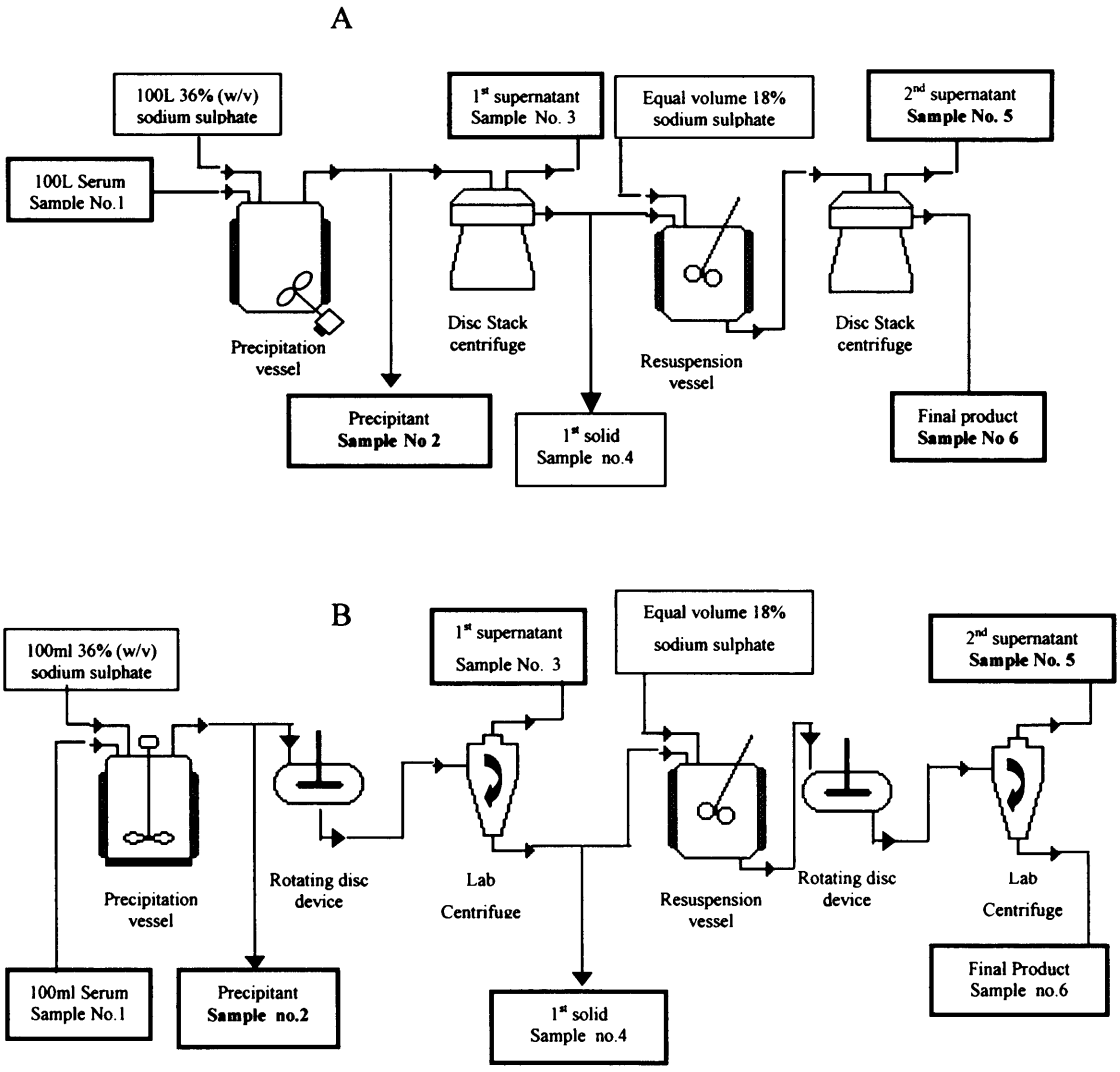

Figure 3.1a & b Process flow sheet detailing the initial stages of the process scale purification process, the ultra scale down mimic of the process and the sampling points

Table 3.1 is a comparison of the physical properties of the antibody particles produced at the industrial scale and by the ultra scale down mimic. The mimic produces a feed stream which closely matches the physical properties of the feed stream produced at the industrial scale (standard error: Viscosity +/- 0.1mPa.s (n=5), Solids content +/- 1.3% (n=5), Density solid +/- 0.16g.cm^{-3} (n=5), Density liquid +/- 0.02g.cm^{-3} (n=5)

	Viscosity (mPa.s)	Solids content (%)	Density solid (g.cm^{-3})	Density liquid (g.cm^{-3})
Scale down	2.5	12.0	1.3	1.17
Industrial scale	2.4	12.0	1.3	1.17

Table 3.1 Comparison of the precipitated antibodies (sample number two in figure 3.1a & b) physical properties produced on an industrial scale and by the scale down mimic

The particle size distribution of the antibody particles produced at the two different operating scales should match, if they do it indicates that the mimic is effective. Figure 3.2 shows the particle size distribution of the industrial scale particles and the ultra scale down particles. The particle size distributions match closely between the two scales indicating a good mimic (standard deviation +/- 3μm at d0.9, n=5).

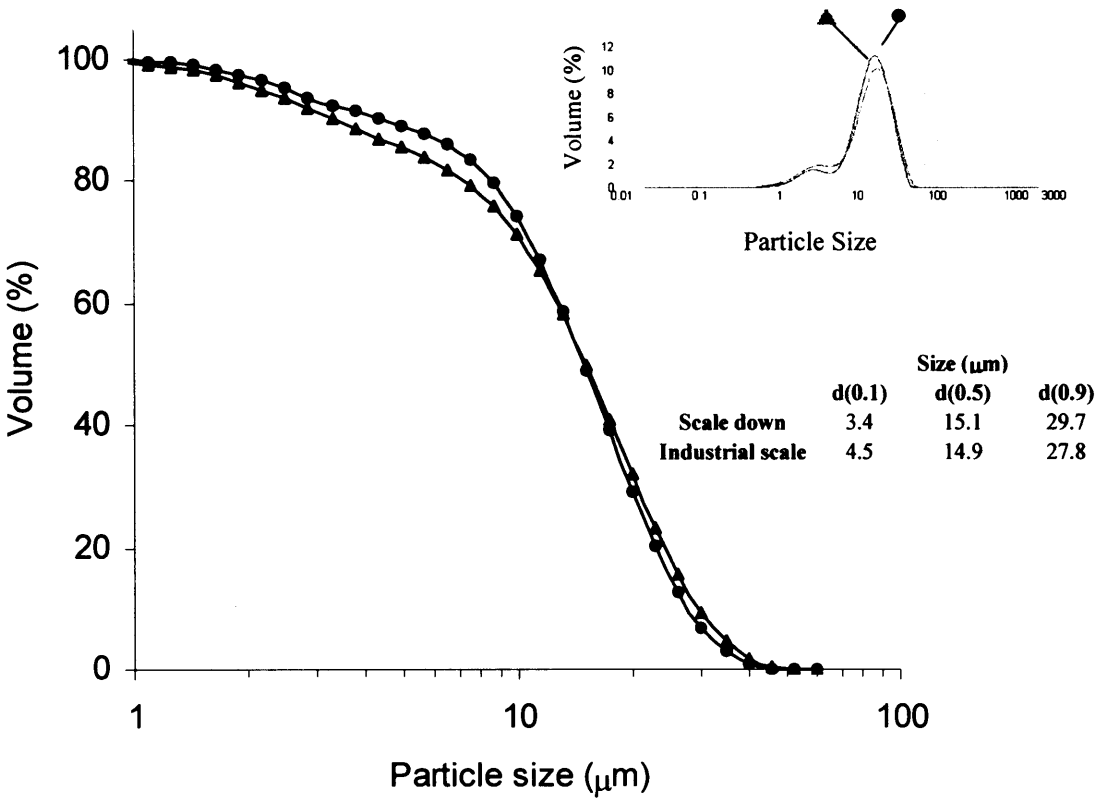

Figure 3.2 Comparison of the particle size distribution produced during the precipitation of antibodies with sodium sulphate on an industrial scale, ● and by a 1000 fold scale down model, ▲ with the same time integrated shear stress value (Ef) (sample point 2 fig 3.1a & b)

Disc stack centrifugation is expected to have some degree of impact upon the particle size distribution of the antibody particles. Figure 3.3 depicts the particle size distribution of the particles before and after their passage through the centrifuge. Disc stack centrifugation results in a 50% decrease in the particle size, it is interesting to note however that no further reduction size occurs during the second passage (standard deviation +/- 3μm at d0.9, n=3).

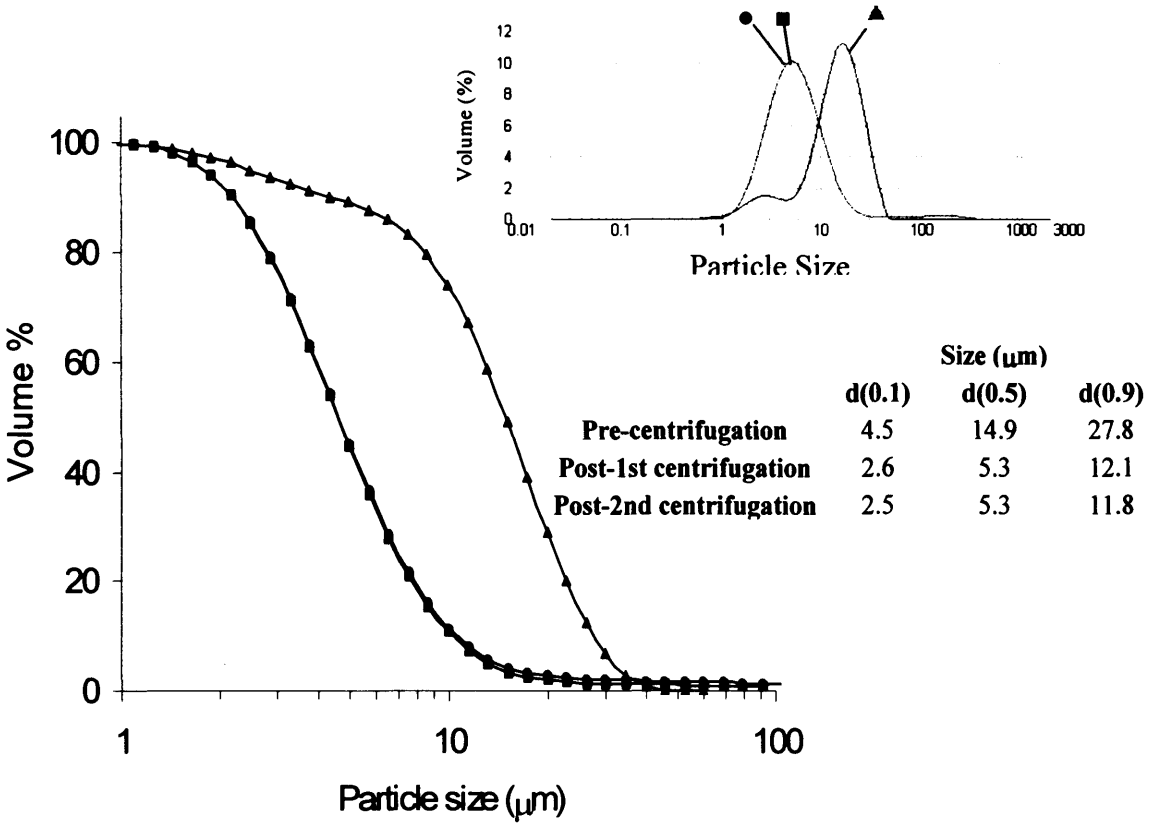

Figure 3.3 Comparison of the precipitated antibodies particle size distribution before, ▲ after, ● 1st industrial scale disc stack centrifugation and after 2nd industrial scale disc stack centrifugation ■ (sample points 2,4 & 6 fig 3.1a)

SDS page gel electrophoresis provides a means of visualising the proteins contained within a sample. Figure 3.4a is a SDS page reducing gel of the proteins contained within the feed and waste streams at various points during the industrial scale purification process. It can be seen that the albumin, which forms the main contaminant, is removed during purification.

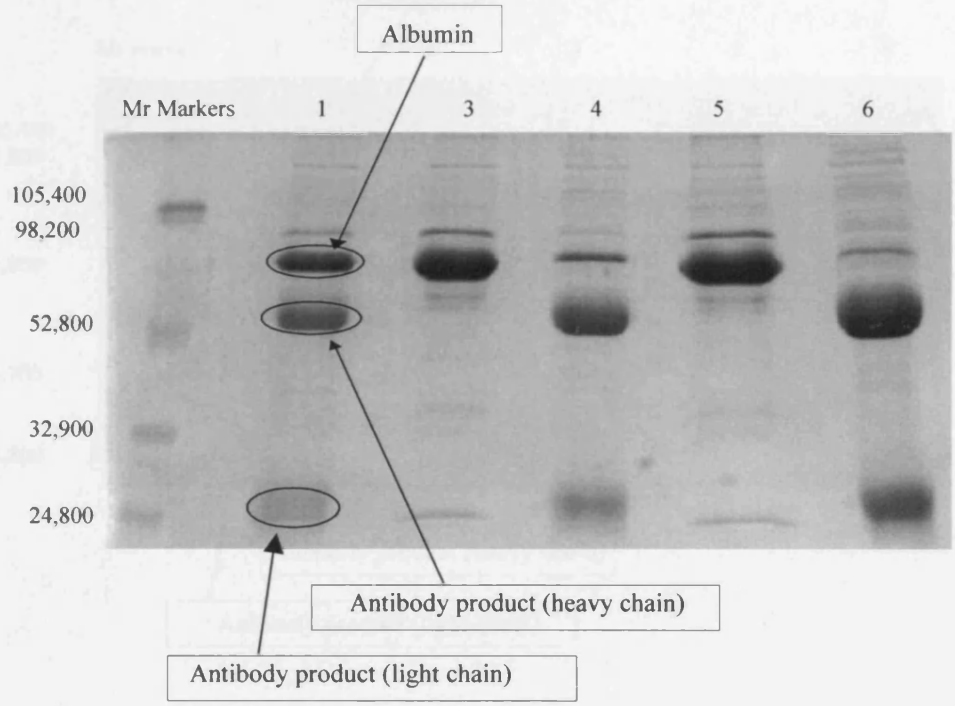

Figure3.4a SDS-page reducing gel showing the contaminants of each feed stream at the industrial scale, lane one contains Serum, three contains 1st supernatant, four contains 1st solid, five contains 2nd supernatant and six contains 2nd solid. Sample numbers refer to figure 3.1a

Figure 3.4b is a SDS page reducing gel of showing the proteins contained in the feed and waste streams of the ultra scale down mimic purification process. The gel shows that the same contaminants are present at both scales.

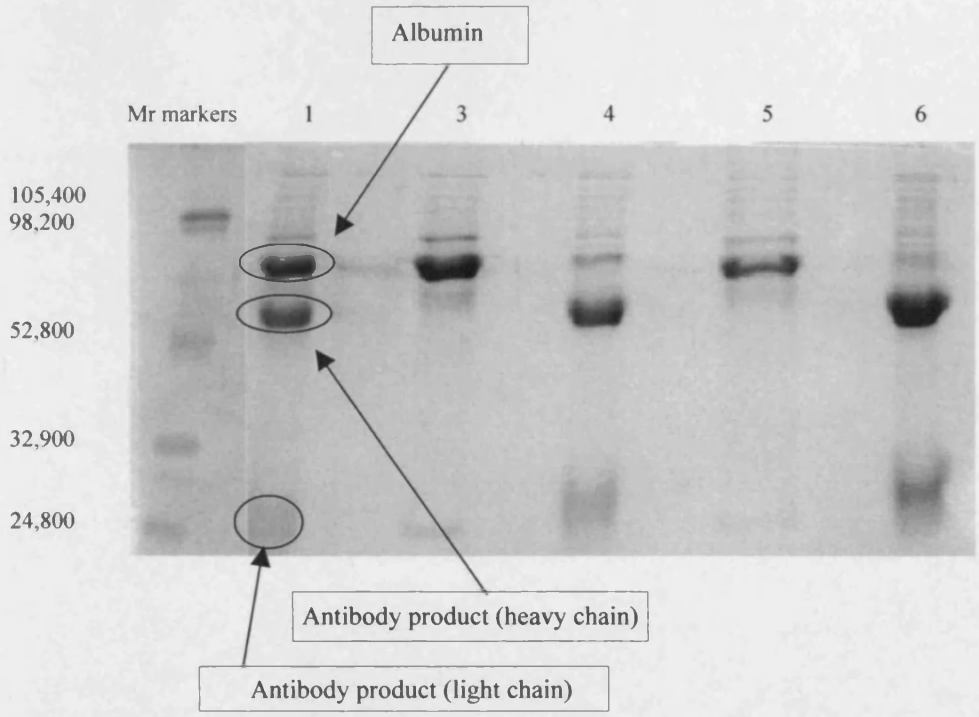

Figure 3.4b SDS-page reducing gel showing the contaminants of each feed stream at the laboratory scale, lane one contains Serum, three contains 1st supernatant, four contains 1st solid, five contains 2nd supernatant and six contains 2nd solid. Sample numbers refer to figure 3.1b

CFD simulations allow predictions of the magnitude of forces acting within the disc stack centrifuge. Figure 3.5 is the CFD simulation of the flow conditions within a disc stack centrifuge. The shear rate is highest within the region of the lock nut.

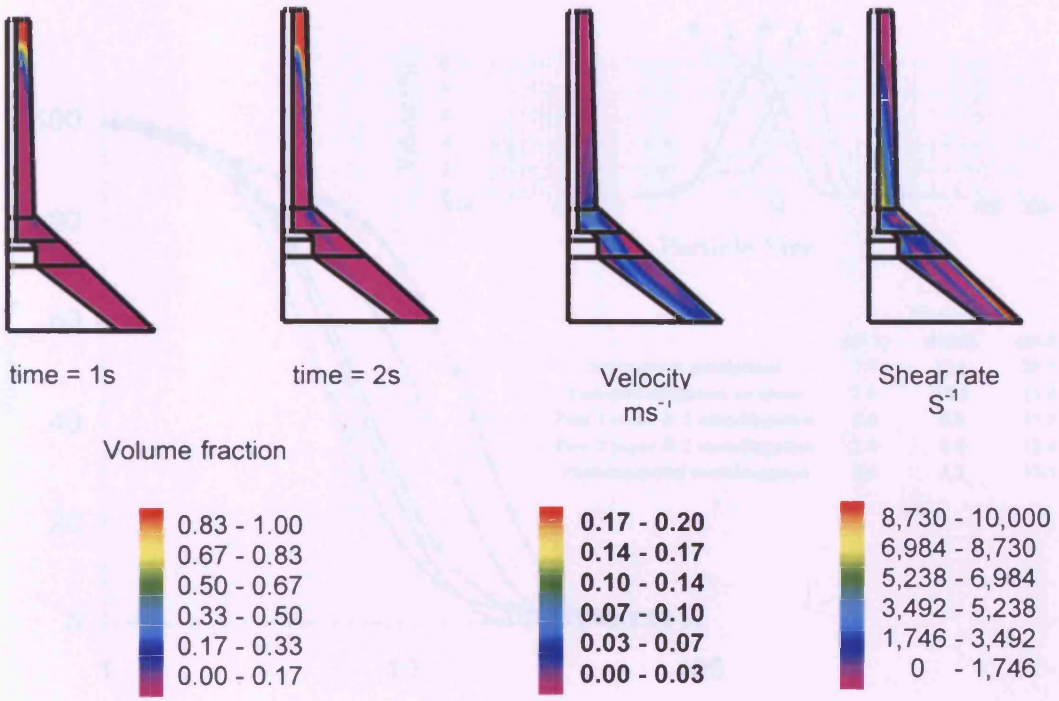

Figure 3.5 CFD simulations of flow and associated hydrodynamic parameters in the entrance region of the disc stack centrifuge

Particle size distribution measurements of the antibody particles at various stages during the ultra scale down purification process are shown in figure 3.6. As can be seen without shearing little degradation of particle size occurs. However the introduction of shear stress results in degradation of the particle size distribution to a size which closely matches the particle size produced during industrial scale centrifugation (standard deviation +/- 3μm at d0.9, n=5).

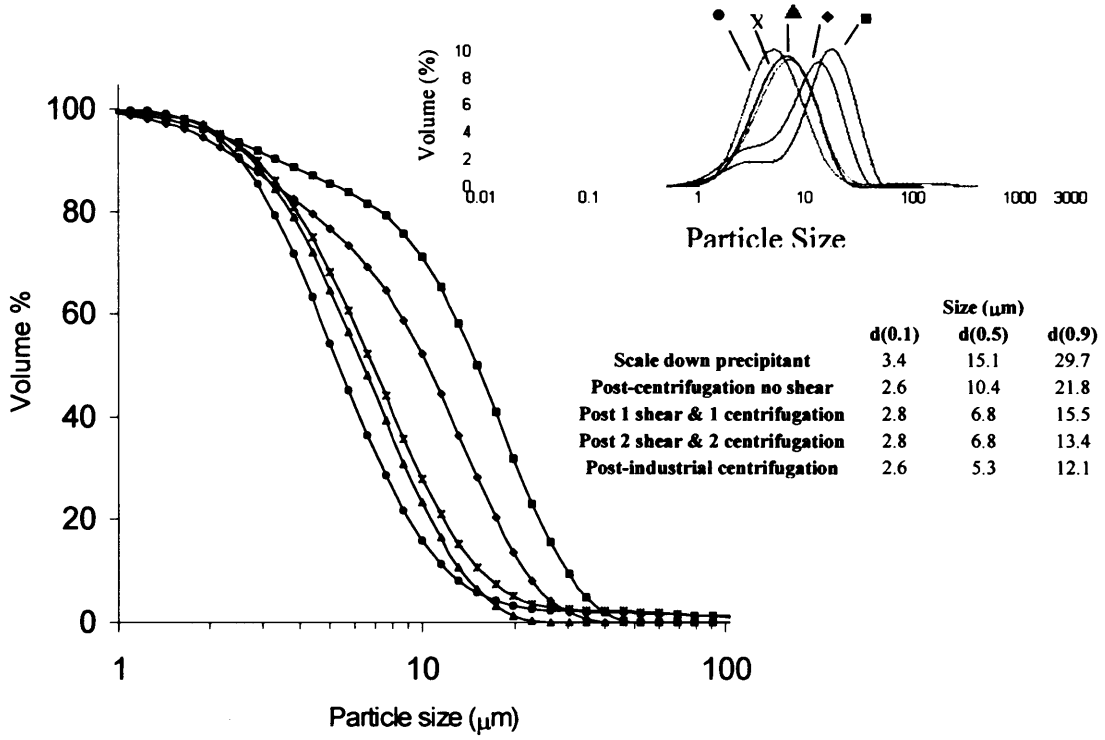

Figure 3.6 Comparison of the precipitated antibodies particle size distribution before, ■ and after, ◆ (sample points 2 & 6 fig 3.1b) centrifugation in a swing out bucket centrifuge at the same flow rate/sigma as the industrial disc stack centrifuge (no shear). After shearing with an air liquid interface followed by centrifugation in a swing out bucket centrifuge, X (sample point 4 fig 3.1b). After shearing twice with an air liquid interface followed by centrifugation twice in a swing out bucket centrifuge, ▲ (sample point 6 fig 3.1b) and after industrial disc stack centrifugation, ● (sample point 6 fig 3.1a)

The levels of total protein, albumin and active antibody were measured in order to produce a mass balance. Figure 3.7a is the mass balance for the industrial scale operation. The balance correlates with the visual information given by the SDS page gels shown in figure 3.5 (standard error: Total protein +/- 3% (n=5), Albumin +/- 5% (n=5), Active antibody +/- 8% (n=3)).

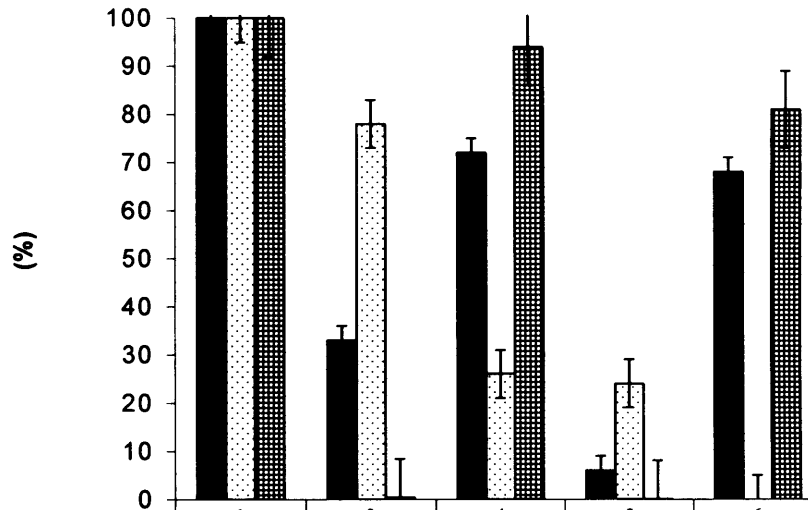

	1	3	4	5	6
■ Average Total protein (%)	100	33	72	6	68
□ Average Albumin (%)	100	78	26	24	0
⊞ Average Active Antibody (%)	100	0.4	94	0.1	81

Figure 3.7a Mass balance for industrial scale purification process showing the levels of total protein, the main contaminant and the product (sample numbers correspond to those in fig 3.1a)

A mass balance was also carried out for the ultra scale down purification process. Figure 3.7b depicts the levels of total protein, albumin and active antibodies within the various samples. It can be seen that they closely match the levels produced at an industrial scale (standard error: Total protein +/- 3% (n=5), Albumin +/- 4% (n=5), Active antibody +/- 9% (n=3)).

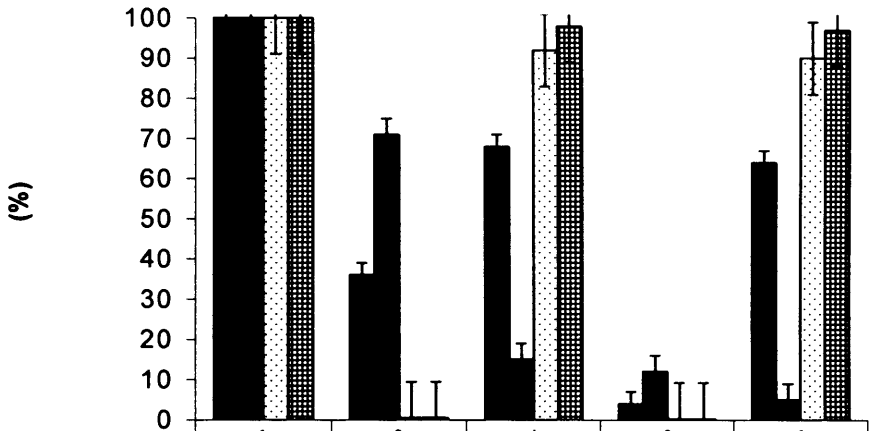

	1	3	4	5	6
Average Total protein (%)	100	36	68	4	64
Average Albumin (%)	100	71	15	12	5
Average Active Antibody (%)	100	0.5	92	0.2	90
Average Active Antibody without shear (%)	100	0.5	98	0.2	97

Figure 3.7b Mass balance for the ultra scale down purification process showing the levels of total protein, the main contaminant and the product (sample numbers correspond to those in fig 3.1b)

A comparison of the levels of total protein, albumin and active antibodies found with the first solid of the industrial scale process and ultra scale down process is presented in Figure 3.8a. The levels of protein closely match between the two differing scales of operation (standard error Scale down: Total protein +/-3% (n=5), Albumin +/- 4% (n=5), Active antibodies = +/- 9% (n=3). Industrial scale: Total protein +/-3% (n=5), Albumin +/- 5% (n=5), Active antibodies = +/- 8% (n=3)).

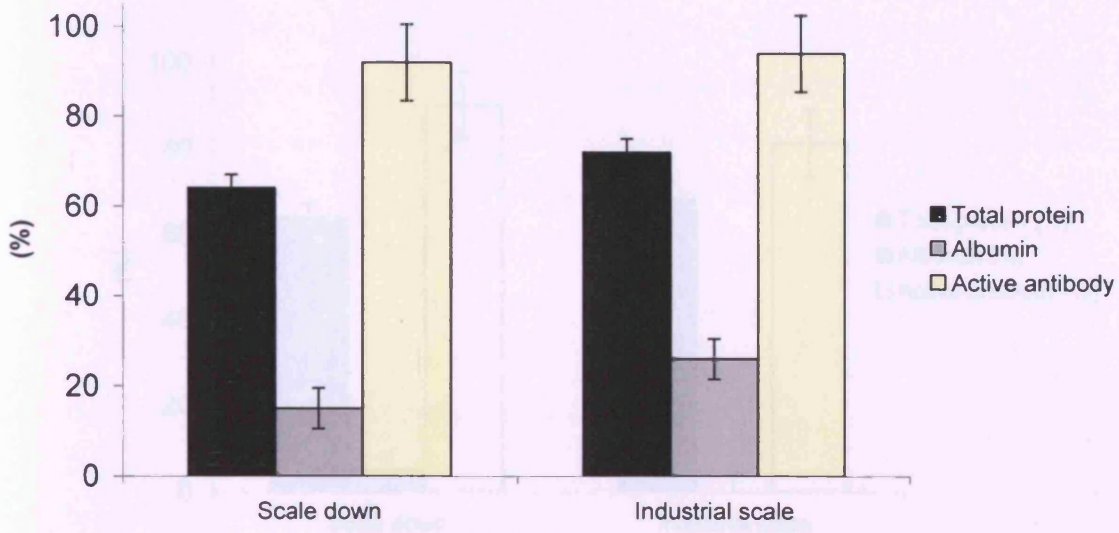

Figure 3.8a Mass balance showing a the quantities of total protein (%), albumin (%) and active antibody (%) present in the 1st solid (sample point 4)

A mass balance of the total protein content, albumin levels and active antibody concentration contained in the final product reveals that the levels match closely between the two scales of operation and that the amount of albumin present has been reduced to almost zero (standard error Scale down: Total protein +/-3% (n=5), Albumin +/- 4% (n=5), Active antibodies = +/- 9% (n=3). Industrial scale: Total protein +/-3% (n=5), Albumin +/- 5% (n=5), Active antibodies = +/- 8% (n=3)).

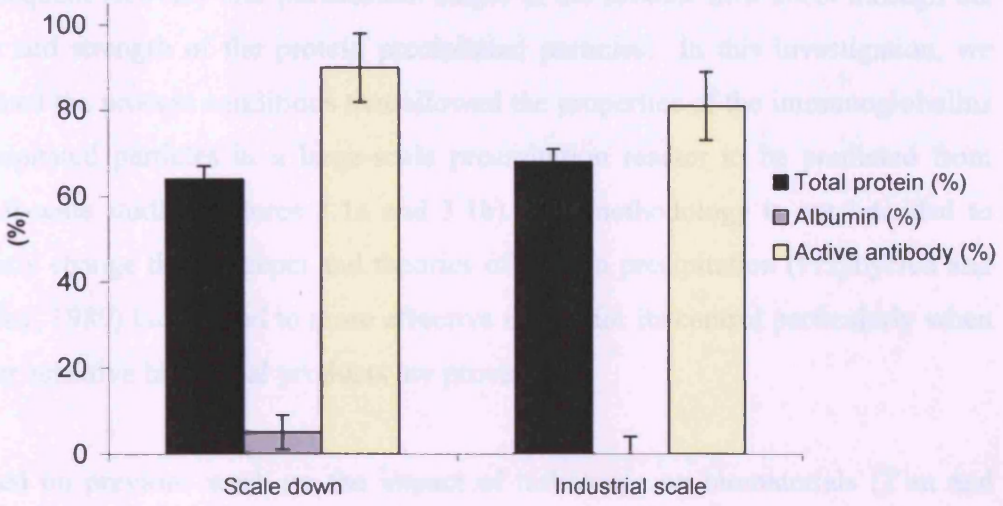

Figure 3.8b Mass balance showing the quantities of total protein (%), albumin (%) and active antibody (%) in the final product (sample point 6)

3.4 Discussion

3.4.1 Precipitation

The recovery of the immunoglobulin fraction from the serum solution containing other biomolecules must ensure conditions, which avoid damage to the protein product. Precipitation is an attractive option that is capable of rapidly isolating the desired product and bringing about product concentration and fractionation simultaneously. The precipitation step also impacts on the efficiency of any subsequent recovery and purification stages in the process flow sheet through the size and strength of the protein precipitated particles. In this investigation, we defined the process conditions that allowed the properties of the immunoglobulins precipitated particles in a large-scale precipitation reactor to be predicted from small-scale studies (figures 3.1a and 3.1b). The methodology is not intended to greatly change the concepts and theories of protein precipitation (Przybycien and Bailey, 1989) but to lead to more effective means for its control particularly when shear sensitive biological products are processed.

Based on previous work on the impact of turbulence on biomaterials (Yim and Ayazi Shamlou, 2000; Henzler, 2000; Kieran, et al. 2000), it was hypothesized that the physical properties of the precipitated particles at the end of the aging process were determined primarily by the total fluid stress, E_f, acting on the particles during the conditioning stage. Assuming that fluid stress is equal, or directly proportional to the fluid energy dissipated in the liquid by the impeller, then E_f was defined as the product of the power input by the impeller, P, per unit volume of suspension, V, and the aging (conditioning) time, t. Thus, $E_f = \varepsilon_v t = [(P/V)t]$. The group $(\varepsilon_v t)$ with the units of Nm^{-2}, may be thought of as a "time-integrated fluid stress" acting on the particles in the aging process and gives a measure of the total work done on the particles during this period. Previous work in our laboratories (Bell, et al. 1982a and 1982b) and elsewhere have used the concept of Camp number, defined as the product of the average shear rate, G, in the precipitating vessel and aging time, t, to correlate experimental data. For a Newtonian system the dimensionless Gt is related to $\varepsilon_v t$ through the kinematic

viscosity. It is proposed that the physical basis of the time-integrated fluid stress, ($\varepsilon_v t$), provides a more rational basis for comparing and correlating experimental results and here we used this approach to compare data from the two scales of precipitation. In both scales the calculation of the operating Reynolds number showed that flow was fully turbulent and power input was obtained from a standard power-curve for each impeller. Suspension viscosity, density and solids contents were measured as described in section 2.2.2 and particles size analysis was performed on samples removed from different points in the process (figures 3.1a and 3.1b). In table 3.1 physical properties are presented for the two scales of precipitation vessel operating at an equal time-integrated shear stress. The data in table 3.1 refers to samples taken at the end of the aging period and prior to the first step centrifugation (sampling point 2 figures 3.1a and 3.1b). Figure 3.2 shows the corresponding size distribution of the immunoglobulins precipitated particles for the two scales. Excellent agreement is observed between the two scales of precipitation. These experiments were carried out at a constant time-integrated fluid stress of $2.6 \times 10^6 Nm^{-2}$, which was calculated based on an aging time of 15h and an operating power input per unit volume of $48.5 Wm^{-3}$, representing the conditions in the large scale precipitation tank. Using the ultra scale-down process, we carried out additional experiments in which E_f was maintained constant for different combinations of P/V and aging times, t. Particle size distributions thus obtained for constant E_f were comparable demonstrating the general applicability of the concept of time-integrated shear stress.

3.4.2 Centrifugation

The plots in figure 3.3 represent the size distribution of samples before (sample point 2, figure 3.1a) and after (sample points 4 and 6, figure 3.1a) the two centrifugation steps. The data refer to samples obtained from the full-scale operation and demonstrate a significant shift in the size distribution towards smaller sizes occurring as the material passes through the first centrifuge. It is notable that the second centrifuge has negligible impact on the size distribution confirming that particle size is determined mainly by the aging conditions and the first stage centrifuge. The SDS-PAGE gel analysis of samples (figure 3.4) allowed the contents of the solids and supernatant streams to be visualised and tracked.

Comparison of samples 1 and 3 shows that a large fraction of the contaminating albumin protein is removed from the immunoglobulin product during the precipitation and first stage centrifugation and according to samples 3 and 6 further albumin is removed during the resuspension and second step centrifugation steps. The remaining contaminating components seen in sample 6 are removed by further downstream processing following treatment with papain. Additionally, these gels indicate that there is no detectable antibody present in the supernatant (Lane 3) of the first centrifuge and mass balances by ELISA carried out on immunoglobulins showed only a small amount of loss of binding (see later discussion).

As described below, we used the ultra-scale down process flowsheet (figure 3.1b) to mimic the large-scale process. Previous work on protein precipitates (Mannweiler and Hoare, 1992) using a disc stack centrifuge concluded that breakage of precipitates occurred in the entrance zone of the centrifuge. This has also been confirmed recently for a multichamber-bowl centrifuge (Boychyn, et al. 2000). The breakage of the feed material increases the proportion of fine particles causing a reduction in the separation performance of the centrifuge (Maybury, et al. 1998). The difficulty in using a conventional laboratory centrifuge to predict the consequences of such breakage on the performance of an industrial centrifuge is that unlike the former, shear damage in the latter is practically negligible since the fluid in the laboratory centrifuge is at rest relative to the centrifuge tube. An approach, which overcomes this difficulty, has been recently reported (Boychyn, et al. 2001; Boulding, et al. 2002). The methodology used to obtain the necessary information is briefly as follows. For a given set of operating conditions, the velocity field and the associated hydrodynamic parameters such as shear rates, energy dissipation rates and shear stresses in the full-scale centrifuge are mapped out by using computational fluid dynamics (CFD) analysis of the prevailing flow. Using CFD simulations the regions of highest energy dissipation rates in the centrifuge are identified. A small laboratory device consisting of a 30mm rotating disc housed in a 40mm diameter, 20mm height, cylindrical chamber described previously (Levy, et al. 1999) is used to create flow conditions inside the chamber that accurately produce the highest predicted energy dissipation rates in the full-scale centrifuge. A small quantity, typically 30ml, of the process material is

subjected to the predetermined flow environment in the chamber of the rotating disc device and the resulting suspension is treated in a standard laboratory centrifuge. In the present study, we used the above protocol with a standard laboratory centrifuge (Beckman J2, UK) equipped with a set of swing out bucket rotors (type J13.1). The Beckman centrifuge was operated at a Q/Σ ratio (Boychyn, et al. 2001) equal to that used in the full-scale centrifuge. Each run was repeated twice and the material pooled and suspended in 18% (w/v) sodium sulphate solution for analysis.

CFD simulations of the entrance region of the disc stack centrifuge are shown in figure 3.5. These simulations indicated that the maximum energy dissipation rate in the centrifuge was in the order of $5x10^4$ WKg^{-1}. We carried out ultra scale-down experiments using the swing out bucket laboratory centrifuge and the rotating disc shear device operating under conditions that matched the maximum energy dissipation rate in the disc stack centrifuge. The results are shown in Figure 3.7 and demonstrate that the laboratory centrifugation on its own fails to mimic the performance of the disc stack centrifuge. However, by shearing the sample in the small scale rotating disc device followed by centrifugation in the swing out centrifuge operating at an equal Q/Σ ratio to that used in the full scale centrifuge it was possible to achieve results that were in excellent agreement with the full-scale unit.

Examination of the size distribution plots in figure 3.6 also shows no significant differences in the size distribution of precipitated particles for solid samples taken at points 4 and 6 (figure 3.1b). This agrees very well with the results shown in figure 3.3 (for samples points 4 and 6, figure 3.1a) and confirms the general applicability of the proposed ultra scale-down approach.

These results are also consistent with previous observations on breakage of precipitates and particles in turbulent flow fields, which suggest that, in these cases the size of the particle that survives an imposed turbulent flow environment is uniquely determined by the intensity of the prevailing fluid stresses. Significant structural changes occurring during the conditioning stage cause the compaction

of the particle and, in the case of precipitate particles, previous work has shown that the degree of compaction is not uniform within the structure. Most particles tend to posses a hard core and a relatively loose structure on the outer region. In a high intensity flow environment, such as that of the centrifuge, the size the particle reduces rapidly as the outer loose structure is removed rapidly by the prevailing fluid stresses. As the outer mechanically weak layers of the particles are removed a point is reached at which mechanical strength of the surface exceeds the magnitude of the imposed fluid mechanical stress. The result is a pseudo-equilibrium size which is determined by the balance of these two forces. Based on the results shown in figures 3.3 and 3.6 it can be concluded that the physical properties of the precipitated antibodies are determined wholly by the aging (conditioning) process in the precipitation step and the first step centrifugation, the re-suspension and the second centrifuge steps have no detrimental impact on the size of the precipitate. The latter stages however have an important role in removing some of the residual contaminating proteins from the precipitate.

Component and total mass balances for the full-scale process flowsheet and its scale-down mimic were also carried out. The results are shown in figure 3.7 and 3.8. The differences observed between the two systems are within the measured level of error of the biological assays used. Comparing the data for the two flowsheets (figures 3.1a and 3.1b) it is notable that shearing of the antibody precipitate in suspension in the chamber of the rotating disc device causes some loss of activity. The differences between the two scales however is within the margin of error and taken together the results support the applicability of the proposed approach to scale-down of both the precipitation and centrifugation stages.

3.5 Conclusion

This chapter describes a new scale-down approach for the primary recovery of a therapeutic protein precipitate based on a full-scale process flowsheet. The process consisted of a sequence of four unit operations including a precipitation followed by a centrifugation, resupension and a final centrifugation step. Using millilitre quantities of process material a new approach was used to define the

important physical properties of the precipitate which impacted upon the recovery process. The results show that protein precipitate size distribution was critically influenced by the precipitation and first stage centrifugation step, the resuspension and second stage centrifugation had no effect on the size of the particles but were significant in removing more of the residual contaminating proteins.

In the case of (first stage) centrifugation, prediction of the performance of a disc stack centrifuge was achieved from the CFD analysis of flow in the full-scale unit combined with shear sensitivity data obtained from a small rotating shear device together with clarification data obtained from a standard laboratory centrifuge. The large scale precipitation step was successfully mimicked at small scale by using the concept of time-integrated fluid stress which was defined as the product of the power input per unit volume of suspension and the precipitation conditioning (aging) time in the reactor.

Taken together the results detailed in this chapter provide a basis for predicting the overall performance of a process by linking the sequence of operations within it via ultra scale-down techniques. Such an approach offers considerable advantages. For example, using millilitre quantities of process material, a series of scale-down tools, such as the rotating shear device, and CFD analysis of flow regimes in the full-scale equipment, process engineers will be able to rapidly assess potential process options for a range of drug candidates early in the development cycle of each drug and reduce the need to carry out numerous pilot-scale runs.

4 The Use Of Ultra Scale Down Mimics To Predict The Effect Of Changes To The Operating Conditions On The Characteristics Of Antibody Particles

4.1 Introduction

Once the initial industrial scale downstream purification process has been developed, trials are carried out in order to optimise the processing conditions. Due however to the constraints discussed in chapter 3 these optimisation trials are often short lived or non-existent. The majority of downstream purification processes are adaptations of old processes that have not been optimised for the new drug candidate. The use of ultra scale down mimics allows a process engineer to study process options cheaply and quickly. The results obtained can then be utilised when designing scale-up or process optimisation schemes.

This chapter describes the use of the ultra scale down mimics developed in chapter 3 to predict the effect that changes to the operating conditions of the purification stage will have on the process and on the characteristics of the process stream. Since the mimic has been verified as being accurate, by comparison with results obtained at an industrial scale, changes made to the operating conditions can be assumed with a reasonable degree of certainty to have the same effect on an industrial scale as they do when carried out with the ultra scale down mimic.

Four types of changes were made to the operating conditions of the precipitation reaction: solid sodium sulphate was used in the place of liquid, the mixing conditions were altered, the temperature of the precipitation reaction was increased and the effect of altering the percentage sodium sulphate was studied. The effects of these changes on the physical properties of the antibody particles (viscosity, density and percentage solids content, particle size distribution and resistance to shearing) were assessed, along with the effect on protein concentration in each phase.

4.2 Using Solid Sodium Sulphate Instead Of Liquid

The use of a solid precipitation agent, as opposed to a liquid one, immediately allows the scale of the operation to be doubled. For example, instead of adding 100L of 36% (w/v) sodium sulphate to 100L of serum to achieve a final concentration of 18% (w/v), 36Kg of sodium sulphate can be added to 200L of serum resulting in the same final concentration. Using a powder as the precipitation agent could effect the kinetics of the precipitation process. Chan, et al. (1986) demonstrated the effect that different precipitation agents have on the precipitation of soya protein. They concluded that the type of precipitation agent influences the precipitate particle formed. The mode and rate of addition of the precipitating agent also influence the reaction (Foster, et al. 1976) and different reagents have different precipitation kinetics (Chan, et al. 1986). For this reason it is necessary to fully investigate the effects of any change to the precipitating agent.

4.2.1 Methodology

200ml of serum were thawed overnight, 0.2μm filtered and placed in the scale down reactor. This was placed in a water bath and the serum was allowed to warm to 30°C. Once the correct temperature had been reached the impeller was set to 555rpm and 36g of sodium sulphate was added at a rate of 1.2g/min, in line with the hypothesised industrial procedure. Once all the sodium sulphate had been added, the impeller speed was increased to 1840rpm and the particles were allowed to condition for 15 hours. At the end of the conditioning period the antibody particles were sized according to the protocol outlined in section 2.3.4.1. The physical characteristics were also determined using the methods in section 2.3.1.

Following the particle size measurements, the antibody particles were sheared in the rotating disc device. 10ml of precipitated antibody solution were sheared at different levels of energy dissipation (shown in table 4.1) for one minute. The sheared material was then particle sized using the standard methodology.

Volts	Rotating disc speed (rpm)	Max energy dissipation (WKg^{-1})
0	0	0
6	10250	12000
8	16000	46000
10	18000	66000
12	20900	100000

Table 4.1 Rotational speed and associated maximum energy dissipation of the rotating disc device

The purpose of these experiments was to determine the impact, if any, of using solid sodium sulphate on the antibody particles characteristics. Additionally, the effect of shear stress on the antibody particles was assessed and predictions of the knock on effects that any changes would have on further downstream purification operations have been made.

4.2.2 Results

The particle size distribution of the particles produced during precipitation with solid sodium sulphate under scaled down conditions was measured and the results are shown in figure 4.1. The particle size distribution of the antibody particles produced by the standard scaled down liquid based precipitation is also included so that a comparison of the results can be made.

The use of solid rather than liquid sodium sulphate results in an increase in the size of the antibody particles from a d0.9 of 29.7μm to a d0.9 of 38.5μm (standard deviation +/-3μm at d0.9 (n=5)).

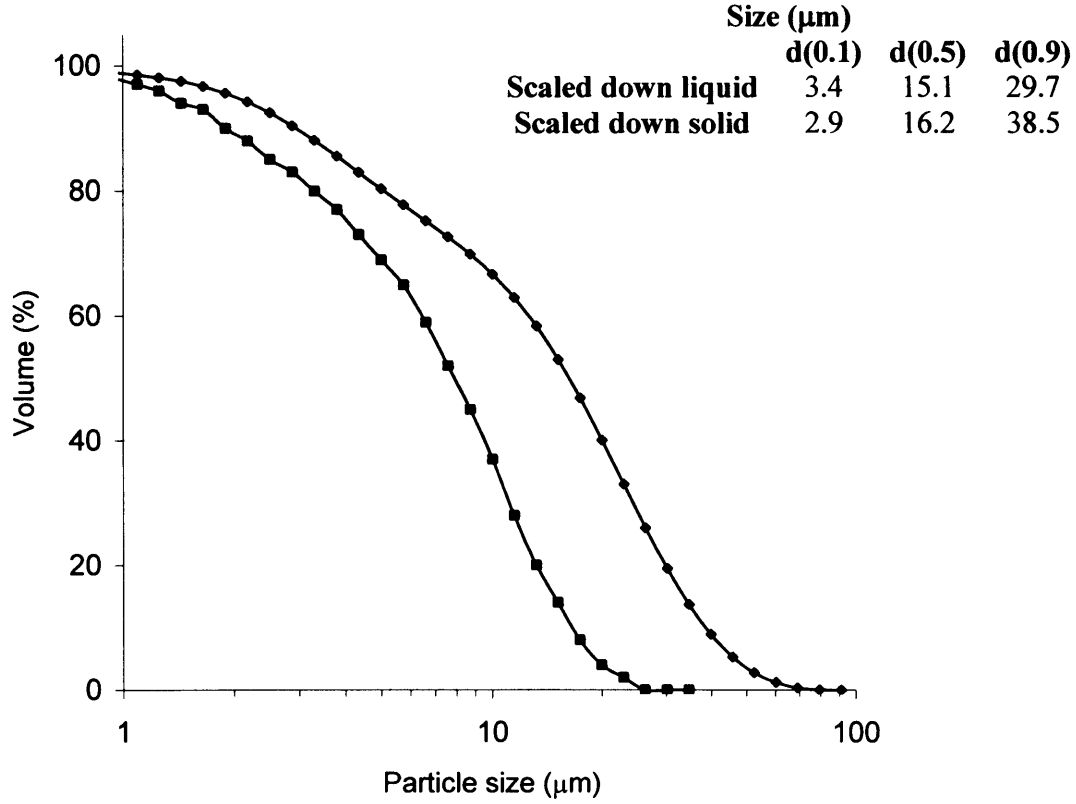

Figure 4.1 Comparison of the particle size distribution of the antibody particles produced with liquid sodium sulphate ■ and with solid sodium sulphate ♦ under the same mixing conditions

Table 4.2 is a comparison of the physical properties of the precipitant solution produced by the liquid and solid sodium sulphate precipitation systems. The use of solid sodium sulphate causes the viscosity of the solution to rise from 2.4mPa.s to 4mPa.s. The solids content of the feed stream also increased from 12% (v/v) to 25% (v/v). The density of the liquid and solid phases remained unchanged (standard error: Viscosity +/- 0.1mPa.s (n=5), Solids content +/- 1.3% (n=5), Density solid +/- 0.16g.cm^{-3} (n=5), Density liquid +/- 0.02g.cm^{-3} (n=5)).

	Viscosity (mPa.s)	**Solids Content (%)**	**Density solid (gcm^{-3})**	**Density liquid (gcm^{-3})**
Scale Down	2.4	12	1.3	1.17
Scale Down using solid precipitant at same Ef	4	25	1.3	1.17

Table 4.2 Physical properties of the antibody particles produced with liquid sodium sulphate and solid sodium sulphate under the same mixing conditions

The precipitate particles were exposed to various levels of shear in order to assess the impact. After exposure the particle size distribution was measured. The resulting particle size data is displayed in figure 4.2.

As the level of energy the antibody particles are subjected to increases so the particle size distribution decreases. Exposure to the highest shear rate results in a decrease in particle size from a d0.9 of 38.3μm to a d0.9 of 26.5μm (standard deviation +/-3μm at d0.9 (n=5)).

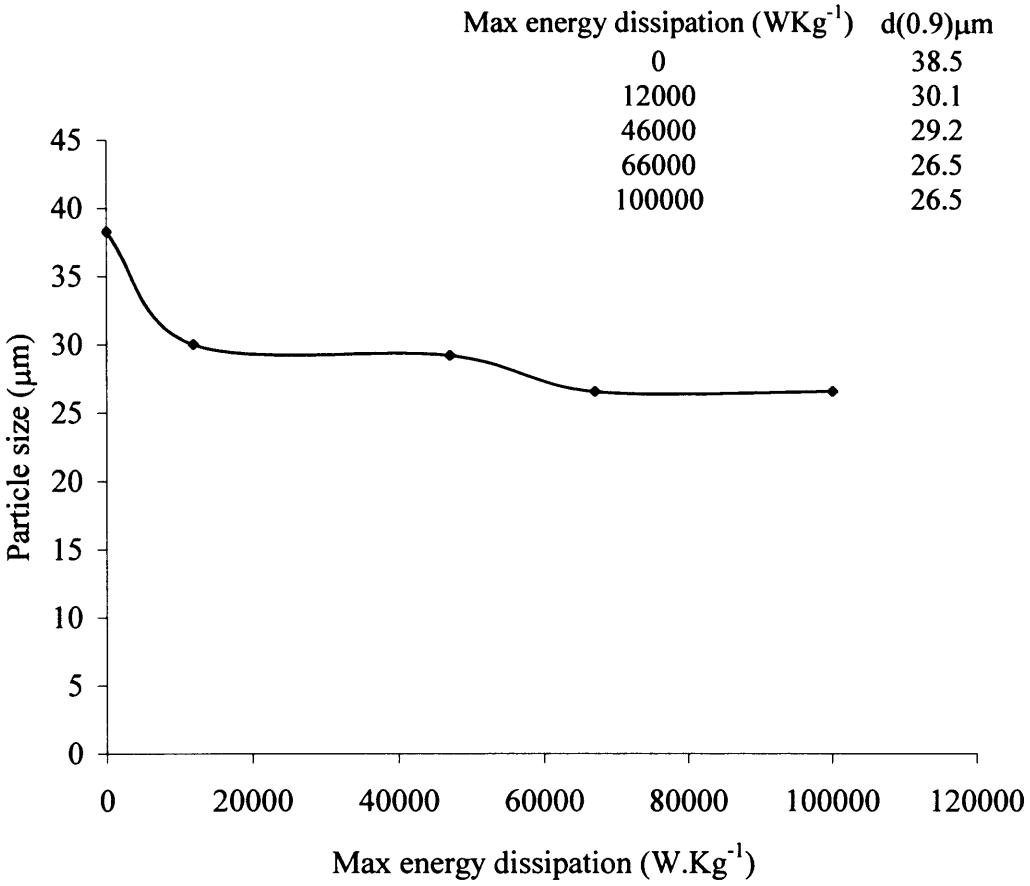

Figure 4.2 Particle size (d0.9) of the antibody particles produced during precipitation with solid sodium sulphate after being subjected to differing maximum energy dissipations in the rotating disc device for one minute

4.2.3 Discussion

It is known that the current scale of manufacturing will be unable to meet the forecasted level of demand for the anti-venom. Therefore, since the anti-venom production process has already been validated, methods of increasing the scale of production or the yield that are easy to implement and validate are of great importance. Using solid sodium sulphate offers the opportunity to double the production scale without having to purchase new vessels and equipment. Since the same basic methodology is utilised to purify the antibodies a bridging study need only be carried out to validate the process.

It can be concluded from figure 4.1 that the use of solid sodium sulphate as opposed to liquid sodium sulphate as a precipitating agent causes an increase in the particle size distribution of 30%. It is believed that the cause of this increase is the fact that the particles have a solid particle in the form of a sodium sulphate crystal to form around. The poor mixing conditions also contribute, resulting in earlier precipitation. This would make it easier for the particles to form and give them longer to grow during the low shear mixing phase resulting in larger particles.

During the addition of the powdered sodium sulphate it was observed that the mixing conditions were not turbulent enough to properly mix the two phases. Large clumps of un-dissolved sodium sulphate were observed at the bottom of the tank. It was also observed that the antibodies began to come out of solution at a lower concentration of precipitant (roughly 10%) than with the liquid version.

Mixing conditions within the precipitation vessel are an important factor; determining the physical characteristics of the particles (Hoare, 1982; Bell and Dunnill, 1982a&b).

It is hypothesised that this earlier precipitation is due to the formation of pockets of high concentrations of sodium sulphate within the vessel, caused by the poor mixing conditions. These pockets cause the premature precipitation of the

antibodies. This earlier precipitation could also be the cause of the larger particles since they would have longer to grow (Spielman, 1978). The particles would have more time to clump together during the addition phase, before the impeller speed is increased and the balance of growth verses shear induced particle break up changes.

From a process engineers perspective, larger particles are easier to separate by centrifugation (Bell and Dunnill, 1982b). This is shown by the following equation. The effective force acting on a spherical particle in a centrifugal field is given by:

$$F_1 = \frac{\pi}{6} d_s^3 \Delta p \omega^2 r$$

(equation 4.1)

Where d_s = the particle diameter, Δp = the density difference between the particle and the suspending fluid, r = the distance from the axis of rotation and ω = the angular velocity and is given by:

$$\omega = 2\pi n$$

(equation 4.2)

This equation indicates a cube relationship between the force acting on a particle and its diameter. Thus, even a small increase in the particle size, results in a large increase in the force acting upon it and hence its sedimentation rate.

By solving equation 4.1 the force acting on a particle 29.7μm in size was found to be $1.1 \times 10^{-9} Kg.ms^{-1}$. Assuming the distance from the axis of rotation is 1 and the speed of rotation remains constant at 125rps. When the particle size increases to 38.5μm, as is the case when solid sodium sulphate is used, the force acting upon these particles becomes $2.4 \times 10^{-9} Kg.ms^{-1}$ (the same assumptions as before were applied). The force has been more than doubled with only a 30% increase in particle size. This increase in the effective settling force acting upon the particle could impact the process time required during centrifugation (Leung, 1998). The time may decrease since the particles should settle out faster.

Table 4.2 indicates that the viscosity of the precipitant solution has increased from 2.4mPa.s to 4mPa.s when solid sodium sulphate is used as the precipitating agent. This increase in viscosity was most likely caused by the increase in solids content also observed. An increase in the viscosity leads to a decrease in the sedimentation velocity. This is shown by the equation below; settling velocity under gravity is determined by:

$$u_g = \frac{\Delta p d^2 g}{18\mu}$$

(equation 4.3)

Where g is gravity and μ is the viscosity.

Solving the above equation for the standard liquid precipitation system where Δp = 130Kgm^{-3} d = 29.7x10^{-6}m and μ = 0.0024Pa.s. gives a sedimentation velocity of 2.6x10^{-5}m.s^{-1}. Solving this equation for the solid based precipitation system where, Δp = 130Kgm^{-3} d = 38.5x10^{-6}m and μ = 0.004Pa.s. gives a sedimentation velocity of 2.6x10^{-5}m.s^{-1}. Therefore the increase in the force acting on the particle caused by the increase in particle size has been countered by the increase in viscosity. This results in particles that, although differ in size, should sediment out at the same velocity. The increase in viscosity will also result in increased pumping costs, another factor to take into account when implementing the process change.

Table 4.2 also shows that the solids content has risen to 25% when solid sodium sulphate is used. This may be due to the fact that solid material has been added to the mixture. As a result, some over precipitation of the albumin may be occurring due to the poor mixing conditions. This may cause local areas of high concentration. The industrial scale centrifuge used at Protherics has a solids holding capacity of 3L. Therefore when the feed is being pumped in at 120L/hr with the liquid precipitation process, the centrifuge needs to be discharged every 12.5 minutes in order to avoid breakthrough. For the solid sodium sulphate process, the centrifuge will need to be discharged every 6 minutes. This is a very small interval of time between discharge cycles. Discharging the centrifuge this

often may interfere with the normal operation. Also during the discharge cycle a small amount of feed material is lost and the centrifuge slows down slightly. This could result in lower yields. If this level of solids were to be processed by centrifugation, the feed flow rate would probably have to be slowed down. This may have knock on effects for the rest of the downstream processing operation such as increased turnaround time.

4.2.3.1 Impact of shear

When subjected to high levels of shear stress, protein precipitates tend to break up (Boychyn, et al. 2001; Neal, et al. 2003). Figure 4.2 reveals that the particle size initially decreases rapidly as energy dissipation increases, until at 66000WKg^{-1} the smallest particle size is reached. Above this level of energy dissipation no further degradation in particle size occurs. The d0.9 produced when the solid particles were exposed to a level of shear equivalent to that found in an industrial centrifuge and spun down at an equivalent Q/Σ as detailed in section 2.1 was 26.6μm. Compared to 13.4μm produced when the liquid system particles were sheared and spun down.

By solving equation 4.3 we can see that this degradation in particle size has altered the settling velocities. The solids system particles now settle at a rate of $1.2x10^{-5}m.s^{-1}$ whilst the liquid system particles settling velocity becomes $0.5x10^{-5}m.s^{-1}$. As a result of the shear stress encountered during centrifugation, the solid system particles now have a settling velocity more than double that of the liquid system particles. This means that in theory, they should be easier to separate. The reason that the solid system particles become easier to separate after centrifugation, is that they are more resistant to shear than those produced by the liquid system. Exposure to shear results in a 30% decrease in size after one minute for those particles produced by the solid system. Whereas exposure to shear for one minute causes a 55% decrease in size for those particles produced by the liquid system.

4.3 Using Solid Sodium Sulphate And Altering The Mixing Conditions

Observation of the reactor vessel whilst mixing the solid sodium sulphate into the serum revealed that the current mixing conditions were not turbulent enough to properly mix the solid and liquid phases. The scale down mimic was therefore used to assess the impact of altering the mixing conditions. The new mixing conditions are more turbulent, thus as a direct result the time integrated shear level was increased.

The aim of these experiments was to assess what impact changing the mixing conditions (to ensure good mixing) would have on the physical characteristics of the antibody particles and on their resistance to shear damage.

4.3.1 Methodology

200ml of serum were thawed overnight, 0.2μm depth filtered and placed into the scale down precipitation vessel. This was placed into a water bath and the serum was allowed to warm to 30°C. Once the correct temperature had been reached the impeller was set to 1840rpm and 36g of sodium sulphate were added at a rate of 1.2g/min, in line with the hypothesised industrial procedure. Once all the sodium sulphate had been added the solution was allowed to condition for 15 hours. This change in the mixing conditions had the effect of increasing time integrated shear stress level (Ef) from $2.6x10^{6}Nm^{-2}$ to $2.7x10^{6}Nm^{-2}$. At the end of the conditioning period the antibody particles were sized according to the protocol outlined in section 2.3.4.1. The physical characteristics were also determined using the method in section 2.3.1.

Once sized, 10ml of the precipitated antibody solution were sheared in the in house shear device at various energy levels as shown in table 4.1. The particles were subjected to each level of shear for one minute, after-which they were re-sized to assess the impact of the shear stress.

4.3.2 Results

By increasing the impeller speed, the balance of orthokinetic growth and shear induced break up of the precipitant particle was altered. Figure 4.3 shows the particle size distribution of the antibody particles, produced by the standard precipitation method, compared to those produced when using solid sodium sulphate and increasing the time integrated shear stress level. The particles produced at the increased shear stress level are significantly smaller than those produced by the standard method. The increased shear stress level particles have a d0.9 of only 7.45μm as opposed to the usual d0.9 of 29.7μm (standard deviation +/-3μm at d0.9 (n=3)).

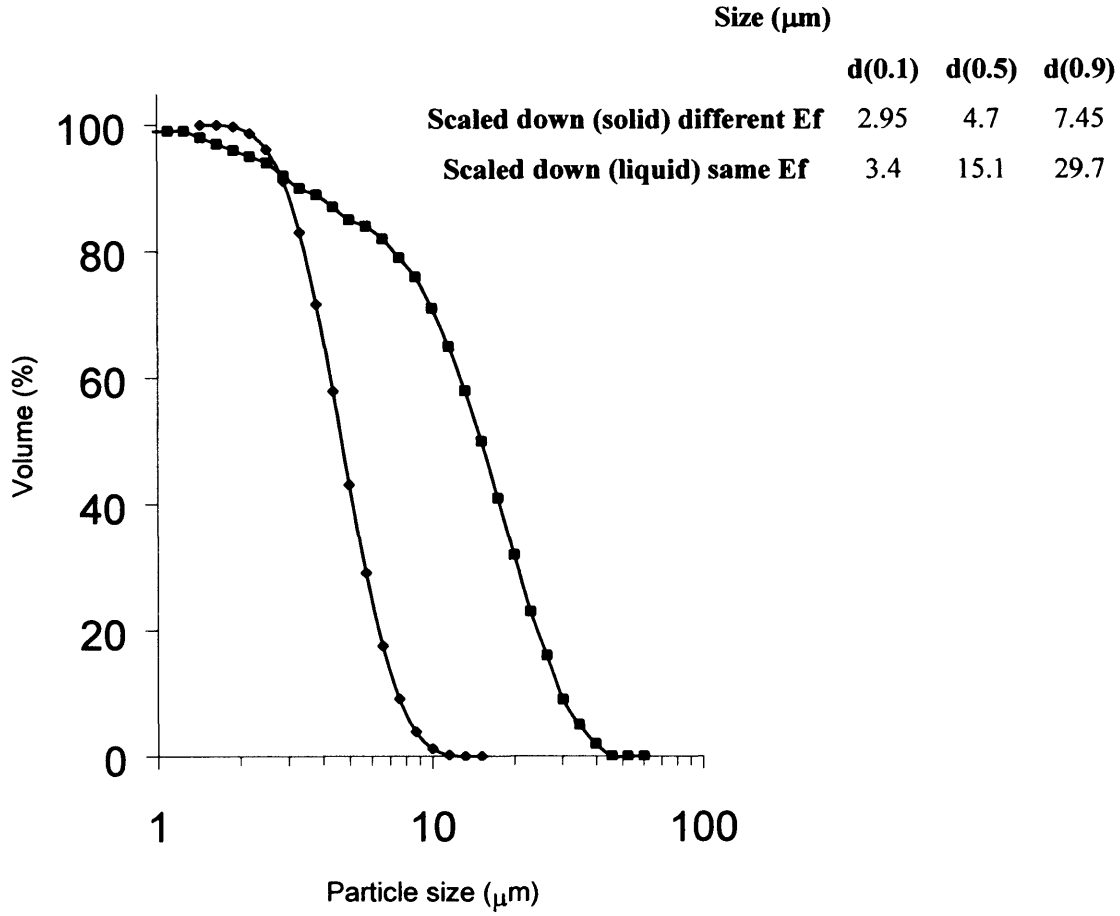

Figure 4.3 Comparison of the particle size distribution of the antibody particles produced using liquid sodium sulphate (■) and solid sodium sulphate with an increased time integrated shear stress level (♦)

The physical properties of the antibody particles were measured and the results can be seen in table 4.3. For comparative purposes the physical properties of the antibody particles produced by the standard liquid system are included. The change in the mixing conditions resulted in an increase in the viscosity from 2.4mPa.s to 3.4mPa.s. The solids content also increased from 12% (v/v) to 18% (v/v). The density of the solid and liquid phases remained unchanged (standard error: Viscosity +/- 0.1mPa.s (n=3), Solids content +/- 1.3% (n=3), Density solid +/- 0.16g.cm^{-3} (n=3), Density liquid +/- 0.02g.cm^{-3} (n=3)).

	Viscosity (mPa.s)	**Solids Content (%)**	**Density solid (gcm^{-3})**	**Density liquid (gcm^{-3})**
Scale Down	2.4	12	1.3	1.17
Scale Down using solid precipitant at different Ef	3.4	18	1.3	1.17

Table 4.3 Physical characteristics of the precipitated antibody particles produced with liquid sodium sulphate and with solid sodium sulphate at an increased time integrated stress level

The particles were subjected to various levels of shear stress. Afterwards the size distribution was measured. The results are shown in figure 4.4. The particle size distribution of the antibody particles, after they were subjected to shear stress, remained unchanged at (d0.9) of 7.5μm even after being subjected to the highest level of shear stress (standard deviation +/-3μm at d0.9 (n=3)).

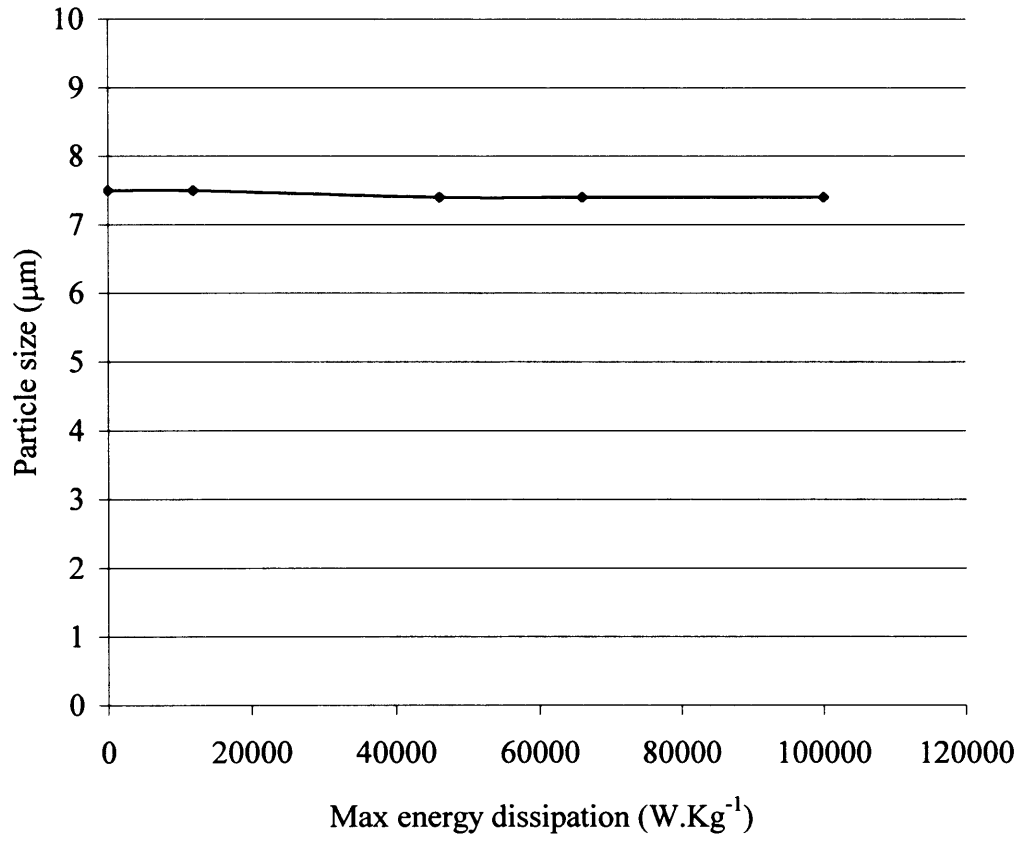

Figure 4.4 Particle size (d0.9) of the antibody particles produced during precipitation with solid sodium sulphate with altered mixing conditions after being subjected to differing maximum energy dissipation

4.3.3 Discussion

The final size of a precipitate particle is determined by the mixing conditions within the reactor vessel (Bell and Dunnill, 1982a; Hoare, 1982; Rothstein, 1994). The mixing conditions influence the balance of particle growth versus particle break up. It can be concluded from figure 4.3 that increasing the stirrer speed during the addition phase of the precipitation reaction results in a decrease in the size of the antibody particles by 75%. It is hypothesised that this decrease is a result of the increased turbulence and levels of shear present during the orthokinetic growth phase. This results in shear induced break up of particles playing a more influential role in the final particle size, resulting in smaller particles. Since the levels of shear are higher right from the start, the particles do not have the chance to form loose particles that are later degraded during the conditioning phase. The result is smaller particles. It was however observed that the increase in turbulence solved the problem of bad mixing; no clumps of un-dissolved sodium sulphate were observed and precipitation began to occur at 12% in line with the liquid precipitation system.

The effective force acting on particles can be calculated by solving equation 4.1. This shows that for particles 7.45μm in diameter the effective force is $1.7x10^{-11}$ $Kg.ms^{-2}$ compared to $1.1x10^{-9}Kg.ms^{-2}$ for the liquid system and $2.4x10^{-9}Kg.ms^{-2}$ for the solid system with out the altered mixing conditions. Taken at face value these figures show that the force acting on the liquid system particles, with the increased mixing conditions, is two orders of magnitude smaller than that acting on the other particles. This would make them harder to separate and increase the processing time. However both the viscosity and shear effects need to be taken into consideration.

Table 4.3 indicates that the viscosity of the final solution increased from 2.4mPa.s to 3.4mPa.s. The cause of this increase attributed to the addition of solid sodium sulphate. The viscosity is not, however, as high as the solid system with the standard mixing conditions. The decrease in particle size and increase in viscosity

results in a decrease in the sedimentation velocity to $1x10^{-6}m.s^{-1}$. This is an order of magnitude smaller than the other two precipitation systems.

Table 4.3 also shows that the solids content increased to 18% this decreases the discharge time in the industrial disc stack centrifuge from 12.5 minutes to 8 minutes, this length of interval between discharges should be long enough not to interfere with the normal operation of the centrifuge.

4.3.3.1 Impact of shear

Figure 4.4 shows that when the particles were subjected to shear no decrease in particle size was observed. This is probably because the conditions already experienced by the particles have strengthened them to the point that no further degradation occurs. Bell and Dunnil (1982b) concluded that the strongest particles result from a Gt of 10^5 and above. The Gt for this system is $8x10^6$. The result is that the sedimentation velocity should not be affected when the particles are pumped through an industrial scale disc stack centrifuge similar to the one mimicked in chapter 3.

4.4 Conclusion

Changing to solid sodium sulphate doubles the volume of serum that can be processed per batch without the need to purchase new equipment. Table 4.4 shown below summarises the particle size, viscosity and resulting sedimentation velocities of the three systems after the particles had been sheared.

Precipitation System	Particle Size (μm) (d0.9)	Viscosity (mPa.s)	% Solids content	Sedimentation velocity ($m.s^{-1}$)
Liquid	13.4	2.4	12	$0.5x10^{-5}$
Solid same mixing	26.6	4	25	$1.2x10^{-5}$
Solid altered mixing	7.45	3.4	18	$1.1x10^{-6}$

Table 4.4 Comparison of the antibody particles characteristics and sedimentation velocity after shearing

This comparison reveals that the particles produced by using solid sodium sulphate, without altering the mixing conditions, should be the easiest to separate. However, the large solids content may make disc stack centrifugation difficult and the poor mixing conditions could result in poor precipitation. The particles produced by the liquid system are next, but the volume would only be 100L per batch. The hardest particles to separate will be those produced by the solid system with the altered mixing conditions. This is the result of the smaller particle size coupled with the increased viscosity. All the factors outlined above plus commercial factors like pumping costs and time considerations need to be taken into account before any changes are made.

4.5 The Impact Of Increasing The Temperature During Precipitation

The effect on particle size distribution of raising the temperature of the precipitation reaction from 30^0C to 40^0C was studied. All other parameters were kept constant in line with the method in section 2.4.1.

According to equation 1.3 (section 1.3.1), at higher temperatures there will be a greater rate of collisions between particles during a precipitation reaction and hence a higher growth rate. This suggests that by increasing the temperature, the precipitation reaction should produce larger particles that will be easier to separate by centrifugation. Therefore the aim of the experiment was to determine the

impact of raising the temperature on the particle size distribution and on the resistance of the particles to the shear stress encountered during an industrial scale centrifugal separation.

4.5.1 Methodology

The precipitation reaction was run as per the method in section 2.4.1 except that the temperature was maintained at a constant 40^0C during the conditioning phase. At the end of the conditioning period the particles were sized as per the procedure in section 2.3.4.1. After-which they were subjected to shear conditions consistent with those found in an industrial scale disc stack centrifuge as per the method in section 2.4.2 and re-sized.

4.5.2 Results

At the end of the conditioning phase the particle size distribution was measured. Figure 4.5 is a comparison of the particle size distribution of the antibody particles produced at 30°C and at 40°C. As can be seen, increasing the temperature by 10°C causes the size of the particles to increase from 29.7μm to 46.2μm (standard deviation +/-3μm at d0.9 (n=3)).

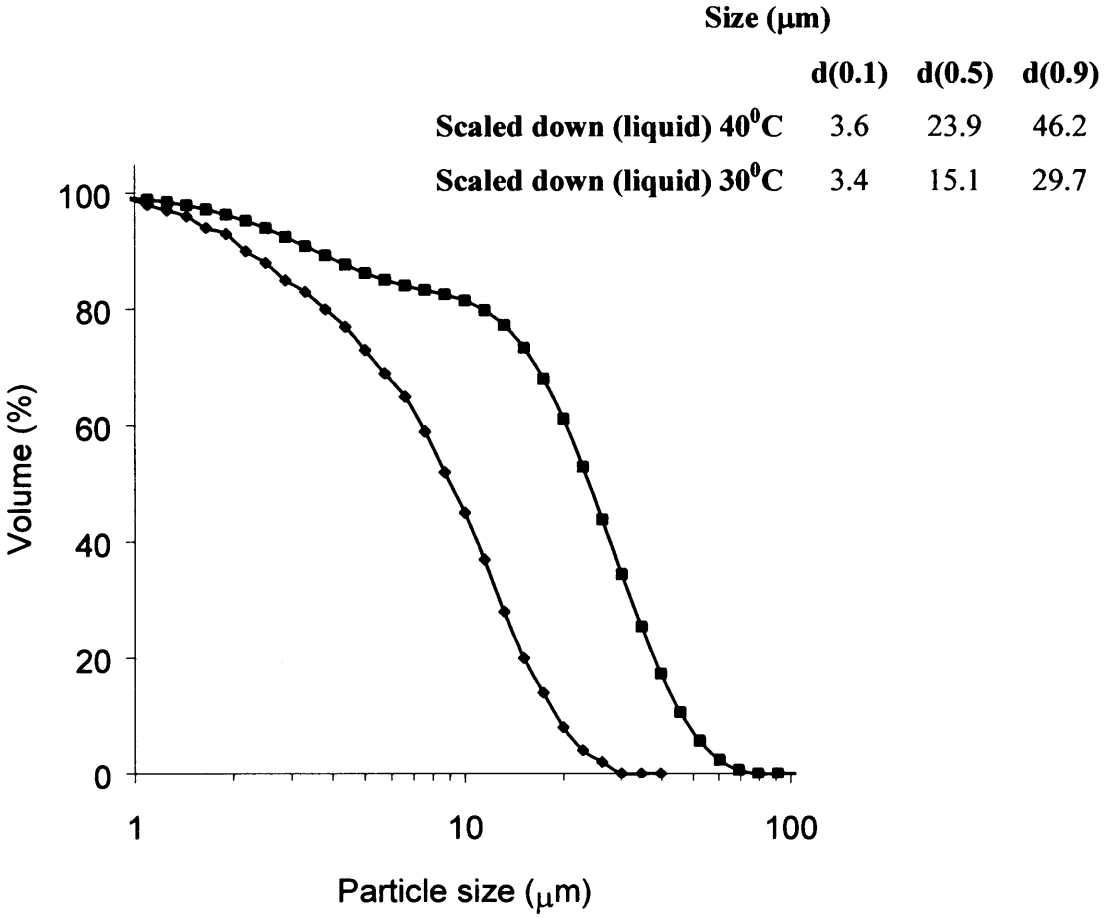

Figure 4.5 Comparison of the particle size distribution of the precipitated antibodies produced at 30°C ◆ and at 40°C ■

The antibody particles were exposed to a level of shear consistent with that found in the industrial scale centrifuge mimicked in chapter 3 and re-sized. Figure 4.6 is a comparison of the particle size distribution before and after shearing. After subjecting the particles to the same level of shear stress as found in an industrial scale centrifuge, the particle size distribution decreased from 46.2μm to 16μm (standard deviation +/-3μm at d0.9 (n=3)).

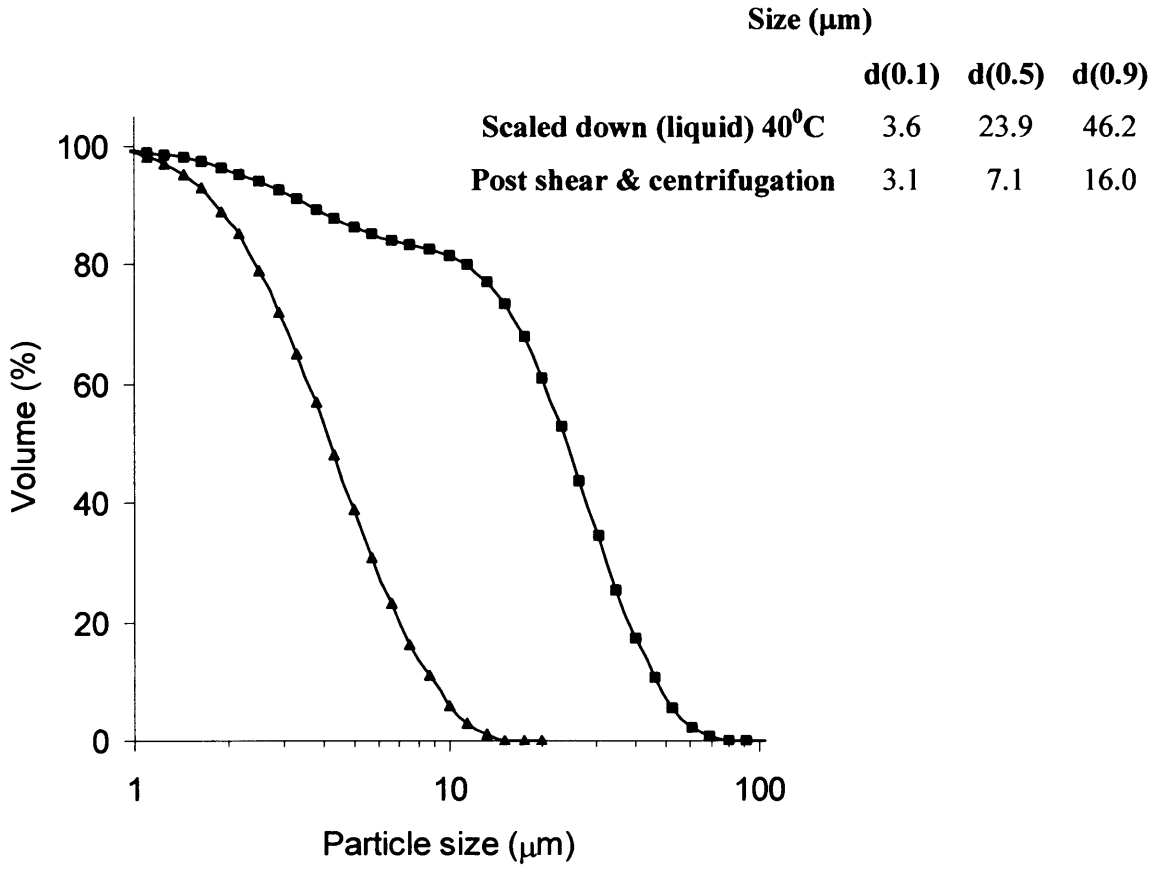

Figure 4.6 Comparison of the particle size distribution of the increased temperature antibody particles before, ■ and after, ▲ shearing with an air liquid interface followed by centrifugation in a swing out bucket centrifuge at the same Q/Σ as the industrial scale centrifuge

4.5.3 Discussion

As indicated by equation 1.3, increasing the temperature results in an increase in the particle size distribution, as shown in figure 4.5. Increasing the temperature by 10^0C results in a 35% increase in the particle size distribution. The extra energy provided by the higher temperature may have increased the number of collisions between precipitate particles, resulting in an increase in the growth rate. This increase in size has more than doubled the settling velocity from $2.6x10^{-8}m.s^{-1}$ to $6.3x10^{-8}m.s^{-1}$. At face value these particles would appear to be easier to separate from the mother liquor by centrifugation.

4.5.3.1 Impact of shear

Precipitant particles aged under the same conditions should have the same relative strength. Therefore subjecting them to the same level of shear stress should result in a decrease in particle size similar to that observed in chapter 3. Figure 4.6 indicates that when the particles were sheared at a level equivalent to that found in an industrial disc stack centrifuge and spun down at an equivalent Q/Σ value (section 2.4.2), the particle size distribution decreased by 65%. When the particles produced at 30^0C were exposed to the same conditions, a decrease in particle size of 55% was observed. This would seem to indicate that the particles produced at the higher temperature are not as strong as those produced at the lower temperature. This could be attributable to the fact that the increase in temperature results in larger particles, with particles that are loosely bound to each other. The degradation in particle size results in particles that are the roughly same size as those produced at 30^0C after shearing.

4.5.4 Conclusion

Although the increase in temperature increased the size of the particles, it lowered their resistance to shear stress; since exposure to shear resulted in a 65% decrease in size as opposed to 55%. This decreased resistance may be due to the fact that the extra energy present has resulted in the formation of particles that are more loosely packed than those formed at 30^0C. The conclusion to be drawn from these experiments is that increasing the temperature would have no impact on the

centrifugal recovery operation; heating the tank an extra 10^0C would merely increase the cost of the purification process.

4.6 Altering The Percentage Of Sodium Sulphate

The concentration of sodium sulphate used to precipitate out the antibody product is of critical importance to the success or failure of the purification operation. According to the Hofmeister series, sulphate is relatively effective at salting the protein out and should only destabilise the protein at relatively high concentrations. The experiments in this section examine the effect of varying the concentration of the sodium sulphate on the precipitation reaction and on the activity of the antibody of interest. The purpose of the experiments was to determine the optimum concentration of sodium sulphate for salting out the antibodies with out destabilising them.

4.6.1 Methodology

90ml of serum, thawed overnight and 0.2μm filtered was separated into 10ml fractions and placed into 9 separate test tubes. An equal volume of liquid sodium sulphate at concentrations of 16, 20, 24, 28, 32, 36, 40 and 44% (w/v) was added slowly to each tube resulting in serum/sodium sulphate mixtures with the following concentrations: 8, 10, 12, 14, 16, 18, 20, 22 and 24% (w/v). Each test tube was mixed thoroughly by inversion and left for 30 minutes to allow the precipitation to take place. After the time had elapsed, the solid and liquid portions were separated by centrifugation in a Beckman J2-M1 centrifuge fitted with a swing out bucket rotor (JA 13) for 30 minutes at 13,000rpm. The solid and liquid phases of each concentration were then assayed for active antibodies, albumin and total protein content following the method detailed in section 2.3.1.

4.6.2 Results

The amount of antibody that binds anti-venom present in the solid phase was measured and the results are depicted in figure 4.7. This shows the concentration of active antibody in the solid phase increasing from zero at 8% and 10% to 38% at 12%. The concentration then levels out at around 75% until at 20% sodium sulphate the level drops to around 63%. The amount of active antibody in the supernatant is seen to decrease from 90% at 8% to 85% at 10% sodium sulphate then 60% at 12%. At 14% there are only 5% of the active antibody remaining in solution. Above this concentration there are no antibodies which bind anti-venom left in solution (standard error +/-9% active antibody (n=3)).

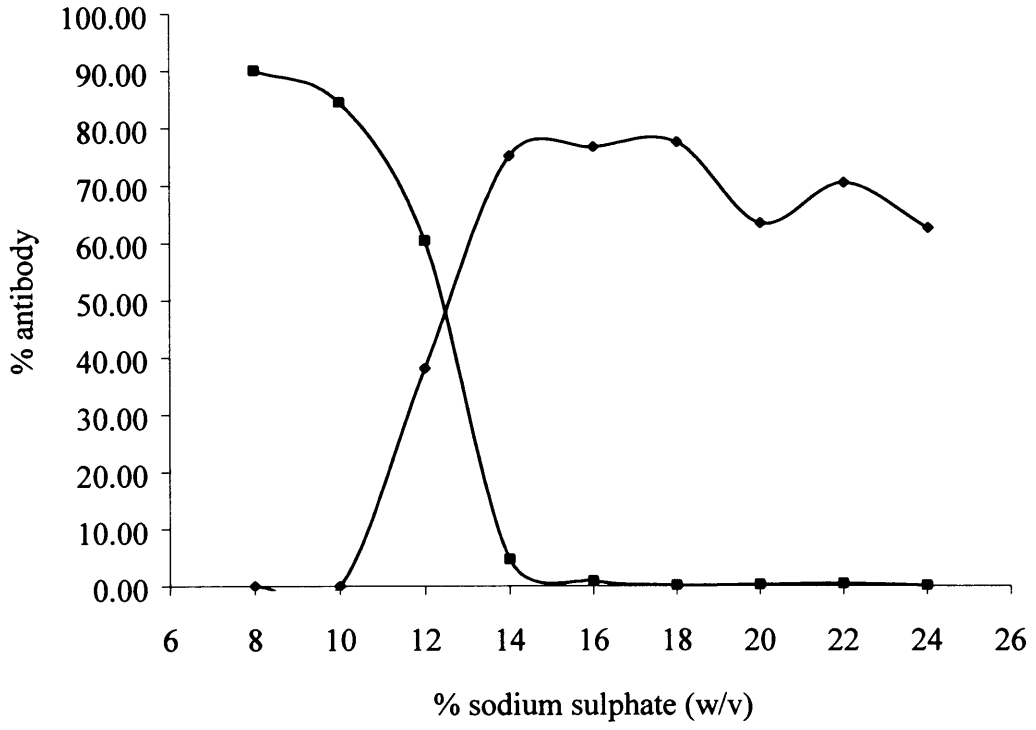

Figure 4.7 Percentage of active antibody present in the solid (♦) and liquid (■) phases at different concentrations of sodium sulphate

The amount of albumin present in the solid and liquid phases was measured and the results are shown in figure 4.8. The concentration of albumin in the supernatant starts at 40mg/ml. Then as the concentration of sodium sulphate increases, so the amount of albumin present decreases until at 24% sodium sulphate only 19mg/ml remains in solution. Juxtaposed to this, the concentration of albumin rises from 0mg/ml to 11mg/ml present in the solid phase at 24% sodium sulphate (standard error +/-0.1mg/ml (n=3)).

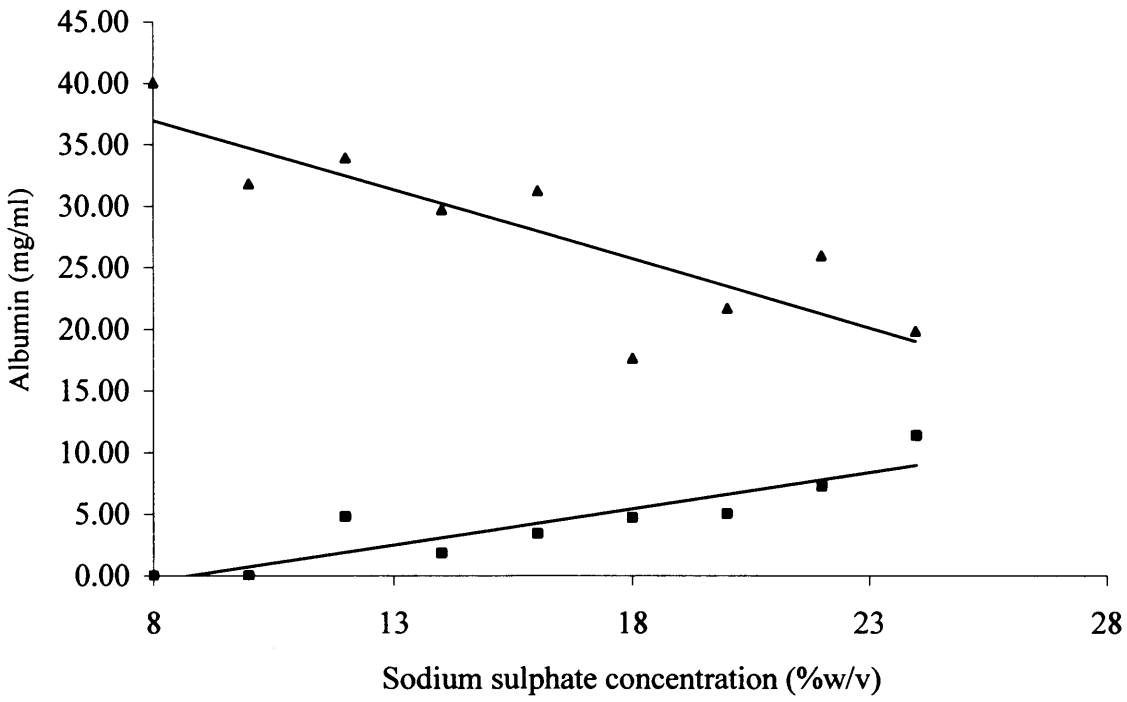

Figure 4.8 Concentration of albumin found in the solid (■) and liquid (▲) phases at different concentrations of sodium sulphate

The total protein content of each phase was measured and is shown in figure 4.9. The figure indicates that there is 75mg/ml of protein present at the start. As the concentration of sodium sulphate increases so to does the total protein level in the solid phase. At 24% sodium sulphate the solid phase contains 38mg/ml and the liquid phase contains 32mg/ml (standard error +/-0.3mg/ml (n=3))

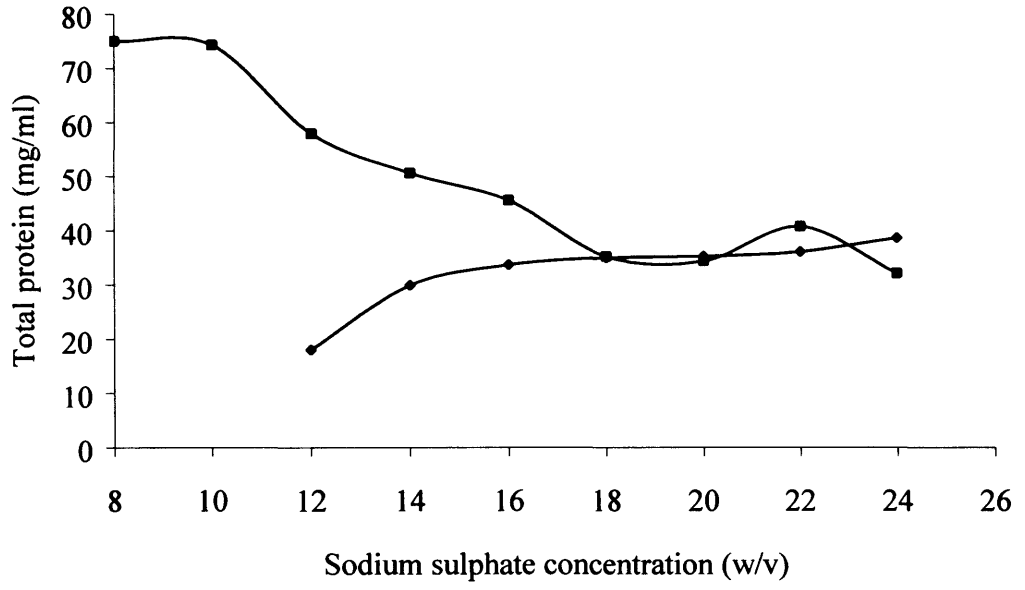

Figure 4.9 Total protein concentration in the solid (♦) and liquid (■) phases at different concentrations of sodium sulphate

4.6.3 Discussion

The amount of sodium sulphate required to precipitate the antibodies out of solution, without precipitating out an excess of contaminating proteins and without denaturing the antibodies has been investigated. As the first step in the purification process it is of critical importance that the efficiency and yield of the separation is as high as possible as well as the reproducibility.

4.6.3.1 Active antibodies

Precipitation reactions provide a quick and simple method of separating the product from the main contaminant (Bell, et al. 1983; Hoare, et al. 1983). The experiments described in this section looked at the process of the precipitation and sought to determine the optimum amount of salt.

Figure 4.7 shows how the antibodies respond to the addition of sodium sulphate. No precipitation occurs between 8 and 10%. However, at 10% saturation the assay reveals that 10-15% of the antibody has been permanently denatured. The samples were diluted to ensure that the sodium sulphate is not interfering with the assay and they were left for 24 hours to allow the antibody to refold into its normal conformation. (A control sample was tested after 24 hours to ensure that no loss of binding activity occurs as a result of the sample being left at room temperature). Thus any antibody not permanently denatured will be detected. It can be safely concluded then that 10% (w/v) sodium sulphate causes 10-15% of the product to be denatured, to the extent that it no longer binds to the snake venom and is therefore no longer biologically active.

Precipitation begins to occur at 12% (w/v). This is the point where supersaturation is just being reached and the "salting in" effect becomes one of "salting out" (Rothstein, 1994). At this point 38% of the antibody has precipitated out, 50% remains in solution and 10% is denatured. By 14% (w/v) 75% of the antibody is in a solid form, 5% remains in solution but 20% has been denatured. At 18% sodium sulphate, the concentration used at the industrial scale 76% of the antibodies have been precipitated, the other 24% have been denatured. The rise in salt of 4% has denatured the remaining active antibody without causing any

further precipitation. Above 18% the sodium sulphate denatures around 40% of the product. The level found in the solid drops to around 65% from 75%. Based on these results a concentration of between 14% and 18% would seem to combine the best recovery of antibody with the least amount of denaturation.

4.6.3.2 Albumin

The initial concentration of albumin in the sheep serum used for these experiments was found to be between 35mg/ml and 40mg/ml. This amount will vary from sample to sample since this is a biological system. In this particular instance the initial concentration was 40mg/ml. A process engineer will wish to see high concentrations of albumin in the liquid phase and only minimal amounts in the solid phase. This will indicate a good purification factor and is the main purpose of the step. Figure 4.8 reveals that up to concentrations of 10% sodium sulphate, no precipitation of albumin occurs. Some denaturation of the protein occurs at 10%, roughly 9mg/ml or 25% has been destabilised. This is seen as a drop in the level present in the liquid phase without an opposing rise in the level present in the solid phase.

Between 12 and 20% the majority (90% of the un-denatured) albumin remains in solution but the sodium sulphate causes some over precipitation, around 10% of the albumin can be found in the solid phase. Above concentrations of 20% the sodium sulphate starts to cause the albumin to precipitate out as well. A sharp rise in the amount present in the solid is seen coupled with a concurrent drop in the amount in the liquid phase. Although the albumin is more soluble than the antibodies, a large concentration of salt still causes it to come out of solution. Based on this assay, a concentration below 20% would seem to offer the best results, since the majority of the albumin remains in solution.

4.6.3.3 Total protein

The serum supplied by Protherics PLC contains between 65 and 80mg/ml of protein. Figure 4.9 which tracks the levels of total protein in each phase, reveals the precipitation process as it occurs. Up to 10% salt no precipitation occurs, at 12% there is a big drop in the amount remaining soluble. This is the point where

the antibodies begin to come out of solution. At 18% the levels of protein found in each phase are roughly equal. This result, coupled with the gels shown in chapter 3 demonstrates that other blood proteins are precipitating out. As a basic rule, proteins will precipitate out of solution in order of decreasing molecular weight (Rothstein, 1994). These proteins will need to be removed by further downstream processing. When 24% is reached it can be seen that the solid phase now contains more protein than the liquid phase. This agrees with the results from the other assays which show antibodies precipitating out and over precipitation of the albumin occurring at the higher concentrations.

4.6.4 Conclusion

The ideal precipitation reaction will remove 100% of the antibodies without denaturing them and without precipitating out any other proteins. Since this is not possible, a balance has to be struck between recovering the antibodies without denaturing them and keeping the albumin and other proteins in solution. The results presented in this section suggest that the optimum concentration of sodium sulphate would be between 16% and 18%. This combines the highest recovery of antibody with the lowest levels of albumin. The SDS-page gels shown in figures 3.5a and 3.5b further back up this conclusion, as they show the majority of antibody product in the solid process stream whilst the majority of the albumin remains in the liquid portion, when 18% (w/v) sodium sulphate is used as the precipitating agent.

4.7 Overall Conclusions

The results presented in this chapter demonstrate the power of scale down experiments to provide valuable process information without the need for large quantities of material. This section demonstrates that utilising solid sodium sulphate; changing the mixing conditions and increasing the temperature alter the kinetics of the precipitation reaction resulting in particles that have different characteristics. It was also determined that the optimum concentration of sodium sulphate for precipitation of antibodies from ovine serum is between 16 and 18%.

5 Separation Of IgG Precipitate From Contaminating Proteins Using Microfiltration

5.1 Introduction

Microfiltration, utilising a dead end filtration technique with a stirrer at the surface of the membrane, as a method to recover the antibody precipitate is an attractive process option, because potentially the current four-step centrifugal separation technique described in chapter three could be integrated into a single unit operation. This is desirable in terms of a possible reduction in process cycle time and an increase in the yield of antibody obtained from a reduction in the number of items of equipment used in the process. This chapter focuses on the use of microfiltration for separating the antibody precipitate.

Membrane separation techniques including microfiltration and ultrafiltration are used for the recovery and purification of many biological materials. Ultrafiltration is traditionally used for separation, concentration and buffer exchange operations involving macromolecules, typically less than about 100nm (Ayazi Shamlou, 2003). These include plasmids, viruses, therapeutic proteins and antibodies. In microfiltration, particle size is typically above 1μm, but normally less 10μm. These include cells, cell debris, protein precipitates and protein crystals (Davies, et al. 2000; Zeman and Zydney, 1996). In this chapter the suitability of microfiltration as a means of recovering, cleaning and concentrating anti-venom antibody precipitate from a serum suspension is assessed. The contaminants are mostly soluble proteins with albumin as the major component. A 200ml (working volume in the range of 75ml to 200ml) stirred cell device, equipped with a 3μm mixed cellulose ester membrane as the filter/sieving medium, was used to separate the anti-venom antibody precipitate from the protein contaminants. An advantage of the stirred cell device is that it allows adjustment of both the shear stress at the surface of the membrane and the transmembrane pressure independent of each other. The stirred cell device has been used in the past to mimic the microfiltration operation of biological materials (Hawrylik, et al. 1994; Kroner, et al. 1987;

Kroner and Nissinen, 1988; Langeloh, et al. 1998; Mercille, et al. 1994; Vogel and Kroner, 1999).

The performance of a membrane separation is affected by fouling of the membrane. Given the method of filtration (microfiltration) and the solids content of the feed stream used in this study, both fouling by adsorption of the contaminating proteins in the pores of the membrane and deposition and formation of a layer on the surface of the membrane are likely to cause clogging of the membrane, limiting continuous operation (Baker, et al. 1985; Belfort, et al. 1994; Chen, et al. 1997; Field, et al. 1995; Howell, 1995; Kelly and Zydney, 1996; Marshall, et al. 1993). This chapter describes how the stirred cell was used to determine the optimum load and wash volume for a batch filtration process and to obtain experimental flux data on the antibody precipitate as a function of time. The information was used to study the effectiveness of microfiltration as a separation technique and the performance of this method of separation was compared with that of centrifugation.

5.2 Methodology

All experiments were carried out with the same stock of anti-venom serum supplied by Protherics (Llandusul, Wales, UK). The stirred cell device described in section 2.4.4 was used to conduct load and wash volume determination experiments, the experiments were conducted under the operating conditions described in section 2.4.4.3. A new 3μm pore size cellulose acetate membrane 60mm in diameter was used for each experiment. It was first necessary to determine the optimum quantities of precipitated serum to load onto the membrane and the optimum volume of washing buffer to be used. The optimum volume is considered the volume which gave the highest antibody yield and best albumin removal within the limits of scale imposed by the stirred cell device.

Figure 5.1(A) shows the sequence of full-scale process operations currently used to recover large quantities of the immunoglobulins as discussed in chapter three. Figure 5.1(B) shows the proposed scale-down microfiltration process against which the industrial centrifugal process is compared.

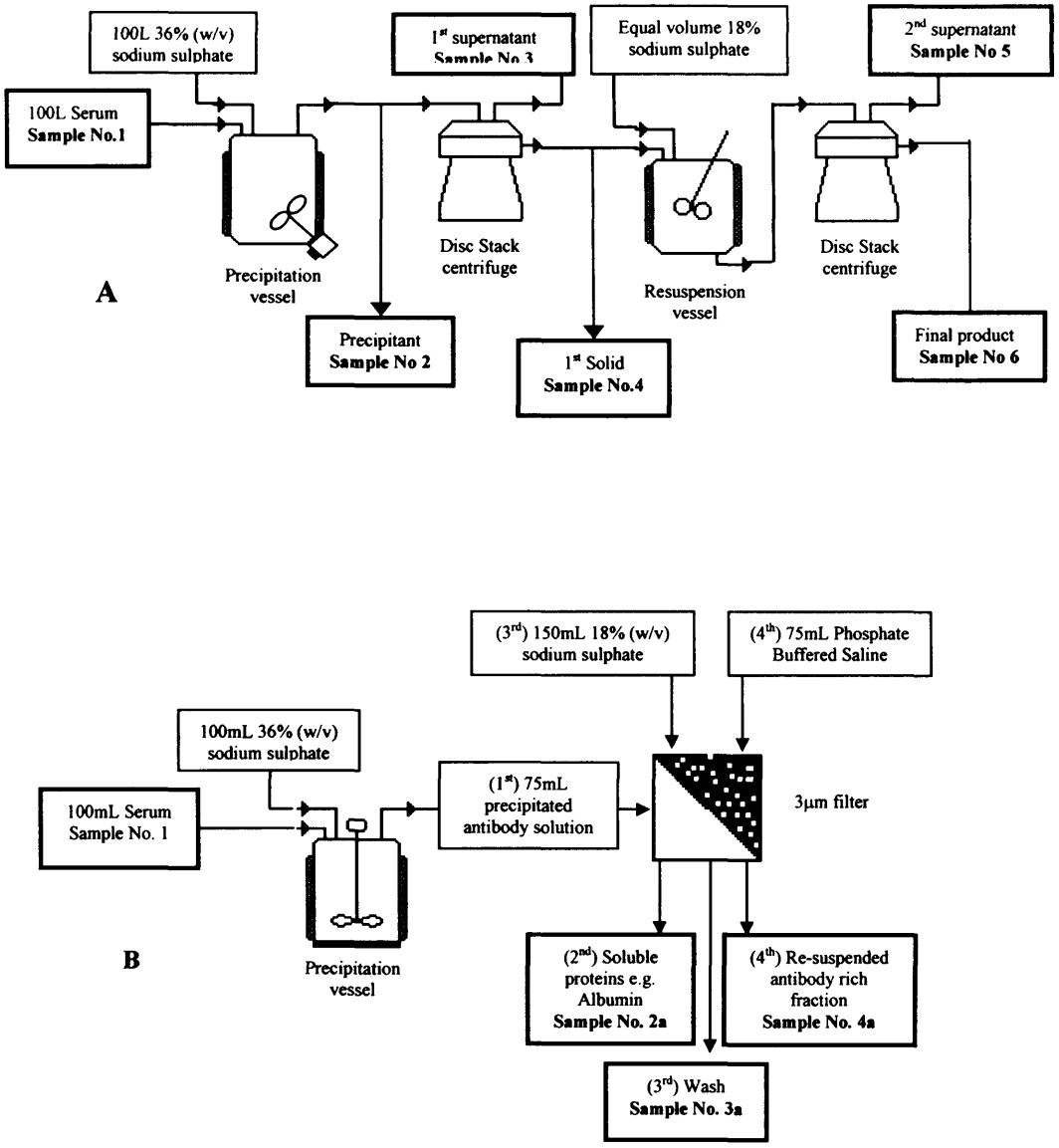

Figure 5.1 Process flow sheet detailing the initial serum purification at an industrial scale (A) and the proposed purification scheme utilising filtration (B)

Load and wash volume determination experiments, batch filtration experiments and continuous filtration experiments were conducted as per the methods described in section 2.4.3. Each sample collected was assayed for active antibody, albumin and total protein content. Sodium dodecyl sulphate polyacrylamide gel electrophoresis (SDS page) was also used to visualise the proteins within each sample as per the methods described in section 2.3.1.

5.3 Results

5.3.1 Load and Washing volume determination

Experiments were conducted with load volumes of 75ml and 100ml respectively and with wash volumes of an equal volume and two times the original load volume.

For the first experiment 100ml of precipitated serum was loaded onto the membrane and the precipitant cake was washed with 100ml of 18% (w/v) sodium sulphate. Samples were assayed for total protein, albumin and active antibodies. The mass balance depicted in figure 5.2 is derived from those assays. 85% of the antibodies were recovered and 20% of the albumin remains contaminating the final product after filtration (standard error: Total protein +/- 3% (n=5), Albumin +/- 5% (n=5), Antibody +/- 6% (n=3)).

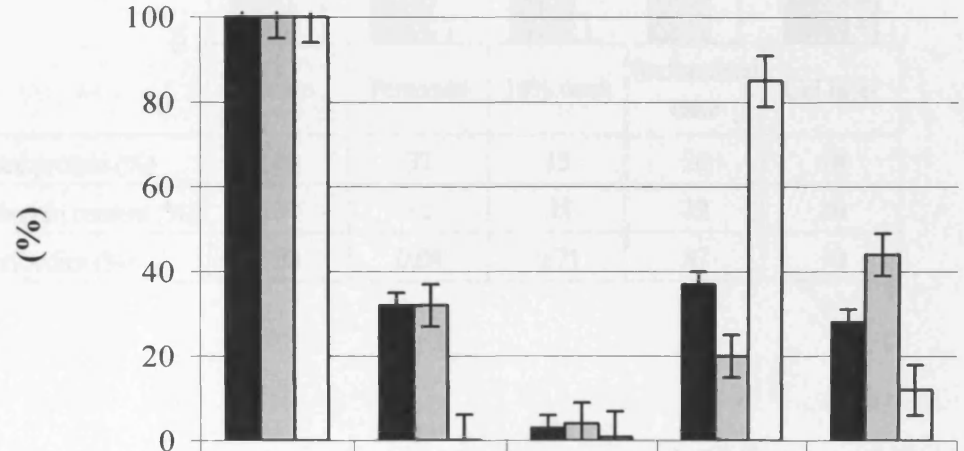

	Serum	Permeate	18% wash	Redissolved cake	Gel layer
Total protein (%)	100	32	3	37	28
Albumin content (%)	100	32	4	20	44
Antibodies (%)	100	0.1	0.9	85	12

Figure 5.2 Total protein, albumin and antibody levels in each fraction produced during the batch filtration of 100ml of precipitated antibody washed by the addition of 100ml of 18% sodium sulphate

The volume of washing buffer was doubled to 200ml and the batch filtration run again. Figure 5.3 shows the mass balance resulting form this experiment. 87% of the antibodies were recovered and 12% of the albumin remains in the final product (standard error: Total protein +/- 3% (n=5), Albumin +/- 5% (n=5), Antibody +/- 6% (n=3)).

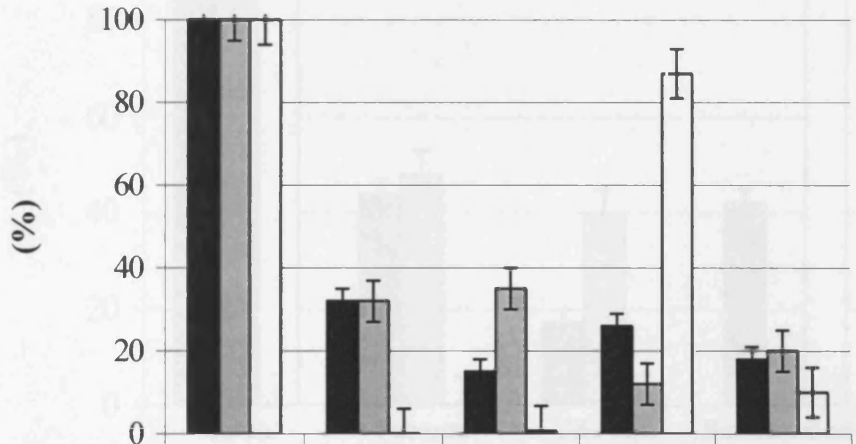

	Serum	Permeate	18% wash	Redissolved cake	Gel layer
■ Total protein (%)	100	32	15	26	18
▨ Albumin content (%)	100	32	35	12	20
□ Antibodies (%)	100	0.04	0.71	87	10

Figure 5.3 Total protein, Albumin and antibody levels in each fraction produced during the batch filtration of 100ml of precipitated antibody washed by the addition of 200ml of 18% sodium sulphate

Figure 5.4 is the mass balance for the batch filtration of 75ml of precipitated serum washed with 75ml of buffer. 94% of the antibodies have been recovered and 10% of the albumin is remaining in the final product after filtration (standard error: Total protein +/- 3% (n=5), Albumin +/- 5% (n=5), Antibody +/- 6% (n=3)).

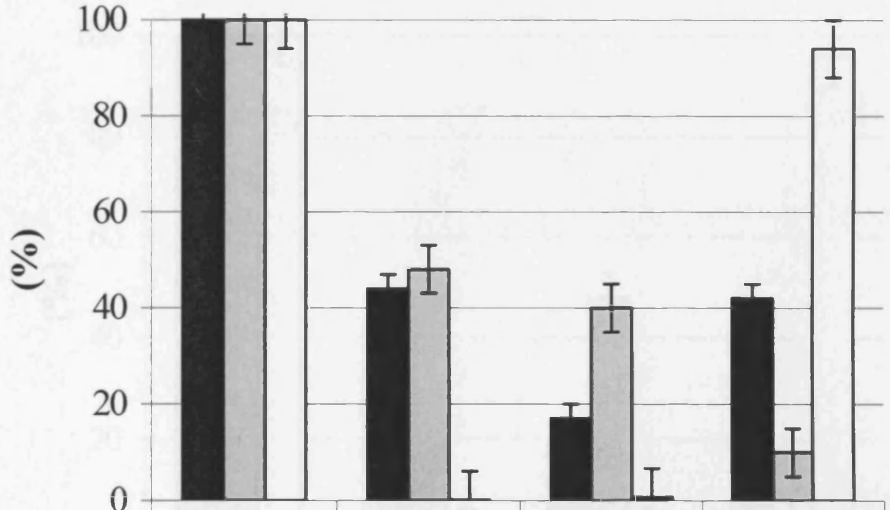

	Serum	Permeate	18% wash	Redissolved cake
■ Total Protein (%)	100	44	17	42
▨ Albumin (%)	100	48	40	10
□ Antibodies (%)	100	0.08	0.67	94

Figure 5.4 Total protein, Albumin and antibody levels in each fraction produced during the batch filtration of 75ml of precipitated antibody washed by the addition of 75ml of 18% sodium sulphate

In the final load and wash volume experiment 75ml of precipitated serum was loaded and 150ml of buffer was used to wash the precipitate cake in an effort to further reduce albumin contamination. Figure 5.5 reveals that the antibody yield is 96% and that only 3% of the albumin is left in the final product (standard error: Total protein +/- 3% (n=5), Albumin +/- 5% (n=5), Antibody +/- 6% (n=3)).

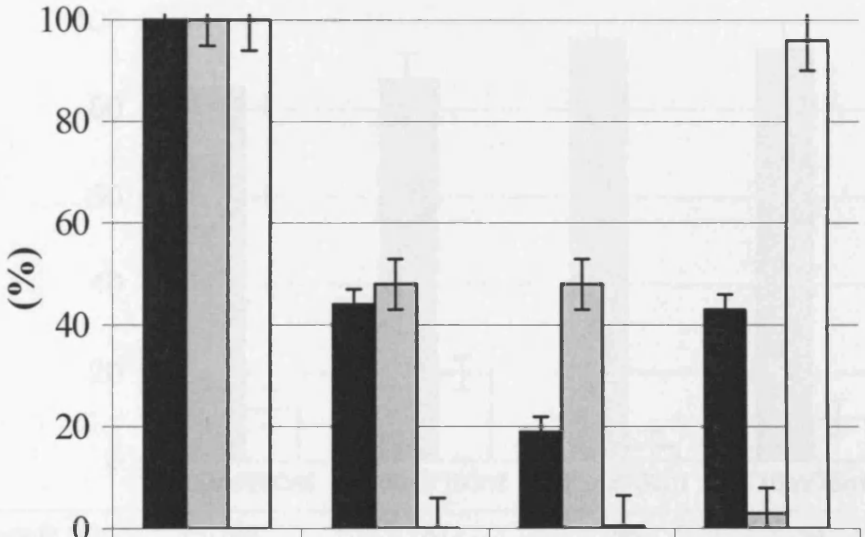

	Serum	Permeate	18% Wash	Redissolved cake
■ Total Protein (%)	100	44	19	43
▣ Albumin (%)	100	48	48	3
□ Antibodies (%)	100	0.06	0.56	96

Figure 5.5 Total protein, Albumin and antibody levels in each fraction produced during the batch filtration of 75ml of precipitated antibody washed by the addition of 150ml of 18% sodium sulphate

A direct comparison of the antibody yields and albumin levels from all the loading and washing volume determination experiments is shown in figure 5.6. Loading with 75ml and washing with 150ml gives the highest antibody yield and the lowest level of albumin contamination (standard error: Albumin +/- 5% (n=5), Antibody +/- 6% (n=3)).

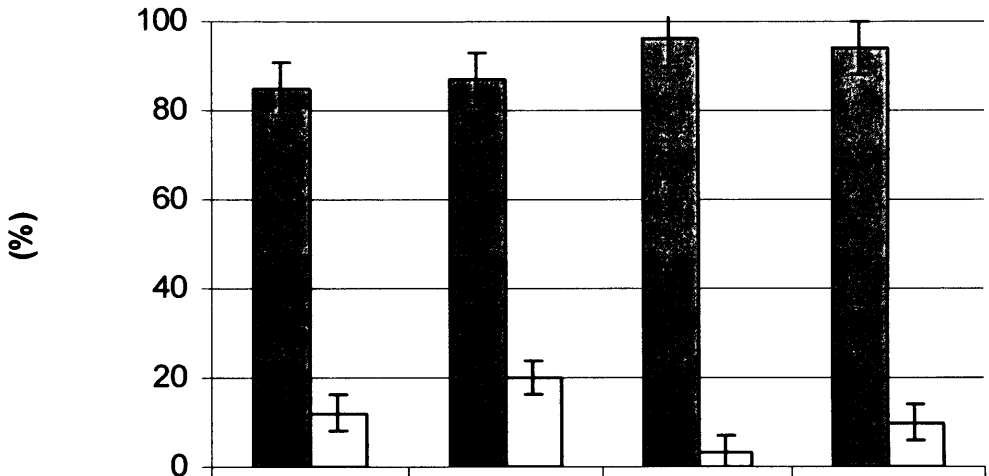

	100ml/200ml	100ml/100ml	75ml/150ml	75ml/75ml
■ Antibody yield (%)	85	87	96	94
□ % Albumin remaining	12	20	3	10

Figure 5.6 Overall antibody and percentage albumin remaining in the final product for each of the batch filtration experiments

5.3.2 Discussion

The amount of antibody precipitant loaded onto the membrane and the volume of buffer used to wash the precipitate particles will determine the yield of the process, in terms of antibody recovery and the degree of purification in terms of the amount of albumin removed. The load volume will also impact on the flux rate across the membrane, which will have a big impact on the process turn around time.

At the end of the filtration, when 100ml of precipitated serum (ratio of precipitated serum to membrane area = 3.5ml/cm^2) filtered and washed with 100ml of 18% (w/v) sodium sulphate, a gelatinous layer of protein was left un-dissolved on the surface of the membrane. Examination of the gel layer revealed it is a layer of glutinous protein that had formed on the surface of the membrane and remained in place after the washing step. The layer contained a large quantity (12%) of the original antibody content which is un-recoverable. It also permanently fouls the membrane as pure water flux rates after cleaning did not return to the pre-operation levels (data not shown). As a direct result of the formation of the gel layer, the final product contained 85% of the anti venom antibodies along with 20% of the original albumin content.

It was hypothesised that increasing the volume of washing buffer may help to dissolve the gel layer and therefore increase the yield and decrease the amount of albumin contaminating the final product. Figure 5.3 shows the mass balance for the batch filtration of 100ml of precipitated serum washed with 200ml of buffer.

Once again the gel layer forms at the surface of the membrane. It contained 10% of the antibody product however the levels of albumin are much lower. The final product also contains a lower level of albumin (12%). This amount of contamination is still higher that the current centrifugal process. So whilst it seems increasing the washing buffer volume had some effect, it did not solve the problem. As a result it was decided to lower the loading volume to 75ml of precipitated serum (ratio of precipitated serum to membrane area = 2.6ml/cm^2).

It can be seen from the mass balance shown in figure 5.4 that the gel layer has disappeared. It is suggested that at 100ml loading volume the membrane is overloaded and as a result the proteins at the membrane surface become compacted together during the course of the filtration. Therefore forming a glutinous un-dissolvable layer. At 75ml loading volume this does not occur. This may be the result of the decreased filtration time. Because the gel layer did not form, the yield rises to 94% and the albumin contamination falls to 10% in the final product. The level of recovery of antibodies is now in line with that seen in the scale-down centrifugal process. The levels of albumin contamination are still high, so again it was decided to increase the quantity of washing buffer.

The amount of washing buffer was increased to 150ml. (The mass balance is shown in figure 5.5). Immediately it is observed that the levels of albumin have dropped to 3% left in the final product.

5.3.2.1 Conclusion

Decreasing the amount loaded from 100ml to 75ml (a decrease in the volume of precipitated serum loaded to membrane area ratio of 3.5ml/cm^2 to 2.6ml/cm^2) resulted in a 10% increase in antibody yield and a decrease in the albumin contamination along with and increase in the flux rate from 99L/m^2/hr to 166L/m^2/hr. The increase in flux rate would result in faster processing times. Washing with double the volume of 18% sodium sulphate buffer also decreased the amount of albumin contaminating the final product. As a result it was decided that the optimum conditions for further filtration experiments within the limitations of the equipment would be to load 75ml of precipitant and wash the cake with 150ml of washing buffer.

5.3.3 Batch and continuous separation of precipitated IgG by microfiltration

The results detailed in this section have been published (Neal, et al. 2004). Microfiltration is an attractive separation option, particularly for protein precipitate in suspension, which may show susceptibility to shear-induced damage in centrifuges (Boulding, et al. 2002; Boychyn, et al. 2001). It is noted that shear rates at the surface of the microfiltration membrane can be high. For example, in tangential flow membrane separation, high linear fluid velocities and large transmembrane pressures are used intentionally to realise wall shear rates, typically in the region of $5x10^3s^{-1}$ to $1x10^4s^{-1}$ (Wilson, et al. 2003) in order to reduce the thickness of any deposited layer on the membrane surface. These values, however, are still typically an order of magnitude lower than shear rates that have been reported in industrial centrifuges (Boychyn, et al. 2001). It was hypothesised therefore that the hydrodynamic conditions in microfiltration are unlikely to cause damage to the antibody precipitate and no loss of product to the filtrate fraction should occur, provided the auxiliary pumps are selected to avoid shear damage during pumping of the suspension. In what follows we provide experimental data to test this hypothesis.

The choice of a 3μm pore size cellulose/acetate membrane filter medium was based on the size distribution of the antibody (precipitate) particles shown in figure 5.7 included below for reference. It is noted that the presence of the fines in the feed material had little impact on the performance of the filter. Measurements of the flux using pure water before and after filtration (data not included) indicated no evidence of permanent fouling of the filter medium.

5.3.4 Methodology

A stirred cell filtration device was operated in two different modes: batch and continuous. It has a diameter of 0.063m with a total volume of 200ml and was modified for use as a small-scale microfiltration device. A 3μm pore size cellulose acetate membrane 90mm in diameter (Millipore, Watford, UK) was cut to the correct diameter, as 3μm pore size membranes were not available in the correct

diameter. These were then placed at the bottom of the cell. The cell was equipped with a single paddle impeller (width = 4.3mm, height = 8.4mm, length = 49.6mm) positioned centrally in the cell in close proximity to the surface of the filter membrane. The shaft was driven from the top by a variable speed motor having a maximum speed of 242rpm. The rotational speed of the shaft was measured using a digital tachometer. The cell was hermetically sealed, once the lid was screwed in place, and was supplied with an air inlet and pressure control system allowing precise setting of the air pressure above the solution in the cell during operation.

Standard batch filtration tests were carried out as follows: 75ml of suspension containing the precipitated antibody was placed in the stirred cell. The rotational speed of the paddle was set at a pre-determined value and an air pressure applied. The permeate was collected (sample 2a, Figure 5.1b) until the permeate flow stopped and a filter cake formed on the membrane. In the second part of the test, the cake was washed, as described next. The operation was stopped, 150ml of 18% sodium sulphate (w/v) was added to the vessel and the paddle speed was set to the same speed as before. The mixture was stirred for ten minutes to break and resuspend the cake of precipitated antibody. The air pressure was re-applied and the filtrate was collected and measured every minute until the permeate flow stopped.

In diafiltration mode, 75ml of precipitated antibody was placed in the cell. The speed of the paddle was set at the pre-determined value and air pressure applied. A buffer solution of 18% sodium sulphate (w/v) was drawn in at the same rate that the permeate was collected, thus maintaining a constant level of liquid in the vessel. The flow of buffer was stopped after 150ml of buffer solution had been added and the operation switched to cake-filtration mode until the permeate flow stopped and a filter cake of the antibody precipitate formed. The 225ml of permeate was collected in three separate 75ml fractions for analysis.

The final step for both modes of operation consisted of adding 75ml of warm (37°C) phosphate buffered saline (PBS) pH 7.4 to the solid cake in the cell. The antibody rich filter cake was allowed to dissolve over approximately ten minutes.

The air pressure was applied as before and the antibody rich permeate collected for analysis.

5.3.5 Results

Figure 3.2 is reproduced below for ease of reference. The precipitate was produced under exactly the same conditions as described in section 2.4.1.

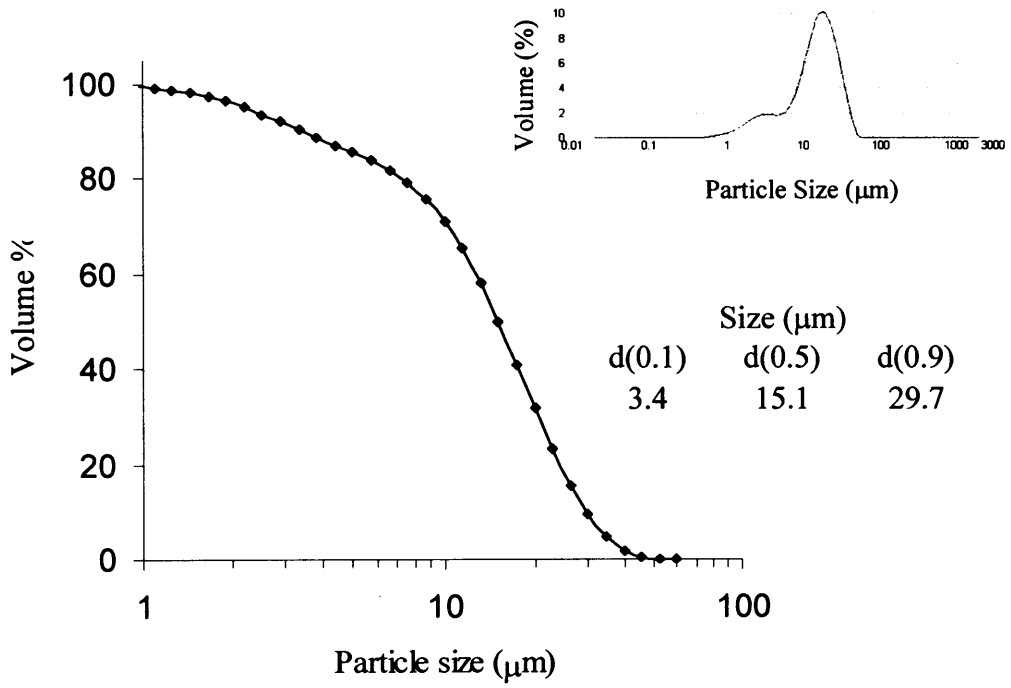

Figure 5.7 Particle size distribution produced during the precipitation of antibodies with sodium sulphate by a 1000 fold scale-down mimic equipment, operating at equal same time-integrated shear stress as the industrial scale (standard deviation +/-3μm at d0.9 n=5)(sample point 2, Figure 5.1a)

The permeate flux rate across the membrane was measured at intervals of one minute for three different pressures and three different stirrer speeds. Figure 5.8A is the flux profile at 0.5bar. It can be seen that the flux rate decreases rapidly and then levels out at roughly 40L/m^2/hr. The data also suggests that altering the stirrer speed did not affect the flux rate.

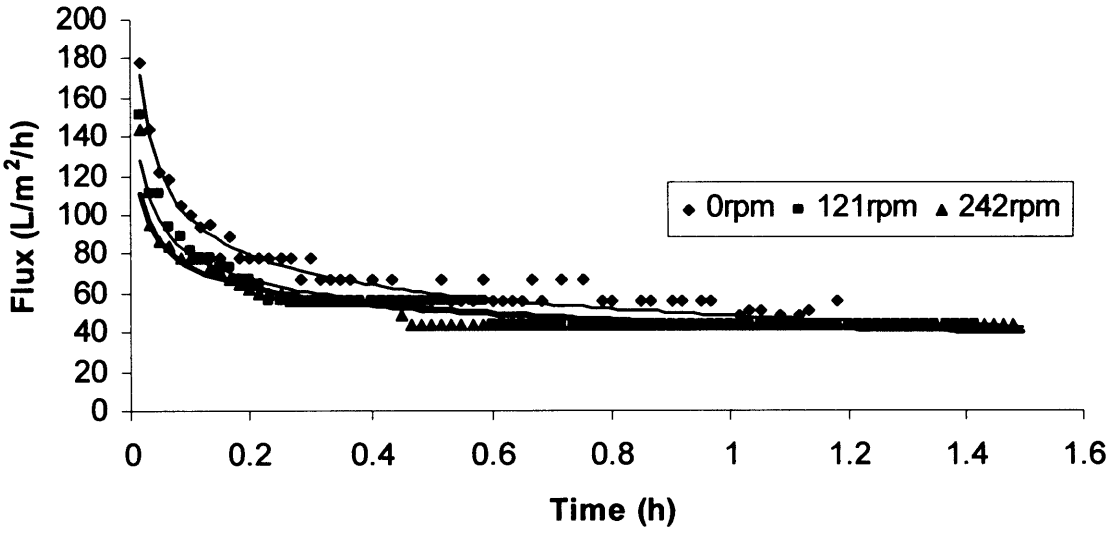

Figure 5.8A Comparison of flux rates measured at 0.5bar and different shear rates during diafiltration (standard deviation +/-5L.m^2.hr, n=3)

The applied pressure was increased to 1.0bar and the flux rate was again measured at one minute intervals. The results are shown in figure 5.8B, again the initial flux rate falls off rapidly and levels out at roughly 60L/m^2/hr.

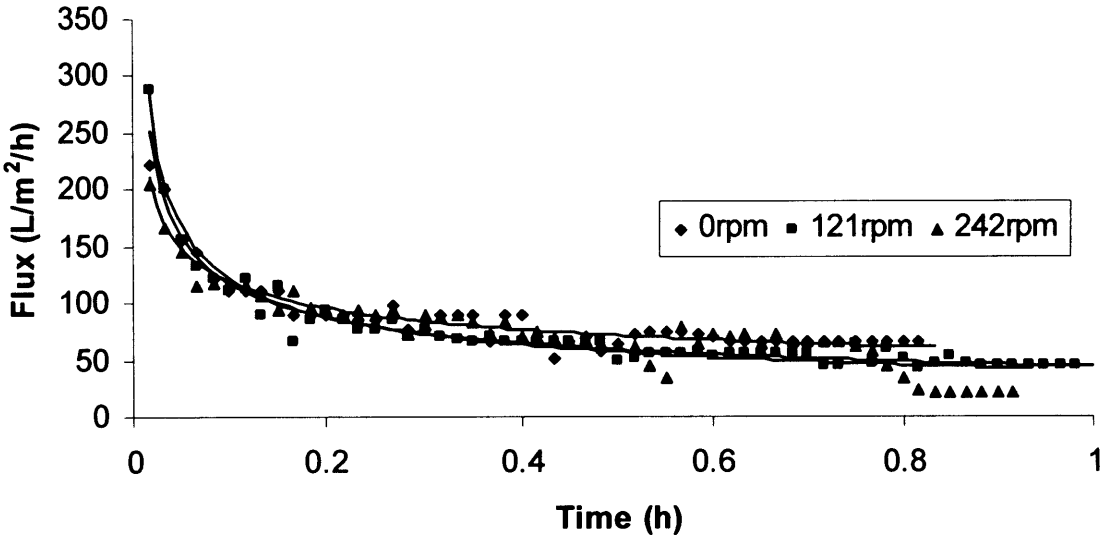

Figure 5.8B Comparison of flux rates measured at 1.0bar and different shear rates during diafiltration (standard deviation +/-5L.m^2.hr, n=3)

The pressure was finally increased to 1.5bar at the flux rate was again measured at one minute intervals. As shown in figure 5.8C the flux rate again decreases rapidly and levels out at around 40L/m^2/hr.

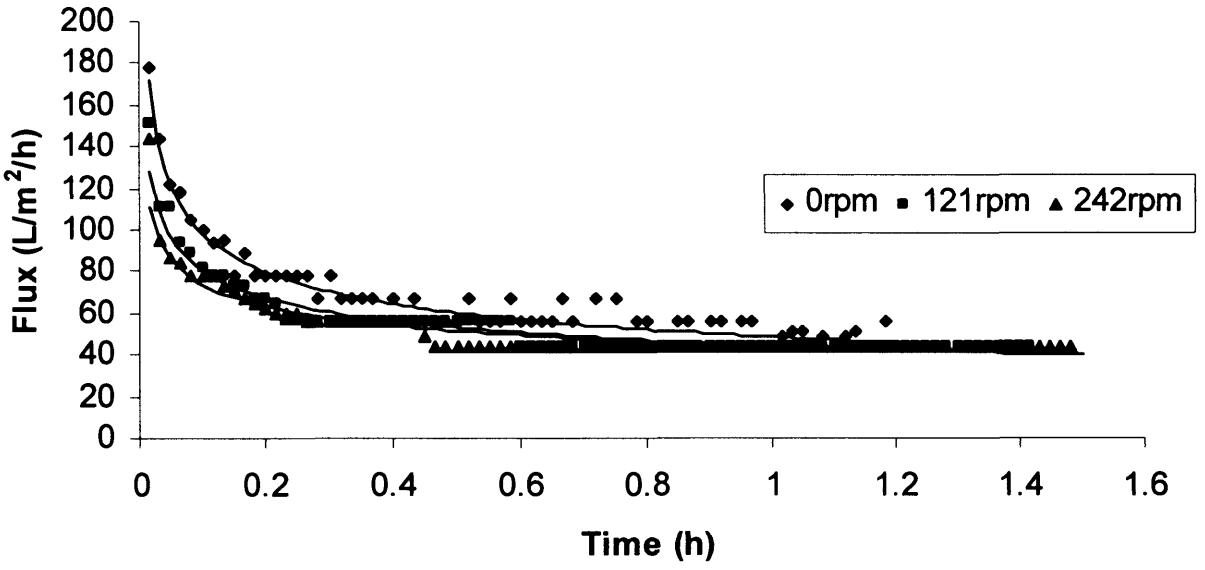

Figure 5.8C Comparison of flux rates measured at 1.5bar and different shear rates during diafiltration (standard deviation +/-5L.m^2.hr, n=3)

The experimental flux data was plotted in terms of the model equations 5.1 and 5.2 described in section 1.3.5.5 in order to determine the method of fouling. These plots are shown in figures 5.9A-C.

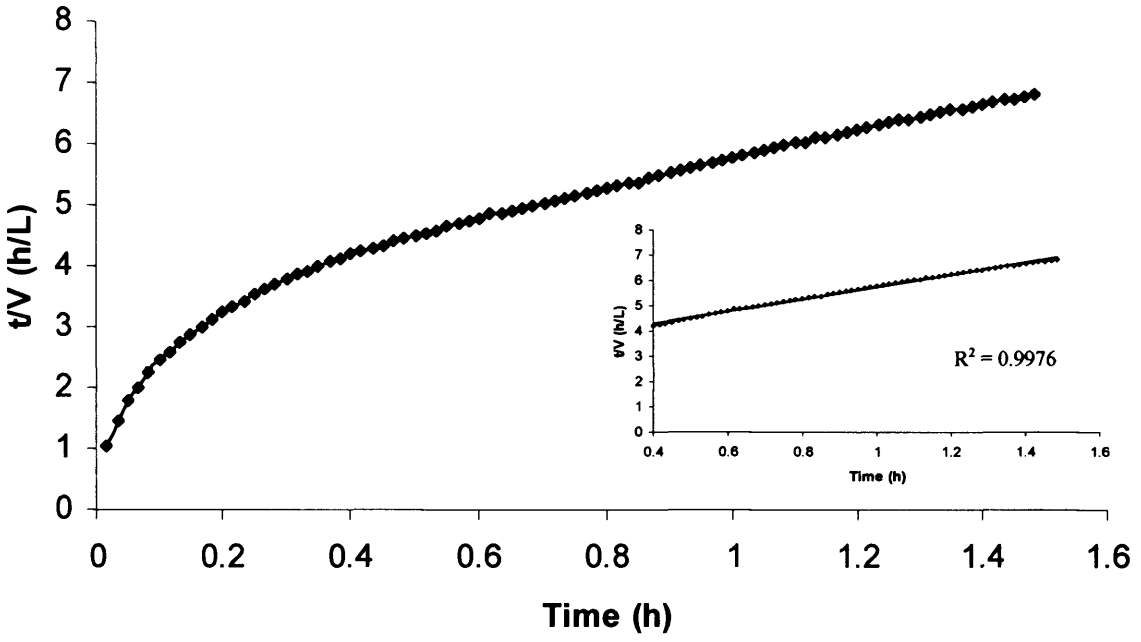

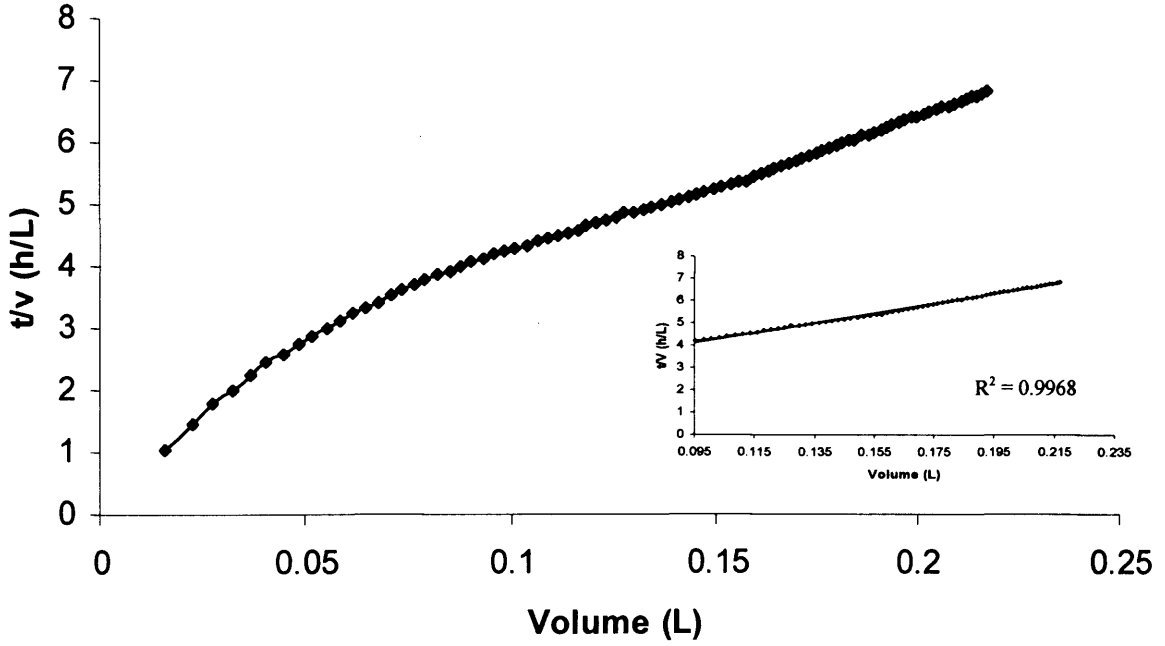

Figure 5.9A Experimental flux data plotted in terms of fouling model equations (5.1) and (5.2). Data refer to experiments carried out under constant volume (continuous/ diafiltration) mode at 242rpm and 0.5bar

Figure 5.9B shows the experimental flux data at 242rpm and 1.0bar plotted in terms of the model equations 5.1 and 5.2.

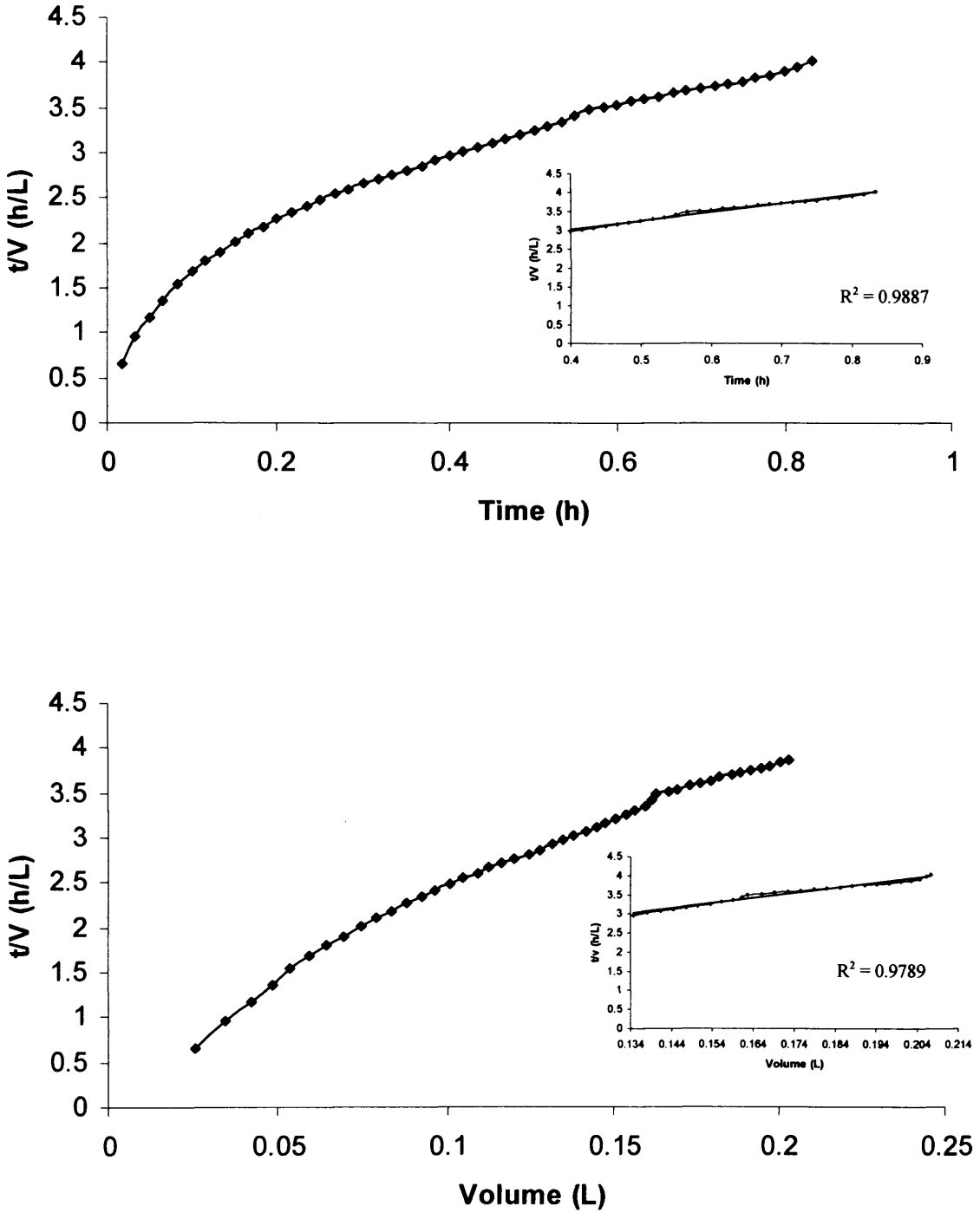

Figure 5.9B Experimental flux data plotted in terms of fouling model equations (5.1) and (5.2). Data refer to experiments carried out under constant volume (continuous/ diafiltration) mode at 242rpm and 1.0bar

Figure 5.9C shows the experimental flux data at 242rpm and 1.5bar plotted in terms of the model equations 5.1 and 5.2.

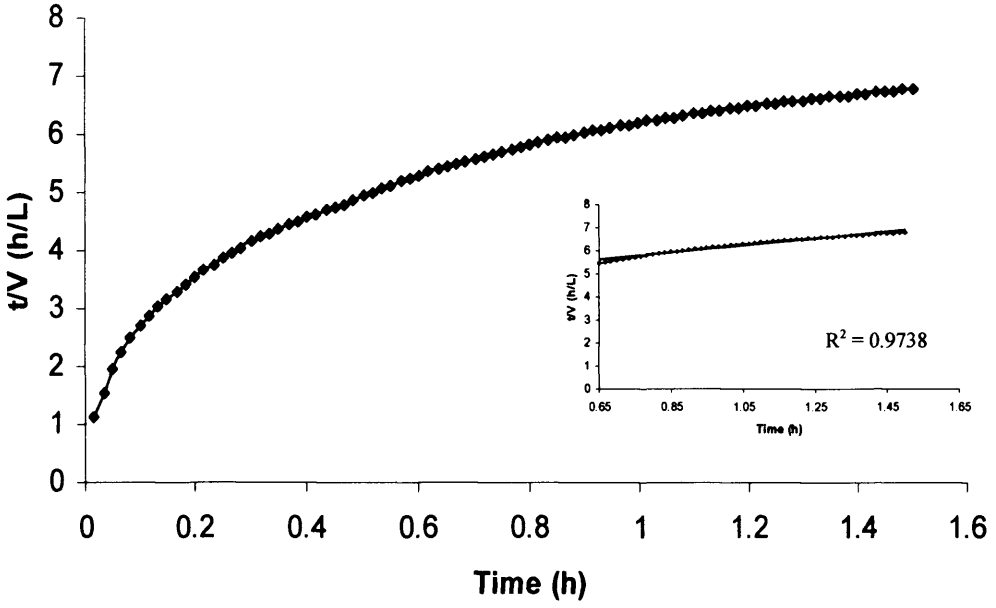

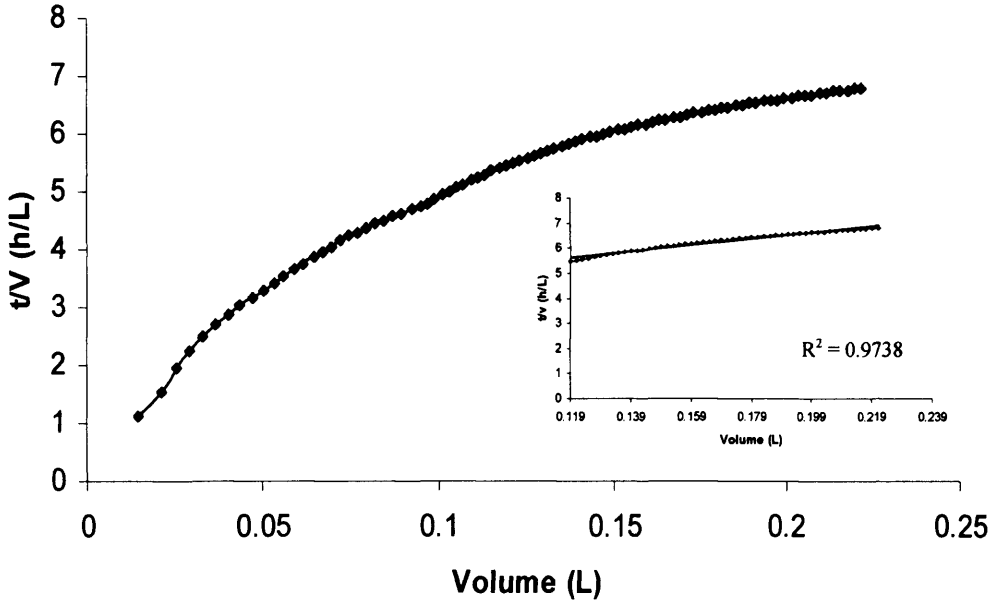

Figure 5.9C Experimental flux data plotted in terms of fouling model equations (5.1) and (5.2). Data refer to experiments carried out under constant volume (continuous/ diafiltration) mode at 242rpm and 1.5bar

Figure 5.10 is a sensitivity analysis of filtration area versus processing time, determined using the values of V_{max} and F_0 obtained from experimental data. This was performed on the experimental flux data in order to determine the membrane area required to process a 250L of precipitated antibody serum at 0.5bar, 1.0bar and 1.5bar.

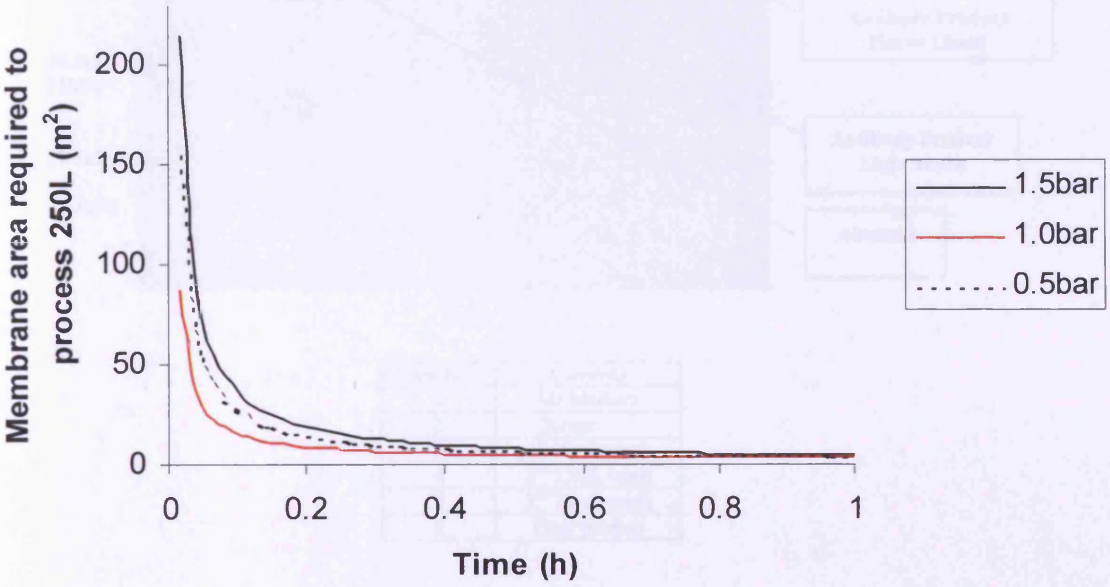

Pressure (bar)	Normalised V_{max} (L/m^2)	Initial Flux ($L/m^2/h$)	Time required to Process 250L with 2.5m^2 of membrane
0.5	148	107	155 minutes
1.0	147	175	107 minutes
1.5	186	86	126 minutes

Figure 5.10 Sensitivity analysis of the area of membrane required to process 250L of precipitated serum versus time

Reducing SDS page gel electrophoresis was used to visualise the proteins contained in various samples. Figure 5.11a is a photograph of the gel produced during the diafiltration process. The albumin is gradually washed away leaving a purified antibody product.

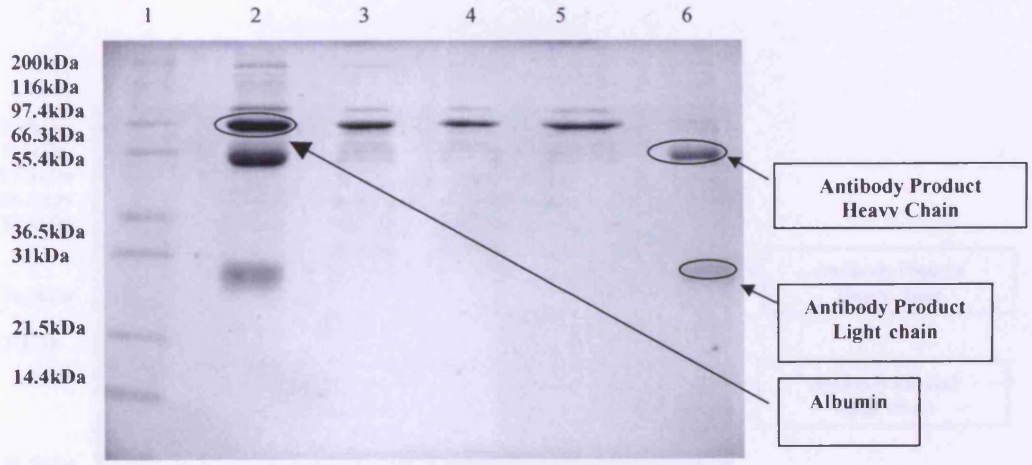

Lane No.	Contents
1	Mr Markers
2	Serum
3	1st 75mL wash
4	2nd 75mL wash
5	3rd 75mL wash
6	Final product

Figure 5.11A SDS denaturing page gels showing a comparison of the protein content of each intermediate purification stage during the diafiltration process

The proteins contained in each sample of the dead end filtration process were also visualised by reducing SDS page. Figure 5.11B is a photograph of the gel showing the different proteins. The photo shows the albumin gradually being removed with some remaining in the final product.

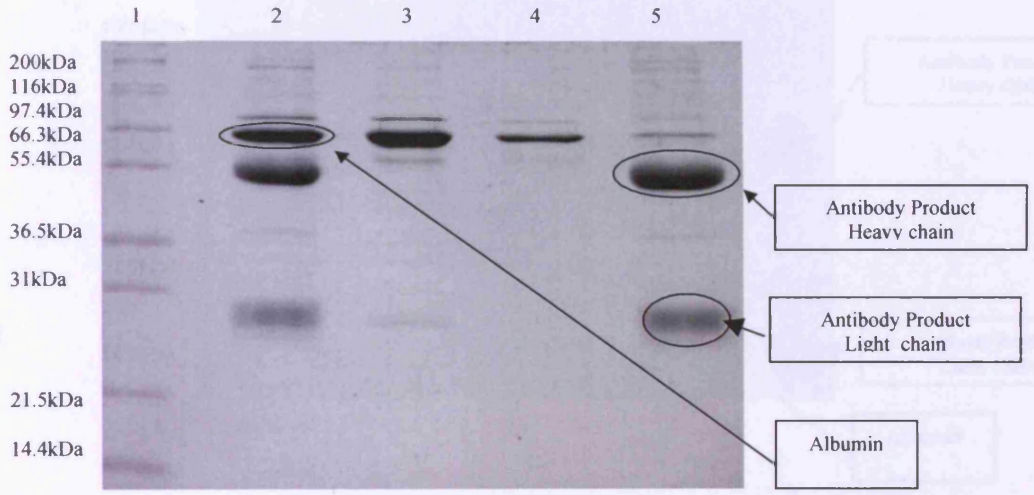

Lane No.	Contents
1	Mr Markers
2	Serum
3	1st Permeate
4	150mL wash
5	Final product

Figure 5.11B SDS denaturing page gels showing a comparison of the protein content of each intermediate purification stage during the dead end filtration process

The reducing SDS-page gel showing the proteins present during the industrial precipitation/centrifugation purification process has been included in figure 5.11C, shown below for reference.

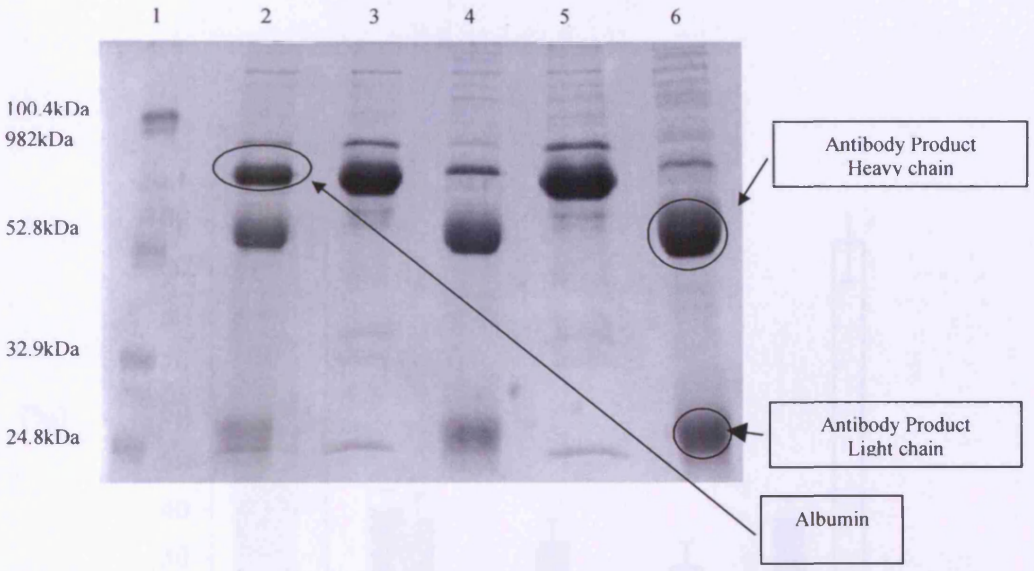

Lane No.	Contents
1	Mr Markers
2	Serum
3	1st Supernatant
4	1st Solid
5	2nd Supernatant
6	2nd Solid

Figure 5.11C SDS denaturing page gels showing a comparison of the protein content of each intermediate purification stage during the industrial centrifugation process

During the diafiltration separation process samples were taken and assayed for total protein, albumin and active antibodies. The results were used to produce the mass balance shown in figure 5.12A. The albumin is removed during the washing phase, whilst the majority of the antibodies are recovered scale (standard error: Total protein +/- 4% (n=5), Albumin +/- 5% (n=5), Active antibody +/- 8% (n=3)).

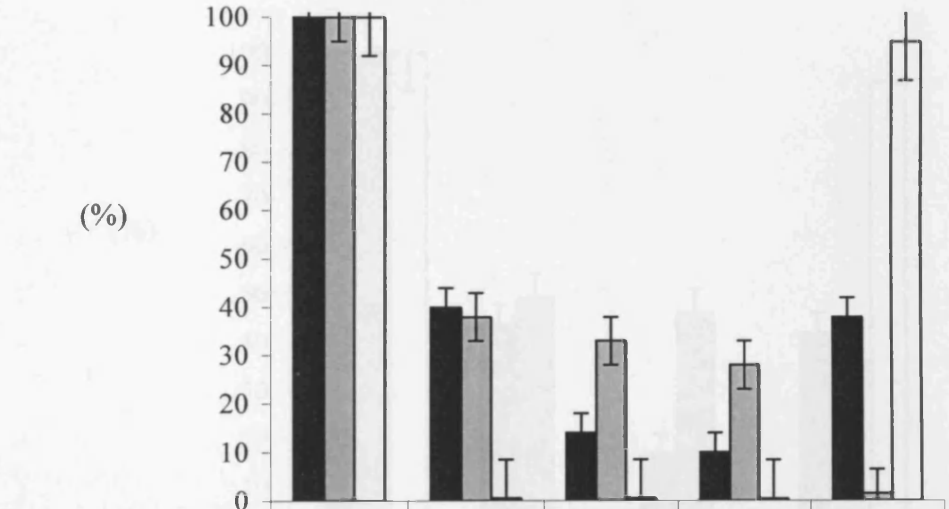

	1	1st 75ml	2nd 75ml	3rd 75ml	4
Average Total Protein (%)	100	40	14	10	38
Average Albumin (%)	100	38	33	28	1.5
Average Active Antibodies	100	0.5	0.5	0.4	95

Figure 5.12A Mass balance for the diafiltration process, showing the levels of total protein (%), the main contaminant albumin (%) and the product (%)(sample numbers correspond to those in figure 5.1)

Samples were also assayed for total protein, albumin and active antibodies during the dead end filtration process. Figure 5.12B shows the mass balance produced as a result of these assays. The albumin is removed during the washing phase leaving a small amount present in the final product and the majority of the antibody is recovered (standard error: Total protein +/- 4% (n=5), Albumin +/- 5% (n=5), Active antibody +/- 8% (n=3)).

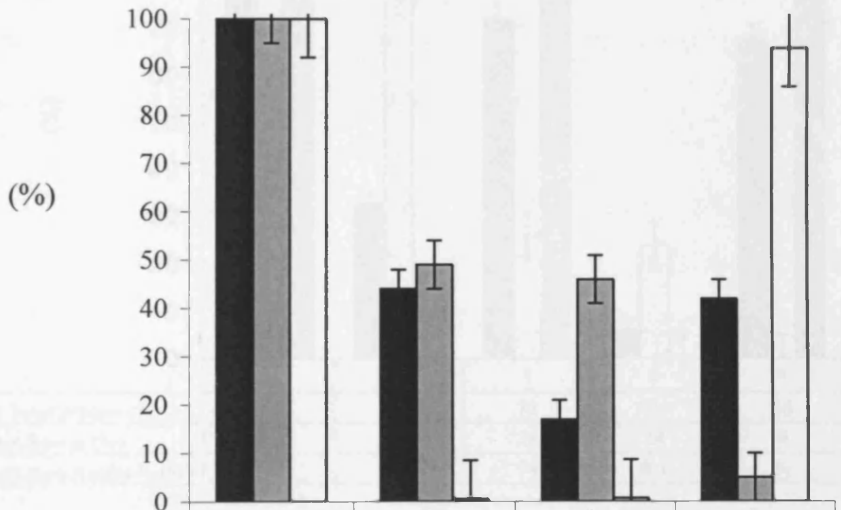

	1	2a	3a	4a
Average Total Protein (%)	100	44	17	42
Average Albumin (%)	100	49	46	5
Average Active Antibodies (%)	100	0.5	0.7	94

Figure 5.12B Mass balance for the batch filtration process, showing the levels of total protein (%), the main contaminant albumin (%) and the product (%)(sample numbers correspond to those in figure 5.1)

The mass balance for the industrial scale centrifugal process is reproduced below in figure 5.12C for reference (standard deviation: Total protein +/- 3% (n=5), Albumin +/- 5% (n=5), Active antibody +/- 8% (n=3)).

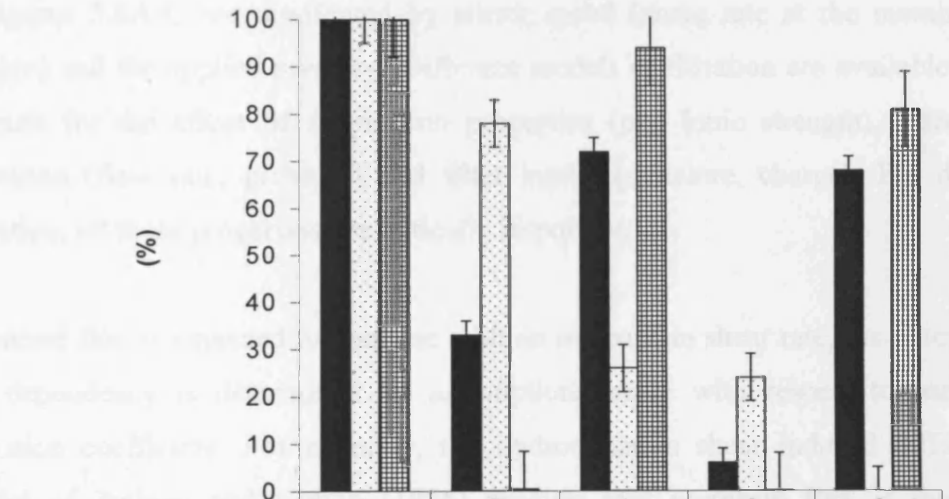

	1	3	4	5	6
Average Total protein (%)	100	33	72	6	68
Average Albumin (%)	100	78	26	24	0
Average Active Antibody (%)	100	0.4	94	0.1	81

Figure 5.12C Mass balance for industrial centrifugation process, showing the levels of total protein (%), the main contaminant albumin (%) and the product (%)(sample numbers correspond to those in figure 5.1)

5.3.6 Discussion

The initial permeate fluxes (F_0) were 107L.m^2.hr, 175L.m^{2}hr and 86L.m^2.hr at 0.5bar 1.0bar and 1.5bar respectively; the reduction in flux rate at 1.5bar is attributed to compaction of the filter cake caused by the higher pressure. In each case the flux declines rapidly indicating the deposition of a layer of particles on the surface of the filter membrane. To a first approximation flux profiles depicted in figures 5.8A-C are unaffected by stirrer speed (shear rate at the membrane surface) and the applied pressure. Different models of filtration are available that account for the effect of suspension properties (pH, ionic strength), filtration operation (flow rate, pressure) and filter media (structure, charge). For depth filtration, all these properties are critically important.

Permeate flux is expected to increase with an increase in shear rate, the extent of the dependency is determined by assumptions made with respect to particle diffusion coefficient. For example, the hydrodynamic shear induced diffusion model of Zydney and Colton (1986) predicts that permeate flux is directly proportional to the applied shear rate, while the inertial lift model of Belfort (1994) predicts an even stronger dependency with permeate flux increasing with the square of the shear rate. These models are essentially extensions of the basic Brownian diffusion theory based on the effect of concentration polarization (the stagnant film) model proposed by Blatt, et al. (1970). In the case of surface (cake) membrane filtration, flux is largely unaffected by operational parameters and the physico-chemical properties of the buffer/suspension. The data shown in figures 5.8A-C and 5.9A-C appear to support the hypothesis that the separation of the antibody precipitate is determined by both surface (cake) membrane filtration and gradual pore blocking filtration mechanisms. Marshall, et al. (1993) concluded that during microfiltration the main mechanism of fouling is pore plugging and that in systems where the concentration of solids within the feed stream is high fouling by surface deposition dominates. In this system microfiltration is the filtration method and the solids content of the feed stream is high, resulting in both methods of fouling occurring. This is supported by further analysis of data discussed below.

The data in figures 5.8A-C show that despite the high permeate flux the rate of filtration decreases continuously and rapidly during the filtration operation. Fouling of the filtration medium is normally presented in terms of two basic models:

(a) Fouling by the deposition of material that forms a layer on the surface of the membrane has been analysed by using Darcy's equation of flow through a porous medium (Jornitz and Meltzer, 1988) which leads to the following cake deposition model (CDM) equation (Jornitz and Meltzer, 1988):

$$\frac{t}{V} = K_1\left(\frac{V}{2}\right) + \left(\frac{1}{F_0}\right)$$

equation 5.1

where V is total volume of permeate collected during the time, t. F_o is the initial flux rate and K_1 is an empirical constant obtained from experimental data.

(b) Adsorption of macromolecules, such as proteins, in the pores of the filter media may also cause a reduction in permeate flux, which may be described by the following expression according to the gradual pore blocking model (PBM) (Jornitz and Meltzer, 1988):

$$\frac{t}{V} = K_2\left(\frac{t}{2}\right) + \left(\frac{1}{F_0}\right)$$

equation 5.2

where K_2 is another constant obtained from experimental data.

According to the gradual pore blocking model a linear plot is expected when t/V is plotted against t, while if cake deposition model controls fouling a linear plot is obtained when t/V is plotted against V. Figures 5.9A-C shows the filtration data

(of figures 5.8A-C) plotted in terms of both model equations (5.1) and (5.2). The plots indicate that for all transmembrane pressures tested, both the cake deposition model and gradual pore blocking model give linear plots. Indicating that both methods of fouling are occurring and contribute to the observed flux.

With gradual pore blocking the flow rate of fluid through the filter follows equation 5.3 shown below:

$$F = F_0\left[1 - k_2\left(\frac{V}{2}\right)^2\right]$$

equation 5.3

When the flow rate drops to zero (F=0) the maximum volume of precipitated antibody serum that could be processed (V_{max}) can be determined.

$$V_{max} = \left(\frac{2}{K_2}\right)$$

equation 5.4

Substituting for V_{max} into equation 5.2 gives the V_{max} equation:

$$\frac{t}{V} = \frac{t}{V_{max}} + \frac{1}{F_0}$$

Therefore using the experimental data obtained from the stirred cell device and assuming that the same filter media and feed composition are employed, it is possible to calculate the operating and process parameters for a large-scale dynamic microfiltration unit based on the scale-up criterion of V_{max} and the initial flux rate (F_0) . The area of membrane needed to process a given volume of precipitated serum can be deduced from equation 5.5, shown below.

$$Area = \left[\left(\frac{V_b}{V_t}\right) \times \left[\left(\frac{V_t}{V_{max}}\right) + \left(\frac{1}{F_0}\right)\right]\right]$$

equation 5.5

Where V_b is the batch volume (L), V_t is the filtration time, V_{max} is the normalised V_{max} (L/m^2) and F_0 is the initial flux ($L/m^2/h$).

The maximum volume (V_{max}) capable of being filter by $1m^2$ of membrane has been calculated for each of the three pressures used and can be seen in figure 5.10. $1m^2$ of membrane could process 148L, 147L and 186L of precipitated antibody serum at 0.5bar, 1.0bar and 1.5bar respectively. At 1.5bar it is possible to process a larger volume of precipitated serum however, the initial flux at 1.5bar was $86L.m^{-2}.h^{-1}$ compared to $107L.m^{-2}.h^{-1}$ at 0.5bar and $175L.m^{-2}.h^{-1}$ at 1.0bar. The flux at 1.5bar has decreased substantially, it is hypothesised that this is due to infilling and compaction of the filter cake leading to increased resistance to flow. This has the impact of increasing the processing time which may effect the process economics. Based on the sensitivity analysis conducted for figure 5.10 an operational pressure of 1.0bar would give the most efficient process, in terms of the time taken to process 250L of precipitated serum.

The stirred cell had a 0.063m diameter disc with an effective filtration area of $0.0028m^2$. Using this information and the V_{max} method for scale-up a sensitivity analysis of filtration area versus processing was carried out. Figure 5.10 is the result of the sensitivity analysis, it can be seen that a stirred filtration machine with an effective filtration area of $2.5m^2$ would be sufficient to process a batch of 250L of antibody suspension in ~2hours. It is noted that agitation did not influence the filtration operation. However its inclusion in a full-scale operation is recommended to provide a means for re-suspending and dissolving the antibody layer in the final stage of the process. The specification of minimum agitation speed of impellers for particle suspension has been studied previously (Ayazi-Shamlou, P. et al. 1994; Ayazi-Shamlou, P. 1993) and is thought to be well within the ability of commercially available stirred microfiltration equipment (Langeloh, et al. 1998).

Figure 5.11A shows the SDS-page gels for samples removed periodically during the continuous (diafiltration) operation of the unit. For comparison, data are also shown for the same starting precipitate in suspension separated by running the

stirred cell in a standard batch (cake filtration) mode of operation, figure 5.11B, and by centrifugation as detailed in chapter three, figure 5.11C.

Lanes 3,4 and 5 in figure 5.11A track the main protein (albumin) contaminant in the permeate fraction. The contaminating albumin is substantially removed from the retentate as the buffer is added to the suspension in the stirred cell during continuous operation. No antibody was detected in the permeate fractions during washing stage as indicated by the gel electrophoresis. At the end of the washing period, the operation was switched to the batch (cake) filtration mode to remove the sodium sulphate buffer used to wash the precipitate. The layer of antibody precipitate formed on the membrane filter was dissolved in a solution of PBS at 37°C by using the stirrer to re-suspend and dissolve the antibody layer in the buffer. Once the dissolution operation was complete, a pressure of 1.0bar ($1x10^5$ N/m^2) was applied and the permeate containing the dissolved antibody fraction collected. It may be seen from lane 6 (figure 5.11A) that the product stream contains only a negligible quantity of the contaminating albumin. In the batch operation the total volume of buffer used to wash the cake was the same as that used during the constant volume operation. The gels in figure 5.11B show that the albumin is removed during both the cake filtration and washing stages (lanes 3 & 4). Again, no antibody was detected in any of the permeate fractions. The gels in figure 5.11C were obtained by separating the antibody precipitate using an industrial centrifuge, details of which are given in chapter three. Comparing the results with the microfiltration operation indicate that the microfiltration scheme provides comparable outcomes in terms of purity of the antibody precipitate.

Figure 5.12A-C provides the results of a mass balance carried out on the key components during the microfiltration of the antibody precipitate. Data are shown for the stirred cell device operating in continuous mode and comparative data are given for batch mode as well as for the industrial disc stack centrifuge (Neal, et al. 2003). The final product for all three systems contains similar percentage of albumin (±5%). However, if we define the relative potency of the final product as the percentage antibody content divided by the percentage total protein content, then it can be seen that the continuous filtration operation has the best relative

potency (2.5) this is followed closely by the dead end filtration (2.2) with the centrifugation process giving the lowest value (1.2).

There are two possible reasons for this. The first is the potential shear associated damage to the product antibody in the high shear zones in an industrial centrifuge (Boychyn, et al. 2001; Boulding, et al. 2002; Neal, et al. 2003). The second is the capacity of the continuous microfiltration to increase the overall process yield by integrating several operations (concentration, diafiltration, washing and buffer exchange) in a single piece of equipment. The improvement in yield may be considered significant given the high cost of the antibody product (Neal, et al. 2003).

5.4 Conclusions

It is known that current manufacturing capacity for rattlesnake venom-specific Fab antibody is unable to keep up with the growth in demand. In this chapter a modified stirred cell device was used to mimic the operation of dynamic microfiltration to separate an intermediate antibody precipitate from a suspension containing contaminating soluble proteins. Constant volume flux data were obtained as a function of shear rate at the surface of the membrane and transmembrane pressure and analysed to establish the limits of the filtration operation. The results were compared with an existing centrifugation process. The analysis indicated that dynamic microfiltration may be used as a single step for separation; purification and concentration of antibody precipitate and offers an attractive process option to centrifugation.

6 Purification Of Ovine Polyclonal Antibodies By Protein G Affinity Chromatography And The Prediction Of Breakthrough Curves

6.1 Introduction

Affinity chromatography is a powerful tool for the isolation and purification of intact proteins. Advances in matrix and ligand technology mean that affinity chromatography has now found widespread use and is a well recognised technique within the biopharmaceutical industry (Subramanian, 1995). This technology has been used for the purification of many different types of product ranging from antibodies (Huse, et al. 2002; Lowe, et al. 2001), to plant proteins (Weselake and Jain, 1992), to proteases (Ibrahim-Granet and Bertrand, 1996).

It is also a potentially attractive process option as a method to purify polyclonal immunoglobulins because in principle the current four-step precipitation/centrifugal recovery technique described in chapter three could be carried out in one step. Protein A affinity chromatography is regularly used for the initial purification of monoclonal antibodies from clarified cell culture fluid (Birch, et al. 1995; Blank, et al. 2001; Fahrner, et al. 1999a; Fahrner, et al. 1999b; Fahrner, et al. 1999c; Grant, et al. 1999; Schwarz, 2000; Walter, 2000) and the same principles could be applied for this purification.

In this instance however, protein G was chosen instead of protein A as it exhibits a higher affinity for ovine IgG antibodies (Bjorrck and Kronvall, 1984). It has been reported that conventional separation techniques, like precipitation, are being replaced by affinity separations (Bonnerjea, et al. 1986). Figure 6.2 details the proposed process flow sheet for the purification process, with the Protein G separation replacing the precipitation and centrifugation steps.

A one step primary separation is extremely desirable because of the potential decrease in process time and potential increase in yield obtained from a decrease

in the number of separation steps used to achieve the purification. The flow sheet detailed in figure 6.1 has eight discrete stages where as the process sheet in figure 6.2 has five. The degree of purification obtained from a protein G (affinity) purification step may also be greater than the current precipitation/centrifugation step, due to the specific nature of the protein G immunoglobulin interaction. There is also general agreement within the biopharmaceutical industry that decreasing the number of steps in a process and increasing the yield will generate higher returns (Lowe, et al. 2001).

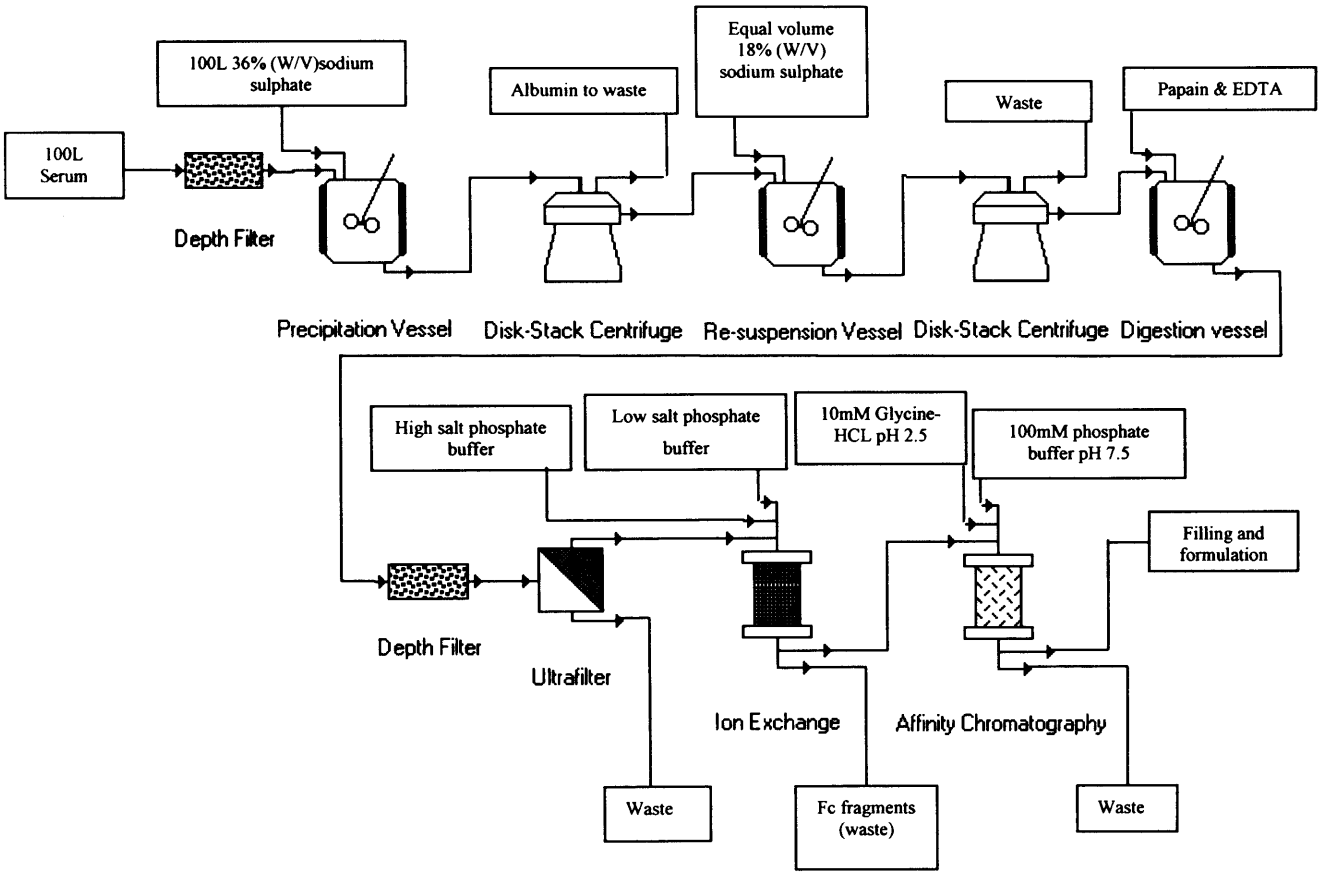

Figure 6.1 Process flow sheet for the purification of polyclonal Fab fragments from ovine serum

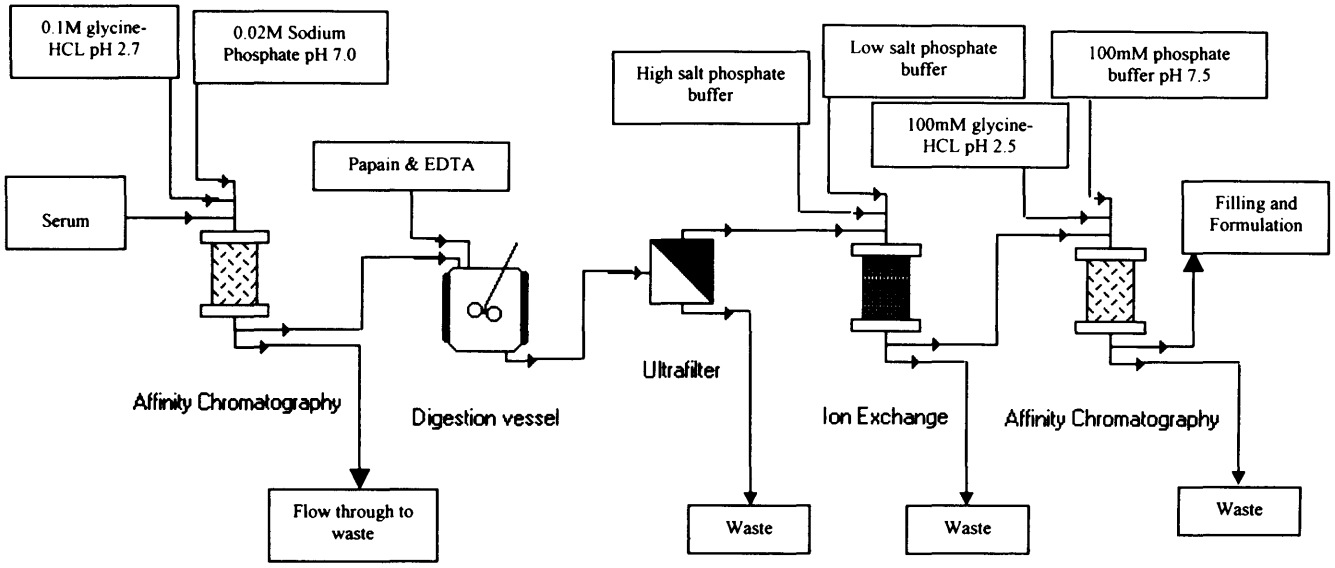

Figure 6.2 Process flow sheet for modified chromatographic separation process

The steps following the protein G affinity purification are required to remove the contaminating Fc fragments produced during the digestion step. Changes to them will not be considered here.

This chapter focuses on the use of protein G for separating polyclonal IgGs from ovine serum and assesses the suitability of affinity chromatography for the initial purification step. This method of separation was also compared to the centrifugal method described in chapter 3 and the filtration separation method described in chapter 5.

Values for the maximum monolayer capacity (q_m), the dissociation constant (K_D), and the apparent adsorption constant (K_1) were determined from batch and rate adsorption data. The results were then used in the kinetic rate constant model developed by Chase (1984) to build a mathematical model capable of predicting the breakthrough curves of IgG separations. Predictions were made for various bed heights/diameters, antibody feed concentrations and feed flow rates. These predictions were tested by comparison to experimentally produced breakthrough curves.

6.1.1 Theory

Adsorption isotherms and modelling

Batch adsorption experiments were conducted to generate information about the binding characteristics of the matrix. The results from the batch adsorption experiments, for both IgG and albumin, were analysed using the Langmuir isotherm (equation 1.19, detailed in section 1.3.6.5 is shown below for reference). It has been used extensively in the past to analyse binding characteristics (Bellot and Condoret, 1993; Chase, 1984; Jacobson, et al. 1984; Mao, et al. 1995; Weaver and Carta, 1996).

$$C_S = \frac{C_M q_m}{C_M + K_D} = \frac{C_M q_m K_A}{C_M K_A + 1}$$

(equation 6.1)

Where C_S is the concentration of absorbed solute at equilibrium, C_M is the concentration of solute in the mobile phase at equilibrium, q_m is the maximum monolayer capacity of the matrix, K_D is the disassociation constant and K_A is the association constant.

The applicability of this model to describe the batch adsorption experimental data was assessed using the Scatchard plotting technique (Andrade, 1985; Blanco, et al. 1989; Scatchard, 1949). A linear Scatchard plot indicates the applicability of the Langmuir model, where as a non-linear plot suggests a violation of the basic assumptions inherent to the model. Rearranging equation 6.1 yields:

$$\frac{C_S}{C_M} = q_m K_A - K_A C_S$$

(equation 6.2)

This equation implies that a plot of C_S/C_M versus C_S should yield a straight line of slope $-K_A$ and intercept q_mK_A if the basic assumptions of the Langmuir model are adhered to. Experimental work (Anspach, et al. 1990; Blanco, et al. 1989; Boyer and Hsu, 1990; Huang, et al. 1990; Ruaan, et al. 1988; Sada, et al. 1986; Whitley, et al. 1989) has however demonstrated that many cases of protein adsorption show deviations from linearity. If the Scatchard plot results in a concave-up curvature, this suggests either negative co-operativity i.e. two different species of protein are competing for the same binding site, or the presence of two or more heterogeneous binding sites. A concave-down curvature indicates positive co-operativity, i.e. one binding site binds more than one protein at a time.

Simulations of the breakthrough process can be conducted by determining the rate constant (K_1) and using the kinetic rate constant model developed by Chase (1984) to describe the adsorption and desorption process. This model assumes that the surface reaction rate is slow compared to the mass transfer rate. This assumption means that the rate at which the antibodies bind to the protein G is slow compared to the rate at which they move from the solution they are contained within to within the matrix. This implies that the protein concentration inside the adsorbant particle is the same as outside. The rate function accounts for the reversible nature of the solute-adsorbent interaction:

$$\frac{dC_S}{dt} = K_1 C_M (q_m - C_S) - K_{-1} C_S$$

(equation 6.3)

$$C_M = C_0 - \frac{v}{V}\left[\frac{(bta)(1-\exp\{-2(av/V)K_1 t\})}{\left(\frac{bta}{b-a}\right)-\exp\{-2(av/V)K_1 t\}}\right]$$

(equation 6.4)

Where

$$a^2 = b^2 - \left(\frac{C_0 V}{v}\right) q_M$$

(equation 6.5)

and

$$b = \frac{1}{2}\left(\frac{C_0 V}{v} + q_M + \frac{K_D V}{v}\right)$$

(equation 6.6)

Where K_{-1} is the reverse reaction rate constant, C_0 is the initial protein concentration, υ is the volume of matrix and V is the volume of solution (Chase, 1984).

This model was originally developed to describe ion-exchange processes. It lumps all the mass transfer resistances into one interaction rate constant. The model also assumes that one protein molecule adsorbs to one functional group.

6.2 Methodology

A 0.7cm diameter, 2.5cm high column with a capacity of 0.96ml, packed with protein G sepharose 4 fast flow (Amersham Biosciences, Buckinghamshire, U.K.) was used to separate polyclonal IgGs from ovine serum. The main contaminants within the serum are albumin and other blood proteins. The column was run according to the method detailed in section 2.5.3. The chromatograms of the first and twentieth purification run on the 0.96ml capacity column are included in the results section in order to show that the column has not significantly deteriorated with repeated use. A mass balance has been produced in order to determine the levels of recovery and the amount of IgG bound to the column. A non reducing SDS-PAGE gel, produced as per the method detailed in section 2.3.3.2, was used to visualise the proteins contained in the un-purified serum, the flowthrough/wash fractions and the elutant fractions. These fractions were produced during the protein G purification.

Column experiments also provided purified IgG for use during the batch and breakthrough curve experiments.

Isotherm measurements

Isotherm measurements were conducted using a batch method. Section 2.5.1 details the method used for the twenty-four hour equilibrium experiments. Solutions of IgG and albumin at various starting concentrations were placed into eppendorfs containing an equal volume of matrix. They were left for twenty-four hours in order to allow the protein concentrations to come to equilibrium. These experiments allow the maximum capacity (q_m) of the matrix to be determined along with the dissociation constant (K_D).

Dynamic equilibrium experiments were used to determine the apparent adsorption constant (K_1). This constant describes the rate of adsorption of the solute to the support; in this case the antibodies to protein G. Section 2.5.2 describes the method utilised to determine the dynamic equilibrium. Known concentrations of IgG and Albumin were placed in a stirred vessel containing an equal volume of protein G matrix. Samples of the mobile phase were then removed at different times. The concentrations of protein were determined by Bradford assay using the methodology detailed in section 2.3.1.1. It was assumed that adsorption and desorption take place simultaneously at the surface of the matrix.

Equation 6.4 was solved using Matlab and the experimentally determined adsorption values. The predicted breakthrough curves were drawn from the results (Dr Hu Zhang, private communication).

The breakthrough curve predictions were tested by comparison with breakthrough curves produced using varying bed heights, different flow rates and different starting concentrations of IgG. The method is described in section 2.5.4.

6.3 Results

The chromatogram for the 0.96ml volume column purification of IgG from ovine serum after the first run are shown in figure 6.3.

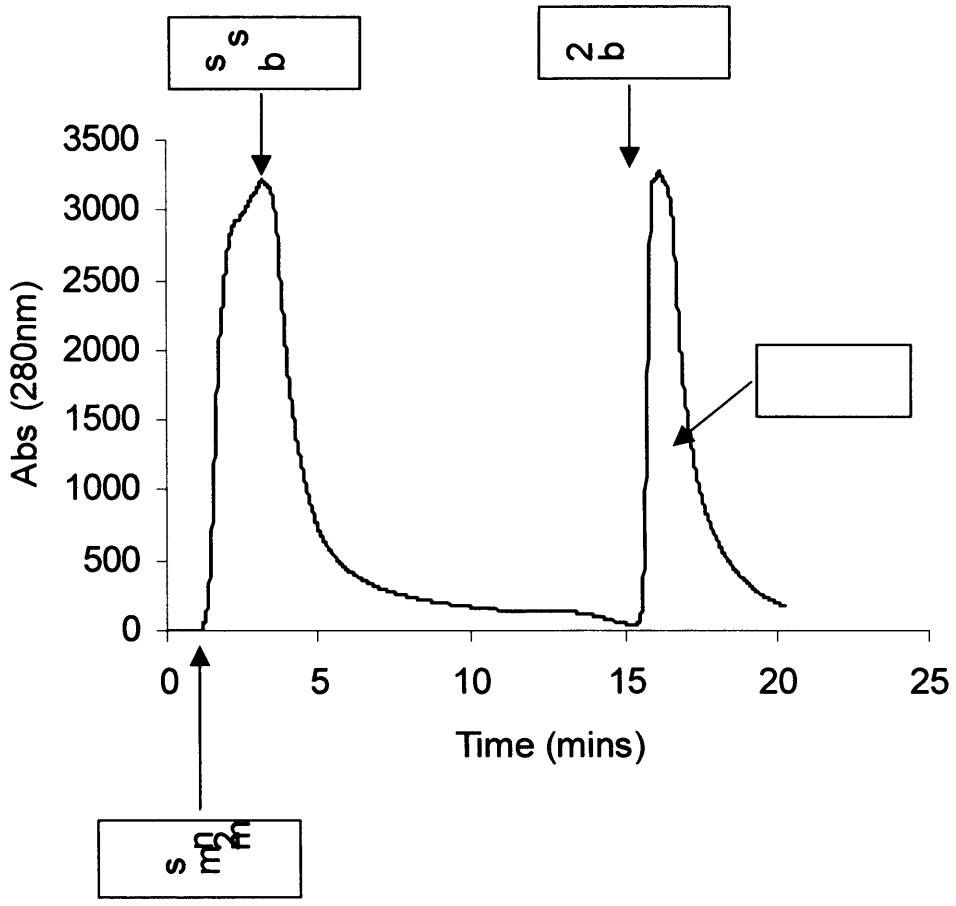

Purification of ovine polyclonal antibodies from serum (run number 1) 2ml of 32.5mg/ml (total protein) 15mg/ml (IgG) at 157.89cm/hr

The chromatogram for the 0.96ml volume column purification of IgG from ovine serum after the twentieth run is shown in figure 6.4.

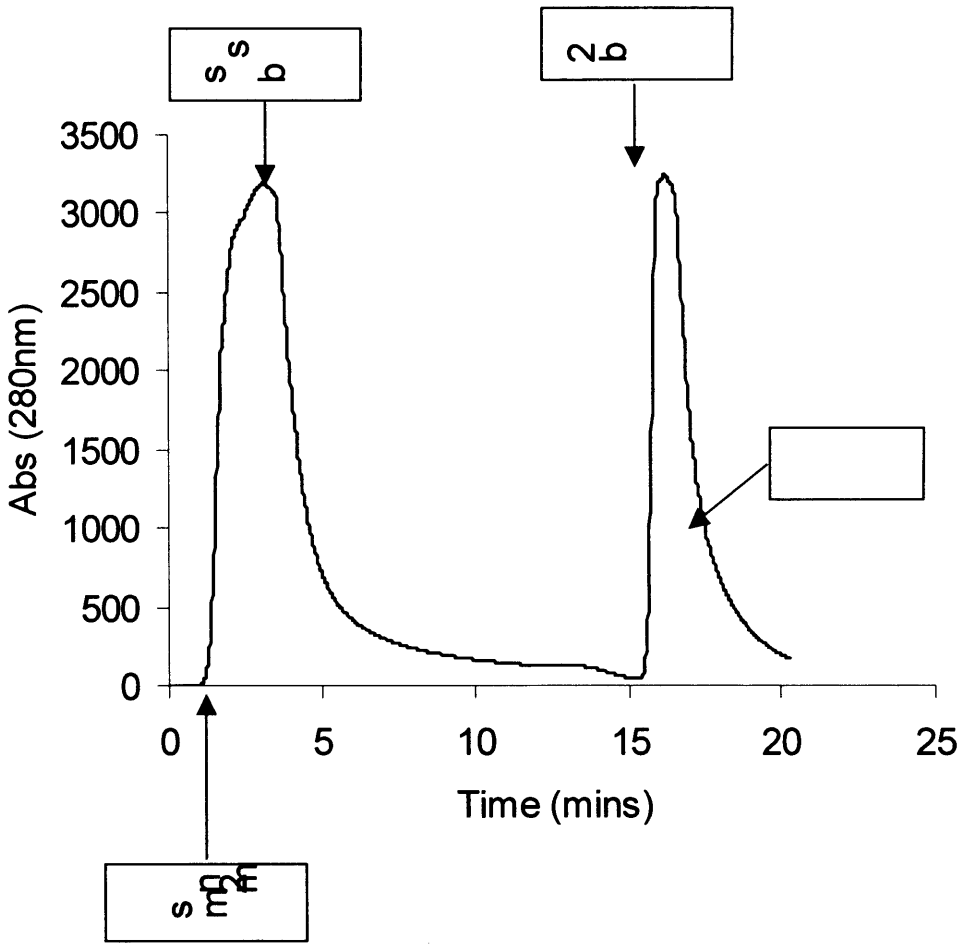

Figure 6.4 Purification of ovine polyclonal antibodies from serum (run number 20) 2ml of 32.5mg/ml (total protein) 15mg/ml (IgG) at 157.89cm/hr

The concentration of proteins in the flowthrough/wash and in the elution portion of the chromatographic run were measured and used to produce the mass balances shown below in tables 6.1 and 6.2. 1ml of protein G matrix binds around 19mg of ovine IgG from within the mixed protein starting serum solution when the flow rate is 157.89cm/hr and the concentration of antibodies in the feed is 15mg/ml.

Run No.	Total protein Loaded (mg)	Total IgG Loaded (mg)	Total protein in Wash/Flowthrough (mg)	Product(eluant) (mg)
1	65	30	46.1	18.9
5	65	30	46.1	18.9
10	65	30	46.4	18.6
15	65	30	46.4	18.6
20	65	30	45.7	19.3

Table 6.1 Mass balance for protein G affinity chromatography runs 1, 5, 10, 15, and 20

Run No.	IgG recovered (mg)	IgG in flowthrough (mg)	% IgG recovered from column	% IgG yield
1	18.9	10	96	63
5	18.9	9.8	96	63
10	18.6	10.2	96	62
15	18.6	9.9	95	62
20	19.3	10	97	64

Table 6.2 Antibody yields for protein G affinity chromatography runs 1, 5, 10, 15, and 20

A non reducing SDS PAGE gel was used to visualise the proteins contained within the various fractions. The antibody is purified out from the other contaminating proteins and is found in the elutant fraction.

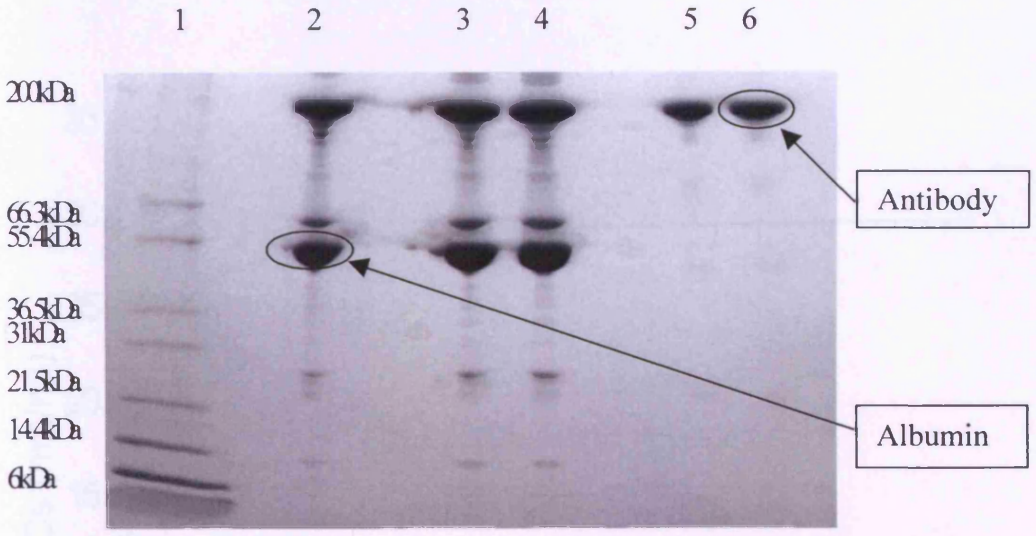

Lane No.	Contents
1	Mr Markers
2	Serum
3	Flowthrough/Wash
4	Flowthrough/Wash
5	Elutant
6	Elutant

Figure 6.5 SDS page non reducing gel showing the protein content of the various fractions produced during the chromatographic separation of antibodies from ovine serum by protein G affinity chromatography

The total protein concentration at equilibrium in the mobile and solid phase at various starting concentrations were determined by batch uptake experiments. The results are plotted below in figure 6.6. The Langmuir equation was used to produce the predicted isotherm based on the experimentally determined value of K_A for IgG antibodies and Albumin.

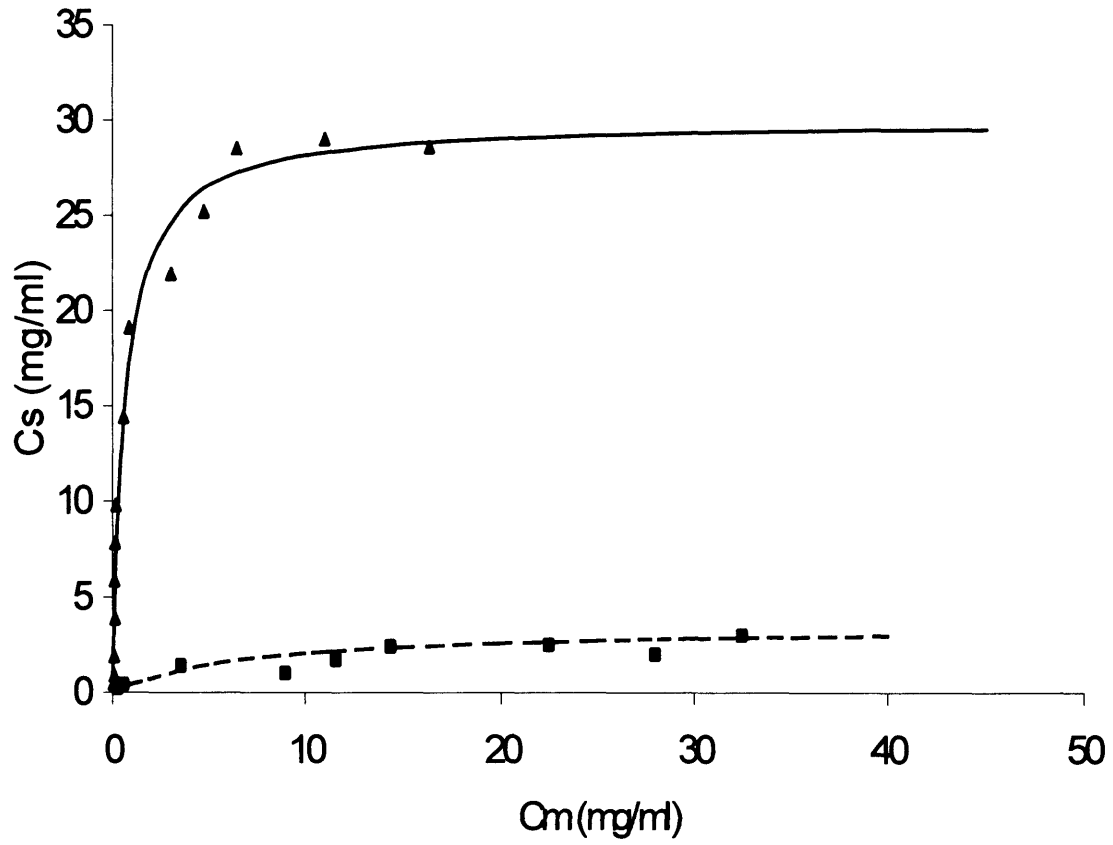

Figure 6.6 Langmuir isotherms showing predicted IgG concentrations (solid line) the predicted Albumin concentrations (dashed line) the measured concentrations of IgG(▲) and the measured albumin concentrations (■) present in the solute fraction and bound to the matrix at different initial starting concentrations after 24 hours

The method of Scatchard was used to determine the applicability of the Langmuir model for describing the IgG experimental data. The plot shown below in figure 6.7 is for the batch uptake of IgG onto protein G matrix.

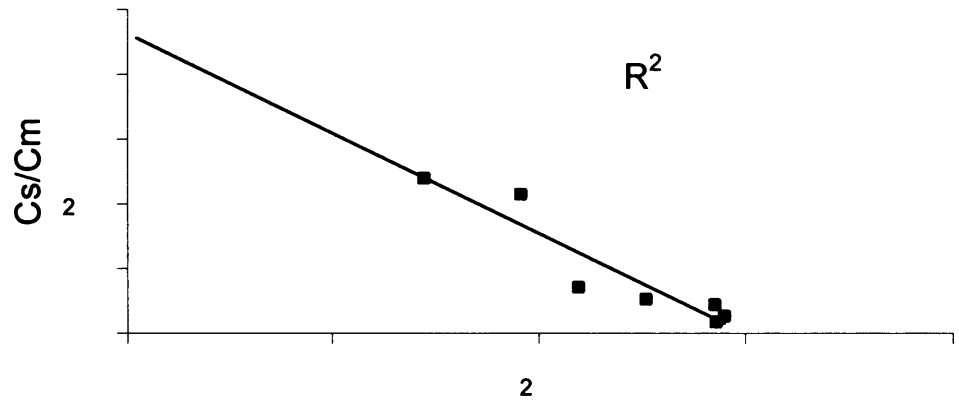

Figure 6.7 Scatchard plot of IgG adsorption data, the solid line is the fitted curve using the Langmuir equation the (■) represent the IgG experimental data

The method of Scatchard was also used to determine the applicability of the Langmuir model for describing the Albumin experimental data. The plot shown below in figure 6.8 is for the batch uptake of Albumin onto protein G matrix.

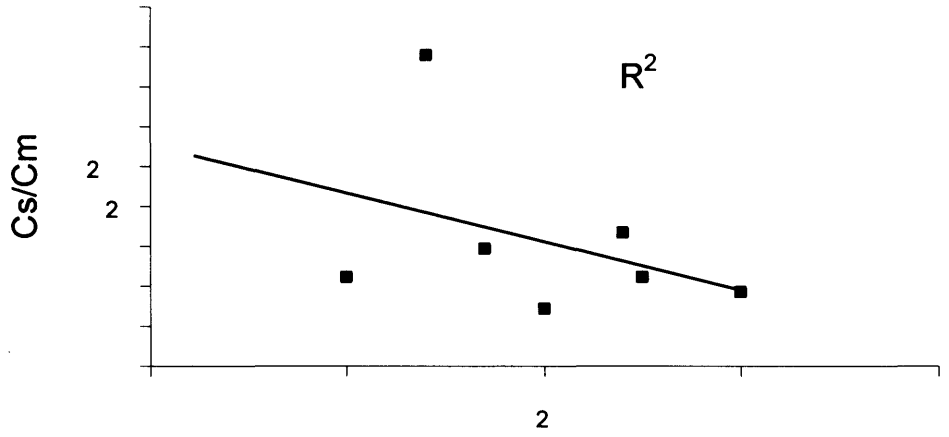

Figure 6.8 Scatchard plot of albumin adsorption data, the solid line is the fitted curve using the Langmuir equation the (■) represent the albumin experimental data

Dynamic equilibrium experiments were conducted and the concentration of both IgG and Albumin remaining in solution were measured after different time intervals. The results are shown below in figure 6.9. The protein G binds IgG in large amounts and reaches its maximum capacity after 5 minutes, whilst the albumin barely binds to the matrix.

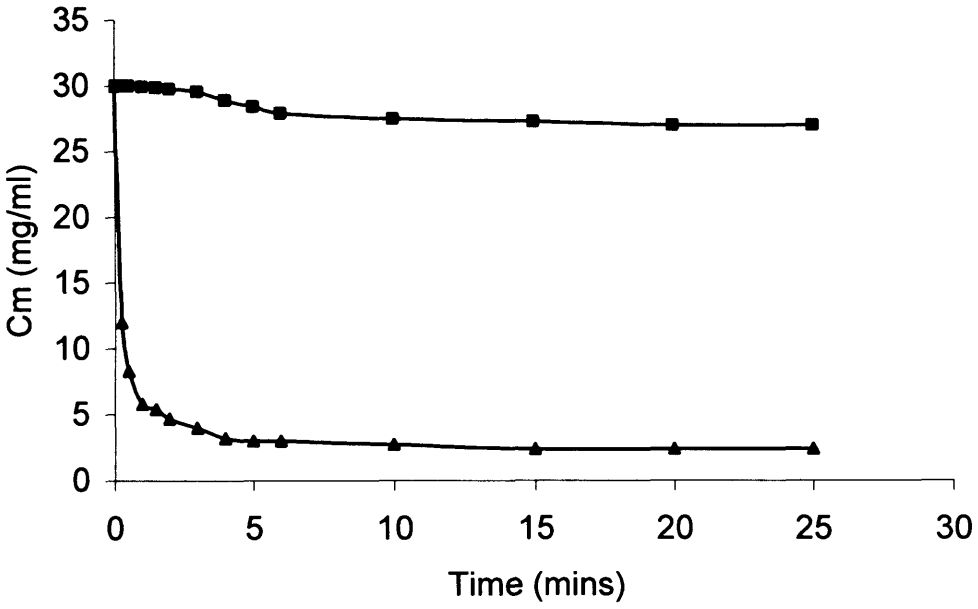

Figure 6.9 Concentration of Albumin (■) and IgG (▲) remaining in the mobile phase at different times after the addition of the protein solution to the equilibrated protein G matrix

Table 6.3, shown below details the experimentally determined values for K_D K_1 and q_m

Protein	K_D (kg/m^3)	K_1 ($m^3/kg/hr$)	Max capacity ($q_m kg/m^3$)
IgG	0.5	12	28.5
Albumin	5	3.6	3

Table 6.3 Experimentally determined values of K_D K_1 and q_m for the interaction of protein G matrix with IgG and albumin

Predicted and experimental breakthrough curves were determined for a variety of different bed heights, flow rates and feed concentrations, in order to test the robustness of the mathematical model. Table 6.4, shown below summarises the conditions.

Experiment No.	1	2	3	4	5
Feed concentration	30mg/ml	30mg/ml	15mg/ml	15mg/ml	30mg/ml
Bed Height	2.5cm	2.5cm	2.5cm	2.5cm	5cm
Flow rate	157cm/hr	316cm/hr	157cm/hr	316cm/hr	76cm/hr
Column diameter	0.7cm	0.7cm	0.7cm	0.7cm	1cm
Experiment No.	6	7	8	9	10
Feed concentration	15mg/ml	30mg/ml	30mg/ml	30mg/ml	30mg/ml
Bed Height	5cm	10cm	10cm	15cm	15cm
Flow rate	76cm/hr	76cm/hr	38cm/hr	120cm/hr	60cm/hr
Column diameter	1cm	1cm	1cm	0.8cm	0.8cm

Table 6.4 Summary of the different conditions utilised during the breakthrough curve experiments

Predicted and experimental breakthrough curves for a bed 2.5cm high, 0.7cm diameter with a feed concentration of 30mg/ml and a flow rate of 157cm/hr and 316cm/hr. The predicted curves closely match the experimental curves.

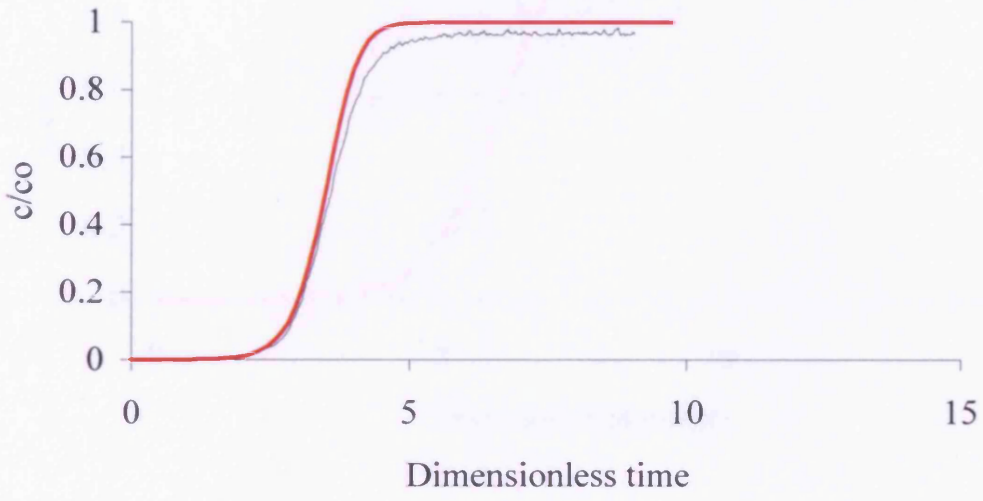

Figure 6.10 Simulated (red line) and experimental (black line) breakthrough curves (2.5cm high column, 0.7cm diameter, 30mg/ml feed concentration, 157cm/hr flow rate)

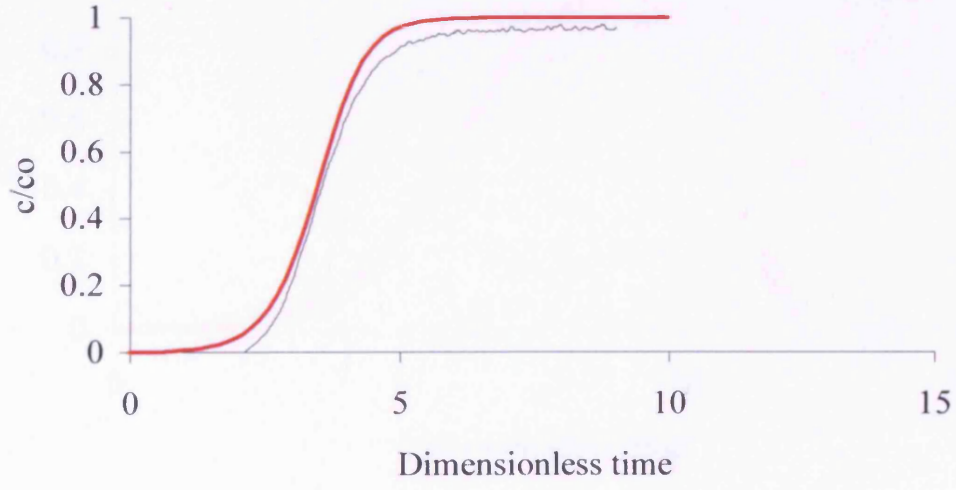

Figure 6.11 Simulated (red line) and experimental (black line) breakthrough curves (2.5cm high column, 0.7cm diameter, 30mg/ml feed concentration, 316cm/hr flow rate)

Predicted and experimental breakthrough curves for a bed 2.5cm high, 0.7cm diameter with a feed concentration of 15mg/ml and a flow rate of 157cm/hr and 316cm/hr. The predicted curves do not closely match the experimental curves.

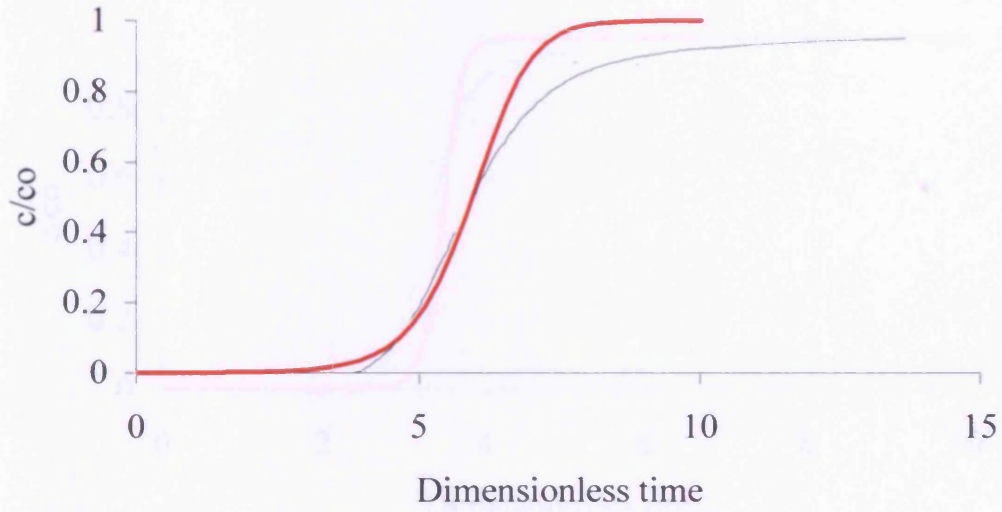

Figure 6.12 Simulated (red line) and experimental (black line) breakthrough curves (2.5cm high column, 0.7cm diameter, 15mg/ml feed concentration, 157cm/hr flow rate)

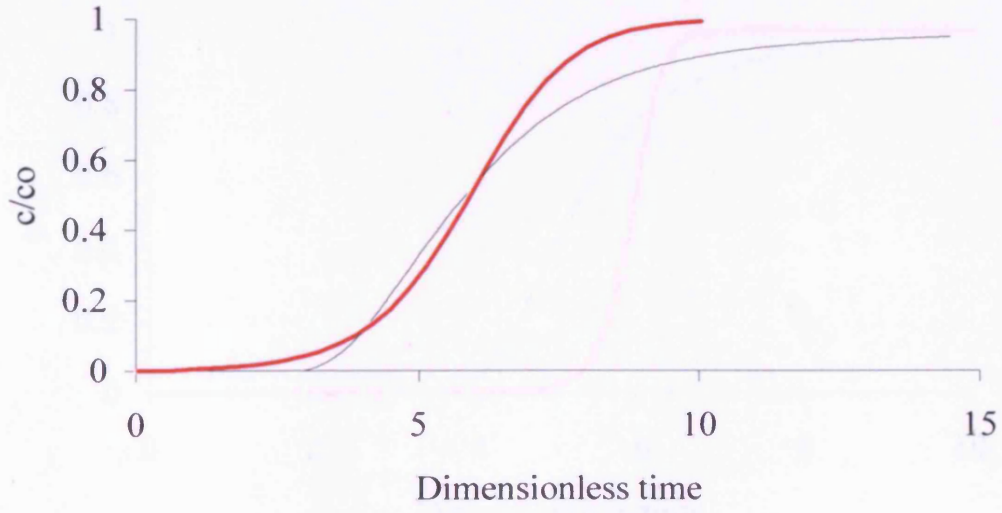

Figure 6.13 Simulated (red line) and experimental (black line) breakthrough curves (2.5cm high column, 0.7cm diameter, 15mg/ml feed concentration, 316cm/hr flow rate)

Predicted and experimental breakthrough curves for a bed 5cm high, 1.0cm diameter with a feed concentration of 30mg/ml and 15mg/ml at a flow rate of 76cm/hr. The predicted curves do not closely match the experimental curves.

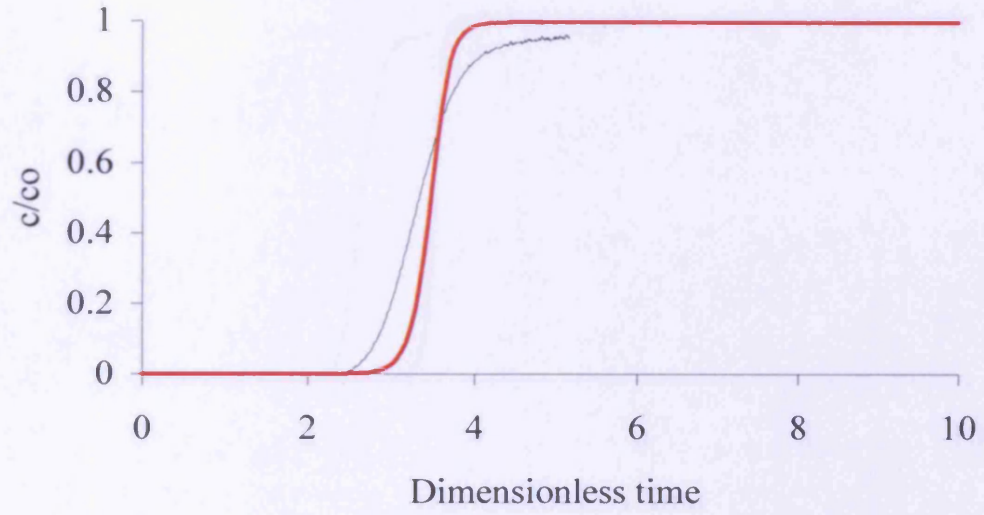

Figure 6.14 Simulated (red line) and experimental (black line) breakthrough curves (5cm high column, 1cm diameter, 30mg/ml feed concentration, 76cm/hr flow rate)

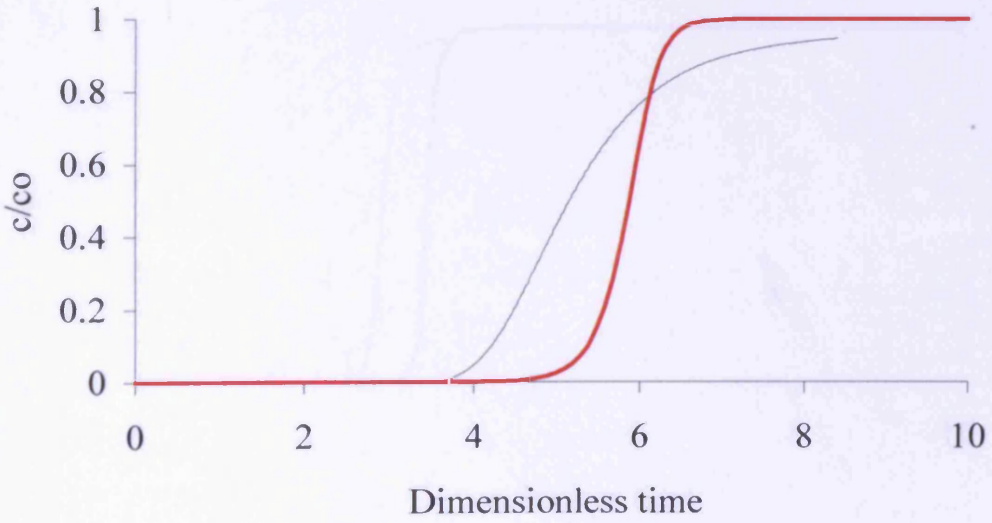

Figure 6.15 Simulated (red line) and experimental (black line) breakthrough curves (5cm high column, 1cm diameter, 15mg/ml feed concentration, 76cm/hr flow rate)

Predicted and experimental breakthrough curves for a bed 10cm high, 1.0cm diameter with a feed concentration of 30mg/ml at a flow rate of 76cm/hr and 38cm/hr. The predicted curves do not closely match the experimental curves.

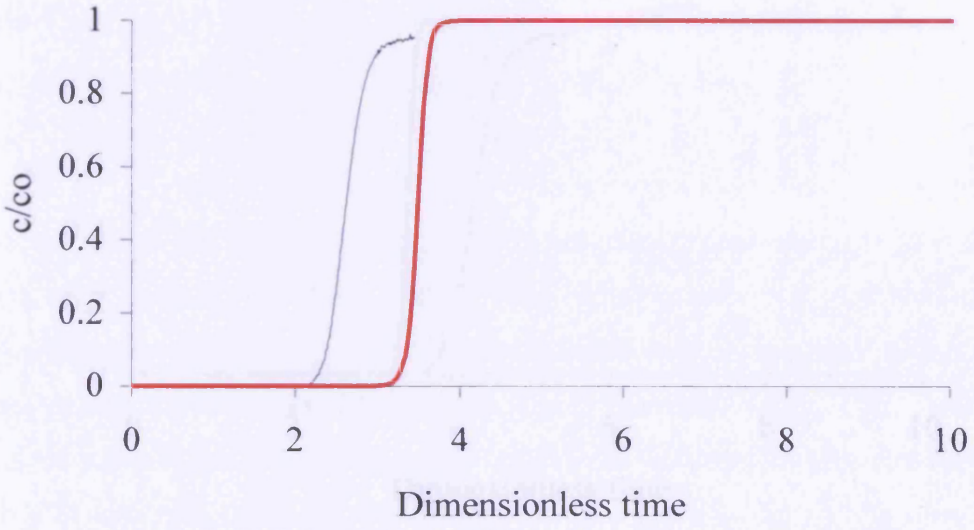

Figure 6.16 Simulated (red line) and experimental (black line) breakthrough curves (10cm high column, 1cm diameter, 30mg/ml feed concentration, 76cm/hr flow rate)

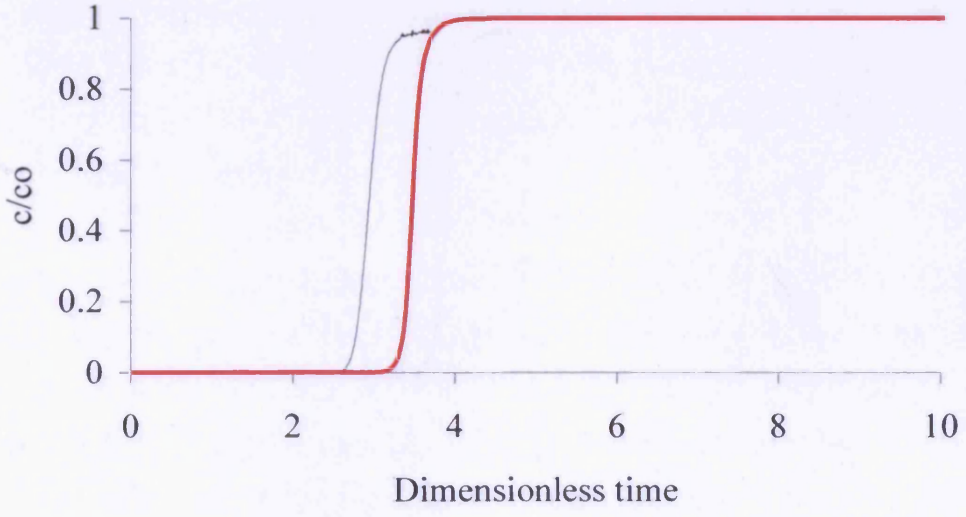

Figure 6.17 Simulated (red line) and experimental (black line) breakthrough curves (10cm high column, 1cm diameter, 30mg/ml feed concentration, 38cm/hr flow rate)

Predicted and experimental breakthrough curves for a bed 15cm high, 0.8cm diameter with a feed concentration of 30mg/ml at a flow rate of 120cm/hr and 60cm/hr. The predicted curves do not closely match the experimental curves.

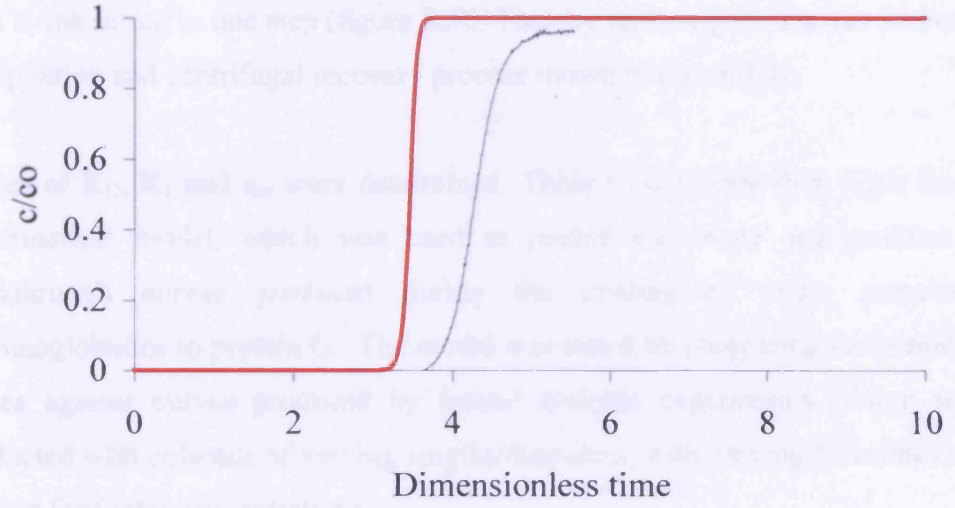

Figure 6.18 Simulated (red line) and experimental (black line) breakthrough curves (15cm high column, 0.8cm diameter, 30mg/ml feed concentration, 120cm/hr flow rate)

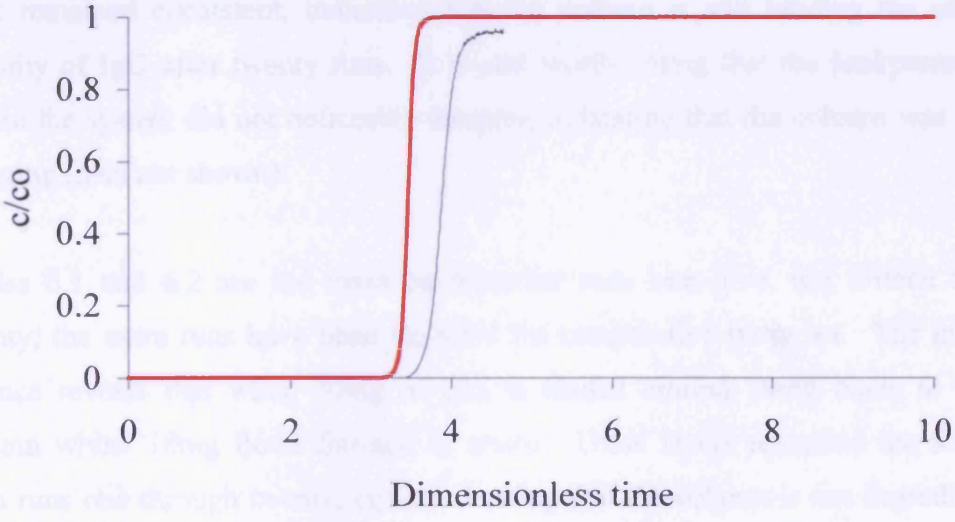

Figure 6.19 Simulated (red line) and experimental (black line) breakthrough curves (15cm high column, 0.8cm diameter, 30mg/ml feed concentration, 60cm/hr flow rate)

6.4 Discussion

A small-scale protein G column (2.5cm x 0.7cm) has been used to study the feasibility of using affinity chromatography to purify polyclonal immunoglobulins from ovine serum in one step (figure 6.2). Thereby replacing the current four-step precipitation and centrifugal recovery process shown in figure 3.1a.

Values of K_D, K_1 and q_m were determined. These values were then input into a mathematical model, which was used to predict the shape and position of breakthrough curves produced during the binding of ovine polyclonal immunoglobulins to protein G. The model was tested by comparing the predicted curves against curves produced by frontal analysis experiments. These were conducted with columns of varying lengths/diameters, with varying flow rates and varying feed inlet concentrations.

Figures 6.3 and 6.4 show the chromatograms produced during the purification of antibodies from ovine serum using the 0.96ml volume protein G column. Figure 6.3 is the chromatogram for the first run and figure 6.4 is the chromatogram produced during the 20^{th} run. As can be seen, the size and shape of the elution peak remained consistent, indicating that the column is still binding the same quantity of IgG after twenty runs. It is also worth noting that the backpressure within the system did not noticeably increase, indicating that the column was not clogging (data not shown).

Tables 6.1 and 6.2 are the mass balances for runs one, five, ten, fifteen and twenty; the extra runs have been included for comparative purposes. The mass balance reveals that when 30mg of IgG is loaded around 19mg binds to the column whilst 10mg flows through to waste. These levels remained the same from runs one through twenty, again indicating that the column is not degrading. It is particularly important from an industrial point of view that the column gives a consistent yield, since a purification process needs to be robust in order for it to be validatable. A long column life will also improve the economics of the process. The mass balance indicates that the yield is 63% compared to 80% for the

industrial scale precipitation/centrifugal recovery process and 95% for the microfiltration process (see figures 3.8b and 5.12a respectively). At first glance this yield does not compare favourably with the yields from the other processes. However, this is an initial set of experiments, designed only to test the feasibility of using protein G to bind and separate the ovine polyclonal antibodies from the rest of the contaminants. Further experimental work would have to be conducted in order to determine the most efficient amount of serum to load as well as the optimum flow rate and buffering conditions required to gain the highest yield, before an accurate comparison could be drawn.

Figure 6.5 is a non-reducing SDS-page gel depicting the proteins contained within the process stream at various points during the protein G separation process. Lane 2 contains the starting serum showing the antibody and the major contaminants. Lanes 3 and 4 contain the flowthrough/column wash fraction. As can be seen a large quantity of IgG remains unbound and is lost. Determining the optimum loading conditions could reduce this loss. Lanes 5 and 6 contain the elution peak. The purity of the final product is excellent, with only one major band of IgG present. This compares very favourably with both the precipitation/centrifugal and microfiltration purification processes (figures 3.4a and 5.11a), where contaminating proteins are still present.

Isotherms

Batch and dynamic experiments were used to determine experimental values which describe the adsorption/desorption process. The Langmuir equation has been used extensively in the past to describe interactions between chromatography media and various substrates (Gritti and Guiochon, 2003; Hahn, et al. 2003; McCue, et al. 2003; Weaver and Carta, 1996). Here it has been used to describe the adsorption/desorption process occurring between protein G and ovine polyclonal antibodies. The applicability of this method to describe the adsorption/desorption process was assessed through the use of Scatchard plots (Scatchard, 1949). The experimentally determined values were used to build a mathematical model capable of predicting the shape of breakthrough curves produced during the protein G separation process. The mathematical model was

tested by comparing its predictions to actual experimental results. However it should be noted that Yang and Tsao (Yang and Tsao, 1982) have highlighted that the assumptions of linear adsorption isotherms or linear adsorption-desorption kinetics, which have been used frequently to describe liquid or gas chromatography systems (Bellot and Condoret, 1993; Chase, 1984; Jacobson, et al. 1984; Mao, et al. 1995; Weaver and Carta, 1996), might not be applicable to affinity chromatography. Another assumption of this model is that the binding sites on the matrix have affinity for only one type of adsorbate. However protein G recognises and binds to many species of IgG and the feed material is polyclonal in nature. This means that reactions with different rate kinetics may be taking place when the matrix and the serum are combined.

Adsorption isotherms were measured for the binding of polyclonal anti-snake venom antibodies and albumin to immobilised protein G. The antibodies/albumin were buffered in 0.2M sodium phosphate buffer pH 7.4. Figure 6.6 is a plot of the experimentally determined values for the concentration of IgG and albumin remaining in the mobile phase at different starting concentrations after the system had reached equilibrium. The plot shows good agreement between the experimental and the Langmuir predicted curves for both the antibodies and the albumin. The shape of the curve shown in figure 6.6 for the antibody-protein G interaction is indicative of a favourable adsorption isotherm (Langmuir, 1918).

The Scatchard plot for the antibody adsorption data is shown in figure 6.7 and the albumin adsorption data is shown in figure 6.8. A straight line indicates that the Langmuir curve can be used to describe the experimental data. The antibody adsorption data, when plotted out, gives a r^2 value of 0.88 indicating a reasonable correlation. The discrepancies could be attributed to the polyclonal nature of the immunoglobulins, which may mean that the different types of antibody have different affinities for the protein G, thus resulting in a mixture of rate constants.

The Scatchard plot for the albumin adsorption data shown in figure 6.8 gives an r^2 value of 0.15, indicating that the Langmuir isotherm does not accurately describe the interaction between albumin and the protein G matrix. This is to be expected since the protein G molecule has been genetically modified to remove its albumin-

binding site. As such the binding of the albumin is probably be due to unspecific interaction with the solid support.

The values for the effective dissociation constant (K_D), forward rate constant (K_1), and the maximum capacity (q_m) for the binding of IgG and albumin to protein G were determined using equations 6.1 to 6.6 with reference to figures 6.6 and 6.9 the results are shown in table 6.3.

For the IgG system at equilibrium the dissociation constant (K_D) equalled 0.5kg/m^3, the forward rate constant (K_1) equalled 12m^3/kg/hr and the maximum binding capacity of the protein G matrix was 28.5kg/m^3 of gel. These values are comparable to those obtained for the interaction between different protein A matrices and polyclonal IgG (Hahn, et al. 2003).

For the albumin system at equilibrium the dissociation constant (K_D) equalled 5kg/m^3, the forward rate constant (K_1) equalled 3.6m^3/kg/hr and the maximum binding capacity of the protein G matrix was 3kg/m^3 of gel.

As expected the association constant for IgG was much larger than for albumin as was the maximum capacity of the resin. This maximum capacity would probably not be achievable under column separation conditions since this value represents the amount bound after 24 hours without any interfering proteins. During column separation the residence time will be a matter of minutes not hours and this is one of the main factors influencing the amount of IgG bound (McCue, et al. 2003). The dynamic equilibrium plot shown in figure 6.9 reveals the rate at which the antibodies and the albumin bind to the matrix. After 5 minutes the matrix has almost reached its maximum capacity for the antibodies or the albumin. This plot was used to calculate the value of K_1.

Breakthrough curves

Experimental breakthrough curves were determined for packed columns in order to study the effect of changing operating variables such as the flow rate, the concentration of the adsorbate and the size and shape of the column on the

position and shape of the curve. These experiments were also conducted to test the mathematical models ability to predict the shape and position of the breakthrough curve under different operating conditions. Table 6.4 summarises the conditions used during the breakthrough curve experiments and figures 6.10 through 6.19 show the experimentally produced curve with the predicted curve overlaid.

Figures 6.10 and 6.11 are the experimental and predicted breakthrough curves for a 2.5cm long bed, 0.7cm in diameter run at a feed inlet concentration of 30mg/ml at a flow rate of 157cm/hr and 316cm/hr. The predicted and experimental curves closely match, indicating a good correlation between the mathematical model and the reaction occurring during the experimental run. The column conditions match those used during the batch update experiments with regard to the feed inlet concentration.

Figures 6.12 through 6.19 are the experimental and predicted breakthrough curves for columns run under different operating conditions as detailed in table 6.4. The predicted and the experimental curves differ in the predicted time it will take for breakthrough to occur; this indicates a possible flaw in the model used to predict the breakthrough curves. The possible reasons for these discrepancies will be discussed later.

The breakthrough curve model is based on several assumptions as well as relying on the accuracy of the experimentally determined values of K_l and q_m to predict the shape and position of the curve. The Langmuir curve and the Scatchard plot of the antibody adsorption data indicated that a simple equilibrium relationship could be used to describe the system and the interactions occurring during the affinity separation (figures 6.6-6.8). However the lack of agreement between the predicted and experimental breakthrough curves suggests that some of the assumptions the model is based on do not fully describe what is occurring within the system. The model assumes that the adsorbent-adsorbate reaction takes place between one molecule and one functional group. However, the antibody solution is polyclonal and contains many different types of antibody, which could have different binding affinities (Bjorrck and Kronvall, 1984). The model also assumes that the protein concentration inside the matrix is the same as outside i.e. the rate

of interaction between adsorbent and adsorbate governs the reaction not the mass transfer rate. Both factors could be contributing to the rate of uptake which impacts the accuracy of the model. The experimentally determined values of K_l or q_m could be inaccurate, which would introduce discrepancies when the model is tested under conditions different from those the values of q_m and K_l were determined at. It should also be noted that the values of the parameters for the interaction between adsorbent and adsorbate are only applicable to the conditions under which they were measured. Differences in the temperature, pH and ionic strength may alter the binding kinetics, resulting in a shift in the position of the breakthrough curve.

The shape of a breakthrough curve can also be used to determine when the most efficient adsorption process is achieved. This is obtained when the curve is at its sharpest. Chase (1984) determined that the sharpest breakthrough curve is seen with the lowest feed flow rate and the highest feed concentration. Within an industrial setting these parameters may not be achievable since time constraints may restrict the flow rate allowable and the feed inlet concentration is governed by the concentration within the ovine serum and the amount of binding buffer added to it.

6.5 Conclusions

This chapter demonstrates the feasibility of using protein G as a replacement for the current precipitation/centrifugation purification process. Although the yield of 63% is less than the current process, optimisation of the technique may improve yields to levels comparable to those of the current purification process. The use of protein G affinity chromatography may also present cost saving opportunities in terms of the time taken to complete the initial purification step.

The mathematical model devised can predict the shape and position of breakthrough curves with some success. Further work is required in order to gain a better understanding of the equilibrium reactions that govern the protein G polyclonal immunoglobulin interaction. The mathematical model provides a

reasonable prediction of the shape of the breakthrough curves. Predictions of the position were only partially successful, possibly due to either one of the assumptions the model is based on is incorrect or the experimentally determined values of K_l or q_m are inaccurate. As it stands the model could not be used to correctly predict the effect of altering separation conditions and parameters i.e. bed height. However with refinement and further experimental work it should be possible to improve the model so that it could be used to predict the impact of changes to the operating parameters; such as the flow rate and the feed inlet concentration.

7 Future Work

This thesis describes the development of an integrated ultra scale down mimic and its use for studying process changes. Future work in this area could be on the optimisation of the current industrial scale manufacturing process and on the production of a whole bioprocess mimic encompassing the ion exchange and affinity chromatography steps. A fully linked bioprocess mimic would afford the opportunity to be able to study the knock on effects of process changes the whole way down the process stream.

Chapter five looked at an alternative purification method. A more in depth study on microfiltration membrane properties and their effect on the flux rate and transmission of the protein would be beneficial in expanding the understanding of filtration.

The ability to purify antibodies from mammalian serum in one step (as demonstrated in chapter six) may reduce both processing time and costs; this could also be the focus of future studies. Work needs to be conducted on the properties of the matrix, such as its life span and capacity as well as the durability of the ligand when dealing with feed solutions that contain large quantities of contaminating material and are of high viscosity. New matrices are also continually being developed. A study into the new types of matrices being produced, their properties and their applicability to antibody purification would be valuable. Work could also be conducted to refine the basic mathematical model developed in chapter 6 for predicting breakthrough curves. A study optimising the process conditions used during the protein G affinity chromatography separation would enable an accurate comparison of the yields between the different separation techniques to be conducted.

The current affinity purification step represents a large proportion of the process costs. Experimental work optimising the process would be beneficial. The theories developed in chapter six could be applied to the current affinity process in order to refine the model and predict beneficial process changes.

8 Ultra Scale Down Solutions

8.1 Introduction

The purpose of the Engineering Doctorate scheme is to ensure that during the four years of the course, candidates receive training in management, validation and commercial awareness as well as carrying out novel research.

The work described in the previous chapters details the research conducted during the completion of this thesis on Ultra Scale Down methods for mimicking downstream operations and small-scale experiments for determining or predicting the behaviour of the process feed stream at a large scale. The purification operations studied include precipitation, centrifugation, filtration and chromatography.

The equipment and methodology used to predict and study the downstream purification process may have commercial uses. The executive summary detailed in this chapter gives a brief overview of the potential commercialisation of Ultra Scale Down, its benefits and drawbacks, if it were to be used in an industrial setting, along with a brief financial appraisal.

8.2 Executive Summary

8.2.1 USD concept

Ultra Scale Down (USD) solutions will provide services to enhance current manufacturing process development activities carried out by the top ten pharmaceutical companies, using the unique, patented USD tools and software developed by University College London (UCL). USD tools accurately mimic the downstream purification process of a biopharmaceutical drug at a laboratory scale. USD is seeking $6 mn in seed funding to finance working capital requirements for the first two years, during which time the technology will be upgraded to meet current industry standards and the benefits further demonstrated in an industrial environment.

The key financial data for the proposed business is shown below:

Year	1	2	3	4	5	6	7	8
Revenues ($ '000)	0	0	9,000	9,000	9,000	9,000	34,000	67,000
Operating Profit ($ '000)	-3,700	-1,800	6,900	6,900	6,900	6,900	30,200	61,500
Operating Profit as % of Revenue	-	-	77%	77%	77%	77%	89%	92%
Head Count	15	16	17	17	18	18	18	18
Cumulative Capital Required ($ '000)	4,000	6,000	6,000	6,000	6,000	6,000	6,000	6,000

Table 8.1 Projected Financial Summary

8.2.2 Value proposition

The key benefits of USD's service are as follows:

1. Enhanced optimisation of the manufacturing process. This would result in better product yields, thereby reducing the costs of manufacturing. Initial estimates suggest a 10-20% potential reduction in manufacturing costs. Furthermore, superior process optimisation may allow better definition of equipment requirements, with resultant capital expenditure savings.
2. Optimising process development increases the probability of being first-to-market with a novel drug, through reduced regulatory review times. Moreover, due to limited patent lives, speeding up drug launch increases the amount of protected sales.
3. A more robust process reduces risk of product recall due to manufacturing problems.
4. Savings in time and costs associated with the process development activities.

8.2.3 The Current Problem

Increasingly, the global biopharmaceutical industry is facing cost and time pressures in the drug development process. These result from:
Cost containment drives by drug purchasers (typically national health organisations) tend to focus on the most visible area – drug pricing;
Increasing competitive pressures call for rapid launch of new drugs. Industry experience indicates that the first entrant in a given therapeutic area can capture up to 80% market share. Advances in other areas of product development (e.g. bioinformatics) have also shifted the bottleneck to the process development activity.

The purification processes for new drugs are becoming increasing complex and costly as a result of increasing complexity of the drugs themselves;
New drug approval times by regulatory authorities (e.g. FDA) are decreasing and these bodies are starting to require that process definition be undertaken earlier in the product development cycle.

Of particular importance in defining the manufacturing process for biopharmaceuticals are "scale-up" effects, i.e. taking a laboratory-scale production process and defining the appropriate parameters to produce equivalent material at bulk scale. Unlike for synthetic chemicals, scale-up effects for biopharmaceuticals are difficult to predict (i.e. during fermentation), because there is little theory or previous experience in this area. Therefore, pilot scale studies are used to generate the requisite empirical data. This procedure is relatively costly, time consuming and may not define an optimum process.

8.2.4 Solution

USD tools accurately mimic the downstream purification process of a biopharmaceutical drug at a laboratory scale. The material produced during USD studies has been proven to be comparable with the material obtained at bulk scale. Therefore, process options can be investigated within a laboratory early on in the drug development cycle and an optimised purification process delivered to the pilot plant for verification. USD tools eliminate the need for continual repetition of pilot plant trials, and because the scale is so small the work can be done at a fraction of the time and cost compared to the current process. Software has also been developed that allows the results from each individual operation to be integrated together into a whole process model. USD tools are available for the seven main purification methods that are used in manufacturing most marketed biopharmaceuticals currently. Further research is being conducted into other key operations (e.g. fermentation). It is expected that working models for these operations will be developed over the next three years by UCL.

8.3 Customers

The biopharmaceutical industry consists of four key segments:

Drug Discovery: small companies which focus on the process of discovering novel drugs. After discovery, the drugs are licensed to larger companies for clinical trials and marketing;

Specialist Biotech: companies which focus on biopharmaceuticals and are active in all areas of the value chain from drug discovery and development to marketing;
Big Pharma: traditional large companies which manufacture biopharmaceuticals as part of a portfolio of both synthetic and bio drugs. The top ten pharma companies dominate the global pharmaceuticals market. Typically, these companies are active in all areas of the value chain.
Contract Manufacturing Organisations (CMO): about ten companies in the UK manufacture biopharmaceuticals on behalf of big pharma and specialist biotech companies. Many of these CMOs also provide manufacturing process development services to their clients.

USD will aim to target Big Pharma companies initially, given that:
This segment stands to gain most directly from the potential benefits of USD, particularly given the intensity of rivalry and the fact that they are active in all areas of the value chain, including process development, manufacturing and marketing;
They offer the best probability of demonstrating USD capability on lead blockbuster drug candidates, thereby maximizing USD's financial returns and market credibility;
The potential for maximizing the financial value of the USD service will be highest, given these companies' scale of operations and hence financial strength and ability to afford the service.
The initial geographic target market will be the UK and US, depending on the location of the development team for the drug candidates to be studied by USD. All the Big Pharma companies have a substantial presence in the UK and US. The UK also leads Europe in growth in the biopharmaceuticals market.

8.3.1 Competitors

Two main process simulation software packages are currently used in the biopharmaceutical industry, sold by Intelligen and Aspentech. USD's key advantages over these are:

The software uses input parameters based on actual empirical data from running the USD tools. The resultant process models are superior in validity and comprehensiveness to the simulation models based on theoretical algorithms only; A more comprehensive offering than Aspentech in terms of number of purification methods simulated (Aspentech focuses largely on a single operation – chromatography).

The USD service will present competition to the CMOs that currently provide process development services. However, USD's market entry strategy of targeting selected Big Pharma clients, should mitigate some of the risk of potential competitive responses by the CMOs. Big Pharma companies represent a relatively small proportion of CMO process definition revenue, as they tend to undertake most process definition work in-house, before contracting out manufacturing.

8.3.2 Accessing the market and extracting financial value

The first two years will be devoted to developing the hardware and software in order to bring it up to current good manufacturing practice standards (cGMP). During this time, we will work in parallel with the process development team of a Big Pharma company such as Pfizer or Glaxo (which have the largest drug development pipelines currently). Work will be undertaken on several different projects encompassing the major drug classes in order to demonstrate the technology. Direct comparison with the traditional process development scheme will enable quantification of the cost benefits obtained using USD.

The Big Pharma company will be persuaded to allow USD to conduct these studies by:
Utilising UCL's contacts and reputation as leverage;
Emphasising that the Big Pharma company has nothing to lose since we will not charge a fee initially, on the condition that we can use the trial results to promote our product. If, however, the company elects to use USD results for the final manufacturing process, a fee will be charged to cover costs.

At the end of the two year development phase the technology will have been proven to be invaluable to any pharmaceutical company that wishes to be successful within the current climate of shrinking profit margins and rising manufacturing costs. Therefore, once the trial is complete, the founders will tour conferences and trade shows marketing USD and demonstrating how effective it is by reference to the trial with the Big Pharma company.

Early studies conducted at UCL show that cost savings to the client will be in the form of decreased manufacturing costs (10-20% per year) and decreased capital costs (~$15mn). A further benefit will derive from the increased chance of being first to market and the associated revenue benefits. Based on these savings, we would negotiate a royalties based method of payment, which is an industry norm. We would expect a 0.5-1.5% share of the future sales revenue for the drug, with the exact clauses and percentages being negotiated on an individual project basis.

8.3.3 Management and culture

The founders will form the initial management team, focusing on technical aspects and business development. The founding team comprises significant experience in the pharmaceutical, biochemical engineering, finance and consulting sectors, specifically:

Greg Neal: EngD (Biochem) will assume the role of Technical Director, with responsibility for the overall technical aspects of studies, management of technical staff and laboratory facilities, and liaison with UCL on technology strategy and development issues. He has significant direct experience with the USD technology.

John McNulty: BEng (Chem) MSc (Pharm Eng) will be one of the Business Development Directors, with responsibility for marketing USD's services and serving as Client Account Manager for selected clients. John is an MBA student at London Business School, with a background in various technology transfer,

technical support and project management roles in the bulk pharmaceutical manufacturing sector, working with Merck Sharp & Dohme (Irl) Ltd.

Stuti Sahajpal: MEng (Chem) will also undertake the role of Business Development Director. She will also undertake financial and accounting tasks initially. Stuti is an MBA student at London Business School. Her previous experience includes management consultancy (including business development) at Arthur D. Little and equity analysis at Citibank. Most recently, Stuti has worked as a planning manager in a small printing firm, giving her exposure to the challenges of managing a small company.

The founding team will manage the process of shaping USD and securing initial funding. Thereafter, USD will seek to recruit, as soon as possible, a Chief Executive Officer with relevant industry experience to enhance USD's market access, visibility and credibility.

8.3.4 Profit potential and funding requirements

The cost of manufacturing a biopharmaceutical drug represents 24% of the sales revenue. Therefore, for an average drug that has annual sales of $265mn, the manufacturing costs are $63mn. A saving of 10-20% is therefore ~$6-12 mn annually. Our fee of 0.5-1.5% of sales would cost the customer ~$1-4 mn. For a blockbuster drug with annual sales typically of $2.5 bn, the profit potential is significantly larger. The cost of manufacturing a blockbuster rises to $600 mn, and therefore the saving for the client rises to $60-120 mn. The royalty charge on sales now represents annual revenues to USD of $13-38 mn.

We estimate that to run a facility with a capacity for six projects per year would cost nearly $3 mn/year. Therefore, even without participating in the development of a blockbuster drug, the profit margin is still substantial. In addition, since the life cycle of a drug is between 10 and 15 year, the royalty revenue would be ongoing over this time, without incurring further costs directly related to that drug.

Given the anticipated growth in drug candidates under development, going from 45 to 620 (15% of which will be Biopharmaceuticals – approximately 100 drugs per year) by 2005, prospects for scaling operations to conduct studies on more than six drugs (i.e. increasing from a 6% market share) per year are promising. See Table 8.1 for Financial Summary.

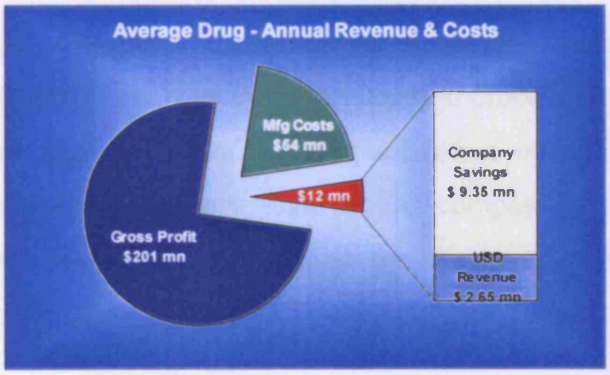

Figure 8.1 Customer Benefits and USD Revenue Model for an "average" drug

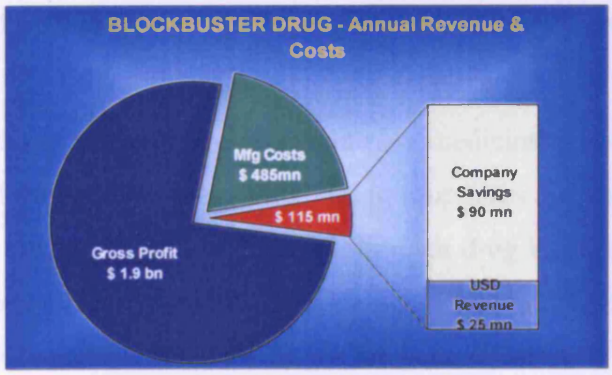

Figure 8.2 Customer Benefits and USD Revenue Model for a "Blockbuster" drug

9 The Impact Of Ultra Scale Down Mimics On The Management Of Purification Process Development And The Regulatory Issues Arising From There Use

Chapters three and four describe the design and use of ultra scale down mimics of precipitation and centrifugation to mimic an industrial scale purification process and study the effects of changes to the purification process. The results presented in chapter three show how individual purification operations can be linked together and how the laboratory scale results compare to the industrial scale process. Chapter four goes on to utilise the mimics to explore the effects of process changes.

The ability to produce information at a laboratory scale, that predicts and mimics the industrial scale, has interesting implications for the initial downstream process design and optimisation and how it is managed.

9.1 The Traditional Biopharmaceutical Drug Development Cycle

The average time to develop and market a new medicine is roughly seven years, but varies widely with some drugs only taking four years and others taking as long as fifteen. The development cycle varies for each drug but the process follows a structure defined by the regulatory environment. The chart below details a typical development cycle and the different stages are generic for every process.

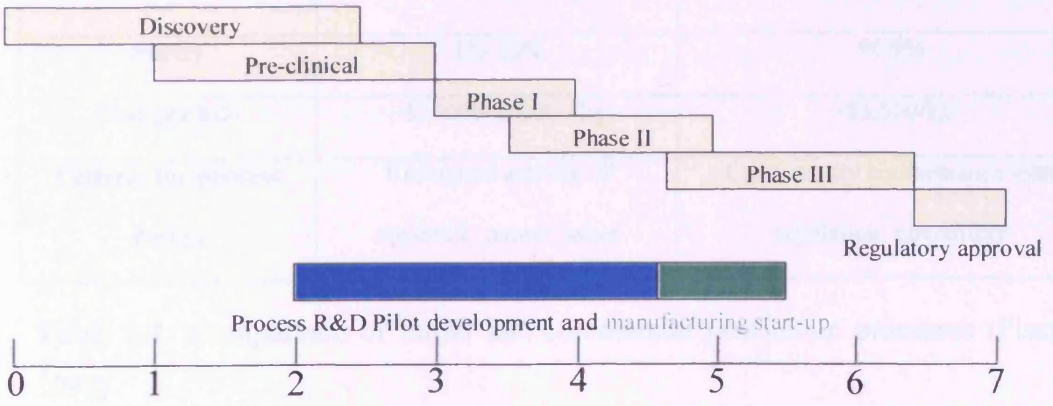

Figure 9.1 Typical Drug Development Process

Process research and development is on the critical path since the manufacturing process needs to be defined before Phase III clinical trails can commence. Any changes after the start of Phase III will result in more consistency and efficacy studies. These can result in a delay to Phase III clinical trials and regulatory approval.

9.1.1 Downstream process research and development

"The goal of process development is to move from a process that has been developed for laboratory developmental work and that is complex, inefficient and potentially unsafe to one that is practical, efficient, robust and safe" (Pisano, 1997). The table below highlights the difference between initial discovery and the full-scale production process. Process development encompasses all the work involved in the transition between these two phases.

	Initial Discovery Process	**Final Commercial Production Process**
Number of purification steps	15	7
Equipment	Test tubes-1 liter flasks	2000-4000 gallon vessels
Batch size (output)	~ 1 gram	100-200 kg
Operators	PhD chemists	Technicians, semi-skilled plant workers
Purity	1%-10%	99.9%
Cost per kilo	~$20000-$50000/kg	~$3,500/kg
Criteria for process design	Biological activity of molecule; patent issues	Cost; quality conformance with regulation; operability

Table 9.1 Comparison of initial and commercial production processes (Pisano, 1997)

Process R&D can be split into two broad sections upstream, which encompasses fermentation design and accounts for roughly 20% of the cost and downstream, which is the actual purification process. Process R&D begins with the search for a manufacturing process. The manufacturing purification process (downstream processing), involves the use of sequential purification equipment to remove the impurities from the feed stream, resulting in a final product that is free from contaminants and suitable for administration to humans. The majority of biological drugs on the market use the same seven main purification methods in variable order to get to a marketable final product. These are: Cell disruption, Centrifugation, Filtration/Ultra-filtration, Expanded bed processes, Column chromatography and Precipitation (Bonnerjea, et al. 1986).

At this point in the cycle, only four pieces of data are available: 1) The protein that needs to be produced; 2) The gene sequence that codes the protein; 3) The host cell used to express the protein and 4) The method for isolating/purifying the protein within the laboratory. The first step is the design of assays that accurately measure the quantity and purity of the protein. The next stage is the design of a manufacture scale process that is efficient and robust - this stage is called pilot development.

9.1.2 Pilot scale development

Traditionally pilot scale studies have been exploratory in nature. This is due to the fact that, at this point in time, very little will be known about the purification of the candidate drug. Of particular importance is the scale of production; this influences the performance of a biotech-process. These "scale-up" effects are difficult to predict because there is little knowledge about what environmental variables might affect the process. The emphasis of process development is to get the process parameters defined as quickly as possible.

Sets of pilot experiments are conducted to determine the influence on performance of a number of process parameters. At this stage, problem solving also focuses on identifying the critical factors affecting process yields and product quality. Getting a process under control requires that a significant amount of data be generated over a large number of controlled pilot runs.

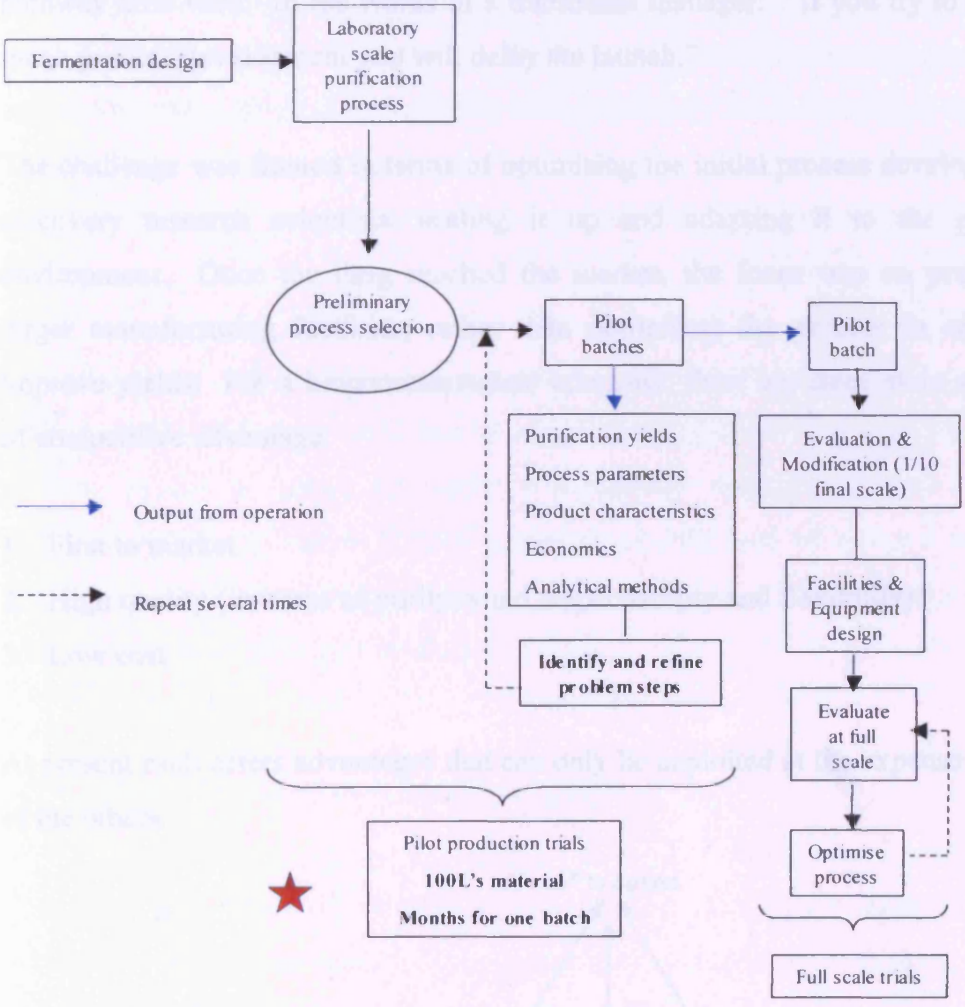

Figure 9.2 Traditional pilot scale process development scheme

9.1.3 The "historical" approach to process development

Considering the fact that pilot plant studies are time consuming, expensive and require dedicated equipment, the traditional attitude among biopharmaceutical companies toward process optimisation has been to delay it until there was a

reasonable certainty that the drug would be approved. In other words, companies hoped to avoid spending resources on drugs that would never make it to market. In practice, this meant investing heavily in process development/optimisation only when drugs got to Phase III clinical trials. Process development was considered a success when it did not get in the way of product launch. Creating a process that gave the drug a competitive advantage was not a high priority, as this was considered a threat to the aim of keeping process development off the critical pathway time wise. In the words of a traditional manager: "If you try to do too much process development you will delay the launch."

The challenge was framed in terms of optimising the initial process developed by discovery research scientists, scaling it up and adapting it to the process environment. Once the drug reached the market, the focus was on providing larger manufacturing facilities, rather than optimising the process in order to improve yields. For a biopharmaceutical company, there are three main sources of competitive advantage:

1. First to market
2. High quality (in terms of purity, yield, dependability and flexibility)
3. Low cost

At present each offers advantages that can only be exploited at the expense of one of the others.

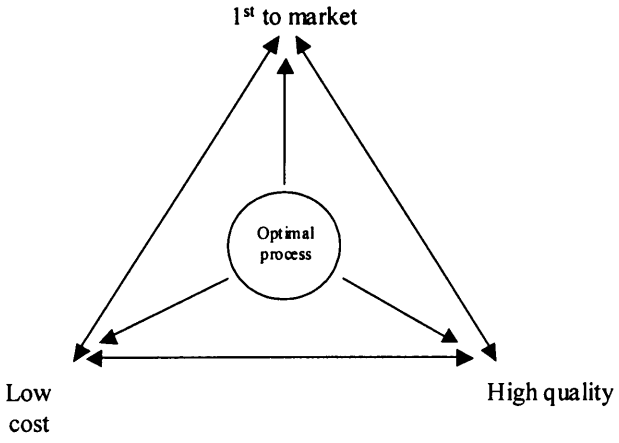

Figure 9.3 Benefits of an optimised manufacturing process

This approach used to make sense when drugs were relatively simple to manufacture and process development involved few major challenges. FDA regulations also stated that the process did not need to be finalised until later on in the development cycle.

However, the industry context is now changing, creating challenges for biopharmaceutical companies. The financial and regulatory environment is creating downward pressure on revenues (caused by shorter product life cycles, pressure by governments to produce cheaper drugs and increased competition) and upward pressure on manufacturing costs (caused by the increasing complexity of new drugs and stricter regulatory requirements). As a result leaving process development until the last minute will almost certainly lead to unaffordable delays.

This changing environment has caused a rethink of process development strategies. It has been proved that thorough investigation of the manufacturing process leads to improved yields, accelerates throughput and reduces manufacturing cycle times. These improvements all lead to reduced costs of manufacture and potentially provide an advantage in terms of the potential for getting to market first with a new class of drug.

9.1.4 The current management problem

The time and monetary constraints surrounding pilot plant trials preclude biopharmaceutical companies from thoroughly optimising a process. The pressure to be first to market and to mitigate the risk of lost capital investment if a drug fails to get to market, out weighs the pressure of having a perfect purification process. **The result is often an unwieldy, inefficient, and costly manufacturing process.** If process improvements are carried out after the product has been launched, which is very costly and time consuming, then the opportunity is missed to reap savings on production costs, since demand normally peaks early in product life cycle. Therefore, improvements need to be made early on. Also, regulatory constraints mean that any major process changes need to be

validated and approved by the appropriate regulatory authority, a process that is by itself time consuming and expensive. However, the high cost and long time line of pilot studies is prohibitive towards carrying out extensive trials and providing an optimised process early in the cycle, when the drugs chances of reaching the market are less than 20%. The result is that the biopharmaceutical companies are now faced with a conundrum; millions cannot be invested early in the drug development cycle to develop a manufacturing process, since the chances of it getting to market are so low. Therefore, the biopharmaceutical company chooses to burden itself with a generic un-optimised manufacturing process in order to reduce time and costs.

9.2 Ultra Scale Sown As The Theoretical Solution To The Process Development Conundrum

Ultra Scale Down (USD) mimics, such as those described in chapters three and four offer process engineers the opportunity to recreate the conditions of a manufacturing scale purification process on a laboratory bench top. At present a fermentation design mimic has not been built, although one is in development (Lamping, 2003). This means that any purification process that utilises the unit operations that USD has the ability to mimic, can be investigated at the start of the development cycle. This is at a fraction of the cost in terms of time, material and facilities. The results from these scale down investigations ensure that process development is kept off the critical path and that a **robust, effective purification process is delivered early** on with a minimum number of pilot scale trials needed to verify it. As a result, a biopharmaceutical company can **be first to market with a low cost and high quality process**. The complementary software allows results from individual operations to be integrated into one whole purification process model. This allows process engineers to make changes to one unit operation and then monitor the effect on the whole process in terms of yield, efficiency and cost.

Utilising USD technology has an effect on the drug development cycle, which is shown below:

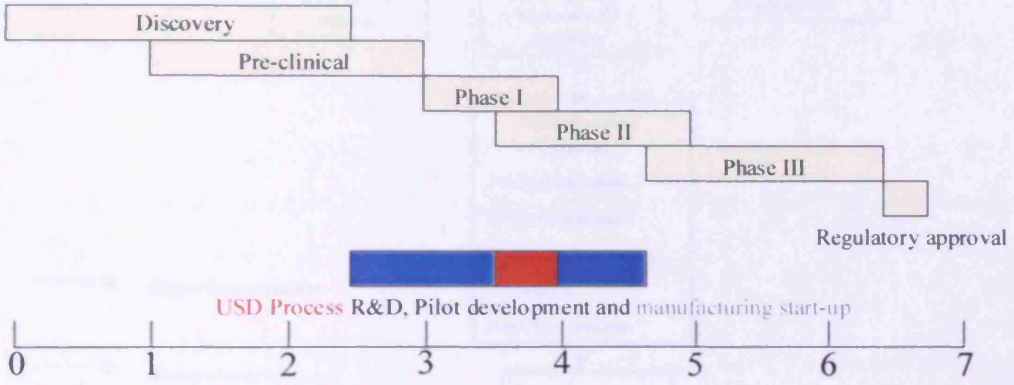

Figure 9.4 Proposed drug development cycle using ultra scale down technology

Process R&D is no longer on the critical path; it takes less time, requires a substantially smaller financial investment and delivers a more robust and efficient process. This in turn helps to decrease the time to market by reducing the time spent at the regulatory approval stage. A robust process that consistently delivers a purified product will take less time to gain approval than a process that has not been thoroughly investigated and optimised.

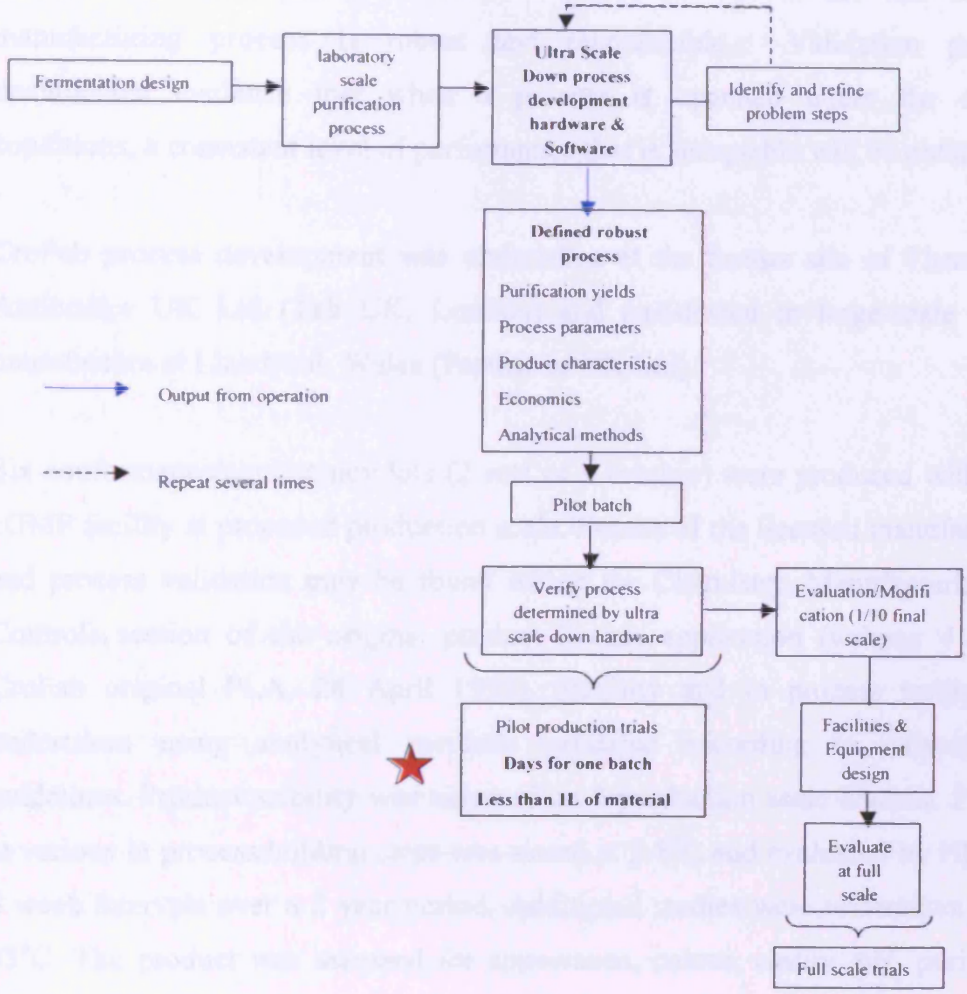

Figure 9.5 Process development scheme utilising ultra scale down technology

9.3 Validation Of The "Crofab" Purification Process

CroFab is the trade name for Protherics anti-rattle snake venom. This section will briefly discuss the validation of the purification process described throughout this thesis and some of the issues arising from the use of Ultra Scale Down mimics during process development.

In order for a company to market a pharmaceutical product within a country, they must first obtain approval from the regulatory authorities governing the countries they wish to sell to. An example is the Food and Drug Administration (FDA) of the United States of America; they require that the product and process be tested

in order to ensure that it is efficacious, safe for human use and that the manufacturing process is robust and reproducible. Validation provides documented evidence that when a process is operated under the defined conditions, a consistent level of performance that is acceptable will be obtained.

CroFab process development was undertaken at the former site of Therapeutic Antibodies UK Ltd (Tab UK, London) and transferred to large-scale cGMP manufacture at Llandysul, Wales (Protherics UK Ltd).

Six conformance/consistency lots (2 sets of 3 batches) were produced within the cGMP facility at proposed production scale. Details of the licensed manufacturing and process validation may be found within the Chemistry, Manufacturing and Controls section of the original product license application (volume 4 of 44, CroFab original PLA, 24 April 1998). Stability and in process testing was undertaken using analytical methods validated according to current ICH guidelines. Product stability was assessed on 3 production scale batches. Product at various in process holding steps was stored at 2-8°C and evaluated by HPLC at 4 week intervals over a 2 year period. Additional studies were undertaken at 27-33°C. The product was assessed for appearance, colour, clarity, pH, purity and potency. Two prior approval clinical studies were undertaken to assess stability, efficacy and dosage of the final product.

As several volumes of the original CroFab license application are held within the Department of Regulatory affairs, Protherics Inc USA and due to confidentiality restrictions regarding the licensed product, further details of process validation are beyond the scope of this thesis. The CroFab purification process outlined in Chapter 1 describes the current, validated method of GMP manufacture.

As a whole process validation involves the characterisation of each stage of the purification process in order to demonstrate that it is robust, repeatable and performs as intended; it should also demonstrate the limits of each step. Cleaning validation also falls under this umbrella. The cleaning of each piece of equipment and the facility needs to be validated to demonstrate removal of proteins whether

they are from the previous process or the environment. It also needs to demonstrate that no trace of the cleaning chemicals themselves remain.

Equipment validation can be split into two phases. The installation qualification provides documented verification that the equipment has been installed inline with the manufacturers recommendations and establishes confidence that the equipment is capable of consistently operating within the established limits. The operational qualification provides documented evidence that the equipment performs as intended over the anticipated operating ranges.

Test methods such as SDS-Page or Gel Permeation Chromatography provide evidence of, for example: the purity, identity, concentration or biological activity of the protein of interest. A test method validation study will have to be carried out which will demonstrate that the method is capable of determining the aspect being examined, for example the concentration. The study will also have to demonstrate that the method is repeatable and accurate. The study involves characterising the method including aspects such as its limits of operation and interfering chemicals. Once completed the test method validation will demonstrate the applicability, repeatability and acceptability of the test.

The purification of CroFab involves eight distinct steps the precipitation step has been chosen to demonstrate how a process step might be validated. The precipitation step is the first major purification step. It is designed to remove the majority of the contaminating albumin and some other contaminating proteins in order to produce a feed stream suitable for chromatographic purification operations.

In order to validate the purification step a characterisation study was undertaken which addressed the parameters influencing the precipitation process. These included; the amount of sodium sulphate used, the rate/mode of addition of the sodium sulphate, the type of sodium sulphate, the temperature of operation and the mixing conditions/time. Each parameter was studied in order to define a range within which the process has to be operated. For example a range of sodium sulphate concentrations from ten to twenty percent (w/v) was studied. The study

determined that precipitation occurs from 12% sodium sulphate upwards. A working value of 18% was then chosen so that any small variation that may occur during routine manufacture will not impact the output of the process. Each aspect was examined and an operational range set which is within the limits studied. In practice the result of a well thought out and applied characterisation study will be a purification step that is robust, repeatable and satisfactory to the governing agencies.

9.4 Regulatory Issues Arising From The Use Of Ultra Scale Down Mimics During Process Development

Ultra Scale Down mimics such as those developed in chapters three and four might enable initial process development work to be carried out at a very small scale, which requires only very small quantities of material. This would allow a company wishing to develop and market a product to conduct more research on the purification process should it wish to. This in turn could generate more evidence that the manufacturing process is robust and reproducible since a number of experiments could be conducted testing the manufacturing process to the very limits of its design.

If however this information were to be submitted as part of the validation process the Ultra Scale Down mimics would first have to be validated. This would involve not only the standard installation, operation and performance qualifications required for any piece of validated equipment but also that the results generated by the small scale experiments be validated as being comparable to the results generated during a full scale manufacturing run.

In order to do this the manufacturer of any Ultra Scale Down device would have to provide evidence and details of the working ranges/conditions within which the device has been tested to show that when used under the tested operating conditions, it will generate results that compare to the full-scale process.

In practice, within the biopharmaceutical industry this may not be possible because every process is different, operated under different conditions with a different product. Therefore, the ultra scale down mimic would have to be validated for each product, process and condition. A restraint which may limit their use to that of a research tool for many years to come.

Ultra scale down mimics have a great potential to provide a wealth of information about a manufacturing process but during the validation of a process their usefulness would be limited by the fact that it would be extremely difficult to validate, that the information generated, accurately mimics what occurs at the larger scale.

10 References

Akerstrom B, Bjork L. 1986. A physicochemical study of protein G, a molecule with unique immunoglobulin G-binding properties. J Biochem Chem 261 (22): 10240-10247.

Akerstrom B, Brodin T, Reis K, Bjork L. 1985. Protein G: A powerful tool for binding and detection of monoclonal and polyclonal antibodies. J Immunol 135: 2589-2592.

Ambler CM. 1952. The evaluation of centrifuge performance. Chem Eng Prog 48: 150-159.

Ambler CM. 1959. The theory of scaling up laboratory data for the sedimentation type centrifuge. J Biochem Microbiol Technol Eng 1: 185-205.

Andrade JD. 1985. Principles of protein adsorption in surface and interfacial aspects of biomedical polymers. Vol 2, Andrade JD. (Ed). Plenum Press, New York. pp. 1-80.

Anspach FB, Johnston A, Wirth HJ, Unger KK, Hearn MTW. 1990. High-performance liquid chromatography of amino-acids peptides and proteins, Part XCV. J Chromatogr 499: 103-124.

Atkinson T, Scawen MD, Hammond PM. 1987. Large scale industrial techniques of enzyme recovery. Chapter 5 in "Biotechnology". Vol 7a Kennedy JF. (Ed) VCH Publishers, Weinheim, Germany.

Attia H, Bennasar M, Delafuente BT. 1991. Study of the fouling of inorganic membranes by acidified milks using scanning electron-microscopy and electrophoresis .1. Membrane with pore diameter 0.2-Mu-M. J Dairy Res 58 (1): 39-50.

Attia H, Bennasar M, Delafuente BT. 1991. Study of the fouling of inorganic membranes by acidified milks using scanning electron-microscopy and electrophoresis .2. Membrane with pore diameter 0.8-Mu-M J Dairy Res 58 (1): 51-65

Axelsson HAC. 1985. Centrifugation. Chapter 21 in "Comprehensive biotechnology". Vol. 2, Cooney, Humphrey AE. (Eds). Pergamon Press, Oxford, U.K.

Axon R, Porath J, Ernback S. 1967. Chemical coupling of peptides and proteins to polysaccharides by means of cyanogen halides. Nature 214: 1302-1304.

Ayazi Shamlou P. (Ed). 1993. In "Processing of Solid-Liquid Suspensions" Butterworth Heinemann, Oxford. pp. 273-285.

Ayazi Shamlou P. Synowiec P. Zolfagharian A. 1994. Critical suspension conditions in stirred crystallizers. Chem Eng J Bioch Eng 55 (1-2): 45-51.

Ayazi Shamlou P. 2003. Scaleable processes for the manufacture of therapeutic quantities of plamsid DNA. Biotechnol Appl Biochem 37 (3): 207-218.

Baker RJ, Fane AJ, Fell CJD, Yoo BH. 1985. Factors affecting flux in crossflow filtration. Desalination 53: 81-93.

Belfort G, Davies RH, Zydney AL. 1994. The behaviour of suspensions and macromolecular solutions in crossflow filtration. J Membr Sci 96: 1-58.

Bell DJ, Hoare M, Dunnill P. 1983. The formation of protein precipitates and their centrifugal recovery. Adv Biochem Eng/Biotech 26: 1-72.

Bell DJ, Dunnill P. 1982a. Shear disruption of soya protein precipitate particles and the effect of ageing in a stirred tank. Biotech Bioeng 24: 1271-1285.

Bell DJ, Dunnill P. 1982b. The influence of precipitation reactor configuration on the centrifugal recovery of isoelectric soya protein precipitate. Biotech Bioeng 24: 2319-2339.

Bellot JC, Condoret JS. 1993. Modelling of liquid chromatography equilibria. Process Biochem 28: 365-376.

Birch JR, Bonnerjea J, Flatman S, Vranch S. 1995. Monoclonal Antibodies: Principles and Applications. Birch JR, Lennox ES. (Eds). Wiley-Liss, New York, pp. 231.

Bjorck L, Kronvall G. 1984. Purification and some properties of *Streptococcal* protein G, a novel IgG binding reagent. J Immunol 133 (2): 969-974

Blanco R, Arai A, Grinberh N, Yarmush DM, Karger BL. 1989. Role of association on protein adsorption isotherms: β-lactoglobulin A adsorbed on a weakly hydrophobic surface. J Chromatogr 482: 1-12.

Blank GS, Zapata G, Fahrner R, Milton M, Yedinak C, Knudsen H, Schmelzer C. 2001. Expanded bed adsorption in the purification of monoclonal antibodies: A comparison of process alternatives. Biosep 10: 65-71.

Blatt WF, Dravid A, Michaels AS, Nelsen L. 1970. Solute polarization and cake formation in membrane ultrafiltration: Causes, consequences and control techniques. Membrane Science and Technolgy. Flinn JE. (Ed). Plenum Press, New York. pp 73-98.

Bonnerjea J, Oh S, Hoare M, Dunnill P. 1986. Protein purification: The right step at the right time. Bio/Technology 4: 954-958.

Bonnerjea J, Jackson J, Hoare M, Dunnill P. 1988. Affinity flocculation of yeast cell debris by carbohydrate-specific compounds. Enzyme Microb Technol 10: 357-360.

Boulding N, Keshavarz-Moore E, Ayazi Shamlou P. 2002. Ultrascale down of basket centrifuge for the recovery of secreted antibody fragments from *Aspergillus awamori*. Biotech Bioeng 79 (4): 381-388.

Bowen WR, Gan Q. 1991. Properties of microfiltration membranes: Flux loss during constant pressure permeation of Bovine Serum Albumin. Biotech Bioeng 38 (7): 688-696.

Boychyn M, Doyle W, Bulmer M, More J, Hoare M. 2000. The laboratory scale down of protein purification processes involving fractional precipitation and centrifugal recovery. Biotech Bioeng 69 (1): 1-10.

Boychyn M, Yim SSS, Shamlou PA, Bulmer M, More J, Hoare A. 2001. Characterisation of flow intensity in continuous centrifuges for the development of laboratory mimics. Chem Eng Sci 56 (16): 4759-4770.

Boyer PM, Hsu JT. 1990. Adsorption equilibrium of proteins on a dye-ligand adsorbent. Biotech Technol 4: 61-66.

Bradford MM. 1976. A rapid and sensitive method for the quantification of microgram quantities of protein utilising the principle of protein-dye binding. Anal Biochem 72: 248-254.

Brown DE, Kavanagh PR. 1987. Cross-flow separation of cells. Process Biochem. 22 (4): 96-101.

Brunner KH, Hemfort H. 1988. Downstream processes: Equipment and techniques, Centrifugal separation in biotechnological processes, Advance in biotechnological processes. Vol 8, Mizrahi A, Alan R. (Eds). Liss inc, New York. pp. 1-50.

Burns D, Zydney AL. 1999. Effect of solution pH on protein transport through ultrafiltration membranes. Biotech Bioeng 64 (1): 27-37.

Cabrera KE, Wilchek M. 1988. Polymeric supports for affinity-chromatography and high-performance affinity-chromatography. Makromolekulare chemie-macromolecular symposia 19: 145-154.

Cacace MG, Landau EM, Ramsden JJ. 1997. The Hofmeister series: salt and solvent effects on interfacial phenomena. Quarterly reviews of biophysics. 30 (3): 241-277.

Chan MYY, Hoare M, Dunnill P. 1986. The kinetics of protein precipitation by different reagents. Biotech Bioeng 28: 387-393.

Chase HA. 1984. Prediction of the performance of preparative affinity chromatography. J Chromatogr 297: 179-202.

Chase HA. 1988. Optimisation and scale-up of affinity-chromatography. Makromol Chem-macromol Symp 17: 467-482.

Chen V, Fane AG, Madaeni S, Wenten IG. 1997. Particle deposition during membrane filtration of colloids: transition between concentration polarisation and cake formation. J Membr Sci 125(1): 109-122.

Cheryan M. (Ed). 1988. Ultrafiltration handbook. Technomic publishing company Inc.

Chippaux JP. 1998. Snakebites: appraisal of the global situation. Bulletin of the World Health Organisation. 76 (5): 515-524.

Chisti Y, Moo-young M. 1991. Large-scale protein separations - Engineering aspects of chromatography. Biotechnol adv 8 (4): 699-708.

Clarkson AI, Lefevre P, Titchener-Hooker NJ. 1993a. A study of the process interactions between cell debris clarification stages in the recovery of yeast intracellular products. Biotechnol Prog 9: 464-467.

Clarkson AI, Bulmer M, Siddiqi SF, Titchener-Hooker NJ. 1993b. Pilot scale verification of Bioprocess models. Computers and Chem Eng 18: 561-655.

Clarkson AI, Bulmer M, Titchener-Hooker NJ. 1996a. Pilot scale verification of a computer based simulation for fractional protein precipitation. Bioprocess Eng 14: 69-80.

Clarkson AI, Bulmer M, Titchener-Hooker NJ. 1996b. Pilot scale verification of a computer based simulation for the centrifugal recovery of biological particles. Bioprocess Eng 14: 81-89.

Corcoran R, Duran S. 1977. Albumin determination by a modified bromcresol green method. Clin Chem 23: 765-766.

Culkin B, Plotkin A, Monroe M. 1998. Solve membrane fouling problems with high-shear filtration. Chem Eng Prog 1: 29-33.

Datar R, Rosen CG. 1987. Centrifugal separation in the recovery of intracellular protein from E.coli. Chem Eng J 34: 49-56.

Davies JL, Baganz F, Ison AP, Lye GJ. 2000. Studies on the interaction of fermentation and microfiltration operations: Erythromycin recovery from *Saccharopolyspora erythraea* fermentation broths. Biotech Bioeng 69: 429-439.

Debye P, Huckel E. 1923. Zur theorie der elektrolyte II. Das Grenzgesetz für die elektrische leifähigkeit. *Phys Z* 24: 305-325.

Dittus FW, Boelter LMK. 1930. Heat transfer in automobile radiators of the tubular type. Univ Calif Pub Eng 13: 443.

El Er, Zaidenzaig Z, Shaltiel S. 1972. Use in the purification of glycongen phosphorylase. Biochem Biophys Res Commun 49: 383-390.

Eriksson K. 1998. Protein purification: High resolution methods and applications. Second edition. Janson JC, Ryden L. (Ed). Wiley-VCH. Inc. pp. 285.

Fahrner RL, Whitney DH, Vanderlaan M, Blank GS. 1999a. Performance comparison of Protein A affinity-chromatography sorbents for purifying recombinant monoclonal antibodies. Appl Biochem 30: 121-128.

Fahrner RL, Iyer HV, Blank GS. 1999b. The optimal flow rate and column length for maximum production rate of protein A affinity chromatography. Bioprocess Eng 21: 287-292.

Fahrner RL, Blank GS, Zapata GA. 1999c. Expanded bed protein A affinity chromatography of a recombinant humanized monoclonal antibody: process development, operation, and comparison with a packed bed method. J Biotechnol 75: 273-280.

Field RW, Wu D, Howell JA, Gupta BB, 1995. Critical Flux concept for microfiltration fouling. J Membr Sci 100(3): 259-272.

Forsgen A, Sjoquist J. 1966. "Protein A" from *S. aureus.* I. Pseudo-immune reaction with human gamma-globulin. J Immunol 97: 822-827.

Foster PR. 1994. Protein precipitation, Chapter 4 in "Engineering processes for bioseparations". Weatherley LR. (Ed). Butterworth-Heinemann, Oxford, U.K.

Foster PR, Dunnill P, Lilly MD. 1976. The kinetics of protein salting out: precipitation of yeast enzymes by ammonium sulphate. Biotech Bioeng 18: 545-580.

Frank MB. (Ed). 1997. Antibody binding to protein A and protein G beads. Molecular Biology Protocals. (http://ornrf.ouhsc.edu/~frank/proteina.html). Oklahoma City. Revision date: January 3, 2001.

Freundlich H. 1907. Ueber die Adsorption in Loesungen. Z physik Chem 57: 385-470.

Gill DS, Roush DJ, Willson RC. 1994. Adsorption heterogenecity and thermodynamic driving forces in anion exchange equilibria of cytochrome b5. J Colloid Interface Sci 167: 1-7.

Grant K, Turner BG. 1999. Understanding biopharmaceuticals-manufacturing and regulatory issues. Grindley JN, Ogden JE. (Eds). Interpharm Press, Denver.

Gritti F, Guiochon G. 2003. Adsorption-desorption isotherm hysteresis of phenol on a C_{18} –bonded surface. J Chromatogr A 1010: 153-176.

Gulich S, Linhult M, Stahl S, Hober S. 2002. Engineering *streptococcal* protein G for increased alkaline stability. Prot Eng 15 (10): 835-842.

Haarstrick A, Rau U, Wagner F. 1991. Cross-flow filtration as a method of separating fungal cells and purifying the polysaccharide produced. Bioprocess Eng 6 (4): 179-186.

Hahn R, Schlegel R, Jungbauer A. 2003. Comparison of protein A affinity sorbents. J Chromatogr B 790: 35-51.

Hammond PM, Scawen MD. 1989. High resolution fractionation of proteins in downstream processing. J Biotechnol 11: 119-134.

Hanemaaijer JH, Robbertsen T, Vandenboomgaard T, Gunnink JW. 1989. Fouling of ultrafiltration membranes - the role of protein adsorption and salt precipitation. J Membr Sci. 40 (2): 199-217.

Harrison R. 2000. Going ballistic. Wellcome News 24: 24-25.

Hawrylik SJ, Wasilko DJ, Pillar JS, Cheng JB, Lee SE. 1994. Vortex flow filtration of mammalian and insect celles. Cytotechnology 15: 253-258.

Henzler HJ, 2000. Particle stress in bioreactors. Adv Biochem Eng Biotechnol 67: 35-82.

Hermia J. 1982. Constant pressure filtration laws - application to power-law non-newtonion fluids. Transactions IChemE 60: 183-187.

Higgins JJ, Lewis DJ, Daly WH, Mosqueira FG, Dunnill P, Lilly MD. 1978. Investigation of the unit operations involved in the continuous flow isolation of β-galactosidase. Biotech Bioeng 20: 159-182.

Hoare M. 1982. Protein precipitation and precipitate ageing, Part 1: "Salting out and ageing of casein precipitates". Transactions IChemE 60: 79-87.

Hoare M, Bell DJ, Dunnill P. 1983. In "Biochemical Engineering III". Venkatsubramanian K, Constantinides A, Vieth WR. (Ed). New York. Acad Sci. pp 254-269.

Hofmeister F. 1888. Arch Exp Pathol Pharmakol (Leipzig) 24: 247–260.

Horstmann BJ, Chase HA. 1989. Modelling the affinity adsorption of immunoglobulin G to protein A immobilised to agarose matrices. Chem Eng Res Des 67: 243-254.

Howel JA, 1995. Sub-critical flux operation of microfiltration. J Membr Sci 107 (1)(2): 165-171.

Huang JX, Schudal J, Guiochon G. 1990. Adsorption behaviour of albumin and conalbumin on TSK-DEAE 5PW anion exchanger. J Chromatogr 504: 335-349.

Huse K, Bohme HJ, Scholz GH. 2002. Purification of antibodies by affinity chromatography. J Biochem Biophys Meth 51: 217-231.

IbrahimGranet O, Bertrand O. 1996. Separation of proteases: Old and new approaches. J Chromatogr B-Biomed App 684: 239-263.

Israelachvili JN. 1985. Measurements of hydration forces between macroscopic surfaces. Chem Scripta 25 (1): 7-14.

Jacobson J, Frenze. J, Horvath C. 1984. Measurement of adsorption isotherms by liquid chromatography. J Chromatogr 316: 53-68.

Janson JC. 1987. On the history of the development of Sephadex. Chromatographia 23: 361-369.

Janson JC, Hedman P. 1987. On the optimization of process chromatography of proteins. Biotechnol Prog 3 (1): 9-13.

Janson JC, Keistiansen T. 1990. Packings and stationary phases in chromatographic techniques. Unger KK. (Ed). Marcel Dekker, New York. pp. 747.

Jin K, Thomas ORT, Dunnill P. 1994. Monitoring recombinant inclusion body recovery in an industrial disc stack centrifuge. Biotech Bioeng 44: 455-460.

Jornitz M, Meltzer T. 1988. In filtration in the pharmaceutical industry. Meltzer T. and Jornitz M. (Eds). New York: Marcel Dekker Inc.

Katoh S. 1987. Scaling up Affinity Chromatography. Trends Biotechnol 5 (12): 328-331.

Kelly ST, Zydney AL. 1996. Protein fouling behaviour during microfiltration: Comparative behaviour of different model proteins. Biotech Bioeng 55 (1): 91-100.

Kieran PM, Malone DM, MacLoughlin PF. 2000. Effects of hydrodynamic and interfacial forces on plant cell suspension systems. Adv Biochem Eng Biotechnol 67: 139-177.

Kroner KH, Schütte H, Hustedt H, Kula MR. 1984. Crossflow filtration in downstream processing of enzymes. Process Biochem 19 (2): 67-74.

Kroner KH, Nissinen V. 1988. Dynamic filtration of microbial suspensions using an axially rotating filter. J Membr Sci 36: 85-100.

Kroner KH, Nissinen V, Ziegler H. 1987. Improved dynamic filtration of microbial suspensions. Bio/Technology 5: 921-925.

Laemmli UK. 1970. Cleavage of structural proteins during the assembly of the head of bacteriophage T4. Nature 227: 680-688.

Langeloh T, Bott R, Ehrfeld E. 1998. Continuous sieving with an agitated cross flow apparatus. Adv filtration separation technol 12: 442-448.

Langmuir I. 1918. The adsorption of gases on plane surfaces of glass, mica and platinum. J Am Chem Soc 40: 1361-1403.

Lamping SR, Zhang H, Allen B, Shamlou PA. 2003. Design of a prototype miniature bioreactor for high throughput automated bioprocessing. Chem Eng Sci 58 (3-6): 747-758.

Lee SS, Burt A, Russotti G, Buckland B. 1995. Microfiltration of recombinant yeast cells using a rotary disk dynamic filtration system. Biotech Bioeng 48: 386-400.

Leung WWF. (Ed). 1998. Industrial centrifugation technology. New York. McGraw-Hill.

Levy MS, Collins IJ, Yim SS, Ward JM, Keshavarz-Moore E, Titchener-Hooker NJ, Ayazi Shamlou P, Dunnill P. 1998. Effect of shear on plasmid DNA in solution. Bioprocess Eng 20: 7-13.

Levy MS, Ciccolini LAS, Yim SS, Tsai JT, Titchener-Hooker NJ. Ayazi Shamlou P, Dunnill P. 1999. The effects of material properties and fluid flow intensity on plasmid DNA recovery during cell lysis. Chem Eng Sci 54: 3171-3178.

Liapis AI. 1989. Theoretical aspects of affinity-chromatography. J Biotechnol 11 (2-3): 143-160.

Lin JK, Karn SJ, Ladisch MR. 1987. Cause and correction of base-line interruptions observed for small-bore liquid-chromatography columns packed with cation-exchange resin in the H+ form. Biotech Bioeng 30 (2): 331-333.

Lojkine MH, Field RW, Howell J. 1992. Crossflow microfiltration of cell suspensions: A review of models with emphasis on particle size effects. Trans IChemE 70 (Part C): 149-164.

Lowe CR, Lowe AR, Gupta G. 2001. New developments in affinity chromatography with potential application in the production of biopharmaceuticals. J Biochem Biophys Methods 49: 561-574.

Maiorella B, Dorin G, Carion A, Harano D. 1991. Crossflow filtration of animal cells. Biotech Bioeng 37: 121-126.

Mannweiler K, Hoare M. 1992. The scale down of an industrial disc stack centrifuge. Bioprocess Eng 8: 18-25.

Mannweiler K, Titchener-Hooker NJ, Hoare M. 1989. Biochemical engineering improvements in the centrifugal recovery of biological particles. IChemE.-Symposium on Adv Bioch Eng 105-117.

Mao QM, Prince IG, Hearn MTM. 1995. High-performance liquid chromatography of amino acids, peptides and proteins. CXXXIX Impact of operating parameters in large-scale chromatography of proteins. J Chromatogr A 691: 273-283.

Marshall AD, Munro PA, Tragardh G. 1993. The effect of protein fouling in microfiltration and ultrafiltration on permeate flux, protein retention and selectivity: A literature review. Desalination 91 (1): 65-108.

Maybury JP. 1999. Scale-down of a bioprocess sequence for the recovery and purification of an intracellular protein. PhD thesis, University College London, U.K.

Maybury JP, Mannweiler K, Titchener-Hooker NJ, Hoare M, Dunnill P. 1998. The performance of a scaled down industrial disc stack centrifuge with a reduced feed material requirement. Bioprocess Bioeng 18: 191-199.

McCormick D. 1988. Chromatography and affinity separations - 1988 report. Bio/Technology 6 (2): 158.

McCue JT, Kemp G, Low D, Quinones-Garcia I. 2003. Evaluation of protein-A chromatography media. J Chromatogr A 989: 139-153.

Mercille S, Johnson M, Lemieux R, Massie B. 1994. Filtration-based perfusion of hybridoma cultures in protein-free medium: Reduction of membrane fouling by medium supplementation with Dnase I. Biotech Bioeng 43: 833-846.

Mignard D, Glass DH. 2001: Fouling during the crossflow ultrafiltration of proteins: a mass-transfer model. J Membr Sci 186: 133-143.

Mikulasek P. 1994. Methods to reduce concentration polarization and fouling in membrane filtration. Collection of Czech Chemical Communications 59: 737-755.

Mosqueira FG, Higgins JJ, Dunnill P, Lilly MD. 1981. Characteristics of mechanically disrupted bakers yeast in relation to its separation in industrial centrifuges. Biotech Bioeng 13: 335-343.

Narayanan SR. 1994. Preparative affinity chromatography of proteins. J Chromatogr A 658: 237-258.

Neal G, Christie J, Keshavarz-Moore E, Ayazi Shamlou P. 2003. An ultra scale-down approach for the prediction of full-scale recovery of ovine polycolonal immunoglobulins used in the manufacture of snake venom-specific fab fragment. Biotech Bioeng 81 (2): 149-157.

Neal G, Francis R, Keshavarz-Moore E, Ayazi Shamlou P. 2004. Separation of IgG precipitate from contaminating proteins using microfiltration. Biotech Appl Biochem 39(2): 241-248.

O'Grady J, Losikoff A. 1996. Virus removal studies using nanofiltration membranes. Dev Biol Stand 88: 319-326.

Omar A. 1996. Virus inactivation by pepsin treatment at pH 4 of IgG solutions: factors affecting the rate of virus inactivation. Transfusion 36: 866-872.

Oscarsson S, Angulotatis D, Chaga G, Porath J. 1995. Amphiphilic agarose-based adsorbents for chromatography - comparative-study of adsorption capacities and desorption efficiencies. J Chromatogr A 689 (1): 3-12.

Parker TG, Dalgleish D. 1977. The use of light-scattering and turbidity measurements to study the kinetics of extensively aggregating proteins: α_s-Caesin. Biopolmers 16: 2533-2547.

Pavlu B, Gellerfors P. 1993. Hydrophobic interaction chromatography of recombinant human growth hormone. Genotropin Biosep 3: 257-265.

Peterson EA, Herbert A, Sober. 1956. Chromatography of proteins. I. cellulose ion-exchange adsorbents. J Am Chem Soc 78 (4): 751-755.

Pisano GP. (Ed). 1997. The development factory: Unlocking the potential of process innovation. Boston: Harvard Business Review Press.

Porath J, Flodin P. 1959. Gel Filtration: A method for desalting and groups separation. Nature. 183: 1657-1659.

Porter MC. 1972. Concentration polarization with membrane ultrafiltration. Ind Eng Chem Prod Res Develop 11 (3): 234-248.

Postlethwaite J, Lamping SR, Leach GJ, Hurwitz MF, Lye GJ. 2004. Flux and transmission characteristics of a vibrating microfiltration system operated at high biomass loading. J Membrane Sci 1: 89-101.

Przybycien TM, Bailey JE. 1989. Aggregation kinetics in salt-induced protein precipitation. AIChE J 35: 1779-1790.

Regnier FE. 1984. Methods in Enzymology. Vol 104. Jakoby WB. (Ed). Acedemic Press, New York. pp. 170.

Reis KJ, Ayoub EM, Boyle MD. 1984. *Streptococcal* Fc receptors. I. Isolation and partial characterization of the receptor from a group C *streptococcus*. J Immunol 132: 3091-3097.

Richardson P. 1987. A biochemical engineering study of fractional protein precipitation. PhD thesis, University College London, U.K.

Rothstein F. 1994. Protein purification process engineering. Harrison RG. (Ed) Marcel Derker Inc. New York.

Ruann RC, Blair JB, Shaeiwitz JA. 1988. Dual-functional affinity protein purification. Biotechnol Prog 4: 107-112.

Rumpus J. 1997. Dewatering and scale down of solids recovery in industrial centrifuges. PhD Thesis, University College London, U.K.

Rushton JH, Costich EW, Everett HJ. 1950. Power characteristics of mixing impellers, part 2. Chem Eng Prog 46 (9): 467-476.

Sada E, Katoh S, Sukai K, Tohma M, Kondo A. 1986. Adsorption equilibrium in immuno-affinity chromatography with polyclonal and monoclonal antibodies. Biotech Bioeng 28: 1497-1502.

Scatchard G. 1949. The attractions of proteins for small moelcules and ions. Ann New York Acad Sci 51: 658-666.

Schlichting H. (Ed). 1979. Boundary layer theory, 7th Ed. Pergamon Press, London.

Schwarz A. 2000. Affinity Chromatography: Methods and Protocols. Bailon P, Ehrlich GK, Fung WJ, Berthold W. (Eds). Humana Press, Totowa, NJ.

Scopes RR. 1981. Quantitative studies of ion-exchange and affinity elution chromatography of enzymes. Anal Biochem 114 (1): 8-18.

Scopes RK. (1988), Protein purification: Principles and practice. 2nd Edition. Springer-Verlag, New york, U.S.A.

Shimizu Y, Matsushita K, Watanabe A. 1994. Influence of shear breakage of microbial cells on cross-flow microfiltration flux. J Ferm Bioeng 78: 170-174.

Skidmore GL, Chase HA. 1988. A study of ion exchangers for protein purification, in "Ion exchange for industry" Streat M. (Ed). Ellis Horwood Ltd, Chichester. pp 520-532.

Skidmore GL, Horstmann BJ, Chase HA. 1990. Modelling single component protein adsorption to the cation exchanger S Sepharose FF. J Chromatogr 498: 113-128

Smith D. 2001. Spitting venom: the search for a cure for a third world killer. The Chemical Engineer (TCE) April: 38-39.

Smoluchowski M. 1917. Mathematical theory of the kinetics of the coagulation of colloidal solution. Z Phys Chem 129-168.

Soon SY, Harbridge J, Titchener-Hooker NJ, Ayazi Shamlou P. 2001. Prediction of drop breakage in an ultra high velocity jet homogeniser. Journal of chemical engineering Japan 34 (5): 640-646.

Spielman LA. 1978. The scientific basis of flocculation. Ives KJ. (Ed). Sijthoff and Noordhoff. Amsterdam.

Subramanian G, (Ed). 1995. Process Scale Liquid Chromatography, VCH, Weinheim.

Van Reis R, Gadam S, Frautschy LN, Orlando S, Goodrich EM, Saskena S, Kuriyel R, Simpson CM, Pearl A, and Zydney AL. 1997. High performance tangential flow filtration. Biotech Bioeng 56 (1): 71-82.

Van Reis R, Leonard LC, Chang HC, Builder SE. 1991. Industrial scale harvest of proteins from mammalian cell culture by tangential flow filtration. Biotech Bioeng 38: 413-422.

Velayudhan A, Horváth C. 1988. Preparative chromatography of proteins: Analysis of the multivalent ion-exchange formalism. J Cromatogr 443: 13-29.

Verdoliva A, Pannone F, Rossi M, Catello S, Manfredi V. 2002. Affinity purification of polyclonal antibodies using a new all-D synthetic peptide ligand: comparison with protein A and protein G. J Immunol Meth 271 (1-2): 77-88.

Versteeg HK, Malalasekera W. 1955. An introduction to Computational Fluid Dynamics. Harlow; Longman Scientific & Technical: New York: Wiley. X. pp: 257.

Virkar PD, Hoare M, Chan MYY. 1982. Kinetics of acid precipitation of soya protein in a continuous-flow tubular reactor. Biotech Bioeng 24: 871-882.

Vogel JH, Kroner KH. 1999. Controlled shear filtration: A novel technique for animal cell separation. Biotech Bioeng 63 (6): 663-674.

Voss T, Falkner E, Ahorn H, Krystek E, Maurer-Fogy I, Bodo G, Hauptmann R. 1994. Periplasmic expression of human interferon-α2c in *Escherichia coli* results in a correctly folded molecule. Biochem J 298: 719-725.

Wakeman RJ, Williams CJ. 2002. Additional techniques to improve microfiltration. Separation and purification technology 26 (1): 3-18.

Walter J. 2000. Protein Liquid Chromatography (Journal of Chromatography Library Vol. 61): Kastner M. (Ed). Elsevier, Amsterdam.

Wankat PC. (Ed). 1986. "Large scale adsorption and chromatography", Vols 1 and 2. CRC Press, Boca Raton, FL.

Weast RC. (Ed). 1978. CRC handbook of chemistry and physics. CRC Press, Florida, U.S.A.

Weaver LE, Carta G. 1996. Protein asorption on cation exchangers: Comparison of macroporous and gel-composite media. Biotechnol Prog 12: 342-355.

Weselake RJ, Jain JC. 1992. Strategies in the purification of plant proteins. Physiolologia Plantarum 84 (2): 301-309.

Whitely RD, Wachter R, Liu F, Wang NHL. 1989. Ion-Exchange equilibria of lysozyme, myoglobin, and bovine serum albumin: effective valence and exchanger capacity. J Chromatogr 465: 137-156.

Wilson JA, Postlethwaite J, Pearce JD, Leach G, Lye GJ, Ayazi Shamlou P. 2003. Vibrating membrane filtration for the recovery and concentration of insect killing nematodes. Biotech. Bioeng, 83: 236-240.

Winston Ho WS, Sirkar KK. (Eds). 1992. Microfiltration. In: Membrane Handbook. Van Nostrand Reinhold. New York. pp: 455-594.

Wu S, Hancock W, Pavlu S, Gellerfors P. 1990. Applications of high-performance hydrophobic-interaction chromatography to the characterisation of recombinant derived human growth hormone. J Chromatogr 500: 596-606.

Yamamoto S, Nakanishi K, Matsuno R, Kamikubo T. 1983. Ion-exchange chromatography of proteins - prediction of elution curves and operating-conditions .2. Experimental-verification. Biotech Bioeng 25 (5): 1373-1391.

Yang CM, Tsao GT. 1982. Packed bed adsorption theories and their application to affinity chromatography. Adv Bioch Eng. 25: 1-18.

Yim SS, Ayazi Shamlou P. 2000. The Engineering effects of fluid flow on freely suspended biological macro-materials and macromolecules. Adv Biochem Eng Biotechnol 67: 83-122.

Yon RJ. 1972. Chromatography of lipophilic proteins on adsorbents containing mixed hydrophobic and ionic groups. J Biochem 126: 765-767.

Yoshida H, Nishikara H, Kataoka T. 1993. Adsorption of BSA on QAE-Dextran: Equilibria. Biotech Bioeng 41: 280-286.

Zeman LJ, Zydney AL. (Eds). 1996. Microfiltration and ultrafiltration: Principles and applications, Marcel Dekker, Monticello, NY.

Zhang Z, Chisti Y, Moo-Young M. 1995. Isolation of a recombinant intracellular β-galactosidase by ammonium sulphate fractionation of cell homogenates. Bioseparations 5: 329-337.

Zydney AL, Colton CK. 1986. A concentration polarization model for the filtrate flux in cross-flow microfiltration of particulate suspensions. Chem Eng Com 47:1-21.

11 Appendix

11.1 Proformas

Date: 16/11/1999

Name: Greg Neal **Supervisor: Eli Keshavarz-Moore**

Registration Date (1999/9/27) **Advisor: Mike Hoare**

Level: (EngD) (with Protherics)

Project title:

A study of the biopurification steps in the production of polyclonal antibody fragments for successful operation and scale-up

Significance:

Investigation into the purification steps will lead to a better understanding of how they interact with each other, resulting in a more efficient, less time consuming purification process. A greater knowledge of how the purification steps interact will also allow results produced at the laboratory bench scale to be more accurately applied to an industrial scale. The scale down is a powerful tool for predicting the optimum design and operation of large scale complex processes. It is particularly challenging because of poor scalability from laboratory to pilot plant, and because of difficulties in the exploration of process optimisation.

Goals:

To create a scale down mimic of the pre-purification steps that accurately describes the industrial scale process utilised by Protherics, and to study the effects of engineering parameters in the application of process options.

Conceptual Challenges:

The behaviour of precipitates in the centrifuge has a large impact on the clarification and separation characteristics. Precipitates are particularly susceptible to shear but the effects are system specific.

Results:

Protherics produce polyclonal antibodies in bulk and final dosage form for therapeutic use. The company's products range from antidotes to snake venom to antibodies against anti-depressant overdose. They are the world's biggest producer of anti snake venom. The company distinguishes itself from its competitors through the use of polyclonal rather than monoclonal antibodies.

At present the serum produced by immunised sheep is processed using several different techniques ranging from, precipitation and centrifugation to affinity chromatography. The company wishes to scale up its production from 100L to 1000L and is investigating alternative process options.

A two week visit was undertaken in order to gain first hand experience of the production of the anti snake venom. A report has been produced on this visit detailing each step of the purification process.

Intellectual Property:

Investigation into pre-purification steps is of value as eventually it should allow the process to be optimised so that valuable product is not lost during purification and it should allow the efficient scale up of the product.

Publications:

None

Previous milestones:

None

Research targets:

6 months:

Understand the purification process used by Protherics with particular emphasis on the precipitation and centrifugation steps. Mimic the precipitation step on a bench top scale in order to study the qualities of the process stream, and determine the characteristics of the precipitate. The conditions of the precipitation step such as the precipitate used may be altered in order to study it further.

Milestones:

- Calculate the sigma value for both Protherics disc stack centrifuge and the bench scale one.
- Mimic the precipitation stage and characterise the process stream, particle size, flow characteristics, density, viscosity and the density difference between the solution and the precipitate will be determined.

Research targets:

6 months to 1 year:

Understand the behaviour of the precipitate in the centrifuge and create a scale down model that accurately predicts the behaviour of the industrial scale centrifuge. Study the interaction between the precipitation and centrifugation steps and how what happens in these steps effects the process further down stream.

Milestones:

- Create a model of the precipitates behaviour in the centrifuge
- Mimic the centrifugation step on a small scale

Training profile

Educational Background: B.Sc (Hons) University of Wales, College of Cardiff

Training profile: Lacks engineering background.

Year 1

Core Training:

Course or Management activity	Dates *	Progress & Assessment
Graduate school board skills e.g. Personal and Professional Management Skills PPSRP	**Oct 99 to June 00**	**Lectures and workshops attended assessment is via course work and examination**
Graduate school technical courses e.g. Statistics Statistics	**14/01/00 24/03/00**	**Lectures and workshops attended assessment is via course work and examination**
Department training modules e.g. Fermentation module Downstream Processing	**Mar 00 to June 00**	**Downstream processing lectures plus course work and a final exam**
Management activities Demonstratorship	**Dec 99 to Mar 00**	**Student assessment Several training sessions attended**
Workshops Attended e.g. Gene meetings		**Shear**
Total number of courses taken		

* these may be checked

Date: 14/07/00

Name: Greg Neal **Supervisor: Eli Keshavarz-Moore**

Registration date (1999/9/27) **Advisor: Mike Hoare**

Level: (EngD with Protherics)

Project title:

A study of the biopurification steps in the production of polyclonal antibody fragments for successful operation and scale-up.

Significance:

Investigation into the purification steps will lead to a better understanding of how they interact with each other, resulting in a more efficient, less time consuming purification process. A greater knowledge of how the purification steps interact will also allow results produced at the laboratory bench scale to be more accurately applied to an industrial scale. Scale down experiments are powerful tools for predicting the optimum design and operation of a large scale complex process. It is particularly challenging because of the poor scalability from laboratory to pilot plant and because of difficulties in the exploration of process optimisation.

Goals:

To create a scale down mimic of the pre-purification steps that accurately describes the industrial scale process utilised at Protherics, and to study the effects of engineering parameters in the application of process options.

Conceptual Challenges:

The characteristics of precipitate particles affect their behaviour in the centrifuge and have a large impact on the clarification and separation process. Precipitate particles are particularly susceptible to shear but the effects are system specific.

Results:

A scale down model of the precipitation process has been built which accurately mimics the industrial scale operation. The model can be used to predict what effects changes in the precipitation operation will have on the precipitate particles characteristics. Material produced by the model can also be used to further study the purification process.

Intellectual Property:

Investigation into pre-purification steps and scale down models is of value as it will allow processing options to be more thoroughly investigated at the early stages of development when only small amount of material are available. It will also reduce the amount of time it takes for a product to get to the market.

Publications:

None.

Previous Milestones:

Understood the purification process used by Protherics, particularly the precipitation and centrifugation steps. Mimicked the precipitation step on a bench top scale and determined the precipitate particles characteristics including, particle size, density, viscosity and percentage solids content.

Research targets:

Next 6 months:

Understand he behaviour of the precipitate in the centrifuge and create a scale down model that accurately predicts the behaviour of the industrial scale machine. Study the interaction between the precipitation and centrifugation steps and how what happens in these steps effects the process further down stream.

Milestones:

- Understand how precipitate particles behave in a centrifuge and how their characteristics affect the performance of the centrifuge.

- Build a scale down model of the disc stack centrifuge that accurately mimics the industrial scale device.

Research Targets:

Next 6 months to 1 year:

Study what effect alterations in the precipitation conditions have on the centrifugation step and what knock on effect this has on chromatography stages. Study what effect changes in engineering parameters during the centrifugation stage have on the performance of the centrifuge. Produce a scale down model of a chromatography column.

Milestones:

- Build a scale down chromatography column
- Understand process interactions

Training Profile

Course or Management activity	Dates *	Progress & Assessment
Graduate school board skills e.g. Personal and Professional Management Skills PPSRP	Oct 99 to June 00	Completed awaiting result
Graduate school technical courses e.g. Statistics Statistics	14/01/00 24/03/00	Completed awaiting results
Department training modules e.g. Fermentation module Downstream Processing	Mar 00 to June 00	Completed awaiting results
Management activities Demonstratorship	Dec 99 to Mar 00	Completed
Workshops Attended e.g. Gene meetings		
Total number of courses taken		

Date: 14/11/00

Name: Greg Neal **Supervisor: Eli Keshavarz-Moore**

Registration date (1999/9/27) **Advisor: Mike Hoare**

Level: (EngD with Protherics)

Project title:
A study of the biopurification steps in the production of polyclonal antibody fragments for successful operation and scale-up.

Significance:
Investigation into the purification steps will lead to a better understanding of how they interact with each other, resulting in a more efficient, less time consuming purification process. A greater knowledge of how the purification steps interact will also allow results produced at the laboratory bench scale to be more accurately applied to an industrial scale. Scale down experiments are powerful tools for predicting the optimum design and operation of a large scale complex process. It is particularly challenging because of the poor scalability from laboratory to pilot plant and because of difficulties in the exploration of process optimisation.

Goals:
To create a scale down mimic of the pre-purification steps that accurately describes the industrial scale process utilised at Protherics, and to study the effects of engineering parameters in the application of process options.

Conceptual Challenges:
The characteristics of precipitate particles affect their behaviour in the centrifuge and have a large impact on the clarification and separation process. Precipitate particles are particularly susceptible to shear but the effects are system specific.

Results:

Bioprocess design and optimisation customarily involves the use of pilot plant and industrial scale experiments to define the process and study the effect that changes to the process have on the level of contaminants or yield of product. These studies require large amounts of time, money and material, all of which are in short supply during the initial stages of process design. The use of scaled down laboratory models that accurately mimic the large scale process allow the process to be studied without the need for costly and material expensive pilot plant trials.

A scaled down model of the precipitation stage has been built which accurately mimics the industrial scale operation. This model has been used to characterise the process stream, it has also been used to determine the effects, if any changes to the process will have on the precipitate particles and hence on operations further downstream.

Protherics wish to change from liquid precipitant to solid in order to scale up production. This change to solid sodium sulphate has been studied and its effects are detailed below:

- Increase in process stream viscosity
- Increase in the amount of solid material
- No change in particle size

The model has also been used to study the effects of higher shear levels during primary particle formation. These were determined to be:

- Increased process stream viscosity
- Decreased particle size
- Increased amount of solid material

Precipitant produced by the mimic has been used in scale down centrifugation studies. The "in house" shear device is being used to mimic a disc stack centrifuge and to study the effects of shear on particle size and biological activity.

Intellectual Property:

Investigation into pre-purification steps and scale down models is of value as it will allow processing options to be more thoroughly investigated at the early stages of development when only small amount of material are available. It will also reduce the amount of time it takes for a product to get to the market.

Publications:

None

Previous Milestones:

Scale down mimic of disc stack centrifuge nearly complete, the scale down model of the precipitation stage has been used to study what effects changes to the process set-up have on the characteristics of the product, i.e. the effect of changing to solid precipitant and changes in mixing conditions.

Research targets:

Next 6 months:

Build a complete picture of the precipitation and centrifugation stage, including mass balances and visual method of tracking the process. Use this picture to optimise the process and study the effects of changes. Produce the first paper on the scale down of precipitation and disc stack centrifugation.

Milestones:

- Use ELISA, SDS-page and total protein assays to create a mass balance and track/visualise exactly what is happening during precipitation and centrifugation.
- Complete paper on scale down of precipitation and centrifugation.
- Finish study on the effect of changing to a solid precipitant.
- Finish study on the effects of shear on particle size and biological activity.
- Determine the Zeta potential of the precipitate particles.

Research Targets

Next 6 months to 1 year:

Study what effect alterations in the precipitation conditions and centrifugation stage have on the chromatography step and how the stages interact. Produce second paper on mixing conditions and process interactions. Produce a scale down model of a chromatography column.

Milestones:

- Second paper
- Build a scale down chromatography column
- Understand process interactions

Training Profile

Course or Management activity	Dates *	Progress & Assessment
Graduate school board skills e.g. Personal and Professional Management Skills PPSRP	Oct 99 to June 00	Completed awarded pass 63%
Graduate school technical courses e.g. Statistics Statistics	14/01/00 24/03/00	Completed awarded pass 63%
Department training modules e.g. Downstream Processing Bioprocess Management	Mar 00 to June 00 Mar01 to June 01	Completed awarded pass 68% In future
Management activities Demonstratorship	Nov 00 to Mar 01	One year completed starting second year
Workshops Attended e.g. Gene meetings		
Total number of courses taken		

Date: 14/06/01

Name: Greg Neal **Supervisor: Eli Keshavarz-Moore**

Registration date (1999/9/27) **Advisor: Parviz Ayazi-Shamlou**

Level: (EngD with Protherics)

Project title:

A study of the biopurification steps in the production of polyclonal antibody fragments for successful operation and scale-up.

Significance:

Investigation into the purification steps will lead to a better understanding of how they interact with each other, resulting in a more efficient, less time consuming purification process. A greater knowledge of how the purification steps interact will also allow results produced at the laboratory bench scale to be more accurately applied to an industrial scale. Scale down experiments are powerful tools for predicting the optimum design and operation of a large scale complex process. It is particularly challenging because of the poor scalability from laboratory to pilot plant and because of difficulties in the exploration of process optimisation.

Goals:

To create a scale down mimic of the pre-purification steps that accurately describes the industrial scale process utilised at Protherics, and to study the effects of engineering parameters in the application of process options.

Conceptual Challenges:

The characteristics of precipitate particles affect their behaviour in the centrifuge and have a large impact on the clarification and separation process. Precipitate particles are particularly susceptible to shear but the effects are system specific.

Results:

A scale down model of the precipitation process has been built which accurately mimics the industrial scale operation. The model can be used to predict what effects changes in the precipitation operation will have on the precipitate particles characteristics. Material produced by the model can also be used to further study the purification process.

The mimic has been used to study the effect that a change from liquid precipitant to solid has:

- Increase the viscosity
- Increase the percent solids
- No change in particle size

It has also been used to study the effect of higher shear levels during primary particle formation:

- Increased viscosity
- Decreased particle size
- Slightly increased percent solids

Precipitant produced by the mimic has been used in scale down centrifugation studies. The "in house" shear device has been used to mimic a disc stack centrifuge and to study the effects of shear on particle size distribution and biological activity. The results are to be published in the first paper.

Intellectual Property:

Investigation into pre-purification steps and scale down models is of value as it will allow processing options to be more thoroughly investigated at the early stages of development when only small amount of material are available. It will also reduce the amount of time it takes for a product to get to the market.

Publications:

Scale down of precipitation and centrifugation. In preparation.

Previous Milestones:

Scale down mimic of disc stack centrifuge complete, the scale down model of the precipitation stage has been used to study what effects changes to the process set-up have on the characteristics of the product, i.e. the effect of changing to solid precipitant and changes in mixing conditions, temperature etc.

ELISA, SDS-page and total protein assays have been used to create a mass balance and track/visualise exactly what is happening during precipitation and centrifugation..

The study on the effect of changing to a solid precipitant has been finished

Finished study on the effects of shear on particle size and biological activity

Research targets:

Next 6 months:

Finish first paper on scale down of precipitation and disc stack centrifugation. Complete three-month new venture development course at the London school of business. Carry out study to determine solubility profile of antibodies in ovine serum. Investigate the effect of temperature on particle size and recoverability.

Milestones:

- Paper finished
- Course completed
- Solubility profile determined
- Effect of temperature determined

Research Targets

Next 6 months to 1 year:

Investigate the next stage in the purification process papain digestion and chromatography for a product in phase two clinical trials, find a way of removing the precipitation and centrifugation stage.

Milestones:

- Complete model of papain digestion
- Complete study into removing the precipitation and centrifugation stage

Training Profile

Course or Management activity	Dates *	Progress & Assessment
Graduate school board skills e.g. Personal and Professional Management Skills PPSRP	Oct 99 to June 00	Completed awarded pass 63%
Graduate school technical courses e.g. Statistics Statistics	14/01/00 24/03/00	Completed awarded pass 63%
Department training modules e.g. Downstream Processing Bioprocess validation Bioprocess management	Mar 00 to June 01	Completed awarded pass 68% Completed Completed
Management activities Demonstratorship	Nov 00 to Mar 01	Two years completed
New venture development at LBS	July 01-Sept 01	
Biobusiness plan competition	Sept 01-Oct01	
Workshops Attended		

e.g. Gene meetings		
Total number of courses taken		

Date: 02/10/01

Name: Greg Neal **Supervisor: Eli Keshavarz-Moore**

Registration date (1999/9/27) **Advisor: Parviz Ayazi-Shamlou**

Level: (EngD with Protherics)

Project title:

A study of the biopurification steps in the production of polyclonal antibody fragments for successful operation and scale-up.

Significance:

Investigation into the purification steps will lead to a better understanding of how they interact with each other, resulting in a more efficient, less time consuming purification process. A knowledge of how the purification steps interact will also allow results produced at the laboratory bench scale to be more accurately applied to an industrial scale. Scale down experiments are powerful tools for predicting the optimum design and operation of a large scale complex process. It is particularly challenging because of the poor scalability from laboratory to pilot plant and because of difficulties in the exploration of process optimisation.

Goals:

To create a scale down mimic of the downstream processing steps that accurately describes the industrial scale process utilised at Protherics, and to study the effects of engineering parameters in the application of process options.

Conceptual Challenges:

The characteristics of precipitate particles affect their behaviour in the centrifuge and have a large impact on the clarification and separation process. Precipitate particles are particularly susceptible to shear but the effects are system specific.

Results:

A scale down model of the precipitation and centrifugation stages has been built. This model has been validated against material provided by Protherics in order to prove the accuracy and validity of results. The model can be used to predict what effects changes in the precipitation operation will have on the precipitate particles characteristics, also the impact of the centrifugation operation can be assessed along with the effects of changes in the operating parameters of this stage. The material produced by the model is representative of the feed stream produced at an industrial scale so all results can be applied to this scale, furthermore the material can also be used to study alternative purification options.

The mimic has been used to study the effect that a change from liquid precipitant to solid has:

- Increase the viscosity
- Increase the percent solids
- No change in particle size

It has also been used to study the effect of higher shear levels during primary particle formation:

- Increased viscosity
- Decreased particle size
- Slightly increased percent solids

London Business School

A three-month course entitled new venture development was undertaken. During the time spent at London Business School my teammates and myself developed a business plan for the commercialisation of Ultra Scale Down technology.

Intellectual Property

Investigation into pre-purification steps and scale down models is of value as it will allow processing options to be more thoroughly investigated at the early

stages of development when only small amount of material are available. It will also reduce the amount of time it takes for a product to get to the market.

Publications:

An Ultra Scale Down Approach For the Prediction of Full Scale Recovery of ovine Polyclonal Immunoglobulins Used in The Manufacture of Snake Venom specific Fab Fragments (Final Draft)

Previous Milestones:

Scale down mimic of disc stack centrifuge complete, the scale down model of the precipitation stage has been used to study what effects changes to the process set-up have on the characteristics of the product, i.e. the effect of changing to solid precipitant and changes in mixing conditions, temperature etc.

ELISA, SDS-page and total protein assays have been used to create a mass balance and track/visualise exactly what is happening during precipitation and centrifugation..

The study on the effect of changing to a solid precipitant has been finished

Finished study on the effects of shear on particle size and biological activity

Solubility study on the Fab fragments has been undertaken and finished.

Three-month course at London Business School finished.

First paper has been completed.

Research targets:

Next 6 months:

Start work to scale down filtration and study this purification process as an alternative to centrifugation.

Milestones:

- Complete scale down model
- Study effect of feed stream (precipitant solution) on filtration

Research Targets

Next 6 months to 1 year:

Investigate alternatives to the existing purification process:

1. Ultra scale down model of membrane filtration
2. Ultra scale down model of chromatographic and papain digestion stages

Milestones:

- Complete model of membrane filtration
- Complete model of chromatographic and papain digestion stages

Training Profile

Course or Management activity	Dates *	Progress & Assessment
Graduate school board skills e.g. Personal and Professional Management Skills PPSRP	Oct 99 to June 00	Completed awarded pass 63%
Graduate school technical courses e.g. Statistics Statistics	14/01/00 24/03/00	Completed awarded pass 63%
Department training modules e.g. Downstream Processing Bioprocess validation Bioprocess management	Mar 00 to June 01	Completed awarded pass 68% Completed Completed
Management activities Demonstratorship	Nov 00 to Mar 01	Two years completed
New venture development at LBS	July 01-Sept 01	Completed

Biobusiness plan competition	**Sept 01-Oct01**	**Final stage qualifiers**
Workshops Attended e.g. Gene meetings		
Total number of courses taken		

Date: 14/08/02

Name: Greg Neal **Supervisor: Eli Keshavarz-Moore**

Registration date (1999/9/27) **Advisor: Parviz Ayazi-Shamlou**

Level: (EngD with Protherics)

Project title:

A study of the biopurification steps in the production of polyclonal antibody fragments for successful operation and scale-up.

Significance:

Investigation into the purification steps will lead to a better understanding of how they interact with each other, resulting in a more efficient, less time consuming purification process. A knowledge of how the purification steps interact will also allow results produced at the laboratory bench scale to be more accurately applied to an industrial scale. Scale down experiments are powerful tools for predicting the optimum design and operation of a large scale complex process. It is particularly challenging because of the poor scalability from laboratory to pilot plant and because of difficulties in the exploration of process optimisation.

Goals:

To create a scale down mimic of the downstream processing steps that accurately describes the industrial scale process utilised at Protherics, and to study the effects of engineering parameters in the application of process options.

Conceptual Challenges:

The characteristics of precipitate particles affect their behaviour in the centrifuge and have a large impact on the clarification and separation process. Precipitate particles are particularly susceptible to shear but the effects are system specific.

Results:

A scale down model of the precipitation and centrifugation stages has been built. This model has been validated against material provided by Protherics in order to prove the accuracy and validity of results. The model can be used to predict what effects changes in the precipitation operation will have on the precipitate particles characteristics, also the impact of the centrifugation operation can be assessed along with the effects of changes in the operating parameters of this stage. The material produced by the model is representative of the feed stream produced at an industrial scale so all results can be applied to this scale, furthermore the material can also be used to study alternative purification options.

The mimic has been used to study the effect that a change from liquid precipitant to solid has:

- Increase the viscosity
- Increase the percent solids
- No change in particle size

It has also been used to study the effect of higher shear levels during primary particle formation:

- Increased viscosity
- Decreased particle size
- Slightly increased percent solids

Ultra Scale Down Filtration

A ultra scale down stirred cell filtration system has been used to study the effect of using filtration to remove the precipitated antibodies instead of centrifugation. Factorial design was used to design a series of experiment studying the effect of pressure and shear rate on permeate flux rate. The yield of antibodies and the purification profile has also been determined and compared to the centrifugation route. This work will form the basis of a second paper

London Business School

A three-month course entitled new venture development was undertaken. During the time spent at London Business School myself and my team mates developed a business plan for the commercialisation of Ultra Scale Down technology.

Intellectual Property

Investigation into pre-purification steps and scale down models is of value as it will allow processing options to be more thoroughly investigated at the early stages of development when only small amount of material are available. It will also reduce the amount of time it takes for a product to get to the market.

Publications:

Neal G, Christies J, Keshavarz-Moore E, Ayazi Shamlou P. 2003. An ultra scale-down approach for the prediction of full-scale recovery of ovine polycolonal immunoglobulins used in the manufacture of snake venom-specific fab fragment. Biotech Bioeng 81 (2): 149-157.

Previous Milestones:

Scale down mimic of disc stack centrifuge complete, the scale down model of the precipitation stage has been used to study what effects changes to the process set-up have on the characteristics of the product, i.e. the effect of changing to solid precipitant and changes in mixing conditions, temperature etc.

ELISA, SDS-page and total protein assays have been used to create a mass balance and track/visualise exactly what is happening during precipitation and centrifugation..

The study on the effect of changing to a solid precipitant has been finished

Finished study on the effects of shear on particle size and biological activity

Solubility study on the Fab fragments has been undertaken and finished.

Three-month course at London Business School finished.

First paper has been completed and accepted for publication by Biotechnology and Bioengineering

Ultra scale down of filtration process has been undertaken and finished

Research targets:

Next 6 months:

Finish second paper on the effect of swapping from centrifugation to filtration on the downstream processing

Milestones:

- Complete second paper
- Produce an Ultra scale down model of chromatographic and papain digestion stages

Research Targets

Next 6 months to 1 year:

- Link all the ultra scale down mimics together to form a whole bioprocess model
- Complete an economic evaluation of the present process compared to the alternatives studied
- Complete third paper on economics of process change

Milestones:

- Production of whole bioprocess model
- Completion of third paper

Training Profile

Course or Management activity	Dates *	Progress & Assessment
Graduate school board skills e.g. Personal and Professional Management Skills PPSRP	Oct 99 to June 00	Completed awarded pass 63%
Graduate school technical courses e.g. Statistics Statistics	14/01/00 24/03/00	Completed awarded pass 63%
Department training modules e.g. Downstream Processing Bioprocess validation Bioprocess management	Mar 00 to June 01	 Completed awarded pass 68% Completed Completed
Management activities Demonstratorship	Nov 00 to Mar 01	Two years completed
New venture development at LBS	July 01-Sept 01	Completed
Biobusiness plan competition	Sept 01-Oct01	Final stage qualifiers

Date: 01/06/03

Name: Greg Neal **Supervisor: Eli Keshavarz-Moore**

Registration date (1999/9/27) **Advisor: Parviz Ayazi-Shamlou**

Level: (EngD with Protherics)

Project title:

A study of the biopurification steps in the production of polyclonal antibody fragments for successful operation and scale-up.

Significance:

Investigation into the purification steps will lead to a better understanding of how they interact with each other, resulting in a more efficient, less time consuming purification process. A knowledge of how the purification steps interact will also allow results produced at the laboratory bench scale to be more accurately applied to an industrial scale. Scale down experiments are powerful tools for predicting the optimum design and operation of a large scale complex process. It is particularly challenging because of the poor scalability from laboratory to pilot plant and because of difficulties in the exploration of process optimisation.

Goals:

To create a scale down mimic of the downstream processing steps that accurately describes the industrial scale process utilised at Protherics, and to study the effects of engineering parameters in the application of process options.

Conceptual Challenges:

The characteristics of precipitate particles affect their behaviour in the centrifuge and have a large impact on the clarification and separation process. Precipitate particles are particularly susceptible to shear but the effects are system specific.

Results:

A scale down model of the precipitation and centrifugation stages has been built. This model has been validated against material provided by Protherics in order to prove the accuracy and validity of results. The model can be used to predict what effects changes in the precipitation operation will have on the precipitate particles characteristics, also the impact of the centrifugation operation can be assessed along with the effects of changes in the operating parameters of this stage. The material produced by the model is representative of the feed stream produced at an industrial scale so all results can be applied to this scale, furthermore the material can also be used to study alternative purification options.

The mimic has been used to study the effect that a change from liquid precipitant to solid has:

- Increase the viscosity
- Increase the percent solids
- No change in particle size

It has also been used to study the effect of higher shear levels during primary particle formation:

- Increased viscosity
- Decreased particle size
- Slightly increased percent solids

Ultra Scale Down Filtration

A ultra scale down stirred cell filtration system has been used to study the effect of using filtration to remove the precipitated antibodies instead of centrifugation. Factorial design was used to design a series of experiment studying the effect of pressure and shear rate on permeate flux rate. The yield of antibodies and the purification profile has also been determined and compared to the centrifugation route. This work will be published in a second paper

Scale Down Chromatography

A small scale study of the equilibrium binding kinetics of ovine polyclonal IgG to Protein G has been conducted and the results used to build a mathematical model capable of predicting the breakthrough curves. The model has been tested by comparison with actual breakthrough curves produced under different conditions.

London Business School

A three-month course entitled new venture development was undertaken. During the time spent at London Business School my team-mates and myself developed a business plan for the commercialisation of Ultra Scale Down technology.

Intellectual Property

Investigation into pre-purification steps and scale down models is of value as it will allow processing options to be more thoroughly investigated at the early stages of development when only small amount of material are available. It will also reduce the amount of time it takes for a product to get to the market.

Publications:

Neal G, Christies J, Keshavarz-Moore E, Ayazi Shamlou P. 2003. An ultra scale-down approach for the prediction of full-scale recovery of ovine polycolonal immunoglobulins used in the manufacture of snake venom-specific fab fragment. Biotech Bioeng 81 (2): 149-157.

Neal G, Francis R, Keshavarz-Moore E, Ayazi Shamlou P. 2004. Separation of IgG precipitate from contaminating proteins using microfiltration. Biotech and Applied Biochem 39(2): 241-248.

Previous Milestones:

Scale down mimic of disc stack centrifuge complete, the scale down model of the precipitation stage has been used to study what effects changes to the process set-up have on the characteristics of the product, i.e. the effect of changing to solid precipitant and changes in mixing conditions, temperature etc.

ELISA, SDS-page and total protein assays have been used to create a mass balance and track/visualise exactly what is happening during precipitation and centrifugation..

The study on the effect of changing to a solid precipitant has been finished

Finished study on the effects of shear on particle size and biological activity

Solubility study on the Fab fragments has been undertaken and finished.

Three-month course at London Business School finished.

First paper has been completed and accepted for publication by Biotechnology and Bioengineering

Ultra scale down of filtration process has been undertaken and finished.

Second paper ahs been completed and submitted.

Research targets:

Next 6 months:

Write up thesis

Milestones:

- Complete Thesis

Training Profile

Course or Management activity	Dates *	Progress & Assessment
Graduate school board skills e.g. Personal and Professional Management Skills PPSRP	Oct 99 to June 00	Completed awarded pass 63%
Graduate school technical courses e.g. Statistics Statistics	14/01/00 24/03/00	Completed awarded pass 63%
Department training modules e.g. Downstream Processing Bioprocess validation Bioprocess management	Mar 00 to June 01	Completed awarded pass 68% Completed Completed
Management activities Demonstratorship	Nov 00 to Mar 01	Two years completed
New venture development at LBS	July 01-Sept 01	Completed
Biobusiness plan competition	Sept 01-Oct01	Final stage qualifiers